Climate processes over the Himalaya – the added value from high resolution regional climate modelling

Jagadishwor Karmacharya

Christ Church

A thesis submitted for the degree of Doctor of Philosophy

University of Oxford

Michaelmas Term 2014

Abstract

The Himalaya plays a vital role in shaping the hydro-climate of South Asia and beyond, but their climate has not yet been monitored and modelled as well as some other regions. As the summer monsoon is the dominant climate system over South Asia, including the Himalaya, realistic simulation of the South Asian summer monsoon (SASM) should be a prerequisite for the satisfactory simulation of the Himalayan climate. The present research tests the assumption that higher resolution modelling will provide improved representation of the SASM, both regionally and over the Himalaya region. The first part of this research assesses the strength and stability of the temporal relationships between the monsoon rainfall indices (MRIs) and the large-scale monsoon circulation indices (MCIs), as a precursor to using such indices for model evaluation. The remainder of the thesis evaluates model performance in simulating various characteristics of SASM, mainly with regard to precipitation. In particular, the sensitivity of a regional climate model (RCM) simulation to domain size and added value of high resolution RCM simulation are evaluated. For this purpose, the Hadley Centre unified model - HadGEM is utilized in its regional and, in few instances, global configurations. The RCM simulations are performed at 0.44° and 0.11° horizontal resolutions and they are forced by the ERA interim dataset. Results show that i) the MRI-MCI relationship exhibits considerable low-frequency variability, ii) RCM simulation of SASM, particularly precipitation, shows sensitivity to domain size and simulation with a moderately sized domain that partially excludes bias prone equatorial Indian ocean outperform those with larger domains, iii) high resolution RCM simulation adds value in many aspects of SASM precipitation, including the seasonal mean, relative frequency distribution, extremes, and active and break monsoon composites, but the improvements are generally seen over the Indo-Gangetic plain rather than the Himalaya. The findings promote use of a high resolution RCM over a moderate sized domain (~25,000,000 sq. km) for the realistic simulation of SASM, but the study needs

to be repeated with multiple realizations and different RCMs before arriving at a robust conclusion.

Table of Contents

Acknowledgements

First and foremost, I would like to thank my supervisors, Mark New and Richard Jones, for their guidance at every stage of the DPhil research with great expertise and patience. Equally, I thank the college advisor Simon Dadson whose constant advice has been very helpful over the years.

I acknowledge the full financial support of The Felix scholarship for the first three years of study and the Christ Church for partially funding the final year of study. I would also like to thank Judith Pallot for her support and proactive role in securing the latter.

The support from the Met Office, which generously permitted use of a recent version of regional climate model developed in the centre and also provided access to its supercomputing facility, has been instrumental for this research. In this connection, I would like to place on record the support from a number of Met Office personnel, in particular Simon Tucker for sharing technical knowhow on post-processing Met Office model output and accessing data via MONSooN, Chloe Eagle for providing step by step guide on pre-processing and running the regional climate model. Special thanks are due to Wilfran Moufouma-Okla for running the high resolution model despite his busy schedule. I am grateful also to Gill Martin, Richard Levine, Carol Mcsweeney and Changgui Wang for their stimulating discussions and debate at various stages.

I must give credit also to Gil Lizcano and Sebastian Engelstaedter for their generosity in downloading and processing some of the datasets. I am thankful to those people who have assisted me personally at the initial stage to get familiar with various programs and interfaces, often sharing considerable time and expertise, in particular Muhammad Rahiz and Said AlSarmi. I would like also to thank everyone in the climate research lab, especially the inhabitants of mezzanine: Rachel James and Christopher Allen, for their help, encouragement and ensuring friendly and vibrant environment in the lab. Rachel James also supported in the write up process at various stages by providing samples of well written pieces of academic work.

I would like also to thank Department of Hydrology and Meteorology, Ministry of Science, Technology and Environment, and Government of Nepal for providing the study leave.

Last, but not the least, I would like to express my gratitude to my father, elder brother, my wife, and kids for their support and constant encouragement to pursue my research by providing conducive environment.

List of Tables

List of Figures

List of Acronyms and Abbreviations

20CR	20 Century Reanalysis
95PDR	95th percentile of the daily precipitation
A/B	Active/Break
AGCM	Atmosphere Only Global Climate Model
AIMR	All India Monsoon Rainfall
AIR	All-India Rainfall
AOGCM	Atmosphere Ocean Global Climate Model
BJF	Betts–Miller–Janjic´
BoB	Bay of Bengal
CEH	Central and Eastern Himalaya
CHMRI	Central Himalaya Monsoon Rainfall Index
CMIP3	Coupled Model Intercomparison Project phase 3
CMIP5	Coupled Model Intercomparison Project phase 5
CORDEX	COordinated Regional Climate Downscaling EXperiment
CRU	Climate Research Unit
CSAD	CORDEX South Asia Domain
CVA	Common Validation Area
DOE	Department of Energy (USA)
ECMWF	European Centre for Medium-Range Weather Forecasts
EIMR	Extended Indian Monsoon Rainfall
EIO	Equatorial Indian Ocean
ENSO	El Nino Southern Oscillation
ERA40	ECMWF 40 year reanalysis

ERAI	ERA-Interim (ECMWF Interim reanalysis)
GA	Global Atmosphere
GCM	Global Climate Model
GLOF	Glacier Lake Outburst Flow
GPCP	Global Precipitation Climate Project
GTS	Global Telecommunication System
HKH	Hindu Kush Himalaya
IGP	Indo-Gangetic Plain
IITM	Indian Institutes of Tropical Meteorology
IMD	Indian Meteorological Department
IMI	Indian Monsoon Index
IOD	Indian Ocean Dipole
ISMR	Indian Summer Monsoon Rainfall
ISV	Intra-Seasonal Variability
ITCZ	Inter-Tropical Convergence Zone
JJAS	June-July-August-September
LBC	Lateral Boundary Condition
LLJ	Low Level Jet
LTL	Lower Tropospheric Level
MCI	Monsoon Circulation Index
MERRA	Modern-ERA Retrospective Analysis for Research and Applications
MetUM	Met Office Unified Model
MHI	Monsoon Hadley Circulation Index
MISO	Monsoon Intra-Seasonal Oscillations
MRI	Monsoon Rainfall Index

NCAR	National Centre for Atmospheric Research (USA)
NCEP	National Centers for Environmental Prediction (USA)
NNRP1	NCEP/NCAR Reanalysis
NNRP2	NCEP/DOE Reanalysis II
NWP	Numerical Weather Prediction
OLR	Outgoing Longwave Radiation
PRECIS	Providing Regional Climates for Impact Studies
R95pTOT	Very Wet Days Cumulative Precipitation
PSS	Peirce Skill Score
RCM	Regional Climate Model
RMSD	Root Mean Square Difference
SASM	South Asian Summer Monsoon
SD	Standard Deviation
SSI	Southerly Shear Index
SST	Sea Surface Temperature
TP	Tibetan Plateau
TRMM	Tropical Rainfall Measuring Mission
UTL	Upper Tropospheric Level
VIMF	Vertical Integrated Moisture Flux
WEIO	West Equatorial Indian Ocean
WSI	Westerly Shear Index
WYI	Webster and Yang Index

1 Introduction

1.1 Importance of the Himalaya

The Himalaya, also called the water tower of Asia, has the third largest reserve of snow and ice outside the two poles (Immerzeel et al. 2010). All the major rivers in Central and South Asia originate from the Hindu Kush Himalayan (HKH) region (Kang et al. 2010), which provides perennial supply of water to the surrounding lowland areas of South and Central Asia. The contribution of snow and glacier melt in the river discharge is especially significant during the dry season. It is estimated that more than 1.3 billion people living in Central and South Asia depend on those rivers (Immerzeel et al. 2010). The Himalaya is also rich in flora and fauna, which provide a source of livelihood for millions of people living on its slopes. The immense volume of water flowing down the Himalayan slopes has the potential to generate huge amounts of clean electricity to irrigate huge swath of arable land spearheading the regional transformation.

The Himalaya also plays a vital role in modulation of climate at local to regional scales and beyond through various mechanisms, such as acting as physical barrier to atmospheric flow from the surrounding regions, as an elevated heat source via production of latent heat of orographic precipitation, and by changing the nature of water and energy exchange between land surface and atmosphere via either increased snow cover, elevated plateaus, or the establishment of rain shadow deserts (Pant and Kumar 1997). In the similar fashion, the mountain massifs of the Himalaya and the Tibetan Plateau (TP) exert profound influence on the monsoon circulation through its dynamical and thermal forcing. While some of these factors, such as orography, are invariant in time, at least on centennial climate scales, others are dynamic (e.g. snow cover) which could vary seasonally or longer time scales. It is the latter which is of more interest to climate researchers in terms of quantifying and projecting their trends

and variability, and understanding interaction of those dynamic elements with other forcings of the regional climate. For example, it is known that spring snow cover over the Himalaya and TP is inversely correlated with the South Asian summer monsoon (SASM) rainfall (Shekhar and Dash 2005) through their control on nature of heat flux (i.e. sensible or latent) over the region, which in turn affect monsoon circulations both at lower and upper levels. So, for example, unravelling the impact of long term fluctuations of the Himalayan glacier cover on the SASM precipitation would be both exciting and challenging from a climate prospective.

1.1.1 Dominant climate systems affecting the Himalaya

The Himalayan region comes under the influence of the monsoon in the summer and western disturbances in the winter. While entire South Asia comes under the influence of the monsoon from June to September, influence of western disturbance over the region is limited to the HKH region in the winter. The summer monsoon has special significance over the entire South Asia as it accounts for more than 75% of annual rainfall over South Asia (Dobler and Ahrens 2010) and about 80% in the central Himalaya (Shrestha et al. 2000). Consequently, monsoonal precipitation has a macro scale control on the regional water availability which in turn affects agriculture, water resources, natural disasters etc. On the other hand, even though western disturbances are active over the HKH region for only a few times each winter, on the average, associated westerly circulations and cyclonic storms contribute about two third of annual snowfall over the western high Himalaya and bring about 25-30% of annual precipitation over the central Himalaya above 3000 m (Barros et al. 2004). Consequently, western disturbances play an important role in replenishing the snow accumulation over the

Himalaya, which is vital for maintaining the glacier mass balance and perennial river flow.

1.2 Impact of climate change over the Himalaya

The Himalayan region is highly sensitive to climate change, similar to other elevated regions. Adverse impacts of global warming have been strongly felt in the Himalayan region where the mountains are warming at much higher rate than a zonal average warming at that latitude (Shrestha et al. 1999). As a consequence, many Himalayan glaciers are undergoing rapid retreat in recent decades (Bolch et al. 2012). This has not only increased the risk of glacier lake outburst flows (GLOFs) in the Himalayan slopes but is also jeopardizes regional water security in the future (Kehrwald et al. 2008). It is anticipated that increasing deglaciation of the Himalaya is leading to changes in the regional hydrology (Barnett et al. 2005). In fact, in recent years, many mid-mountain regions of Nepal are facing severe water stress in non-monsoonal months causing huge societal impacts, such as forcing whole communities to migrate in a number of places. While the prime cause of this water scarcity appears to be rooted in hydro-climatic changes associated with climate change (e.g., more erratic weather patterns, shift in seasonal cycle of snow and glacier melt, depletion of snow and water reservoirs), mismanagement of resources (e.g. deforestation) might also have aggravated the situation.

The strong role of the Himalaya in modulation of the regional climate implies that any impact of the climate change on the Himalaya will not be confined locally but likely generate strong regional feedback perturbing the climate at regional scale. Hence there is strong incentive to enhance our understanding on the Himalayan climate, its

interaction with other major elements of the regional climate and then to produce reliable estimate of future changes in climate and its potential impacts.

1.3 Available tools for future climate projections

While understanding of the current climate can be enhanced by strengthening the in-situ and remote observation network, and processed based interpretation of those observations, the most advanced tool to generate plausible climate projections is to run climate models, which are constantly being upgraded with advances in our understanding of the climate system.

Global climate models (GCMs) are the most comprehensive scientific tool for global climate projection which takes into account interaction among different forcings of the climate system. At global and continental scale, the GCMs are able to simulate broad features of the current climate reasonably well and can reproduce the historical observed large-scale changes in climate, but due to constraints in the computing resources they still operate at resolution (grid scale) of around 100-200 km. Their effective resolution is about 6-8 grid distances, i.e. of the order of 1000 km (Grotch and MacCracken 1991). Hence, they are not able to represent the heterogeneity of the land surface and topography with sufficient details and many processes, which operate at finer resolution than the grid spacing, have to be parameterized. As a consequence, GCMs often have problems capturing the fine-scale structures that affect regional climate (Rajendran et al. 2013) which could then have detrimental impact even on the representation of the large scale process. For example, their depiction of regional and local atmospheric circulations (e.g. narrow jet cores, mesoscale convective systems, sea-breeze type circulations) and representation of processes at high frequency temporal scales (e.g.

precipitation frequency and intensity) are inadequate (Christensen et al. 2007). Similarly, their ability to reproduce the effects of mesoscale influences such as convective systems embedded in depressions and the most intense and localised precipitation events may also be limited (Stowasser et al. 2009).

In the similar fashion, GCMs do not have proper representation of the Himalayan topography (maximum elevation ~4.75 km at ~2° horizontal resolution), nor can they resolve climate with sufficient details to be relevant for projecting Himalayan climate. Obviously, very high resolution global models are able to simulate regional and local aspects of climate (e.g., Mizuta et al. 2006) but such simulation is still not commonly feasible due to their high computational cost.

Regional climate models (RCMs) are limited area models, derived from the GCMs or operational numerical weather prediction models and operate at horizontal resolution of few kilometres to few tens of kilometres. They are used to dynamically downscale GCMs or reanalysis to add finer details, and they have potential to add values to GCMs for a number of reasons. For example, RCMs have a more realistic representation of fine scale forcings of weather and climate, such as topography and land use (Chan et al. 2012) and generally improved representation of physical processes and interactions (e.g. the dynamical structure of weather systems of cloud complexes, mesoscale structures, the location of major circulation features) etc. (Rauscher et al. 2010). For these reasons, RCMs are expected to simulate local and regional weather phenomena more accurately (Marvel et al. 2013) leading to improved simulation of the distribution of events at finer temporal scales e.g. daily and in particular extreme events (Frei et al. 2003, Kendon et al. 2012, Rummukainen 2010). Hence, compared to GCMs, RCMs have great potential to improve the representation of the SASM as well as the Himalayan climate. Furthermore, at higher resolution increasing number of processes can be explicitly

resolved and there is evidence that explicitly resolving, rather than parameterizing nonlinear processes may improve the fidelity of models (Hack et al. 2006) as has been demonstrated in convection permitting RCMs at kilometre-scale (Kendon et al. 2012).

Statistical downscaling is another option available for site specific downscaling of coarse resolution GCM outputs, which involves identifying statistically robust relationships between large scale climate variables (e.g., the mean sea level pressure field) and local variable of interest such as temperature and precipitation (Rummukainen 2010), and using those relationships for future projection based on the GCM future scenario. There is an array of specific methods for this but the main limitation of the statistical downscaling technique is that it assumes stationary relationship between the predictor and predictand, which might not hold in future.

Climate model's skill in simulating the Himalayan climate is briefly presented next. But as described above, summer monsoon is the most important season in South Asia and the monsoon system has macro level control on the hydro climate of the region. Hence, any study of the regional climate, such as over the Himalaya, should necessarily involve study of the monsoon as well. So, the review also makes assessment of performance of climate model in SASM simulation.

1.4 Brief review of previous work on climate modelling over South Asia and the Himalaya

1.4.1 GCM simulations

As mentioned above, GCMs are too coarse to represent the Himalayan climate, so they have not been used for such purpose. However, GCMs are able to reasonably well

capture the broad-scale features of the summer monsoon circulation such as establishment of the trough of low pressure along the Indo-Gangetic plain (IGP), the cross-equatorial flow from the Southern Hemisphere across the east African coast, low level wind flow over South Asia (Kripalani et al. 2007). They are also able to simulate the massive Tibetan anticyclone dominated upper level flow (Stowasser et al. 2009) and three intense rainfall or deep convection centres (Viz. Indian monsoon, Western North Pacific monsoon and Equatorial Indian Ocean) of the Asian summer monsoon (Annamalai et al. 2007a). However, they have deficiencies in reproducing important aspects of the regional distribution of the monsoon precipitation, partly due to their coarse resolution (Rajendran et al. 2013). This is because SASM precipitation involves fine scale processes of interaction between the large-scale monsoon circulation and local complex terrain, heterogeneous land surface. Nevertheless, gradual improvements have been made with recent models. For example, Sperber et al. (2013) found that GCMs participating in Coupled Model Intercomparison Project-5 (CMIP5) has overall better performance than those from Coupled Model Intercomparison Project-3 (CMIP3) in simulation of various characteristics of late twentieth century Asian summer monsoon.

Recent studies show that very high resolution GCMs show marked improvement in simulation of SASM precipitation. From evaluation of atmosphere only GCM (AGCM) simulations at different horizontal resolutions of 20, 60, 120 and 180 km, Rajendran et al. (2013) found marked skill of very high resolution (20 km) AGCM in capturing spatial pattern of monsoon seasonal mean precipitation and its frequency distribution, where as coarser resolution simulations fail to capture the observerved characteristics of monsoon precipitation and its spatial heterogeneity. Similarly, the very high resolution GCM is also able to capture the observed contrasting trend in precipitation over

different regions and projects future heterogeneous change in mean precipitation over India with increase in some region but decrease in others (Rajendran and Kitoh 2008). This is in sharp contrast to the coarser GCM projections that fail to capture the observed characteristics of monsoon precipitation such as its spatial heterogeneity, and the projections that depict a rather uniform change in future. This is an indication that monsoon rainfall is strongly controlled by parameterized physics and high-resolution processes, which need to be resolved with adequately high resolution (Rajendran and Kitoh 2008). Furthermore, high resolution GCMs project substantial, spatially heterogeneous increase in both extreme hot and heavy rainfall events in future. Sabin et al. (2013) also found similar improvements in a variable resolution AGCM simulation with zooming over India (~35 km) compared to that with uniform 1° X 1° grid, such as improved representation of the southwesterly monsoon flow, realistic monsoon trough together with large improvements in representation of associated precipitation and circulation features. Hence, the benefit of using high resolution models in simulation of the SASM is evident.

1.4.2 RCM simulations

RCMs are being used extensively in the study of climate over all regions of the globe. Over the South Asian domain, RCMs have mostly been used for simulation of the SASM (e.g., Ashfaq et al. 2009, Dash et al. 2013) highlighting the importance of the monsoon in the region, where they were typically run at horizontal resolution of about 50 km. Those studies show that compared to GCMs, RCMs have better skill in reproducing a number of important features of the summer monsoon dynamics, including the monsoon trough (Kumar et al. 2006), low level flow patterns (Pal et al. 2007), atmospheric circulation (Polanski et al. 2010), the seasonal structure of the

meridional tropospheric temperature gradient, local Hadley circulation and easterly vertical shear) (e.g., Ashfaq et al. 2009, Saeed et al. 2012). However, recent RCM simulations are not necessarily more accurate than the driving data in simulating these large scale features (e.g., Dobler and Ahrens 2010), which is likely due to the contraints imposed by realism of large scale flows from GCMs. Even in better RCMs, there are departures from the observed large scale circulation patterns, such as weaker upper-level easterly flow, stronger westerly flow, weaker easterly vertical shear (e.g., Ashfaq et al. 2009, Saeed et al. 2012).

Assessment of monsoon rainfall climatology and the variability shows that RCM simulations are generally in better agreement with observations and can deliver added value compared to coarser driving data sets (e.g., Polanski et al. 2010). For example, Kumar et al. (2006) found that the most notable advantage of using a RCM is a more realistic representation of the spatial patterns of summer monsoon rainfall such as the maximum along the windward side of the Western Ghats. Pal et al. (2007) noted that a RCM fairly well simulated the observed precipitation patterns, including the locations of high precipitation areas such as the Western Ghats, east central India, Nepali upslopes, and Indo-China Peninsula coastal areas. They attributed this improvement to spatial resolution and the model physics. Apart from rainfall pattern, RCMs are also able to improve other aspects such as capture the timing of monsoon onset, the correlation between local Hadley circulation and rainfall (e.g., Ashfaq et al. 2009, Saeed et al. 2012).

RCM studies that focus on the Himalaya are rare. As stated above, most of the RCM based evaluation and projection studies over South Asia have been focused on the SASM. In addition, the majority of those studies focused geographically on India (e.g.,

Kumar et al. 2011b, Kumar et al. 2006). Although, some visual inferences about the Himalayan climate could be made by inspecting maps plotted in such studies, many of those studies simply blank out regions outside India (e.g., Kumar et al. 2011b). Nevertheless, some RCM based studies focusing on the Himalaya have been undertaken in the last decade. For instance, climate scenarios for the central Himalaya were developed under the APN CAPaBLE program[1]. A scientific and socio-economic study[2] gave a glimpse of future climate projections for the central Himalaya using GCMs and RCMs. Akhtar et al. (2008) used an RCM to develop climate change scenarios for the western Himalaya and applied those in hydrological models to investigate impacts on water resources. There are also few studies on weather and climate over the western Himalaya (e.g., Dimri 2004, Dimri and Mohanty 2009, Dimri 2013). Yadav et al. (2010) developed climate change scenarios for Northwest India winter season using a RCM and a high resolution GCM. It can be inferred from most of those studies that RCMs at 25-50 km resolution do not adequately resolve the Himalayan climate so as to be relevant for planning adaptation, mitigation and disaster reduction at local scale, which indicates the need of RCM simulations at even higher resolutions. This is because important processes and topographic features in the Himalaya are not properly resolved at those intermediate resolutions.

[1] Karmacharya et al. (2007) Climate Change Scenario for Nepal based on Regional Climate Model RegCM3 (unpublished technical report synthesized in "Final Report for APN CAPaBLE Project: 2005-CRP1CMY-Khan" available at www.apn-gcr.org/resources/archive/files/ae45cb3f153b3a2b082ae980ec90eb46.pdf)

[2] NCVST (2009) Vulnerability Through the Eyes of Vulnerable: Climate Change Induced Uncertainties and Nepal's Development Predicaments, Institute for Social and Environmental Transition-Nepal (ISET-N, Kathmandu) and Institute for Social and Environmental Transition (ISET, Boulder, Colorado) for Nepal Climate
Vulnerability Study Team (NCVST) Kathmandu. (available at www.i-s-e-t.org/images/pdfs/Climate%20Scenarios%20Report%20%28High%29_10%20November%2009.pdf)

1.5 Need of high resolution RCM simulation for projection of the Himalayan climate/SASM

Nepal, located along the central Himalaya and its foothills, is a land of complex topography with steep slopes and deep valleys. This topographic heterogeneity has a strong control on local climate. For instance, precipitation patterns in the Tropical Rainfall Measuring Mission (TRMM) show large variations over spatial scales in the order of a few kilometres with strong topographic control (Anders et al. 2006) such as up to 5 fold differences in mean precipitation between major valleys and their adjacent ridges. But representations of topography in GCMs and even intermediate resolution RCMs are much smoother. As a result such model simulations lack sufficient local detail even when they are able to capture the large scale regional features.

For various purposes, for instance adaptation, mitigation and disaster management etc., climatic information is increasingly being sought at finer spatial and temporal details as consideration of fine scale processes is critical for accurate assessment of local and regional scale vulnerability to climate change (e.g., Rajendran and Kitoh 2008). For example, such information is needed to run impact assessment models (Berg et al. 2013), some of which operate at resolution of hundreds of meters or even less.

Obviously, representation of the complex topography improves with increasing model resolution. It is also expected that higher resolution model simulations have enhanced skill to capture the spatial heterogeneity of the climate, their variability and extremes. However, simply increasing the horizontal resolution does not necessarily lead to improved climate simulation unless the model physics is configured to operate at such resolution via tuning the model (Rauscher et al. 2010).

RCMs are increasingly being run at resolution of 10-12 km or even less, at convective resolving resolution of 1-4 km, for simulation over various regions with mostly, but not always, improved representation of the climate. Model performances are found to be sensitive to the season, geographic region etc. (e.g., Chan et al. 2012, Iorio et al. 2004, Rauscher et al. 2010). Over South Asia, very high resolution AGCMs (20-35 km) have shown great improvements in simulation of the SASM compared to coarser GCMs. But studies employing very high resolution RCMs (~12 km resolution or less) are generally lacking. Though a few studies employed spatial resolution of 25 km or higher, they did not focus on the added value aspect of the higher resolution simulation. Hence there is a need to explore the added value of high resolution RCM simulation over the region focusing on key regional and local climatic processes.

1.6 Observational datasets and associated uncertainty

Traditionally, observations are made at point locations using an array of station network and it is anticipated that they provide fair representation of climatic condition of the whole region. But it is worth noting that dense and uniform station network is required to capture spatial heterogeneity of climate with sufficient details, especially for fine scale variables such as precipitation. However, it is challenging to establish and maintain such network and virtually impossible to do so in hostile environments like the Himalaya, where, ironically, greatest microclimatic variability possibly prevails due to strong orographic control on near surface climate.

It is also challenging to continuously maintain the standard of an observatory for an extended period of time. Hence, it is not uncommon to find a few missing and/or erroneous data in long time series. Such discontinuity could also make the time series

temporally inhomogeneous, however filling missing data is quite challenging. Though several techniques exist for the purpose, none of them could exactly match with the missing observation. In any case, use of different techniques introduces a layer of uncertainty. Furthermore, while there are statistical means (e.g. homogeneity test) to check the data integrity, it is not easy to deal with time series that fail quality control procedures. In addition, despite best efforts, errors could creep in observation made at station itself due to several factors. For example, Frei et al. (2003) noted that precipitation measurements at high alpine sites generally inherits considerable uncertainty emerging from a systematic measurement bias, mainly caused by wind field deformation and deflection of hydrometeors over the rain gauge opening resulting in large undercatchment of precipitation. Similarly, Andermann et al. (2011) found that datasets vary significantly along the Himalayan orographic front but are more consistent toward the adjacent flatter regions.

Despite these uncertainties, observations are the "best guess" of the ground truth available for assessing model skills in simulating current climate. However, there is a mismatch of scale between point station observations and the areal average output of climate models (Chen and Knutson 2008). For this reason gridded datasets are generally sought for model assessments. However, observed gridded datasets are also affected by uncertainty (Haslinger et al. 2013).

One common approach used to generate gridded datasets is to interpolate point observation made at different locations. Several interpolation or gridding techniques exist for this purpose. But different techniques have their own merits and limitations. However, some are better suited for particular variable that the others. But the use of different technique potentially introduces uncertainty in the gridded datasets as they would differ from each other even when they have same undelaying point datasets

(Hofstra et al. 2008). Quality of gridded datasets is also affected by the spatial distribution of the undelaying station network. High quality gridded datasets can be generated from dense and uniformly distributed station network, which well captures spatial heterogeneity of the climatic variable. But gridded datasets developed from unevenly distributed stations and/or spare station network has detrimental impact in resultant grid point average estimates, especially by changes in variance (Hofstra et al. 2010). For example Hofstran et al. (2010) noted that if fewer stations were used for interpolations, both precipitation and temperature are over-smoothed, leading to a strong tendency for interpolated daily values to be reduced relative to the "true" area average. Furthermore, extremes are affected more than the means, especially for variables with large spatio-temporal variability like precipitation in mountainous regions (Haslinger et al. 2013). These aspects are also relevant for temperature even though they are generally less affected compared to precipitation (Hofstra et al. 2009). However, in mountainous terrain, temperature can depict a very complex vertical structure even in narrow space leading to an additional uncertainty in the gridded data (Daly 2006).

Another dilemma encountered in developing gridded dataset is decide whether to use data from all the available stations, many of which might only span for shorter durations than the whole time period of the dataset being developed, or use only those stations that covers the entire period. The first approach generates gridded dataset with detail spatial variations but this comes at the cost of the dataset being temporarily inhomogeneous (Huffman et al. 2009). As fixed stations, which spans over entire duration, are used in the second approach temporal homogeneity is ensure but the resulting dataset likely miss out many spatial details due to sparser station density.

In recent decades, gridded datasets has also been developed from entirely new class of observation, namely satellite observations using remote sensing technology. As the observation is made from orbiting satellite using remote sensing technology, they provide a snap shot of environmental/meteorological condition over an extended area and hence the observation, by default, is two dimensional (gridded). Also depending on resolution of the sensor they can provide information at very high resolutions. However, there are some limitations in satellite generated gridded datasets as well.

Firstly, remote sensing techniques themselves may have limitations in making accurate estimates of the field being monitored (e.g. precipitation rate) in a diverse climatic conditions. For example, remote sensors cannot determine accurately snowfall which is the major contribution at high elevation. Hence, remote measurements often underestimate precipitation rate at high elevation, where they mainly fall as snow or light drizzle and during short intense storms (Andermann et al. 2011). Consequently, even though TRMM – 3B42 has provided good measurements of precipitation patterns over various parts of globe, it underestimate precipitation in mountainous regions, especially where high snowfall contribution has been reported (Kamal-Heikman et al. 2007). Similarly, main source of uncertainty in precipitation estimates made by remotely sensing cloud top temperature using Infrared sensors resides in the calibration of the cloud top temperature to estimate precipitation (Huffman et al. 2007).

In addition, satellite records often need to be calibrated and validated against the ground observations. However this could introduce error over the regions where the ground observation is sparse or are of poor quality. For example, most of the rain gauges used to calibrate satellite precipitation estimates are derived from the Global Telecommunication System (GTS) with reportedly poor spatial coverage in the Himalaya (Yatagai and Kawamoto 2008), which might partly explain their

underestimation of precipitation. Additionally, Yatagai and Kawamoto (2008) reported that the GTS database includes erroneous entries in the Himalayan region, where 0 mm precipitation values were reported instead of missing values, thus contributing to precipitation underestimation. Also, for fine scale variable such as precipitation, a single rain gauge does not capture variability at the scale of kilometres seen in complex terrain such as the Himalaya; consequently caution should be exercised while using sparsely distributed station data to calibrate corresponding remotely sensed pixel values (Andermann et al. 2011).

Lastly, many remote sensed datasets are generally derived from multiple sensors which have an irregular return interval and therefore, likely miss major events (e.g. precipitation events) (Huffman et al. 2007). Consequently, such estimates often underestimate cumulative values when compared against ground observations.

In summary, various sources of uncertainties inherent in observational datasets are described in the section. This is to highlight the need to exercise caution in treating single dataset as the "truth" while assessing model performance against them and to promote use of multiple observations for the same purpose.

1.7 Aims and objectives and structure of the thesis

The overall aim and objective of this thesis is to test the hypothesis that high resolution (~12 km) regional climate modelling provides improved representation of the SASM, both regionally and over the Himalaya. This is achieved through the assessment of the added value of high resolution simulation of SASM focusing on the Indian peninsula and the Himalaya region.

The investigation is arranged into three main sections. The first section is an assessment of the strength and stability of the temporal relationships between monsoon rainfall indices (MRIs) and the large-scale monsoon circulation indices (MCIs), as a precursor to employ such indices for model evaluation. In the second section of the thesis, the sensitivity of RCM simulation to domain size in SASM simulation is investigated. The final section evaluates the added value of high resolution simulation of SASM by comparing a coarse and high resolution RCM simulation run over an optimal domain identified in Chapter 4.

The thesis is structured as follows: **Chapter 2** reviews the literature to-date of relevance to the simulation of the SASM in contemporary climate models, the sensitivity of RCM simulation to domain size, and horizontal resolution. Areas requiring further research are identified, and the specific research objectives for this work are specified in the light of these findings.

Chapter 3 investigates the evolution of relationship between monsoon rainfall indices and monsoon circulation indices at interdecadal time scale to assess their potential use as benchmark metrics for model evaluation in simulating SASM.

Chapter 4 evaluates the sensitivity of RCM simulation of SASM to domain size. A climate model is run in global and regional configuration to identify the nature of the systematic error in SASM simulation and interaction of different elements of bias so as to identify an appropriate domain for SASM simulation.

Chapter 5 evaluates the added value of high resolution RCM simulation of SASM climatology when run over an identical domain and forced by realistic lateral boundary. RCM simulations are performed at 0.44° and 0.11° horizontal resolutions (i.e.

approximately 50 and 12 km resolution respectively) over an optimal domain identified in chapter 4.

Chapter 6 assesses the added value of high resolution RCM simulation of intraseasonal variability of the SASM. This involves analysis of same pair of simulations employed in Chapter 5.

Conclusions and recommendations for further research are presented in **Chapter 7.**

1.8 Notes on the thesis format

The thesis follows the "paper route". The substantive research chapters are academic papers, as submitted to, or published in, peer reviewed journals. Four first authored papers are included as required by the regulations. These papers present a coherent set of research, investigating the sensitivity of RCM simulation of SASM to domain size and horizontal resolution. At the time of writing, one paper has been published and three submitted, as follows:

Published

Karmacharya J, Levine RC, Jones R, Moufouma-Okia W, New M (2015) Sensitivity of systematic biases in South Asian summer monsoon simulations to regional climate model domain size and implications for downscaled regional process studies. Clim Dyn 45:213-231. doi: 10.1007/s00382-015-2565-6

Submitted

Karmacharya J, New M and Jones R (2015) Contrasting temporal relationships between zonal and meridional wind based monsoon circulation indices and South Asian summer monsoon rainfall.

Submitted to: Geophysical Research Letters

Karmacharya J, Jones R, Moufouma-Okia W and New M (2015) Evaluation of the added value of a high-resolution regional climate model simulation of the South Asian summer monsoon climatology.

Submitted to: International Journal of Climatology

Karmacharya J, New M and Jones R (2015) Added value of a high resolution regional climate model in simulation of intraseasonal variability of the South Asian summer monsoon.

Submitted to: International Journal of Climatology

The text, figures and tables in each paper are same as those in the papers listed above. The references to figures and citations have been standardized to provide a coherent format throughout the thesis and the references have been summarized into a single list at the end of the thesis. Supplementary information for each article has been included in the thesis at the end of the relevant chapter, and it is referred to with prefix S (e.g. Table 1.S1, Fig. 1.S1 etc.).

2 Literature review

2.1 Introduction

Some of the issues surrounding the skilful simulation of SASM and its evaluation have been described in Chapter 1. In this literature review, these issues are explored in greater detail through critical appraisal of the existing literature, which reveals key research gaps.

Section 2.2 makes the case for rapid model appraisal using concise metrics. Required attributes of such metrics are discussed and suitability of various indices, such as monsoon precipitation and monsoon circulation indices, as rapid appraisal metrics, are investigated.

Section 2.3 briefly reviews the performance of climate models in simulating SASM with a focus on precipitation.

Section 2.4 addresses the issue of sensitivity of regional climate model simulation of SASM to domain size and location.

Section 2.5 investigates the issue of added value in high resolution simulations. Various methods used to investigate added value are discussed. Literature on the added value of SASM simulation is explored with a focus on the precipitation.

Finally, section 2.6 summarises the findings of the review, and identifies the gaps addressed in the thesis.

2.2 Rapid appraisal of climate model simulations

2.2.1 Need of rapid appraisal

Recent years have seen consolidated efforts on simulating global and regional climate from a host of global and regional climate models respectively, by various modelling centres, which could be directly compared with each other (e.g., Giorgi et al. 2009). They come under the auspices of CMIP for global models and under the auspices of COordinated Regional climate Downscaling EXperiment (CORDEX) for regional modelling and statistical downscaling. This is done primarily to intercompare model performance for present climate over various regions as well as to get an estimate of uncertainty in the future projections. Most of these model outputs are freely available and many of these simulations have multiple realizations. It provides the scientific community unprecedented opportunity to utilize an array of model outputs in evaluation of model performance over their areas of interest as well as for further downscaling. However, it poses also a challenge as the researches have only a finite amount of resources for model evaluation, or further downscaling. Hence, the first step in model evaluation study, which considers a number of similar models, generally involves a rapid evaluation of the model outputs so as to segregate satisfactory models from the poor ones. Once well performing models have been identified, further analysis or downscaling could be limited to only those models or its subset there by saving time or allowing for more in depth analysis (e.g., McSweeney et al. 2012). However, it should be noted that realistic simulation of a model for present climate does not guarantee its skill for future climate although it gives some confidence in those models (at least compared to those models that have poor skill to simulate present climate)

For example, Cook and Vizy (2006) used the circulation characteristics and physical processes of a “rainfall dipole” variability mode as assessment criteria to identify CMIP3 GCMs that simulate the climatology and a prominent mode of variability of the West African monsoon well. Based on the assessment, they selected only three, out of the 18 GCMs considered, for future climate projection. Kim et al. (2013) selected three best performing CMIP5 GCMs (out of 15) based on their ability to represent the global climatological mean interdiurnal variability of surface variables (e.g. maximum and minimum temperature, wind speed and precipitation) for present climate condition. Cook et al. (2008) chose GCMs (8 out of 18 CMIP3 GCMs) over Midwest America based on their ability to produce realistic representations of the low level meridional flow during June-July and used only those for a climate change impact assessment. They cross evaluated the selected models using other criteria such as horizontal wind vectors and geopotential heights and found them reasonable. In general, application of the large space scale dynamic fields that are resolved well in GCMs is preferred for their evaluation than using precipitation based criteria, which are more difficult to simulate.

2.2.2 Potential rapid appraisal metrics on monsoon simulation

The metrics used for rapid evaluation would generally be specific to the region / climate system as model performance varies from region to region, or even season to season within a region. So, it is seldom possible to know beforehand a given model’s performance over an area of interest without an assessment of its performance. In this context, use of concise and meaningful indices to characterize monsoon and its variability not only facilitate objective assessment of climate model skill in simulating

monsoon, but it can also assist empirical studies on the relationship between the monsoon and drivers of its variability (Wang and Fan 1999).

Use of indices (that give numeric values) rather than spatial maps for model evaluation has the advantage that results can be presented concisely (in tabular form) and evaluated in an objective manner (e.g. by considering the deviation from the observed values). These indices are derived from a simple or elaborate computation using various metrics/ statistics. For a rapid assessment it is sufficient to compute seasonal mean values of such indices and then compare the observed and simulated interannual time series.

2.2.2.1 Existing indices for assessment of model simulation of the SASM

The following table provides a brief summary of indices used to quantify various characteristics of SASM. They can also be used for model evaluation. Only those indices are considered which can be aggregated for the whole season reflecting the behaviour of SASM at the seasonal scale as the aim here is to make rapid assessment of model skill in capturing SASM at the fundamental but computationally easiest level. So, indices such as mid atmospheric (200-600 hpa average) temperature difference between a north area (15°-35° N, 40°-110° E) and a southern area (10° S-15° N,40°-110° E), which is used to derive the monsoon onset (e.g., Goswami et al. 2006b) is not considered.

Table 2.1 Indices describing various characteristics of monsoon.

Name	Definition	Reference
Rainfall		
All India monsoon rainfall (AIMR)	Monsoon mean rainfall derived from All-India rainfall monthly rainfall time series developed by IITM	Parthasarathy et al. (1994)
Indian summer monsoon rainfall (ISMR)	Monsoon mean rainfall averaged over 70°–90° E, 5°–25° N (land points only)	Parthasarathy et al. (1992)
Extended Indian monsoon rainfall (EIMR)	Monsoon mean rainfall averaged over 70°–110° E, 10°–30° N (both land and ocean)	Goswami et al. (1999)
Circulation		
Monsoon Hadley circulation index (MHI)	Monsoon mean meridional wind shear at lower tropospheric level (LTL) (850 hpa) and upper tropospheric level (UTL) (200 hpa), averaged over 70° –110° E, 10°–30° N	Goswami et al. (1999), Lau et al. (2000)
Webster and Yang index (WYI)	Monsoon mean zonal wind shear at LTL and UTL, averaged over 40°–110° E, 0°–20° N	Webster and Yang (1992)
Modified WYI	As WYI but at upper level average of 150 and 100 hpa is considered	Chen et al. (2007)
Westerly shear index (WSI)	Monsoon mean zonal wind shear at LTL and UTL averaged over 40°–80° E, 5°–20° N	Wang and Fan (1999)
Indian monsoon index (IMI)	Difference in monsoon mean LTL zonal wind averaged over 40°–80° E, 5°–15° N and 70°–90° E, 20°–30° N	Wang et al. (2001)
Southerly shear index (SSI)	Monsoon mean meridional wind shear at LTL and UTL, averaged over combined regions of 85°-100° E, 15°–30° N and 40°-55° E, 10° S–0° N	Wang and Fan (1999)

Others		
Temperature gradient	Temperature difference between Indian landmass (27.5°–17.5° N and 72.5°–82.5° E and i) Arabian Sea (10°–20° N and 60°–70° E), ii) Bay of Bengal (10°–20° N and 85°–95° E) from 100 to 1000 hpa.	Bawiskar (2009)
	Seasonally averaged mid atmospheric temperature difference between a north area (15°-35° N, 40°-110° E) and a southern area (10° S-15° N,40°-110° E)	Dobler and Ahrens (2010)
Outgoing longwave radiation	Averaged over 10-25° N and 70-100° E	Wang and Fan (1999)
Integrative monsoon index	Leading principal component series of the multivariate dataset constituted by analysis on three fields – Sea level pressure, zonal wind shear, and meridional wind shear over the region 40°-105° E, 0°-60° N	Fan et al. (2009)
Vorticity circulation index	Difference of 850 hpa zonal wind averaged over 5°-15° N, 40°-80° E from that averaged over 25°-35° N, 70°-90° E	Yim et al. (2013)

The following table presents a few monsoon indices defined for other regions.

Table 2.2 Monsoon indices over other regions.

Region	Description	Reference
East Asian summer monsoon	Differences of sea level pressure	Chen et al. (2007) and the reference in there
	East Asian land-sea thermal contrast index: land-sea temperature contrasts between the east and west and between the north and south	Chen et al. (2007) and the reference in there
	Zonal wind shear	Lau et al. (2000)
	Combined differences of the sea level pressure between east and west and the zonal wind shear between the upper and lower troposphere in the low latitude	Chen et al. (2007) and the reference in there
	Zonal wind difference between the tropics and subtropics in East Asia	Chen et al. (2007) and the reference in there
South China Sea summer monsoon	Divergence differences between the upper and lower troposphere	Chen et al. (2007) and the reference in there
Defined for seven tropical monsoon regions including South Asia	Vorticity circulation index	Yim et al. (2013)
Australian summer monsoon index	850 hpa zonal wind averaged over 100°-150° E, 15°-5° S	Zhang and Zhang (2010)

There are many other indices associated with a particular phase of monsoon, such as onset and retreat of monsoon (e.g., Xavier et al. 2007 and the references there in), intraseasonal variability of monsoon (e.g., Xavier et al. 2010). However, as mentioned above, they are not considered here as the aim of the rapid assessment is to distinguish models that have realistic representation of monsoon at the seasonal mean scale (i.e. overall monsoon) and involves only simple computations,

Apart from consideration of the above indices for rapid model assessment, it is also important to evaluate model fidelity in simulating the large scale modes of variability that affect the monsoon – such as India Ocean dipole (IOD, Ashok et al. 2001, Saji et al. 1999), ENSO (Webster and Song Yang 1992) etc. while selecting GCMs for further downscaling (e.g., Annamalai et al. 2007a). This is because RCMs receive those teleconnection signals through the lateral boundary, so it is important that the driving models realistically simulate those features. Hence there is a need of assessment of this aspect as well. A further extension to this is assessment of the relationships, both contemporaneous and lagged, between the large scale modes of variability (e.g. IOD. ENSO) and the local monsoon indices (e.g. those based on precipitation or circulation).

The aim of the rapid model appraisal is to assess with minimal efforts, whether a given model has satisfactory skill in representing a given climate system of interest. So, the metric in question should be easy to compute. But at the same time it should well represent dynamics of the system and its variability. As an illustration, suitability of two common SASM indices as rapid model assessment metric in simulating SASM is examined below.

2.2.2.2 Monsoon rainfall indices

One of the best measures of strength of SASM and its variability is arguably provided by the regionally averaged MRIs such as the all India monsoon rainfall, and they are still used as a robust measure of the SASM (Turner and Annamalai 2012). Hence, at first glance, MRIs appears to be an appropriate index to be used as a rapid model evaluation metric. However, precipitation is a synthesis variable that is the sum of numerous processes within a climate model (Rauscher et al. 2010). So, good simulation of precipitation is notoriously difficult to achieve as this requires accurate simulation of many other processes. In agreement with this, McSweeney (2007, page no. 30) and Dia (2006) state that "*Precipitation is a particularly complex atmospheric process to model, relying on the accurate representation of difficult physical processes, including cloud micro-physics, cumulous convection, planetary boundary layer processes, and large-scale circulations*".

Also, the main issue preventing the use of MRIs as a rapid evaluation metric is the high sensitivity of the simulated precipitation to parameterization, particularly to the convection scheme. This is particularly true for tropical precipitation which is more convective in nature. Hence its reliable modelling heavily depends on realistic representation of the complex convective process (McSweeney 2007). But convection is very difficult to model reliably at coarse resolution as they are highly sensitive to parameterization of convection scheme (Kharin and Zwiers 2005, Scinocca and McFarlane 2004). So, it is not surprising that substantial differences in simulated monsoon precipitation could arise from different convection schemes (Srinivas et al. 2013). Hence, even though precipitation is one of the most widely studied variables in model simulation, it has significant limitations to be used as a metric for rapid model assessment.

2.2.2.3 Monsoon circulation indices

Large-scale MCIs are useful diagnostic tools for studying the SASM dynamics and its variability. A number of MCIs have been defined in order to study the monsoon system and its interannual variability (See Table 2.1). They can be computed readily by taking difference of areal average of upper level zonal or meridional wind at different levels or regions. In fact, MCIs have been used as model evaluation metrics in several recent studies of the SASM that utilize GCMs and RCMs (e.g., Ashfaq et al. 2009, Dobler and Ahrens 2010, Dobler and Ahrens 2011, Kumar et al. 2011a, Saeed et al. 2012, Saeed et al. 2011). Moreover, MCIs represent the large-scale and three dimensional structure of SASM system, so they should be less sensitive to the model parameterization, in particular to convection scheme. Hence, MCIs has the potential to qualify as a metric for rapid model appraisal for the SASM simulation.

However, thermodynamic energy arguments postulate weakening of the monsoon circulation with global warming (Held and Soden 2006, Vecchi et al. 2006). In fact, studies indicate that some aspects of the SASM circulation are already weakening in recent decades (Bawiskar 2009, Fan et al. 2009, Kulkarni 2012, Murugavel et al. 2012). As MCIs are reliant on the monsoon circulation, it raises questions whether and in what ways MCIs could still be used as good representative of monsoon dynamics in the future.

As MRIs are still taken as a robust measure of monsoon, the representativeness of MCIs as indicators of monsoon system can be gauged by comparing the MCI-MRI correlations over different periods. Though studies that define MCIs show relatively strong MCI-MRI correlations for different MRIs and MCIs, such studies evaluated the relationships only over a short period, typically from 1970s to early 1990s. However, a

weaker MCI-MRI relationship for few years in 1990s was noted by Wang and Fan (1999). Moreover, correlation between any two pair of variables generally exhibits low frequency variation (Gershunov et al. 2001); especially as the monsoon circulation is known to weaken in recent decades despite relatively stable MRIs, there is a need to investigate long term evolution of the MRI-MCI relationship. If such investigation reveals presence of persistent strong and relatively stable correlation between the two indices, then the correlation could also be used as an additional metric for rapid model assessment as it would have larger representativeness of the whole monsoon system.

2.3 Simulation of SASM in contemporary models

This section describes the skill of contemporary climate models in simulating SASM, mainly the precipitation. Prominent areas of model deficiencies are also highlighted.

2.3.1 GCM simulation of SASM

Substantial improvements have been made in performance of GCMs at the global and continental scales in recent decades, and they are able to simulate broad features of the current climate reasonably well. But they still have problem resolving many important small to medium scale processes resulting in systematic regional biases (Rajendran et al. 2013). For example, their depiction of regional and local atmospheric circulations (e.g. narrow jet cores, mesoscale convective systems, sea-breeze type circulations) and representation of processes at high frequency temporal scales (e.g. precipitation frequency and intensity, surface wind variability) are insufficient (Christensen et al. 2007). Similarly, their ability to reproduce the effects of mesoscale influences such as convective systems embedded in depressions, and the most intense and localised precipitation events may also be limited (Stowasser et al. 2009).

The SASM can be suitably described as a fully coupled ocean-land–atmosphere system, and hence it should be better reproduced by coupled atmosphere-ocean GCMs (AOGCMs, Webster et al. 1998). For example, in assessment of five GCMs, Martin et al. (2000) found that they simulate the SASM circulation reasonably well. Indeed, the broad-scale features of the monsoon circulation like establishment of the trough of low pressure along the Indo-Gangetic plains, the cross-equatorial flow from the Southern Hemisphere across the east African coast, and the low level wind flow over South Asia are reasonably well captured by the recent models (Kripalani et al. 2007). Similarly, GCMs are generally able to simulate the upper level flow dominated by massive Tibetan anticyclone (Stowasser et al. 2009), as well as three intense rainfall or deep convection centres (Viz. Indian monsoon, Western North Pacific monsoon and Equatorial Indian Ocean) of the Asian summer monsoon (Annamalai et al. 2007b).

However, climate models have had traditionally considerable difficulty simulating the characteristics of the SASM precipitation (Webster et al. 1998). Even the simulation of monsoon precipitation climatological distribution has proven to be rather difficult in current generation of models (Martin et al. 2000) and therefore provides a severe test of the climate models. They generally suffer from systematic wet bias over the equatorial Indian Ocean (EIO) (Oouchi et al. 2009) and dry bias over central India during the monsoon (Sperber et al. 2013). In fact, overestimation of precipitation over warm ocean and underestimation over land in tropical regions is a common problem in many climate models (Rockel and Geyer 2008). This is consistent with previous studies such as Kharin and Zwiers (2005) that reported relatively poor model skill in simulating rainfall in tropics compared to that in mid and high latitudes. They attributed this to larger fraction of convective rainfall in tropics, which are very difficult to model reliably. Likewise, GCMs are known to simulate excess precipitation over high and narrow

mountain ranges that stand perpendicular to main wind direction all over the globe (Rockel and Geyer 2008).

Some studies have shown that compared to AGCMs, AOGCMs perform marginally better in simulating monsoon rainfall (Kumar et al. 2006). However, Rajendran et al. (2013) showed that a super high resolution AGCM (~20 km), that employ suitable physics schemes, is also able to realistically simulate SASM precipitation, including finer spatial scales, which even the highest resolution AOGCM participating in CMIP3 failed to achieve.

Further, simulation of the mean monsoon by the GCMs participating in CMIP3 is diverse. For example, Annamalai et al. (2007b) found that, of the 18 GCMs considered; only six could reproduce monsoon precipitation climatology with some fidelity. Of these only four GCMs exhibit a robust ENSO–monsoon contemporaneous teleconnection, including the known inverse relationship between ENSO and rainfall variations over India. While there have been some improvements in CMIP5 model compared to CMIP3 models, many of the systematic model biases in the mean climate in CMIP3 are present also in the CMIP5 models. For example, Sperber et al. (2013) evaluated the late twentieth Century simulation of Asian summer monsoon in CMIP5 and CMIP3 models using diagnostics and skill metrics to assess the climatology, annual cycle, intra- and inter- seasonal variability. They noticed some progress in modelling these aspects of the monsoon. For example, the CMIP5 multi-model mean is more skilful than the CMIP3 multi-model mean for all diagnostics in terms of the skill of simulating pattern correlations with the observations, but no single model stands out as the best performer and significant biases still persist.

Irrespective of the skill of GCMs in simulating SASM, their coarse resolution imply that they cannot be expected to capture the fine scale feature of precipitation such as orography induced heavy precipitation bands along the Western Ghats, the Himalaya and Myanmar coast. Nor can they capture the meso scale and finer phenomenon leading to extreme events such as precipitation extremes, which results in whole intensity distribution of precipitation being shifted to lower intensity values.

2.3.2 RCM simulation of SASM

RCMs have been widely used for dynamical downscaling over various parts of the globe, including South Asia. Some of those studies over South Asia focused on validation of RCMs under present climate (e.g., Dobler and Ahrens 2010, Philippe et al. 2011, Polanski et al. 2010, Saeed et al. 2012), while others tested the linkage of SASM with other climatic forcings such as Eurasian snow cover (e.g., Shekhar and Dash 2005). Yet others made future projection of the SASM (Ashfaq et al. 2009, Kumar et al. 2011a, Kumar et al. 2011b, Kumar et al. 2006, Syed et al. 2014).

RCMs generally have relatively better skill in reproducing a number of important features of the SASM dynamics compared to GCMs. A number of studies show RCMs have better skill than GCMs in simulating various component of SASM dynamics such as monsoon trough (Kumar et al. 2006), low level flow patterns (Pal et al. 2007), atmospheric circulation and its variability (Polanski et al. 2010), the seasonal structure of the meridional tropospheric temperature gradient, local Hadley circulation and easterly vertical shear (e.g., Ashfaq et al. 2009, Saeed et al. 2012). But not all recent RCM simulations are necessarily more accurate than the driving data in simulating these large-scale features. For example, Dobler and Ahrens (2010) obtained mixed result in a study on representation of SASM in an RCM. They found RCM driven by

reanalysis does not better simulate large-scale indices such as vertical wind shear indices and outgoing longwave indices compared to reanalysis. However, the RCM when forced by a GCM showed improvement in simulating those aspects relative to driving GCM. Based on the study, they concluded that the transfer of an RCM to different regions is not trivial, rather it needs severe testing before application. Furthermore, even in better simulating RCMs, there are departures from observed features such as weaker upper-level easterly flow, stronger westerly flow, weaker easterly vertical shear etc. (e.g., Ashfaq et al. 2009, Saeed et al. 2012).

Overall, RCM simulated SASM rainfall climatology and its variability is in better agreement with observation. For example, Pal et al. (2007) noted that RegCM3 fairly well simulate observed precipitation patterns with correct locations of high precipitation areas such as the Western Ghats, east central India, Nepal upslopes, and Indo-China Peninsula coastal areas. They attributed this improvement to spatial resolution and the model physics. Similarly, Kumar et al. (2006) have found that the most notable advantage of PRECIS simulation is more realistic representation of the spatial patterns of summer monsoon rainfall such as the maximum along the windward side of the Western Ghats. Kumar et al. (2011b) shows that PRECIS, driven by HadCM3, also has reasonable skill in simulating the monsoon climate over India. Furthermore, Polanski et al. (2010) have found HIRHAM simulated precipitation is in better agreement with high resolution observation over central India, the Himalayas and Tibet compared to ERA40.

However, there is still considerable spread in the RCM simulation of the SASM precipitation. For example, Philippe et al. (2011) have found that though RCMs are generally able to capture the spatial pattern of monsoon precipitation, their amounts and the regional distribution differs substantially among the four RCMs compared. This

spread indicates that important feedbacks and processes are poor, or not adequately, taken into account in the RCMs. Similarly, Dobler and Ahrens (2010) noted large biases in the spatial distribution of precipitation. As for GCMs, convection scheme is one of the key sources of variability in RCM simulated spatio-temporal pattern of the SASM precipitation (Srinivas et al. 2013).

However, in general, along with improved distribution of seasonal mean precipitation, RCMs are generally able to better simulate several other characteristics of SASM precipitation such as the timing of monsoon onset (Philippe et al. 2011), the meridional propagation of precipitation (Philippe et al. 2011), the correlation between local Hadley circulation and rainfall (e.g., Ashfaq et al. 2009, Saeed et al. 2012), though monsoon withdrawal is not well simulated (Philippe et al. 2011).

Furthermore, RCMs ability to capture various aspects of SASM other than precipitation has been showcased in several studies. For example, Dash et al. (2013) have found that the interannual characteristics of both the rainfall and temperature extremes simulated by RegCM3 in Central India are well in phase with those observed. Polanski et al. (2010) have also found HIRHAM is able to simulate SASM temperature climatology and its variability.

Other improvements in high resolution simulation of SASM are discussed later but the sensitivity of RCM simulation of SASM to domain size and location of the boundary is described next.

2.4 Sensitivity of the RCM simulation to domain setup

The most common approach in dynamical downscaling is to use the one way nesting technique in which RCM receives the meteorological field from the coarse resolution

(GCM or reanalysis) driving data at its lateral boundaries at regular intervals. Based on that information, the RCM generates its own simulation within the domain while maintaining consistency with the driving field at the lateral boundary. RCMs, being limited area models, have some specific constraints associated with them, which do not affect GCMs. Dependency of the RCM simulation to the quality of the driving data is a concern. Irrespective of the quality of the RCM, good output cannot be expected unless driven by good quality driving data (Giorgi and Mearns 1999). This is why assessment of driving model is important as noted earlier. Still, this adds another level of uncertainty as RCM output could vary with the use of different driving data as input.

Also, a number of techiques has evolved for feeding the large scale driving fields to RCMs. While the traditional approach is to carry out contious integration of RCMs with a single initialization of the atmospheric fields and frequent updates of lateral boundary conditions (LBCs) from the global field, some of the recent techniques employ - consecutive integrations with frequent reinitialization, grid point nudging etc. Sensitivity studies show that use of these different techniques lead to different downscaled outputs (e.g., Lo et al. 2008), introducing another layer of uncertainity associated the choice of 'nudging' technique.

Another limitation specific to RCM, is its sensitivity to the domain size and location of the boundary. This has been focus of many studies, mainly over the mid latitude domains. The control exerted by the LBCs on nested simulations increases as the size of the domain is reduced. The large-scale component of the simulation, which is forced by the LBC, influences the small-scale features that develop along the large-scale flow but they need adequate space and time to develop well, which could be hindered by small domain (Leduc et al. 2011). Jones et al. (1995) found improved performance of a RCM

simulation with larger domain. Based on their result, they have advised for selecting a domain that is large enough so that RCM is free to generate circulation within its domain, but not so large that the RCM integration diverges significantly from the large-scale features of the driving field. In partial agreement with this, Diaconescu and Laprise (2013) showed slight reduction in skill of RCM at reproducing the large scales with increasing domain size when driven by perfect LBC. However, they have found that RCM reduces some large-scale errors when driven by imperfect LBCs with very large domains. In contrast, Colin et al. (2010) have showed that RCM simulation of extreme precipitation events over Europe is relatively insensitive to domain size.

All the studies mentioned above were carried out over mid-latitude regions. But there are hardly any such studies over South Asia. In one such study, Bhaskaran et al. (1996) have noted that a Met Office RCM's (which is a predecessor of the RCM used in this study) simulation of SASM large-scale circulation, is relatively insensitive to the domain size. They attributed this to the inherent difference in climate regimes in mid-latitudes and tropics. Most of other RCM simulations over South Asia have been performed either over the domain used by Bhaskaran et al. (1996) (e.g., IITM studies), or domains selected in ad-hoc basis as done in other regions (Leduc et al. 2011). For example, very large domains are employed in CORDEX framework to minimize the number of domains and to promote maximum number of RCM simulation in each domain in order to facilitate comprehensive model intercomparison (Giorgi et al. 2009).

However, some recent studies indicate that RCM simulations over the tropical regions, particularly those related with precipitation are also sensitive to domain size. For example, Bhaskaran et al. (2012) have found that simulation of SASM seasonal mean hydrological cycle and daily precipitation variability at a sub domain is sensitive to the

domain size. Also, the need of careful selection of domain is highlighted by other studies over the tropics. For example, in a recent study Browne and Sylla (2012) noted the critical role of the size and location of the RCM domain in realistic simulation of the West African summer monsoon precipitation through their control on the inclusion of the main regional forcings within the domain. Hence, there is a need to revisit the issue of sensitivity of RCM SASM simulation to domain size. Identification of optimal domain for SASM simulation is of interest also for the following reasons:

i) Similar to other parts of the global, CORDEX simulations for South Asia have been run over a relatively large domain compared to many previous studies. Hence, unless the influence of the RCM simulation of the SASM is quantified, or insensitivity of the RCM simulation of SASM is re-established, it would be difficult to compare results from the CORDEX simulation with those from previous studies. In particular, it would be difficult to distinguish whether the differences in results in the previous studies from those in CORDEX simulation are solely due to improvement in model physics and parameterizations, or the size of the domain also plays a role.

ii) Secondly, RCM simulations are progressively being run at higher and higher resolutions. Over many regions they are now routinely run at resolution of 12 km or less. However, this involves additional costs. For example, doubling of horizontal resolution increases the computational cost by more than four times (e.g., Jones et al. 2004) and trebling of resolution costs about 20 times (Kusunoki et al. 2011) with comparable increase in storage and data processing costs. So, unless there are compelling reasons for performing high resolution RCM simulation using huge domain (such as CORDEX South Asia domain), it makes more sense to run those simulations in an optimal domain.

In addition, it was noted in section 2.3.1 that most of the GCMs still have problems simulating important features of the SASM, particularly those related with precipitation. In this connection, it is worth noting that RCM model physics are derived either by modifying the existing limited area model, or by implementing GCM physics in regional dynamical framework (Giorgi and Mearns 1999). So, an obvious question is: can an RCM, derived from GCM, depict good skill over the regions where its parent GCM shows poor skill? However, it might be possible to exploit the sensitivity of the RCM simulation to its domain (provided that exists) to identify suitable domains. But, this would require that parent model's inherent systematic errors over the region are largely forced by local processes but their key source regions lie at the periphery of the main area of interest.

2.5 Added value of high resolution simulation

Despite the great importance of identifying added value in RCM simulations, this has not received much attention until recently (Feser and von Storch 2005). But this is likely the single most important issue in regional climate modelling, which arises virtually in every RCM application (Giorgi 2014). However, it has received greater attention in recent years and has become the main subject of several studies (e.g., Kanamitsu and Dehaan 2011, Lee and Hong 2014, Racherla et al. 2012). For example, added value of RCM simulation has been assessed against the driving GCM or reanalysis (e.g., De Sales and Xue 2011, Winterfeldt and Weisse 2009) in recent years. Similarly, added value of high resolution RCM simulation has also been evaluated against the coarser RCM simulation (e.g., Sanchez-Gomez et al. 2009). Also, given the existing demand of computational resources from various aspects of climate model simulations such as generating multiple realizations, using more comprehensive physics, and longer

integrations, more studies are needed to evaluate the potential benefits of increased horizontal resolution (Pope and Stratton 2002).

2.5.1 The definition

According to Di Luca et al. (2012) added value of high resolution simulation refers to relative improvement in the RCM simulation relative to the driving fields. But, this definition can be extended to include other types of experiments that involve evaluation of high and low resolution simulations such as:

i) An RCM versus a GCM, even when the RCM is not driven by the GCM

ii) Two RCM simulations at high and low resolution (this thesis)

2.5.2 Source of added value

A model's performance can depend on horizontal resolution for various reasons such as a more accurate representation of fine scale forcings (e.g. topography, coastlines and land use) (Chan et al. 2012), the better representation of physical processes and interactions (e.g. the dynamical structure of weather systems or cloud complexes), the location of major circulation features, and the direct dependence of physical parameterizations on the model grid size (Rauscher et al. 2010). With these improvements, they are expected to simulate local and regional weather phenomena more accurately (Marvel et al. 2013) leading to improved simulation of small scale features (Diaconescu and Laprise 2013) and distribution of events at finer temporal scales e.g. daily and, in particular, extreme events (Frei et al. 2003, Kendon et al. 2012).

Moreover, the large-scale dynamics of the climate systems are partially determined by nonlinear processes whose characteristic scales might be unresolved at coarse

resolutions (Marvel et al. 2013). Hence, model fidelity could also improve by explicitly resolving, rather than parameterizing those processes (Hack et al. 2006) as has been demonstrated in convection-permitting RCMs (Kendon et al. 2012).

2.5.2.1 Where does added value lie?

The main aim of the one-way nesting approach of high resolution regional climate modelling is to add information not resolved by the driving model (Jones et al. 1995) in order to provide more realistic fine scale information, which enhances that of the coarse scale GCMs (Giorgi et al. 2014). So, according to Chan et al. (2012), some of the pertinent questions in evaluation of added value are: For what climate statistics should one hope to find added value from dynamic downscaling? How does added value vary with the temporal scale of the climatic variable? For example, where and when can added value be found in monthly mean values?

Large scale features resolved in numerical data are typically on the order of four grid boxes or above (Pielke 2002). For global reanalysis or simulation products, this means that phenomena smaller than about 500-800 km (e.g., mesoscale phenomena such as fronts, mesoscale convective systems and disturbances, polar lows, typhoons etc.) are not represented well (Feser et al. 2011). RCMs have the potential to give more realistic results on small to medium spatial scales (600 km and less) (Feser 2006, Feser et al. 2011) with improved local to regional representation of climate processes (Rummukainen 2010). Thus added value of regional climate modelling is expected mainly at these medium scales (e.g., Feser et al. 2011, Laprise 2003), although RCMs might be able to improve imperfect large scales supplied as driving LBC (Diaconescu and Laprise 2013, Gao et al. 2006, Giorgi et al. 1998). The latter possibly arises from a better description of the atmospheric dynamical processes (Feser 2006), which leads to

the formation of mesoscale features such as fronts or mesoscale disturbances (e.g., Denis et al. 2002), resulting in improvement in large-scale pattern.

Identification of added value in RCM simulation depends on several factors. A key factor is related with the climate variable considered in the assessment (Di Luca et al. 2012). Added value can be anticipated in variables with fine scale features, both temporal and spatial, such as precipitation or even surface temperature because the regional dynamics of this variable depend strongly on the high resolution details. But little added value is expected in more uniform variables such as geopotential height and sea level pressure (Feser et al. 2011). Indeed, added value has been generally found in RCMs for the surface variables (e.g. surface temperature, wind speed) in the reanalysis driven downscaling studies over regions characterized by small-scale orographic features such as mountainous regions (Feser 2006) and coastal areas (Winterfeldt and Weisse 2009) and lakes. But little added value and even degradation is found in regions devoid of important small-scale physiographic forcing (Winterfeldt and Weisse 2009). Similar results are seen in GCM driven RCM simulations. For example, RCMs generally improve the precipitation simulation compared to GCMs in regions where small-scale surface forcings are important or GCMs do not perform well, but RCMs simulated climate might degrade those regions where GCMs perform well or large-scale forcings are dominant (De Sales and Xue 2011, Seth et al. 2007).

Another factor influencing the evaluation of added value is concerned with statistics considered for evaluation. For example, Panitz et al. (2014) have found that the increase of the model resolution does not bring evident improvements to the results for monthly means statistics. Similarly, in a review of recent studies, Giorgi (2014) has concluded that the added value is not necessarily found in climatological means, which depends more on the physics of the specific models rather than the model resolution, but rather

in higher order statistics and regional circulation features/feedbacks. For example, compared to the driving GCMs, the RegCM4 consistently improved the simulation of the tails of the daily (Giorgi et al. 2014) and seasonal (Coppola et al. 2014) precipitation distributions, while not systematically improving the climatological means (Coppola et al. 2014). The dissimilar sensitivity to changes in spatial resolution exhibited by different precipitation intensities has important implications in added value (Di Luca et al. 2012). The absence of added value reported in some studies might be related to "the failure of the assumptions from which added value is expected" (page no. 1233, Di Luca et al. 2012). As mentioned above, very little added value can be found in monthly mean precipitation in regions without important surface forcings because monthly scales are predominantly associated with large-spatial scales, probably well resolved by GCMs. This suggests that different statistics will show different potential for added value depending on which part of the distribution is sampled. This means higher moments of the distribution (e.g., intensity and frequency of heavier precipitation rate events) show a much higher sensitivity to changes in resolution than central moments (e.g., low-moderate precipitation rate events) (Di Luca et al. 2012).

A third factor that influences added value is concerned with the sampling frequency/duration of the variable in concern. Di Luca (2012) has showed that potential added value of RCMs is much higher for shorter temporal scales (e.g., 3-hourly data) than for long temporal scales (e.g. bi weekly average data) due to the filtering resulting from time averaging process.

Furthermore, studies show that added value of RCMs is strongly dependent on the regional geography (De Sales and Xue 2011) and seasonality (Di Luca et al. 2012) possibly due to intrinsic differences in model performance in different climate regimes.

In addition, added value of RCM is generally clear in those regions where mesoscale phenomena are more common (Feser et al. 2011). For example, Di Luca (2012) found higher potential of added value over continental America in warm season compared to cold season because of higher proportion of precipitation falling from small-scale weather systems in the warm season. However, they found additional component of potential added value in regions of complex topography induced by orographic forcing in all seasons and temporal scales. Other studies also found the geographic dependency of the increased skill at high resolution simulation. For example, Rauscher et al. (2010) noticed added value over the topographically complex regions such as United Kingdom in their simulation over European domain, which they linked with the availability of high resolution observation that capture the complex climatology and provide a means to validate model simulations. Likewise, Kendon et al. (2012, 2014) utilized radar data to establish added value of very high resolution (1.5 km) RCM precipitation simulation over south UK at subdaily time scale compared to its coarser resolution counterpart (12 km)

However, it is not entirely clear whether high resolution modelling leads to larger improvements for convective or large-scale precipitation, as different studies show contrasting results. For example, some studies found improved precipitation distribution at higher resolution over the regions/seasons where precipitation is mainly produced by resolved schemes rather than the convective parameterizations but fewer improvements when convective schemes dominate (Chan et al. 2012, Iorio et al. 2004), while others reported improvements even for summer convective precipitation (Prein et al. 2013). In contrast, others have found improved precipitation simulation at higher resolution when convection is dominant process but little difference for large-scale precipitation (Gao et

al. 2006, Giorgi et al. 1998). These differences likely arise from the different model physics or parameterization or convection schemes.

2.5.2.2 Why is it often difficult to find added value?

As noted by Marvel et al. (2013), finer spatial resolution does not universally lead to better performance. Achieving added value from a high resolution RCM simulation is not a trivial issue as simply increasing model resolution does not automatically result in improved model performance (e.g. Jacob et al. 2007, Rauscher et al. 2010). A high resolution simulation may lack any added value or even show degradation owing to problems in the lateral forcing of the RCMs (Warner et al. 1997), domain size (Leduc and Laprise 2009, Vannitsem and Chomé 2005), parameterization inadequacies (Jiao and Caya 2006), or a combination of several of those factors (e.g. Castro et al. 2005).

Simulating precipitation has proven to be especially difficult, with insufficient evidence that higher resolution improves performance. Masson and Knutti (2011) have found that higher model resolution in the Coupled Model Intercomparison Project Phase 3 (CMIP3) ensemble does not lead to better simulation of large-scale precipitation climatologies. Regionally, Rauscher et al. (2010) found that improvement in precipitation with resolution is dependent on season and geography, while Caldwell (2010) finds that improved model resolution does not translate into improved simulation of California wintertime precipitation.

High resolution simulations do not necessarily produce results closer to the observed values, in part because the approximations in model do not converge monotonically with resolution and the performance strongly depends on the behaviours of parameterizations (Di Luca et al. 2012). So, before undertaking high resolution simulation, one should check whether parameterizations are scale dependent and, if so,

whether they are adjusted to or fit for the scales of the high resolution simulation being sought (Jacob and Brasseur 2013[3]). This is necessary as increasing resolution without tuning model physics could increase the model bias (Rauscher et al. 2010). For example, if simulated precipitation at low resolution is already high, it may increase even more at higher resolution. In a study using Hadley Centre AGCM, HadAM3, Pope and Stratton (2002) noted an overall degradation in the precipitation climatology at higher resolution. In a study of the East Asian rain band using GCMs with 60 and 20 km grids, Kusunoki et al. (2011) have found that merely increasing the horizontal resolution gives rise to large biases in precipitation and temperature, much less organization of convection, and suppression of tropical cyclone generation. But careful model tuning such as changing the parameters in the evaporation process, cloud water content diagnosis, vertical transport of horizontal momentum in cumulus, and gravity wave drag improve simulated climatology. In particular, overestimation of global average precipitation of the 20 km model was suppressed by decreasing the amount of detrainment of cloud water at the top of the cumulus, as well as decreasing transformation speed from cloud water to precipitation in the cloud scheme (Mizuta et al. 2006).

In a study on sensitivity of RCM simulation of summer precipitation over southeastern United States to physical parameterization and resolution, Li et al. (2014) found that choice of cumulus scheme that could realistically represent the convective rainfall triggering mechanism may be more effective in a realistic precipitation simulation than solely increasing model resolution. Similarly, in RegCM3 simulation of SASM precipitation at high and low resolutions (90 and 30 km) and three different convection

[3] Oral presentation at International Conference on Regional Climate – CORDEX 2013, Brussels, Belgium, available at: http://cordex2013.wcrp-climate.org/plenary_A6/Pl_A6_01_jacob.pdf

schemes (viz. Greel, Anthes-Kuo and MIT-Emanuel), Sinha et al. (2013) found that different convection scheme performed better at different resolution. These results indicate the need of improvement in model parameterizations and model tuning for improved model performance at higher resolution (Duffy et al. 2003, Pope and Stratton 2002, Sinha et al. 2013).

However, parameterisation schemes, in particular the cumulus convection schemes, are often designed for coarser resolution and may become less valid at increasingly high resolution (Chan et al. 2012). Molinari and Dudek (1992) argue that the assumption of traditional convection scheme begins to break down at horizontal resolution of about 50 km as some convection processes begin to be partially resolved by the model at resolutions of about 20-25 km. In an effort to overcome deficiencies in model simulation arising from the dependency on the convection schemes, a few modelling centres have started to test RCM simulation at spatial resolution of up to 4 km and less with partial shutdown of convection scheme, although even at grid scales of the order of 1 km, not all convection is fully resolved (Roberts and Lean 2008).

2.5.2.3 "Diminishing returns" with increasing resolution

But, while model simulations are being performed at higher and higher resolutions, one aspect that has not received much attention is the prospect of diminishing return at higher resolution. For example, Mass et al. (2002) demonstrated improved representation of precipitation at higher model resolutions over the western United States using a short-range NWP model but noted ''diminishing returns'' with increasing resolution, a result found in previous studies (e.g., Boville 1991). Likewise, Rojas (2006) found large improvement in MM5 simulation of precipitation from 135 to 45 km over the topographically complex country of Chile, but smaller changes from 45 to 15

km. Similarly, in a recent study using Hadley Centre model Chan et al. (2012) did not find any clear evidence of improvement in daily precipitation over England at 1.5 km simulation compared to 12 km simulation. Also, Li et al. (2014) found no obvious advantage of a 3 km convection permitting simulation of summer precipitation over southeastern United States compared to 15 km simulation run with best performing convection scheme.

From the analysis of the same set of simulations as in Chan et al. (2012), Kendon et al. (2012) found clear improvements at the sub-daily time scale for metrics such as variability, duration and spatial extent of precipitation. Similarly, Wang et al. (2013) found added values in RCM simulation even at 500 m resolution compared to its 1.5 km counterpart in simulating very fine local mesoscale climate patterns, including diurnal variations of temperature and winds over parts of south west coast of England. Likewise, in multiscale evaluation of summer and winter daily heavy precipitation events in the Colorado Headwaters at 36-, 12- and 4-km resolution Prein (2013) concluded that the main advantages of the 4 km simulation were the improved spatial mesoscale patterns of heavy precipitation.

Hence, the issue of "diminishing return" with progressively higher resolution also seemingly depends on several factors, similar to those outlined in section 2.5.2.1 such as seasonality, geography, statistic/metrics and temporal and spatial scale.

One important aspect that should be borne in mind in investigation of the return of a model simulation is the potential benefit of the return being sought, if achieved. This could differ substantially in different operating contexts. For example, for weather forecasting the benefits of high resolution has been proven in tracking the trajectory and intensity of extreme events such as cyclones, mid-latitude intense lows and localised

extreme events. But the prime purpose of climate change modelling is to gain insight on changes in characteristics of weather and climate of relevance to impact rather than getting individual events right so higher resolution might not be that critical.

2.5.3 Methods for evaluating added value

Added value of high resolution simulation is an emerging area of research with much ongoing debate. Several factors affecting added value have been discussed in the preceding sections such as variables, timescale, geographic region, season etc. being evaluated. However, several studies have suggested employing specific techniques for systematic detection of added value over and above simple visual and/or simple statistical comparison of RCM simulations. For example, Marvel et al. (2013) argues that simply increasing horizontal model resolution is of limited use if it degrades the ability of models to capture large-scale features or global mean states even if it leads to better representation of small-scale processes. It is, therefore, important to examine the performance of models at multiple spatial scales. Some of the techniques used in evaluation of added value in various studies are listed in Table 2.3 and key points described subsequently.

Table 2.3 Various methods used for evaluating added value.

Method	Variables/ metric	Complexity	Reference
Difference of squares of GCM bias from RCM bias	Precipitation climatology	Simple	Pinto et al. (2013)[4]
Spatial aggregation	Precipitation climatology	Simple	Tselioudis (2012)
Spatial filter (running spatial average)	Precipitation climatology	Simple	Philippe et al. (2011)
Spatial filter (isotropic digital filter)	Surface pressure and temperature	Complex	Feser (2006)
Optimal statistical filter (Optimal fingerprint technique)	Observed and projected annual temperature and precipitation time series	Complex	Paeth and Mannig (2012)
Scale space framework	Seasonal climatology of surface air temperature, sea level pressure, total precipitation rate	Complex	Marvel et al. (2013)
Intensity scale verification technique	Seasonal precipitation and inter-annual precipitation difference	Complex	De Sales and Xue (2011)

Pinto et al. (2013) used a simple error measuring technique to evaluate added value of a RCM compared to a GCM. This technique involves computing the difference of the square of the GCM bias from the RCM bias. They used this technique to compute added value in the spatial distribution of precipitation climatology.

Tselioudis (2012) investigated the added value (introduction of novel information) of a RCM simulation of precipitation compared to the driving GCM simulation by employing a simple technique of upscaling (based on averaging the value of all the high

[4] Oral presentation at International Conference on Regional Climate –CORDEX 2013, Brussels, Belgium, available at: http://cordex2013.wcrp-climate.org/plenary_A1/PL_A1_11_Pinto.pdf

resolution grid points that correspond to each lower-resolution grid point) the high resolution RCM output to match that of the GCM. They found that RCM produced more precipitation compared to the GCM in both the present and future climate. The additional precipitation is mostly concentrated over the mountain range which they attributed to the increase in topographic height in the RCM compared to the GCM.

Philippe et al. (2011) computed approximate added value by employing a simple spatial filter. This technique involved subtracting a smooth field (generated by computing 5 X 5 grid point running spatial average) from the original precipitation climatological field in order to extract the small-scale (mesoscale) features and identify the mesoscale signals. They showed that a comparison of the observed and simulated residual fields gave an indication of sensitivity of RCM precipitation simulation to the orographic forcing and the treatment of precipitation in different models. However, the authors noted that this analysis did not identify the "real added value", which could only be obtained by comparing a GCM and a RCM.

Paeth and Mannig (2012) applied an optimal statistical filter (optimal fingerprint technique) to compare the coherence between observed and simulated patterns of Mediterranean climate change from a global and a regional climate model. The optimal fingerprint technique computes a detection variable d which is derived from the scalar product between an observed state vector and a simulated state vector (the so called guess pattern or fingerprint). The scalar product is then weighted by the inverse matrix of natural variability in order to maximize the signal-to-noise ratio, which is equivalent to a rotation of the state vector in the multidimensional variable space away from the direction of strongest noise. The resulting detection variable d_{opt} is optimized through an optimal statistical filter. They used 30 year trend patterns of Mediterranean annual temperature and precipitation from the Climate Research Unit (CRU) data set as

observed state vectors and guess patterns were once taken from a GCM and once from a RCM. They found that RCM did add value in the detection of regional climate change as the RCM's trend patterns of annual temperature and precipitation were more consistent with the recently observed changes in the Mediterranean Basin than the GCM's trend patterns.

Feser (2006) compared the scale dependent skill of a RCM and a driving reanalysis data set employing appropriate spatial filters. They used an isotropic digital filter which was able to separate the model outputs into different spatial scales by filtering certain wave number ranges. The filter weights are determined so that the 2D response function is approximately isotropic, and for the predetermined wavenumber ranges close to either one or zero. For the low pass filter a wavenumber range of 0-6 was chose which allows weather phenomena larger than about 700 km (i.e. those best resolved in GCMs) to pass this filter. The medium-pass filter was set to allow wavenumbers 8-16, which correspond to scales of about 250-550 km (i.e. best resolved in RCMs). The skill of the reanalysis or the RCM is measured by computing the pattern correlation coefficients on the filtered data of the reanalysis or the RCM against the filtered data from an operational regional weather analysis at the two space scale ranges specified above. It is expected that RCM has similar skill as the driving reanalysis for large scales, though larger skill on the medium scale. They found that the RCM generated significant added values, more obvious for regionally more structured variables such as near surface temperature than for spatially smooth variables such as air pressure.

De Sales and Xue (2011) used the intensity scale verification technique to quantitatively assess the RCM's ability to add value to simulation of seasonal precipitation and inter-annual precipitation difference. This verification method evaluates the forecast skill

score and energy of precipitation as a function of different spatial scales and precipitation intensities. The scale components are obtained by a 2-D Haar discrete wavelet transform and different precipitation intensities are selected by thresholds. Generally, intensity-scale decompositions of skill score tend to show low skill for very intense rainfall rates and very small spatial scales, which represent small-scale convective storms. In contrast, frontal and non-convective large precipitation systems are more often properly simulated, yielding higher scores. Negative scores are associated with the model's performances, not better than a random prediction.

Marvel et al. (2013) evaluated RCM's performance across spatial scales using a technique based on the "scale space" framework. This technique involves progressive smoothing (removal of fine scale structure) of two dimensional climate data using a diffusion equation. Here smoothing refers to a process by which variability on fine spatial scales is systematically removed to generate filtered, coarser resolution versions of the data. This process can aid in understanding the persistence of certain features in data across the spatial scales, and it allows for the evaluation of model performance as a function of spatial scale.

Following Pinto et al. (2013), in this thesis added value is defined as the difference of absolute biases in coarser RCM simulation from finer RCM simulation.

I.e. Added value = absolute bias in coarser RCM simulation - absolute bias in finer RCM simulation

This method is chosen because of the ease of the computation and direct linkage of added value with the reduction in magnitude of bias. However the magnitude of added value computed in this manner is sensitive to the observation used as reference, which

demands the use of high quality data at fine scale as reference as has been identified in previous studies.

2.5.4 Survey of literature on added value of high resolution simulation

In this section, a brief survey of literature on added value is presented. Studies over various parts of the globe are presented followed by those on SASM.

2.5.4.1 Added value of high resolution simulation over different regions

In this section some recent studies on added value of high resolution simulation over different regions of the globe are presented. Table 2.4 provides a summary of those studies which is elaborated below.

Table 2.4 Studies on added value of high resolution simulation over the globe.

Models compared	Region	Variables/ metrics	Reference
45 CMIP5 GCMs with horizontal resolutions ranging from 0.75° to 5°	5 tropical and subtropical CORDEX domains	Seasonal mean surface temperature and precipitation	Elguindi et al. (2014)
MetUM (GA3) at N96, N216, N320 resolutions	Global	Precipitation	Walters et al. (2011)
3 RegCM4 simulations and its 3 driving GCMs	5 tropical and subtropical CORDEX domains	Extreme hydroclimatic indices and precipitation PDFs	Giorgi et al. (2014)
9 simulations from 3 different RCMs and their driving GCMs	Double nest with outer nest over Europe and inner nest over Germany	Seasonal mean surface temperature and precipitation	Berg et al. (2013)
WRF at 0.33° and 0.11° resolutions, ERA-Interim	Germany	Monthly and seasonal mean precipitation	Warrach-Sagi et al. (2013)
REMO and ERA40	South-West Africa	temperature and precipitation	Haensler (2011)
NCEP GCM and ETA	South America	Seasonal mean precipitation	De Sales and Xue (2011)
AGCM at 60 and 20 km	East Asian summer monsoon	precipitation	Kusunoki et al. (2011)
MetUM RCM at 1.5 and 12 km	South England	Precipitation at daily and sub-daily scale	Kendon et al. (2012) Chan et al. (2012)
Canadian Global Environmental Multiscale model in its global and regional configurations	North America	Precipitation, specific humidity and zonal wind	Diaconescu and Laprise (2013)
2 RCMs at 25 and 10 km resolutions	Czech Republic	Annual cycle of precipitation	Zikova et al. (2013)

Double nesting (27, 9 km) of WRF and driving ERA-Interim	Portugal	Temperature and precipitation on daily to seasonal timescales	Soares et al. (2012)
COSMO-CLM at 10 km	Greater Alps	Various simple statistics on temperature and precipitation	Haslinger et al. (2013)
RegCM3 (15, 3 km)	Greater Alps	Surface temperature and other surface hydrological parameters	Im et al. (2010)
WRF at 27 and 9 km, and driving ERA-Interim	Iberian Peninsula	Various statistics of precipitation	Cardoso et al. (2013)
RegCM4 at 50 and 12 km	Tibetan Plateau	Monthly and seasonal temperature and precipitation	Ji and Kang (2013)

Very few of the studies in Table 2.4 indicate dependency of model performance to resolution even among the GCMs. For example, Elguindi et al. (2014), from an assessment of 45 GCMs participating in CMIP5 experiments over a subset of CORDEX domains (Africa, Mediterranean, South and Central America, and South Asia), found that high resolution GCMs (resolution < 2°) had higher skill in most regions and seasons for both seasonal mean temperature and precipitation compared to the low resolution GCMs (resolution >2°). However, the result does not hold for all seasons and regions as majority of models exhibit varying degrees of skill depending on the region and season, only a few models (UKMO models, NCAR models and CSIRO-AC10) perform well globally. Hence, it is not clear whether they would have reached at the same conclusion had they used different threshold to differentiate low and high resolution GCMs. Also, the horizontal resolution of the GCMs they considered varies

from 5° to 0.75°. But it is not clear whether skill of the GCMs progressively increases from lower to higher resolution (that is above and below their 2° threshold).

Likewise, Walters et al. (2011) assessed the performance of Hadley Centre's unified model GA3 (model configuration used in thesis) at a range of horizontal resolutions (N96, N216, N320) and found that increased resolution enabled the model to represent both regional and local climate better, e.g. by improving precipitation distributions and amounts, especially near areas of orography. Also, enhanced resolution allows the more accurate modelling of extremes, including the number, intensity, and interannual variability of tropical cyclones. Increased errors in the precipitation were noted over tropical land regions at N216 and N320 compared to N96, although June-August precipitation deficit over India is reduced. Hence, there is regional variation in the model performance at high resolution. The performance of the model at even higher resolution but confined to South Asia will be investigated in detail in this thesis.

Giorgi et al. (2014) analysed extreme hydroclimatic indices simulated by RegCM4 and its three driving GCMs over 5 CORDEX domains (same as those mentioned in preceding paragraph). They found that the RCM consecutive dry day index and 95th intensity percentile are generally in line with the TRMM data (which is of high resolution), and yield improvement in the simulation of precipitation empirical probability density functions (compared to the driving GCMs). Conversely, the GCMs results are generally in line with the coarser resolution GPCP dataset with mostly underestimation of occurrence of most extreme events. These results illustrate the added value of the increased resolution of the regional model as well as need of high resolution observational datasets for evaluation of such models.

Similar to results of Giorgi et al. (2014), Berg et al. (2013) found that GCMs performed well in simulating the intensity distribution of precipitation at their own resolution, but the RCMs add value to the distributions, especially for the extremes, when compared to observations at similar resolutions. They draw this conclusion from a study employing multiple RCM simulation for Europe (at 50 km) with a high resolution nest over Germany (at 7 km) using three different RCMs (CLM, WRF and REMO) and three driving datasets (two GCMs and a reanalysis). However, on the down side biases in the GCMs are generally carried over to the parent RCMs in enhanced or reduced forms, which is then carried over from the parent RCMs to daughter RCMs without a change in amplitude. In addition, pattern of bias in a given RCM simulation remained similar for different driving data but differed among the RCMs indicating sensitivity of the RCM simulation to its model physics. This points to the need of selecting well performing RCM over the region of interest, especially if only one RCM is to be used for downscaling.

In partial agreement with Berg et al. (2013), Warrach-Sagi et al. (2013) found that WRF simulations at both 0.33° and 0.11° resolutions show a systematic positive precipitation bias over Germany, not apparent in ERA interim and an overestimation of wet day frequency. But they improved the annual cycle of the precipitation intensity, underestimated by ERA interim. Further, even the high resolution (0.11°) simulation depicts typical systematic errors in precipitation associated with orographic terrain such as the windward-lee effect. In contrast, they found high value from a season long RCM simulation on the convection-permitting scale (~4 km) in terms of improvements in location of precipitation maxima in the mountainous regions and spatial correlation of precipitation. They argue that improved performance of convective permitting simulation comes from switching off of the deep convection scheme, which shows

strong spatial and case dependent sensitivity and brings in high systematic errors. The contrasting performance of the model at convective permitting and slightly coarser resolutions indicate the potential of huge improvements at the former resolution. Hence, it needs to be seen how RCM at such high resolution performs over the Himalaya.

Haensler (2011) claimed clear benefit of using a regional climate model especially in regions with complex topography and climate characteristics. In particular, they found clear added value of downscaling of ERA40 reanalysis with REMO (at 18 km resolution) in terms of the RCMs ability to realistically simulate precipitation over South-West Africa in both summer and winter seasons where the driving ERA40 has poor representation of precipitation. However, this result should be interpreted with caution as the limitations of reanalysis dataset in precipitation simulation are well known.

De Sales and Xue (2011) found regional dependency of the RCM performance owing to differences in climate regimes operating in different region. In particular, they found that a RCM was able to add value to summer and winter precipitation over southern South America where a comparable mix of frontal and convective precipitation occurs with largest improvements associated with precipitation events at spatial scales of about 400-800 km and rainfall rates above 4 mm/day. But the RCM generally failed to yield added value over northern South America where convective storms were the dominant source of precipitation. In terms of inter-annual precipitation difference, the RCM produced better results over southern South America, by simulating the increase in intense small-scale events in the wet years.

Kusunoki et al. (2011) compared the performance of an AGCM, at 20 and 60 km resolutions, in simulating rain band of East Asian summer monsoon and found that the

20 km model reproduced the rain band better than lower resolution model in terms of geographical distribution and seasonal march.

Kendon et al. (2012) compared a MetUM RCM's simulation at a low and high resolution over south UK and found much more realistic precipitation at sub-daily scale in 1.5 km simulation compared to 12 km simulation. They found that in the 12 km RCM heavy rain events were not heavy enough, and tended to be too persistent and widespread. While the 1.5 km model have a tendency for heavy rain to be too intense, it still gives a much better representation of its duration and spatial extent. Long-standing problems in climate models, such as the tendency for too much persistent light rain and errors in the diurnal cycle are also considerably reduced in the 1.5 km RCM. They concluded that biases in the 12 km RCM appeared to be linked to deficiencies in the representation of convection. However, analysing same set of simulation Chan et al. (2012) concluded that overall there was no evidence of 1.5 km simulation being superior to 12 km or vice versa in simulation of daily precipitation. In particular they found no benefit of increasing model resolution beyond 12 km for winter season. They attributed this to scale of dynamical process that drove winter precipitation events in Europe, caused by fronts and depressions at scale of the order of 100-1000 km, which was 2-3 order of magnitude larger than highest model resolution (1.5 km) in their study. These results again indicate dependency of high resolution RCM skill on the seasonality/climate regime over study region. In addition, time scale (i.e. daily, sub-daily) selected for assessment also have influence on the model skill.

The primary objective of dynamical downscaling using RCM is to add fine scale details to the GCM. However, the driving GCMs often contain large scale regional biases. In this connection Diaconescu and Laprise (2013) assessed the effect of RCM domain size

on the larger scales; in particular they investigated whether an RCM when run over very large domains, could actually improve the large scales compared to those of the driving data. They found that domain size did not have much effect when an RCM was driven by perfect LBC as its skill at reproducing the large scales decreases only slightly with increasing the domain size. On the other hand, RCMs can reduce some large scales errors present in the driving imperfect LBC, when run with very large domains. This study suggests the need to carry out RCM simulations over very large domain when forced by GCMs as they generally contain some errors. However, this study is conducted over mid latitude (North America) and it remains to be seen if same applies over tropical domains such as South Asia. In addition to above results, they reaffirmed the main advantage of RCM lay in the added value it provided at small scales and extremes, particularly for precipitation, while the coarse resolution model simulations had difficulties in simulating heavy precipitation events, and as a result their precipitation distributions were systematically shifted toward smaller intensity.

Zikova et al. (2013) assessed two RCMs (RegCM3 and ALADIN-CLIMATE/CZ) simulations at an intermediate (25 km) and high resolution (10 km). They found that generally the effects of increased horizontal resolution varied with RCM and evaluated characteristic which was in line with some other studies (e.g., Berg et al. 2013, Chan et al. 2012, Kendon et al. 2012). For the simulation of annual precipitation cycle and the precipitation half-time, RegCM3 results improved with the increased horizontal resolution, whereas ALADIN-CLIMATE/CZ results worsened. For the precipitation amount and the dependence of precipitation amount on altitude, the increase in horizontal resolution decreases the accuracy of results in both models. These results indicate the need to tuning the model physics and parametrization for setting up RCM at

very high resolutions. This study also suggests the need of using multiple RCMs to reach to a robust conclusion.

Soares et al. (2012) assessed the performance of ERA-Interim forced WRF model at an intermediate (27 km) and high resolution (9 km) run in double nest over Portugal. They found that high resolution RCM simulation had better skill compared to ERA-Interim when compared with station observations comprising daily temperature and precipitation, through the computation of mean climatologies, standard statistical errors on daily to seasonal time scales and distribution of extreme events. Out of which, the largest gain of the high resolution modelling was found geographically over the wet regions of Portugal where orographic enhancement was dominant, which resulted in better representation of the extreme precipitation events. Hence, this study suggests that high resolution RCM simulation might also result in similar improvements over the Himalaya.

However, contrary to the finding of Soares et al. (2012), Haslinger et al. (2013) found rather large temperature and precipitation biases over greater Alps even on a seasonal scale in a high resolution (9 km) RCM simulation. The contrasting results of the two studies might be due to the large difference in elevation of the highest peak in the two domains. However, the authors pointed out the need of detailed analysis to detect processes responsible for model shortcomings. Also, the need of improved gridded observational datasets was highlighted in order to reduce uncertainty in model assessment. In this context similar study over the Himalaya would be really useful given the complex topography and even higher elevation of the region. In this regard, the region poses a severe test bed for high resolution climate models.

Im et al. (2010) found contrasting results from that of Haslinger et al. (2013) over the same region (Alps) when they employed a mosaic type parameterization of subgrid-scale topography and land use for a high resolution (3 km) RCM simulation over the region. In particular, they achieved much finer detail of temperature and snow distribution over the Alpine region at higher resolution (3 km) (compared to it RCM simulation at 15 km which already produce good quality temperature and precipitation statistics) along with improved simulation of the surface hydrological cycle, in particular snow and runoff at high-elevation sites. This result again shows the dependency of the RCM performance at high resolution on the model physics.

In agreement with the majority of the studies mentioned above (e.g., Diaconescu and Laprise 2013, Haensler 2011, Kendon et al. 2012), Cardoso et al. (2013) found significant improvement in representation of precipitation fields at all timescales in the higher resolution WRF simulation (9 km) as well as the representation of variability and of extreme weather statistics over Iberian Peninsula. In contrast, Ji and Kang (2013) found clear improvements for temperature but not for precipitation at high resolution (10 km) RCM simulation (compared to coarser simulation at 50 km) in their study over the Tibetan Plateau employing double nesting. They attribute improvement in temperature simulation to improved representation of complex topography at the higher resolution. So, this study provides yet another evidence that precipitation simulation over complex regions such as the Himalaya does not necessarily improve simply by increasing the model resolution.

2.5.4.2 Added value of high resolution simulation of SASM

Higher resolution climate models, not limited to RCMs, are increasingly being used to simulate the SASM. For example, Rajendran et al. (2012) and Rajendran and Kitoh

(2008) assessed the skill of a high resolution (20 km) AGCM to simulate SASM and illustrated that SASM rainfall was strongly controlled by processes and parameterised physics which needed to be resolved with adequately high resolution for accurate assessment of local- and regional- scale climate and its changes. Also, Rajendran et al. (2013) evaluated AGCM simulations over India at a range of horizontal resolutions (20 to 180 km) and found marked skill of super high resolution (20 km) in capturing fine scale spatial pattern of monsoon seasonal mean precipitation and its frequency distribution. However, at lower resolution, the simulations fail to capture the observed characteristics of monsoon precipitation and its spatial heterogeneity. Similarly, Sabin et al. (2013) found large improvement in variable resolution global climate model zoomed over South Asia (resolution < 35 km) in simulating various aspects of SASM such as more realistic precipitation distribution and circulation features (e.g. monsoon trough and synoptic disturbances) compared to coarser uniform AGCM simulation.

Higher resolution RCMs have also been used in a few studies on SASM in recent years. For example, Akhtar et al. (2008) ran a RCM (PRECIS) at 25 km forced by a GCM (HadAM3P) and used the outputs to drive hydrological models in order to estimate impact of climate change in three small river basins in the western Himalaya. They found rather uniform warming throughout the year and across the basin in future (i.e. in late 21st century compared to base line). Similarly, in all three basins precipitation was projected to increase in all seasons but with larger increase in winter than summer. They also noted that projected changes were comparable to those made for neighbouring regions using coarser RCM and statistical methods. Ashfaq et al. (2009) found that a RCM (RegCM3) simulation at high (25 km) and medium (50 km) resolution had very similar spatial pattern of changes in mean convective precipitation. They further noted that despite higher resolution of the RCM, its convective parameterization was

inadequate to resolve interaction among convective organization, orography and the diurnal cycle, which influenced the life cycle and spatial coherence of large scale circulation.

Similarly, Bhaskaran et al. (2012) ran a Met Office RCM (HadRM3P) at 50 and 25 km to study sensitivity of the hydrological cycle to domain size and showed that seasonal mean hydrological cycle and the day-to-day precipitation variations of a sub-region within the model domain were sensitive to the domain size but largely insensitive to resolution. Ménégoz et al. (2013) ran RCM at 20 km to simulate precipitation and snow cover over the Himalaya for few years and noted that although the RCM was able to capture the spatial variability of precipitation and snow cover over the Himalaya, it underestimated precipitation and snowfall. Moreover, a season-long very high resolution (1.5 km) integration of the SASM has been performed recently in Met Office (Webster S, personal communication) but it will take more time to extend this work to climate time scale given the tremendous computational cost involved. However, none of those RCM based studies directly compared the performance of RCMs at higher and coarser resolutions.

However, Sinha et al. (2013) employed a double nesting technique to run RegCM3 at 90 km and 30 km, forced by a GCM at outer domain, to simulate SASM for three seasons (dry, wet and normal) and three different convection schemes. They found that rainfall intensity and distribution was best captured by different convection schemes at different resolutions. Nevertheless, the high resolution model captures those aspects better compared to the coarser simulation, as well as generates more rainfall over most parts of India. Further, based on the findings they argued that it was adequate to run the model at 30 km resolution for assessment of the results against the observation at 1° resolution (the highest they were able to find). Clearly, daily precipitation data over

South Asia is available at much higher resolution so they might have concluded differently about adequacy of the model resolution had they compared their result with such dataset. In addition, even the horizontal resolution of 25 km seems to be generally inadequate for the realistic representation of spatiotemporal variability of SASM such as precipitation particularly over complex regions such as the Himalaya. In any case, there have been only a few RCM based studies on SASM that employ high resolution compared to host of such studies over other regions, in particular over mid-latitudes, in recent years.

The high resolution model simulations of SASM described in this section and their key results are summarized in the table below.

Table 2.5 High resolution model simulation of the SASM.

High resolution models	Coarse resolution model	Key result related with model resolution	Reference
AGCM at 20 km	No low resolution baseline	Model able to capture observed increasing and decreasing trend of precipitation at interannual time scale	Rajendran et al. (2012)
AGCM at 20 km	No low resolution baseline	Model able to capture spatial distribution of seasonal mean precipitation with great details	Rajendran and Kitoh (2008)
Stretched AGCM with ~35 km resolution over South Asia	Same AGCM without stretching (i.e. uniform 1°X1° resolution)	More realistic precipitation distribution and circulation features (e.g. monsoon trough and synoptic disturbances)	Sabin et al. (2013)
AGCM at 20 km	AGCM at various resolutions up to 180 km	High resolution models better capture fine scale spatial pattern of monsoon seasonal mean precipitation and its frequency distribution	Rajendran et al. (2013)
PRECIS at 25 km	No low resolution baseline	Projected change in mean temperature and precipitation comparable to those from coarser models for neighbouring regions	Akhtar et al. (2008)
RegCM3 at 25 km	RegCM3 at 50 km	Both models project very similar spatial pattern of changes in mean convective precipitation	Ashfaq et al. (2009)
MetUM (HadRM3P) at 25 km	MetUM (HadRM3P) at 50 km	Seasonal mean hydrological cycle and the day-to-day precipitation variations of a sub-region within the model domain are sensitive to the domain size but largely insensitive to resolution	Bhaskaran et al. (2012)
RCM at 20 km	No low resolution baseline	Though the RCM is able to capture the spatial variability of precipitation and snow cover over the Himalaya, it underestimate precipitation and snowfall	Ménégoz et al. (2013)
RegCM3 at 30 km	RegCM3 at 90 km	Rainfall intensity and distribution is best captured by different convection schemes at different resolutions. But high resolution simulation generates more rainfall over India.	Sinha et al. (2013)

2.6 Summary of literature review and research objectives

The literature review has led to the identification of a number of gaps and areas for further research. A summary of the literature review in the preceding sections is drawn below:

- As more and more climate model outputs are becoming readily accessible, climate scientists are now in a position to choose the more realistic model outputs for the assessment of the climate projections or further downscaling. However, the performance of a model depends on variety of factors such as geographic region, season, variable etc. being considered for evaluation. So, it is not known beforehand which models perform well over the area of interest. Availability of numerous model simulations, in some cases with multiple realizations and versions, makes the selection of model outputs even more challenging. So, this calls for a framework in which available models can be rapidly assessed in order to rank the models and select satisfactory models for downscaling (in case of GCMs) or application in impact assessments (in case of RCMs). Given the regional and seasonal dependency of model performance it requires that metrics selected for rapid model appraisal are region and season specific. In general, such metrics is likely to be related with large scale fields in the case of GCMs and performance metrics or diagnostics relevant to impacts assessments in the case of RCMs.

- There are few studies that intercompare the skill of climate models in simulating SASM, but they undertake a range of evaluation. But it remains to be seen whether this can be done rapidly with a minimal set of evaluation metrics

without compromising overall results and, if so, which are the suitable metrics for this purpose.

- RCMs being limited area models require regular updates of meteorological field at its lateral boundary. The need to specify the domain in RCM simulation added one more layer of uncertainty in its simulation as RCM simulations are known to be sensitive to the size of the domain and its location. There is some consensus that the RCM domain should not be too small (e.g. lesss than ~10,000 grid boxes) even if the region to be assessed is small. However, it is not entirely clear how big a domain could be. Early studies over mid-latitudes suggest that domain should neither be too small (e.g. lesss than ~10,000 grid boxes) nor too big (e.g. more than ~50,000 grid boxes) so that there is just level of control of the boundary forcing on the integration at interior of the domain. However, some recent studies seemingly deviate from this view. Some recommend having domain as large as feasible while others show relative insensitivity of RCM simulation of certain aspects to domain size.

- However, very few studies exist on the sensitivity of the RCM simulation of SASM to domain size. In contrast to the finding over the mid-latitudes, one early study reported that RCM simulation of SASM circulation is relatively insensitive to the size of the domain, which they attributed to intrinsic differences in tropical and mid-latitude climate. But a recent study reported that simulation of SASM seasonal mean hydrological cycle and daily precipitation variability at a sub domain is sensitive to the domain size. So, the issue of sensitivity of RCM SASM simulation to domain size is far from settled.

Moreover, ongoing CORDEX simulations over the huge South Asian domain (~7,00,00,000 sq. km) call for an early assessment of sensitivity of RCM SASM simulation to the domain size.

- Even though investigation of added value of RCM simulation has received attention only recently, it is arguably the single most important issue in the regional climate modelling. In any case, it is implicit in every RCM application as the main aim of regional climate modelling is to provide realistic fine scale information not resolved by the coarser driving model.

- In anticipation of improvements, and driven by user demand and affordability of ever increasing computational power, there is a drive to undertake the RCM simulations at increasingly higher resolutions. Until few years back, the RCM simulations were performed at spatial resolution of 50-60 km. But over the last few years, advanced modelling groups have been routinely performing the RCM simulation at horizontal resolution of about 10 km or even less going down to convection permitting scale of 1-4 km. However, the clear benefit from high resolution simulations especially for precipitation simulation (which is postulated to significantly improve) has not been clearly established, and even less so for the simulation of the SASM. But, this is an important question from an operational viewpoint as well because of the many fold additional cost involved with even the doubling of the resolution. Further, there is competing demand for the computation resources even in the regional climate modelling, including simulation of multiple realizations, creating multi-model ensemble (using combination of multiple GCMs and RCMs), carrying out longer

integrations, and doing various sensitivity studies etc. So there a need to establish clear benefit of high resolution simulations over South Asia to justify allotment of resources for this task.

- Though added value of the high simulation is anticipated i) in fine-scale variables such as precipitation, ii) extremes and higher order moments, and iii) over the complex and heterogeneous regions, the results from the literature to date are rather mixed. Many studies do report the added value on some or all of the above aspects, but there are sizeable numbers of studies that fail to find any added value or even deterioration at the higher resolution. A number of other studies report sensitivity of the high resolution simulation to season and geography. Others report difficulty in finding added value or even deterioration in simulation of the precipitation at higher resolution, which has been partly attributed to the model sensitivity to parameterization of convection. In this connection, a few studies report improvements on various aspects, including precipitation in convective permitting simulation, which has been attributed to the circumventing model dependency on convection parameterization. While other studies report lack of improvement even at convective permitting simulation or diminishing return with increasing spatial resolution.

- The summary drawn in the preceding point is based on studies over mid-latitudes. Though the SASM has been studied extensively using GCMs and RCMs, at about 50 km resolution, very few studies specifically investigate the added value aspect. There are few studies using the RCM simulation at 25 km or less but even those studies did not explore the issue of the added value.

However, there have been few studies on SASM using very high resolution AGCMs (about 20 km) and they all report improvement in the SASM simulation including precipitation, compared to their coarser resolution counterparts.

Based on the conclusions drawn above, the following three questions are identified for the further research and are addressed in this thesis.

1) How reliable are monsoon circulation indices for evaluation of climate model in a changing climate?

This is addressed through the investigation of the strength and stability of monsoon precipitation indices and a number of large scale monsoon circulation indices at interdecadal scale. This work is motivated by the fact that presence of strong and stable relationship between those indices would likely qualify circulation based indices to be used as one of the metrics for rapid model assessment.

2) To what extent the choice of domain size and location affect the "added value" that an RCM can offer?

This is investigated through the evaluation of the sensitivity of RCM simulation of SASM climatology, mainly the precipitation, to the size and location of the domain**.** Provided the simulation is sensitive to domain setup, the objective is to identify a potential optimum domain which can be used to assess the added value of high resolution RCM simulation of SASM.

3) To what extent the Hadley Centre regional climate model add value in going from 50 km to 12 km resolution, and if so, where does the added value lie?

This assessment of the added value focuses mainly on the evaluation/comparison of the high and moderate resolution model's ability to simulate the SASM, in particular various characteristics of its precipitation, compared to the observations. In the first

part, added value is explored at the climatological scale and the intraseasonal aspect is investigated in the second part so as to assess the added value of high resolution simulation on various aspects of SASM at the range of time scales and different geographic regions within South Asia. The results would assist in informed decision making regarding undertaking the RCM simulation at higher resolution verses doing so at coarser resolution so as to utilize surplus resources for other activities such as generating multiple realizations.

3 Contrasting temporal relationships between zonal and meridional wind based monsoon circulation indices and South Asian summer monsoon rainfall.

Synopsis

Following the review of the current state of knowledge regarding the skill of climate models, particularly related with the SASM, and identification of the gaps and the research objectives, this is the first of the four substantive chapters aimed at answering the thesis research questions. In this connection, this chapter seeks to unravel the first research question, which is: How reliable are monsoon circulation indices for evaluation of climate model in a changing climate.

The thesis seeks to use monsoon circulation indices as evaluation metrics to assess whether climate models correctly capture the interannual and intraseasonal variability of the monsoon circulation; but the preliminary exploration revealed the interdecadal variations in the correlation between the indices and rainfall indices. Hence this analysis is undertaken to understand whether the variations were statistically significant, and to be able comment on the fact that empirically derived indices may vary in usefulness over time and they should perhaps be used with caution.

To achieve this objective, the linkage between monsoon rainfall and the monsoon circulation is examined through the assessment of the relationships between the respective indices at decadal time scales. For a comprehensive assessment a number of indices were considered from multiple datasets. As seen later, results show considerable low frequency variability in the relationship between SASM rainfall indices and circulation indices. Nevertheless, interdecadal variability of the relationship between meridional wind based monsoon circulation indices and monsoon rainfall indices are within the limit of sampling variability (as computed from bootstrapping) for 1948-2011 but that between zonal wind based circulation indices and monsoon rainfall indices exceeds the limit of sampling variability.

Findings of the study suggest that relationships between the monsoon circulation and monsoon rainfall, represented through their indices, in model simulations should be interpreted with caution. In particular, high correlation between the two indices in model simulations does not necessarily imply higher model skill as they show considerable low frequency variability in observation, which needs to be investigated further.

Authorship Declaration

I did all the analysis and writing for this paper. The methodology and structure of the paper were discussed with M. New. R. Jones advised on the methodology and soundness of the paper in terms of the scientific content. Both M. New and R. Jones help on interpretation of the results. All authors were involved in editing the drafts.

Contrasting temporal relationships between zonal and meridional wind based monsoon circulation indices and South Asian summer monsoon rainfall.

J. Karmacharya[1,2], M New[1,3] and R Jones[1,4]

Affiliations:

[1] School of Geography and the Environment, University of Oxford, Oxford, United Kingdom

[2] Department of Hydrology and Meteorology, Kathmandu, Nepal

[3] African Climate and Development Initiative, University of Cape Town, Cape Town, South Africa

[4] Met Office Hadley Centre, Exeter, United Kingdom

Submitted to: *Geophysical Research Letters*

Abstract

Large scale monsoon circulation indices (MCIs) represent readily computable diagnostic tools for studying the South Asian summer monsoon (SASM), and have also been used for model assessments. Also, monsoon rainfall indices (MRIs) provide reliable estimate of the SASM so good correlations between the two indices are anticipated. MRIs have remained largely stableover the decades, but recent studies show significant weakening of the monsoon circulation in recent decades which is projected to weaken further and might then decouple the relationship between the two indices. We examined the MCI-MRI relationships using different MCIs and reanalyses and found that they exhibit considerable low-frequency variability. Correlations between zonal wind-based MCIs and a MRI were significantly more variable than expected due to sampling variability (Standard deviation of MRI and zonal MCIs: ~0.25) for 1948-2011 but that was not the case for meridional wind-based indices (Standard deviation of MRI and meridional MCIs: ~0.1). An asymmetric response of zonal circulation and rainfall to increasing aerosol loading over north India might partly account for the former.

3.1 Introduction

Large scale monsoon circulation indices (MCIs) are useful diagnostic tools for studying the South Asian summer monsoon (SASM) dynamics and its variability. Use of concise and meaningful indices to characterize monsoon variability can facilitate empirical studies on the relationship between the monsoon and drivers of its variability, and can also aid objective assessment of climate model skill in simulating monsoon variability (Wang and Fan 1999). MCIs have been used as model evaluation metrics in several recent studies of the SASM using global and regional climate models (GCMs and RCMs) (e.g., Ashfaq et al. 2009, Dobler and Ahrens 2010, Dobler and Ahrens 2011, Kumar et al. 2011a, Saeed et al. 2012, Saeed et al. 2011). Similarly, Fan et al. (2010, 2012) used an integrative monsoon index, defined in terms of the common pattern among multiple fields (sea level pressure, zonal and meridional tropospheric wind shear) associated with the monsoonal dynamics, to evaluate skill of GCMs in simulating the SASM and their reliability for projecting changes in the SASM.

Regionally-averaged monsoon rainfall indices (MRIs) such as the All-India Monsoon Rainfall (AIMR) (e.g., Parthasarathy et al. 1994) have been used to measure the strength of SASM and its interannual variability, and MRIs are continue to be used as a robust measure of the SASM (Turner and Annamalai 2012). As both MRIs and MCIs provide a measure of SASM variability, arguably they should have good correlations with each other; this has often been a precondition in defining MCIs (Goswami et al. 1999). Unsurprisingly therefore, each new MCI was generally shown to have higher correlation with MRIs, compared to previous MCIs. Earlier studies on MCI-MRI relationships covered relatively short durations, typically from the 1970s to early 1990s when those relationships were particularly strong. Nevertheless, a weaker MCI-MRI relationship for

few years in 1990s was noted by Wang and Fan (1999) and they speculated on several reasons for that; such as divergence in those indices in strong ENSO warming years, interdecadal variability of SASM convection and the intrinsic chaotic nature of the SASM.

However, the correlation between any pair of linearly related or unrelated climatic series that vary on interannual timescales should necessarily exhibit low-frequency variation (Gershunov et al. 2001). For example, the low frequency variation of the ENSO-MRI relationship is well documented (e.g., Kumar et al. 1999). Here, we find that most of the MCI-MRI correlations previously analysed have decreased in recent decades. This contrasts with higher MCI-MRI correlations in some recent reanalysis-driven RCM simulations for the same period (e.g., Dobler and Ahrens 2010, Saeed et al. 2012). This was suggested as evidence of the added value of downscaling, but might equally indicate limitations in the modelling system in capturing observed weakening in MCI-MRI relationships, rather than added value. Hence, there is a need to quantify the strength of MCI-MRI relationships over different periods, establish the significance of any observed low frequency variations of MCI-MRI relationships and, if possible, identify their drivers. This could provide new basis for evaluating MCI-MRI relationships in GCM and RCM simulations.

Thermodynamic energy arguments postulate that global warming could cause weakening of the tropical overturning circulation via increased atmospheric stability in response to a slower rate of rise in global rainfall relative to the increase in lower tropospheric moisture (Held and Soden 2006, Vecchi et al. 2006). There is evidence that some aspects of the SASM circulation has weakened in recent decades (Bawiskar 2009, Fan et al. 2009, Kulkarni 2012, Murugavel et al. 2012), which may simply form part of the larger global weakening of the tropical circulation with warming (Turner and

Annamalai 2012). For example, Fan et al. (2009) showed a weakening trend of an integrated monsoon index for 1948-2000. Similarly, Kulkarni (2012) reported a weakening mid tropospheric geopotential height gradient, a weakening lower tropospheric cross equatorial wind flow, and an eastward shift of the Walker circulation for 1948-2004; similarly, Bawiskar (2009) showed weakening of lower tropospheric temperature gradient during 1948-2004. Other recent studies also provide evidence of a weakening SASM circulation (e.g., Bansod et al. 2012, Joseph and Simon 2005, Krishnan et al. 2013). In contrast, some other studies reported a strengthening of some components of SASM circulation (Konwar et al. 2012, Ratnam et al. 2013) or the entire northern hemisphere summer monsoon circulation (Wang et al. 2013). Closer inspection of their results indicates that the northern hemisphere summer monsoon circulation showed a weakening trend before the mid-1980s but intensified thereafter (e.g., Fig. 4, Wang et al. 2013), which they attributed to internal natural variability.

In contrast, SASM rainfall lacks any significant long term trend (e.g., Goswami et al. 2006a, Krishnan et al. 2013), which is somewhat surprising given the warming in the recent decades and projection of increased rainfall under global warming (e.g., Turner and Annamalai 2012). The lack of an increasing trend of SASM despite recent warming has been attributed mainly to weakening monsoon circulation; however, the large increasing trend of aerosol concentration over South Asia might also be partly responsible (Turner and Annamalai 2012). The direct radiative effect of aerosol limits the solar radiation reaching the surface, reducing the surface meridional thermal contrast thereby reducing monsoon rainfall. However, indirect effects of increasing aerosol on cloud lifetime or aldedo as well as role of absorbing aerosols are less clear. Notwithstanding the uncertainty related to aerosol forcing, theoretical consideration and model projections suggest the warming impact to prevail in the long run leading to

further weaken of monsoon circulation but strengthening of monsoon rainfall, which might well decouple MCI-MRI relationships (Fan et al. 2009). It is possible the decoupling is already underway, given the substantial warming in recent decades.

In this context, we investigated the historical evolution of MCI-MRI relationships and evaluated their stability in recent decades. The aim of this study is to i) test the statistical significance of multidecadal variability of MCI-MRI relationships, ii) investigate possible mechanism of such variability, and iii) highlight the implications of such variability for model evaluation.

3.2 Methodology

3.2.1 Data and monsoon indices

Upper air data is required for computing MCIs and quasi-observed values are available from reanalyses. Hence, we used six reanalysis datasets: i) 20 Century reanalysis (20CR) (Compo et al. 2011), ii) NNRP1 (Kalnay et al. 1996), iii) ERA40 (Uppala et al. 2005), iv) ERA Interim (ERAI) (Dee et al. 2011), v) NNRP2 (Kanamitsu et al. 2002) and vi) MERRA (Rienecker et al. 2011). Depending on the individual reanalysis time coverage, we considered 1871-2011, 1948-2011, 1958-2001 periods from the first three reanalyses respectively, and 1979-2011 for the remaining data. We used multiple reanalyses to increase robustness of our findings, as spurious long-term trends might be present in individual reanalysis data (e.g., Hurrell and Trenberth 1998, Krueger et al. 2013). We computed five MCIs: i) monsoon Hadley circulation index (MHI) (Goswami et al. 1999), ii) southern shear index (SSI) and iii) western shear index (WSI) (Wang and Fan 1999), iv) Indian monsoon index (IMI) (Wang et al. 2001), and v) Webster and Yang index (WYI) (Webster and Song Yang 1992). Details of these indices are listed in

Table 3.S1. Note that MCI refers to reanalysis-derived MCI hereafter unless stated otherwise, and that in their original definitions, some MCIs were calculated by first taking the anomalies from their climatologies but we have used the actual values; this should not affect our results as the correlation coefficient is not affected by changes in mean or scale in the two variables. Moreover, note that in our definition of SSI, the southern box extends only down to 10°S (rather than 15°S in the original definition). However, in all the datasets, the original and modified SSI series are in very good agreement (not shown); hence our results should not be affected by using a slightly different region. We also note that WYI quantifies variability of the entire tropical Asian monsoon (both the Indian subcontinent and vicinity of the Philippines) but does not reflect the regional characteristic, and so it does not properly measure SASM rainfall variability (Jianhua Ju and Slingo 1995, Wang 2000). Nevertheless, we included this index as it is still used in studies of SASM variability and the objective of this paper is to intercompare MCI-MRI variability for different datasets and indices.

We used three precipitation datasets: All-India rainfall (AIR) data – based on a weighted mean of 306 well distributed land stations over India (Parthasarathy et al. 1994), and two gridded datasets: APHRODITE (APHRO_MA 1003R1) (Yatagai et al. 2009) and Global Precipitation Climate Project version 2.2 (GPCP) (Adler et al. 2003). AIR is the longest series (1871-2011) and, APHRODITE and GPCP are available for 1951-2007 and 1979-2011 respectively. We computed three MRIs: AIMR from AIR, Indian summer monsoon rainfall (ISMR) (Parthasarathy et al. 1992) from APHRODITE and extended Indian monsoon rainfall (EIMR) (Goswami et al. 1999) from GPCP. Multiple MCIs and MRIs are considered to intercompare the results and to get an estimate of robustness of the results. However, most of the MRI analyses are limited only to AIMR as this is the longest series and MCIs showed similar low frequency

variations for all three MRIs for the overlapping periods as the MRIs are well correlated (e.g. see Fig. 3.S1). Note that MRI refers to AIMR hereafter unless stated otherwise.

3.2.2 Analysis methods

We used bootstrapping of the sliding correlation analysis to identify whether a low frequency variation of the MCI-MRI relationship is significantly different to that expected from two random series (i.e. noise) with the same statistical properties. However, bootstrapping can only be used for normal and serial independent series as this assumption is made in generating random test series (Gershunov et al. 2001). Accordingly, MCIs and MRI were tested for normality and independence. Normality was tested using the one-sample Kolmogorov-Smirnov test and independence was tested using the lag-1 autocorrelation (Table 3.S2). For the full period (1871-2011) 20CR MCIs does not satisfy the criteria of independence. Hence, the series does not meet the requirement for bootstrapping. NNRP1 is the second longest series (1948-2011), so we considered this period for normality and independence test, as this allows for the results to be compared in the two reanalyses. Here, AIMR and most MCIs from both reanalyses pass the normality test (two NNRP1 MCIs only just fail). Hence, we considered those series for 1948-2011 periods for bootstrapping. Details of bootstrapping of the sliding correlation analysis are explained by Gershunov et al. (2001), but we made following refinements for this study. Corresponding to each pair of MCI-MRI sliding correlation, 5000 pairs of correlated white noise series of equal length (64 years) were simulated with correlation coefficient set equal to the population correlation coefficient of the corresponding MCI-MRI sliding correlation. Then sliding correlation analysis was applied to each pair of white noise series for sliding window widths of 31, 21 and 11 years respectively. Next, the standard deviation (SD) of each

sliding correlation series is computed. Finally, SD values corresponding to 90th (95th, 99th) and 10th (5th, 1st) percentiles were computed from the 5000 SDs corresponding to each of the three sliding window widths and MCI-MRI sliding correlation (Table 3.S3). The SD of sliding correlations between observed series (i.e. MCI-MRI sliding correlation) must be outside 90th (95th, 99th) and 10th (5th, 1st) percentile limit to be considered significantly more or less variable than expected from sampling variability (i.e. noise) at 90% (95%, 99%) confidence level (in a one-tailed test).

3.3 Results

3.3.1 Variability of MCI-MRI relationship

We begin by examining how the relationship between circulation-based and rainfall-based monsoon indices has evolved over time, and whether the fluctuation, if any, is consistent across the indices and/or datasets. This is achieved by plotting the 21 year sliding correlation time series between AIMR and each MCI (Fig. 3.1). The most noticeable feature in the figure is the evidence of decadal and multi-decadal shifts in the strength of the correlation between 20CR MCIs and AIMR. These shifts occur must prominently in around 1890, 1930, 1955 and then a more gradual shift to lower correlations in the 1980s. Those early fluctuations in AMIR-20CR MCI correlations could not be verified because of unavailability of the other reanalysis data prior to 1948, however the broad agreement between MCIs for other reanalyses and those for 20CR after 1950 gives some confidence that the earlier fluctuations are not specific to 20CR, though it may well relate to low data input to reanalysis prior to 1948 (Fig. 3.S1).

Another interesting feature of Fig. 3.1 is the broad agreement in evolution of MCI-AIMR relationships among the MCIs. For example, the MCI-AIMR correlations were

highest for 1960-1980 but they have declined in the recent decades. The decline appears to be higher for zonal wind-based MCIs (zonal MCIs, viz. IMI, WSI and WYI) than meridional wind-based MCIs (meridional MCIs, viz. MHI and SSI). But, it should be noted that subtle inter-reanalysis difference persist for each MCI-AIMR relationship. Moreover, inter-reanalysis spread have generally increased for zonal MCI-AIMR relationships in recent decades. Also, 20CR IMI-AIMR correlation is less than corresponding correlation for other reanalyses for the entire data overlapping period. Similarly, ERAI meridional MCI-AIMR correlation is less than corresponding correlation for other reanalyses for most of the data overlapping period.

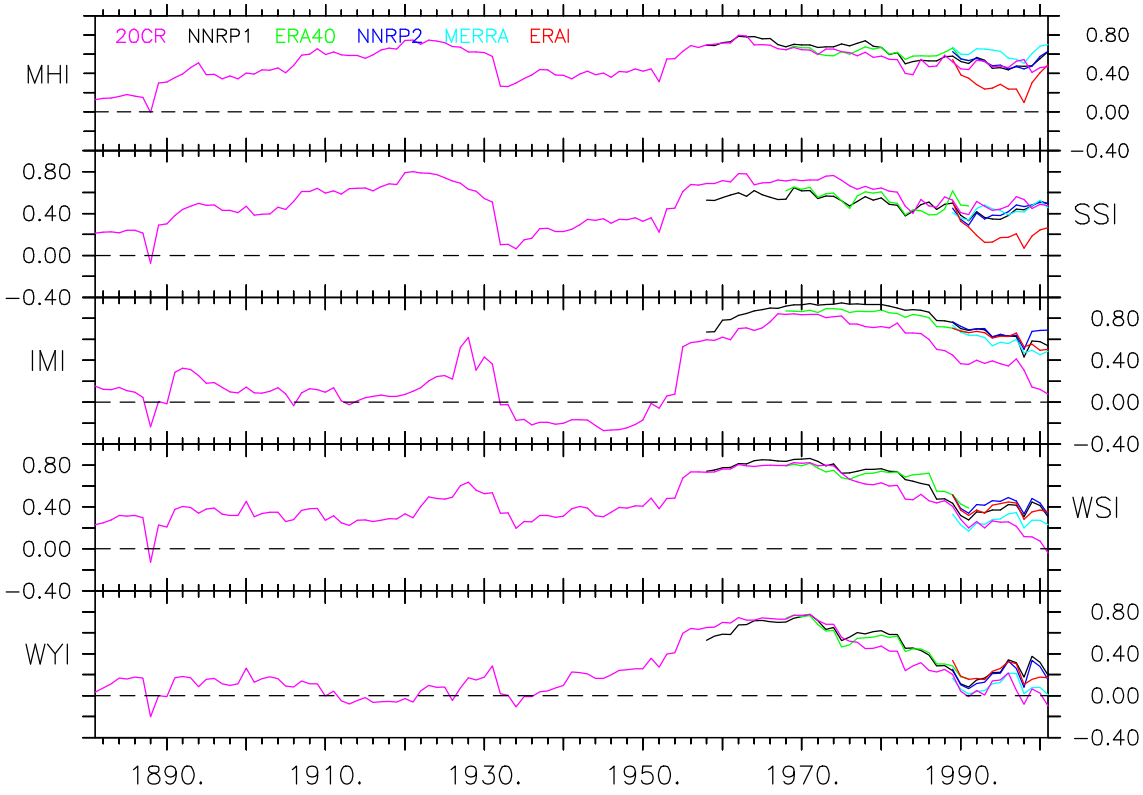

Fig. 3.1 Sliding correlation (21 year window) between MCIs and AIMR. Each MCI-AIMR sliding correlation is computed from six reanalyses.

3.3.2 Statistical significance of fluctuations in MCI-MRI relationships

The statistical significance of fluctuations in the MCI-AIMR correlations for 1948-2011 is tested using the method of bootstrapping (see analysis methods). For both 20CR and NNRP1, the SD of zonal MCI-AIMR sliding correlations (21 year sliding window) were higher than that expected due to sampling variability at 90% or higher confidence level, while the SDs of meridional MCI-AIMR sliding correlations were within the limit of sampling variability (Table 3.1). To address the issue of sensitivity of the results to sliding window width, we also computed above SDs for 11 year and 31 year sliding windows, but the results remained the same except in two instances, in which case SDs of NNRP1 zonal MCI-AIMR were within the sampling variability limit at 90% confidence level.

Table 3.1 Standard deviation of sliding correlation between 20CR (NNRP1) MCIs and AIMR for 1948-2011, and for 31, 21 and 11 year sliding windows.[1]

	20CR			NNRP1		
MCIs	31 year	21 year	11 year	31 year	21 year	11 year
MHI	0.071	0.104	0.125	0.076	0.103	0.143
SSI	0.076	0.119	0.225	0.072	0.080	0.199
IMI	**0.134**[c]	**0.209**[c]	**0.326**[c]	0.077	**0.136**[c]	**0.222**[c]
WSI	**0.188**[a]	**0.253**[b]	**0.330**[b]	**0.143**[b]	**0.196**[b]	**0.274**[c]
WYI	**0.220**[a]	**0.284**[b]	**0.375**[b]	**0.148**[c]	**0.204**[c]	0.280

[1] Numbers are rounded off to 3 digits. Significant values are indicated by boldface ([a, b] and [c] correspond to significance at 1%, 5% and 10% level respectively).

3.3.3 Possible causes of more significant fluctuations in MCI-MRI correlation

Given the consistent result of fluctuations in multi-decadal MCI-MRI correlation that are greater than that expected from a purely stochastic process, we next explored for possible physical causes behind this result.

3.3.3.1 Trend of monsoon indices

First, it is investigated whether trends in indices over the correlation sliding window play any role in fluctuation of strength of corresponding indices. To isolate the impact of local trend on variability of MCI-AIMR relationship, we plotted scatter plot between MCI-AIMR sliding correlation (21 year sliding window) and MCI (AIMR) sliding trend (21 year sliding window) corresponding to four different periods (viz., 1871-2011, 1948-2011, 1958-2001 and 1979-2011) taking consideration of availability of different reanalysis (not shown). Those plots did not depict strong relation between MCI-AIMR sliding correlation and MCI (AIMR) sliding trend. For further insight, we computed correlation between MCI-AIMR sliding correlation and MCI (AIMR) sliding trend for each of those periods (not shown). We found low correlation in almost all case except for two instances (where they exceed 0.707), which are likely chance occurrences.

In addition we detrended MCIs and AIMR using the method of least square fit and 21 year sliding window and plotted sliding correlation (21 year sliding window) between the detrended AIMR and each of the detrended MCIs. The resulting plot is remarkably similar to Fig. 3.1 (not shown). The scatter plot between MCI-AIMR sliding correlation and sliding correlation of corresponding detrended indices confirm this (Fig. 3.S2). Hence, local trend of indices does not have any influence in fluctuation MCI-MRI relationships.

3.3.3.2 Spatial shift: Shifts in center of action of monsoon circulation

Shifts in center of action of monsoon circulation is another potential cause for higher variability of AIMR and zonal MCI relationships. Such shifts may arise due to change in wind shear pattern associated with change in convection patterns. This is investigated by plotting i) monsoon climatological zonal (meridional) wind shear pattern and ii) temporal correlation maps between AIMR and monsoon mean zonal (meridional) wind shear pattern during the 21 year periods of high (1960-1980) and low (1990-2010) correlations. Here we present the results for NNRP1 but it remains essentially same for 20CR. Zonal (meridional) wind shear pattern over South Asia for the high and low correlation periods were very similar (pattern correlation >0.99) (Fig. 3.S3). But there was large difference in the correlation map between AIMR and zonal (meridional) wind shear during the high and low correlation periods (pattern correlation <0.5) (Fig. 3.2). During 1990-2010, correlation decreased not only inside the boxes (which represent the MCI averaging regions) but throughout South Asia. Hence, this rules out a shift in domain of high correlation from inside the MCI computation region to outside (i.e. to new center of action in monsoon circulation) or change in the wind shear pattern as a cause for change in zonal MCI-AIMR relationship for the two periods. Rather, this indicates break down in wind shear and MRI relationships over whole South Asia in the recent decades.

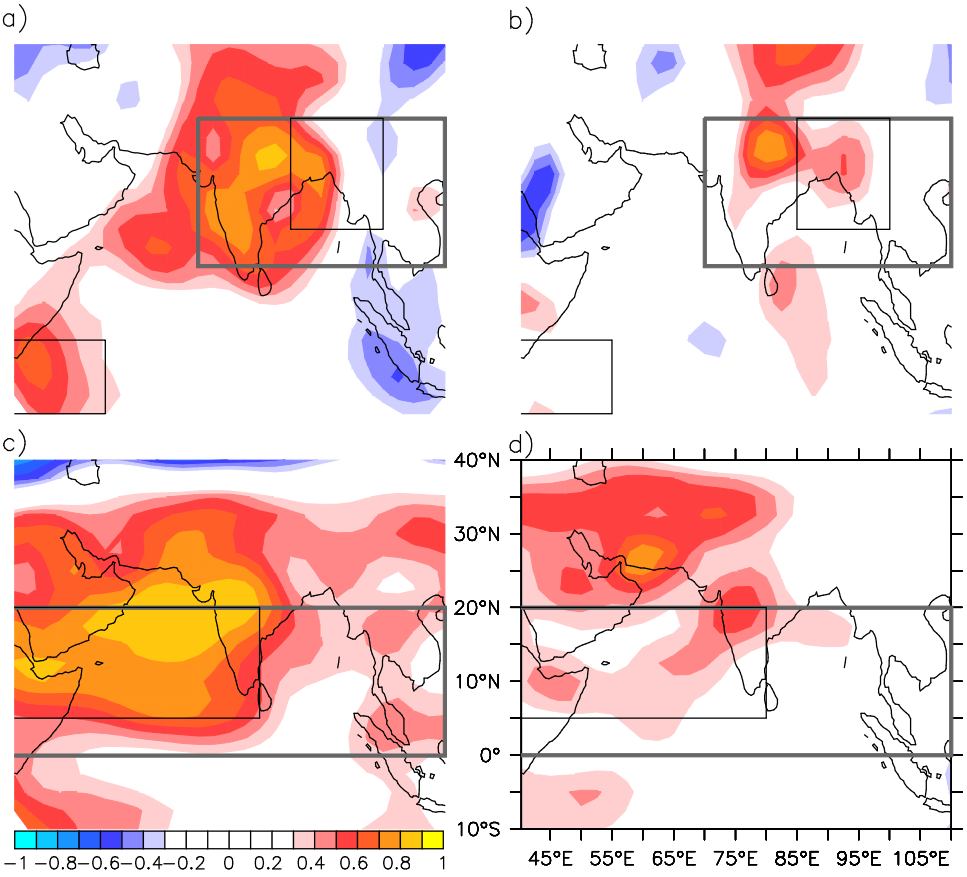

Fig. 3.2 Correlation map of NNRP1 meridional wind shear and AIMR for a) high (1960-1980) b) low (1990-2010) MCI-AIMR correlation periods. (c-d) Same as (a-b) but for NNRP1 zonal wind shear. Boxes enclose different MCI averaging regions.

3.3.3.3 Temporal shift: Shift in annual cycle of mean or variance of indices

The variation in strength of MCI-AIMR relationships could also arise due to temporal shift, for example, shifts in annual cycle of one or both the indices. Such shifts could either be a shift in the mean annual cycle or a shift in variance annual cycle. However, we did not find any shift in mean annual cycle for the indices we considered (one each from three different types of monsoon indices; i.e. MHI, WYI and AIMR) during the low and high correlation periods for both reanalyses (not shown). There were some differences in monthly variance of those indices but that did not alter the overall shape of seasonal cycles themselves.

3.3.3.4 Change in interannual variance of indices

Correlation between two indices might depend on their variability; with high variability associated with higher correlation. To investigate this, we examined scatter plots of MCI-AIMR sliding correlation and corresponding MCI sliding SD for different period (not shown). Those plots indicate some connection between the two. For further insight we computed the correlation between MCI-AIMR sliding correlation and corresponding MCI sliding SD for different period. In general, these correlations are found to be particularly good for the medium period (1948-2011, 1958-2001) (Table 3.S4). A similar result is seen for correlation between MCI-AIMR sliding correlation and AIMR sliding SD (Table 3.S5). Hence, the results are generally in conformity with the idea that higher variability of two variables could potentially increase their correlation though this relationship is not very well established for the recent period (1979-2011) when MCI-MRI sliding correlation has gradually declined. Moreover, this does not provide an insight for contrasting variability of zonal and meridional based MCIs with MRI.

3.3.4 Similarity of MCI correlations with observed and reanalysis MRIs

Finally we examined whether the fluctuations in correlations between MCIs and observed MRIs are also seen for MRIs derived from reanalysis precipitation. This provides insights on whether climate models can internally capture these changing relationships. For this we plotted the sliding correlation between MCIs and reanalysis-derived ISMR (EIMR) (Fig. 3.S4). We chose ISMR and EIMR here as AIMR is based on station average, which could not be computed using gridded data. Nevertheless, observed AIMR and ISMR are highly correlated (Fig. 3.S1). EIMR was also considered

to compare/ contrast among different MRIs, given EIMR is argued to be better correlated with MHI (Goswami et al. 1999). From a comparison of Fig. 3.S4 with Fig. 3.1, the sliding correlations show broadly consistent variations in the post 1950 period. For example, the temporal evolution is broadly consistent across the MCIs with the sliding correlation attaining maximum values around 1960-1980 but gradually declining in recent decades. However, compared to Fig. 3.1, the reanalysis MCI-ISMR sliding correlations were more broadly spread, but this was expected as both MCI and ISMR vary for each reanalysis here, unlike a unique AIMR for all reanalyses in Fig. 3.1. Another difference was the consistent higher sliding correlation for 20CR ISMR-zonal MCIs prior to 1950s for most of the period. Variations of reanalysis MCI-EIMR sliding correlations are broadly consistent with reanalysis MCI-ISMR sliding correlations (not shown). We also compared the sliding correlation between MCIs and APHRODITE ISMR/GPCP EIMR, and found that evolution of sliding correlation was comparable to that between MCI and AIMR for the data overlapping period (not shown). This shows that evolution of observed MCI-MRI relationship is broadly captured by the reanalysis simulations (i.e. reanalysis MCI and reanalysis MRI) and is independent of the MRI considered.

3.4 Conclusions and discussion

MCIs can provide useful insight in the study of SASM and its variability, and also form potentially useful metrics for model evaluation. From a modelling perspective, one advantage of MCIs compared to MRIs is they are not directly sensitive to the convective scheme and represent the large scale and three dimensional structure/dynamics of SASM system. However, since MRIs are the primary indicators of on the ground impact of SASM variability, evaluation of MCIs should ideally

provide information on the link between large scale processes and precipitation, which was certainly the case between the 1960s and 1980s – the period used for defining those MCIs.

We investigated the stability of several MCI-MRI relationships and found that interdecadal variability of meridional MCI-MRI relationships were within the limit expected due to sampling variability for 1948-2011. But, interdecadal fluctuations of zonal MCI-MRI relationships were significant at 90% or higher confidence level for the same period. Local variability of the indices generally show good correlation with the contemporary strength of MCI-MRI relationships, however, our investigation did not reveal any further insight in contrasting variability of zonal and meridional based MCIs with MRI. Nevertheless, it is possible that the high variability of zonal MCI-MRI relationships is physically based, such as low-frequency variability in the large-scale ocean atmosphere system. For example, the increasing trend in the frequency of El Ninos has been linked to weakening easterly shear over the Indian monsoon region through eastward shift and weakening of the east-west Walker circulation (Tokinaga et al. 2012, Vecchi et al. 2006, Zhang and Song 2006).

There has been large increase in concentration of Atmospheric Brown Cloud aerosols over South Asia in recent decades (Turner and Annamalai 2012), particularly over north India (north of 20°N) (Bollasina et al. 2011). Although the overall impact of aerosol on the SASM is still unclear, this might be partly responsible for contrasting relationship of the zonal and meridional MCIs with MRIs in recent decades, given the meridional MCIs include north and/or northeast India region in their domains but zonal MCIs do not. A plausible explanation is that any local circulation and rainfall changes induced by change in aerosol concentration are in tandem, leading to analogous changes in meridional MCIs and MRIs (as they both include north India in their domain) leaving

the meridional MCI-MRI relationships relatively intact. On the other hand, north India lies at the fringe of the zonal MCIs domain so any aerosol related impact on those and MRIs are likely to be asymmetric leading to destabilisation of the zonal MCI-MRI relationships.

Similarly, Murugavel et al. (2012) noted a small increase in all-India summer monsoon rainfall despite large increase in the all-India averaged convective available potential energy (CAPE) and speculated that increasing trend in CAPE may be compensating for weakening monsoon circulation and, thus, maintaining the Indian summer monsoon rainfall.

In order to understand the possible influence of other factors in fluctuating MCI-MRI relationships, monsoon mean interannual time series is plotted for a few other indices or variables averaged over appropriate regions (Fig. 3.S5 and Table 3.S6). There is no clear trend for indices/metrics such as Nino 3.4 index and soil moisture content averaged over South Asia but clear trend exist in others. For example, snow cover averaged over Tibetan region is sharply declining and surface temperature averaged over South Asia is clearly increasing. Arguably, slight increasing trend also exists for IOD and atmospheric water vapour pressure especially since around 1960 and 1970 respectively. It is plausible that some of these time series, especially those having clear increasing or decreasing trend depict good correlation with MCI-MRI sliding correlation. Under such scenario, one might be tempted to argue that those indices/ metrics “explain” the fluctuations in MCI-MRI correlations. However, it should be borne in mind that good correlation between two parameters does not imply a causal relationship between the two, unless it is substantiated by a clear physical mechanism.

Here also, significant decreasing trend of snow cover over Tibet likely have a tendency to enhance summer monsoon rainfall as suggested by Shekhar and Dash (2005) through modulation of sensible and latent heat flux. But in reality this might be compensating for weakening monsoon circulation and, thus, maintaining the Indian summer monsoon rainfall.

In summary, even though some inference can be made by comparing Fig. 3.1 and 3.S5 on likely factors contributing to fluctuating MCI-MRI relationships, further research is needed to arrive at a firm conclusion.

Nevertheless, the variable nature of MCI-MRI relationships likely has a few implications. Firstly, in evaluation of MCIs, as well as MCI-MRI relationships in models they should not necessarily be expected to generate higher values, rather shifts in the correlations are probably as important as the correlation themselves. Secondly, though dynamic factors have been considered while defining MCIs, as for many other indices, the common approach used to identify a MCI is to construct correlation map between MRI and the wind shear field and then isolate local regions with large correlations and finally compute the spatial average over the region as an index. According to Delsole and Shukla (2012), this methodology is a form of screening and Delsole and Shukla (2009) showed that this kind of screening typically leads to large bias in skill measures. So it is advisable that all MCIs are revisited and their usefulness re-evaluated employing longer period data as well as avoiding screening problem.

Acknowledgements

Three reanalyses (NNRP1 NNRP2, 20CR) and a precipitation dataset (GPCP) were downloaded from Earth System Research Laboratory, National Oceanic and

Atmospheric Administration (http://www.esrl.noaa.gov/psd/data/gridded). MERRA dataset was downloaded from Goddard Earth Science Data and Information Services Center (http://disc.sci.gsfc.nasa.gov/mdisc). Similarly, ERA40 and ERA Interim dataset were downloaded from European Centre for Medium-Range Weather Forecasts (http://data-portal.ecmwf.int). AIR data is downloaded from Indian Institute of Tropical Meteorology (ftp://www.tropmet.res.in/pub/data/rain/iitm-regionrf.txt). APHRODITE data was downloaded from APHRODITE's Water Resources

(http://www.chikyu.ac.jp/precip/products/index.html). We also acknowledge use of the Ferret program, a product of NOAA's Pacific Marine Environmental Laboratory, for analysis and graphics in this paper. First author thanks the Felix Scholarships for funding his DPhil. R. Jones was supported by the Joint DECC/Defra Met Office Hadley Centre Climate Programme (GA01101).

Supplementary Information: Chapter 3

Table 3.S1 List of monsoon indices and their definition.

Name	Definition	Reference
All India monsoon rainfall (AIMR)	Monsoon (JJAS) mean rainfall derived from All-India rainfall monthly rainfall time series developed by IITM	Parthasarathy et al. (1994)
Indian summer monsoon rainfall (ISMR)	Monsoon mean rainfall averaged over 70°–90° E, 5°–25° N (land points only)	Parthasarathy et al. (1992)
Extended Indian monsoon rainfall (EIMR)	Monsoon mean rainfall averaged over 70°–110° E, 10°–30° N (both land and ocean)	Goswami et al. (1999)
Monsoon Hadley Circulation Index (MHI)	Monsoon mean meridional wind shear at lower tropospheric level (LTL) and upper tropospheric level (UTL), averaged over 70° –110° E, 10°–30° N	Goswami et al. (1999)
Southerly Shear Index (SSI)	Monsoon mean meridional wind shear at LTL and UTL, averaged over combined regions of 85-100° E, 15°–30° N and 40-55°E, 10° S–0° N	Wang and Fan (1999)
Indian Monsoon Index (IMI)	Difference in monsoon mean LTL zonal wind averaged over 40°–80° E, 5°–15° N and 70°–90° E, 20°–30° N	Wang et al. (2001)
Westerly Shear Index (WSI)	Monsoon mean zonal wind shear at LTL and UTL, averaged over 40°–80° E , 5°–20° N	Wang and Fan (1999)
Webster and Yang index (WYI)	Monsoon mean zonal wind shear at LTL and UTL, averaged over 40°–110° E, 0°–20° N	Webster and Yang (1992)

Table 3.S2 Test of normality and independence of MCIs and AIMR[1].

	1871-2011		1948-2011			
	p-value	Lag-1 auto-correlation	p-value	Lag-1 Auto-correlation	p-value	Lag-1 Auto-correlation
MCIs	20CR		20CR		NNRP1	
MHI	**0.410**	0.345	**0.588**	**0.119**	**0.955**	**0.028**
SSI	**0.952**	0.280	**0.758**	**0.034**	**0.85**	0.181
IMI	0.019	0.527	**0.867**	**0.039**	**0.549**	**0.013**
WSI	**0.887**	0.319	**0.911**	**0.009**	**0.491**	**0.022**
WYI	**0.347**	0.320	**0.965**	**0.081**	**0.732**	0.279
AIMR	**0.192**	**-0.092**	**0.342**	**-0.076**		

[1] Normal and independent values are shown in boldface.

Table 3.S3 Percentiles of the bootstrapped standard deviation of sliding correlations corresponding to 20CR/NNRP1 MCIs and AIMR mean correlation coefficients for 1948-2011 (64 years), and for 31, 21 and 11 year sliding windows[1].

MCI	R	31 year						21 year						11 year					
		10	5	1	90	95	99	10	5	1	90	95	99	10	5	1	90	95	99
20CR																			
MHI	0.597	0.036	0.032	0.025	0.112	0.13	0.169	0.06	0.052	0.04	0.172	0.196	0.255	0.123	0.109	0.087	0.277	0.307	0.366
SSI	0.552	0.039	0.034	0.027	0.12	0.14	0.183	0.065	0.057	0.045	0.183	0.21	0.263	0.134	0.118	0.097	0.293	0.324	0.37
IMI	0.497	0.042	0.036	0.029	0.13	0.15	0.193	0.071	0.063	0.051	0.196	0.222	0.281	0.145	0.132	0.106	0.31	0.336	0.399
WSI	0.549	0.04	0.034	0.027	0.121	0.139	0.181	0.067	0.058	0.045	0.183	0.209	0.262	0.134	0.12	0.095	0.291	0.319	0.378
WYI	0.441	0.046	0.039	0.032	0.138	0.16	0.205	0.077	0.067	0.053	0.208	0.236	0.289	0.16	0.143	0.116	0.323	0.35	0.411
NNRP1																			
MHI	0.636	0.033	0.028	0.022	0.105	0.123	0.163	0.056	0.048	0.038	0.16	0.182	0.228	0.113	0.101	0.078	0.263	0.293	0.354
SSI	0.504	0.043	0.037	0.029	0.129	0.15	0.193	0.072	0.063	0.048	0.198	0.225	0.282	0.143	0.128	0.104	0.305	0.337	0.391
IMI	0.742	0.024	0.021	0.017	0.081	0.096	0.124	0.041	0.035	0.027	0.126	0.147	0.187	0.084	0.073	0.058	0.211	0.24	0.31
WSI	0.636	0.033	0.028	0.022	0.102	0.118	0.154	0.056	0.049	0.037	0.16	0.185	0.239	0.114	0.101	0.08	0.26	0.287	0.346
WYI	0.472	0.045	0.039	0.03	0.134	0.155	0.199	0.073	0.064	0.05	0.201	0.228	0.286	0.151	0.134	0.107	0.312	0.34	0.394

[1] Because of stochastic nature of computation, the percentiles computed slightly differ in each computation with identical setting.

Table 3.S4 Correlation between MCI-AIMR sliding correlation (21 year window) and corresponding MCI sliding SD (21 year window)[1].

	1871-2011	1948-2011		1958-2001			1979-2011				
MCI	20CR	20CR	NNRP1	20CR	NNRP1	ERA40	20CR	NNRP1	NNRP2	MERRA	ERAI
MHI	**0.13**[c]	**0.81**[a]	**0.89**[a]	**0.82**[a]	**0.94**[a]	**0.74**[a]	0.15	0.26	0.34	**0.53**[b]	-0.22
SSI	0.05	**0.87**[a]	**0.66**[a]	**0.92**[a]	**0.68**[a]	**0.48**[a]	**0.66**[a]	**0.88**[a]	**0.8**[a]	**0.49**[b]	-0.78
IMI	-0.31	**0.92**[a]	**0.77**[a]	**0.92**[a]	**0.84**[a]	**0.74**[a]	**0.83**[a]	**0.4**[c]	**0.85**[a]	**0.83**[a]	**0.73**[a]
WSI	**0.57**[a]	**0.96**[a]	**0.76**[a]	**0.96**[a]	**0.79**[a]	**0.55**[a]	**0.71**[a]	0.29	0.21	0.26	**0.52**[b]
WYI	**0.20**[b]	**0.96**[a]	**0.62**[a]	**0.96**[a]	**0.68**[a]	**0.52**[a]	-0.18	-0.12	0.13	0.24	**0.46**[c]

[1] Significant values are indicated by boldface (a, b and c correspond to significance at 1%, 5% and 10% level respectively).

Table 3.S5 Correlation between MCI-AIMR sliding correlation (21 year window) and AIMR sliding SD (21 year window) [1].

	1871-2011	1948-2011		1958-2001			1979-2011				
MCI	20CR	20CR	NNRP1	20CR	NNRP1	ERA40	20CR	NNRP1	NNRP2	MERRA	ERAI
MHI	**0.33**[a]	**0.66**[a]	**0.81**[a]	**0.69**[a]	**0.81**[a]	**0.67**[a]	**0.4**[c]	0.2	0.16	**0.42**[c]	0.05
SSI	**0.56**[a]	**0.78**[a]	**0.73**[a]	**0.79**[a]	**0.75**[a]	**0.63**[a]	0.28	-0.06	-0.09	0.34	0.06
IMI	**0.56**[a]	**0.88**[a]	**0.87**[a]	**0.89**[a]	**0.92**[a]	**0.92**[a]	**0.41**[c]	**0.62**[b]	**0.46**[c]	**0.45**[c]	**0.53**[b]
WSI	**0.39**[a]	**0.86**[a]	**0.91**[a]	**0.84**[a]	**0.92**[a]	**0.86**[a]	**0.44**[c]	-0.33	**0.52**[b]	**0.39**[c]	**0.42**[c]
WYI	**0.39**[a]	**0.84**[a]	**0.9**[a]	**0.82**[a]	**0.92**[a]	**0.88**[a]	**0.4**[c]	-0.66	0.16	0.27	0.29

[1] Significant values are indicated by boldface (a, b and c correspond to significance at 1%, 5% and 10% level respectively).

Table 3.S6 List of indices / metrics plotted in Fig. 3.S5 and their computation region

Index / metric	Computation region	Dataset / Data Source	Reference
ENSO (Nino 3.4)	SST averaged over 5 S-5 N, 170-120 W	HadISST1 www.esrl.noaa.gov/psd/gcos_wgsp/Timeseries/Data/nino34.long.data	(Rayner et al. 2003)
IOD	Difference of SST averaged over 50-70 E, 10 S-10 N and 90-110 E, 10 S-0 N	HadISST1	(Rayner et al. 2003)
Snow cover	Averaged over Tibetan region (65-105 E, 26-46 N)	NHSC - Northern Hemisphere EASE-Grid Snow Cover and Sea Ice Extent ftp://ftp.cdc.noaa.gov/Datasets/snowcover/snowcover.mon.mean.nc	(Robinson et al. 1993)
		NSIDC - Global monthly satellite-derived snow water equivalent climatology	(Armstrong et al. 2005)
		MODIS/Terra snow cover (MOD10CM)	(Hall et al. 2006)
Surface temperature	Averaged over South Asia (60-90 E, 5-30 N)	Climatic Research Unit (CRU) High Resolution Gridded Data of Month-by-month Variation in Climate	(Harris et al. 2014)
Water vapour pressure	Averaged over South Asia (60-90 E, 5-30 N)	CRU High Resolution Gridded Data of Month-by-month Variation in Climate	(Harris et al. 2014)
Soil moisture	Gangetic plain (70-90 E, 23-27 N)	CPC soil moisture water height from a model ftp://ftp.cdc.noaa.gov/Datasets/cpcsoil/soilw.mon.mean.v2.nc	(Van den Dool et al. 2003)

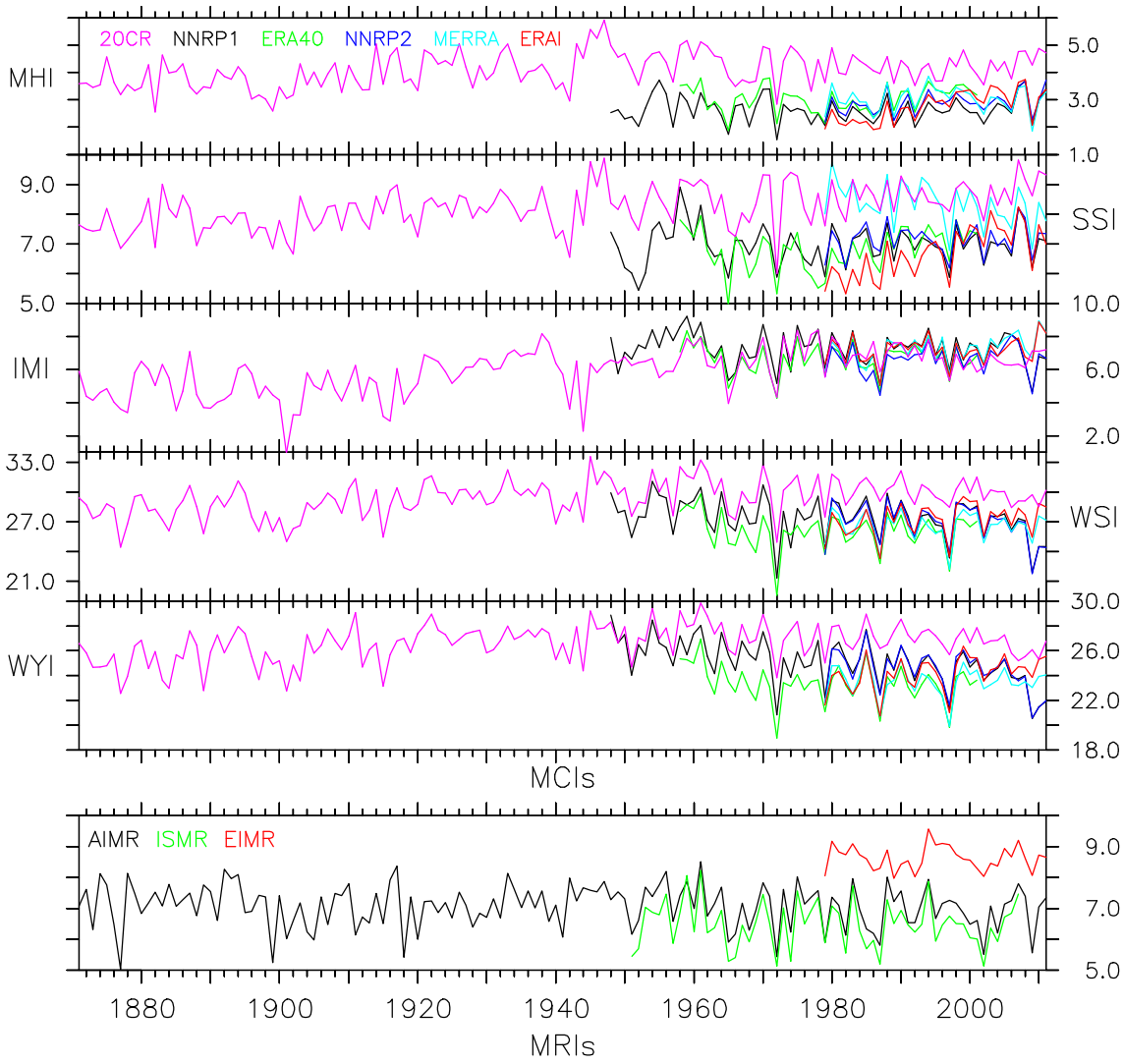

Fig. 3.S1 MCIs and MRIs time series[1].

[1] Each MCI is computed from six reanalyses.

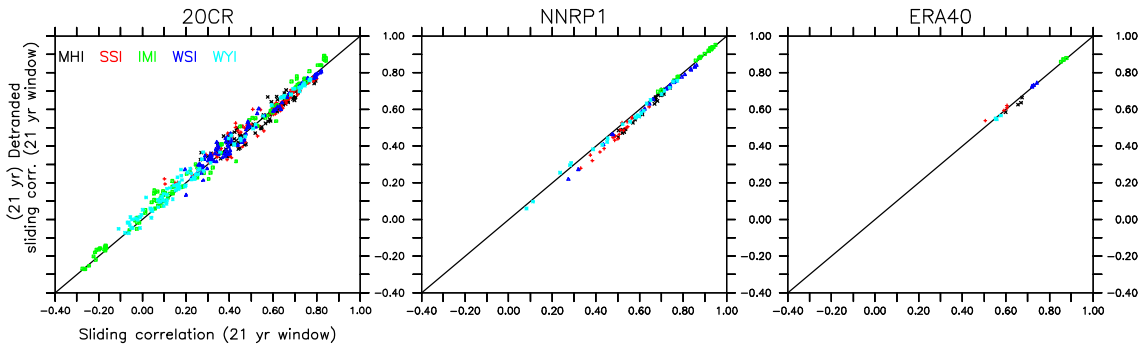

Fig. 3.S2 Scatter plot of MCI-AIMR sliding correlation and sliding correlation of corresponding detrended indices for full data available period[1].

[1] As 21 year sliding window is used for detrending and computing sliding correlation of the detrended data, this result in reduction of 40 data points (years) from the time series, hence no point remains for plotting from the shorter datasets (i.e. NNRP2, MERRA and ERAI).

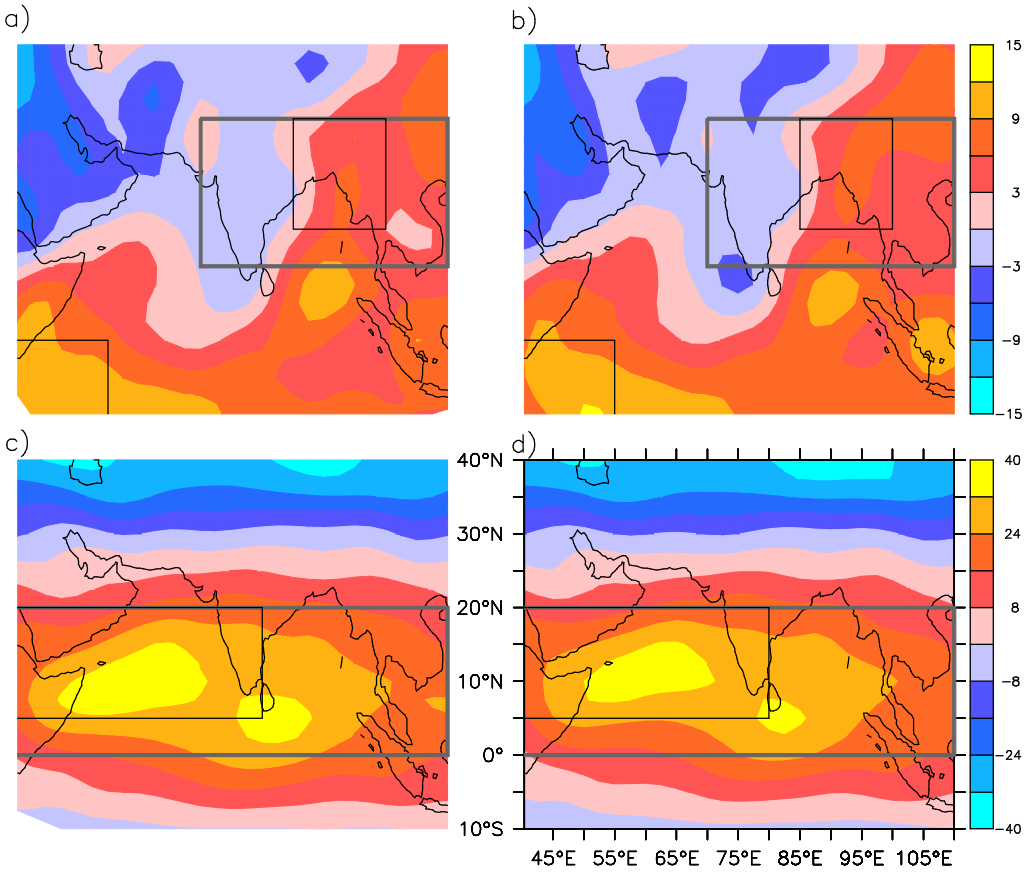

Fig. 3.S3 NNRP1 climatological meridional wind shear for the period of a) high (1960-1980) b) low (1990-2010) correlation with AIMR. (c-d) Same as (a-b) but for NNRP1 zonal wind shear.

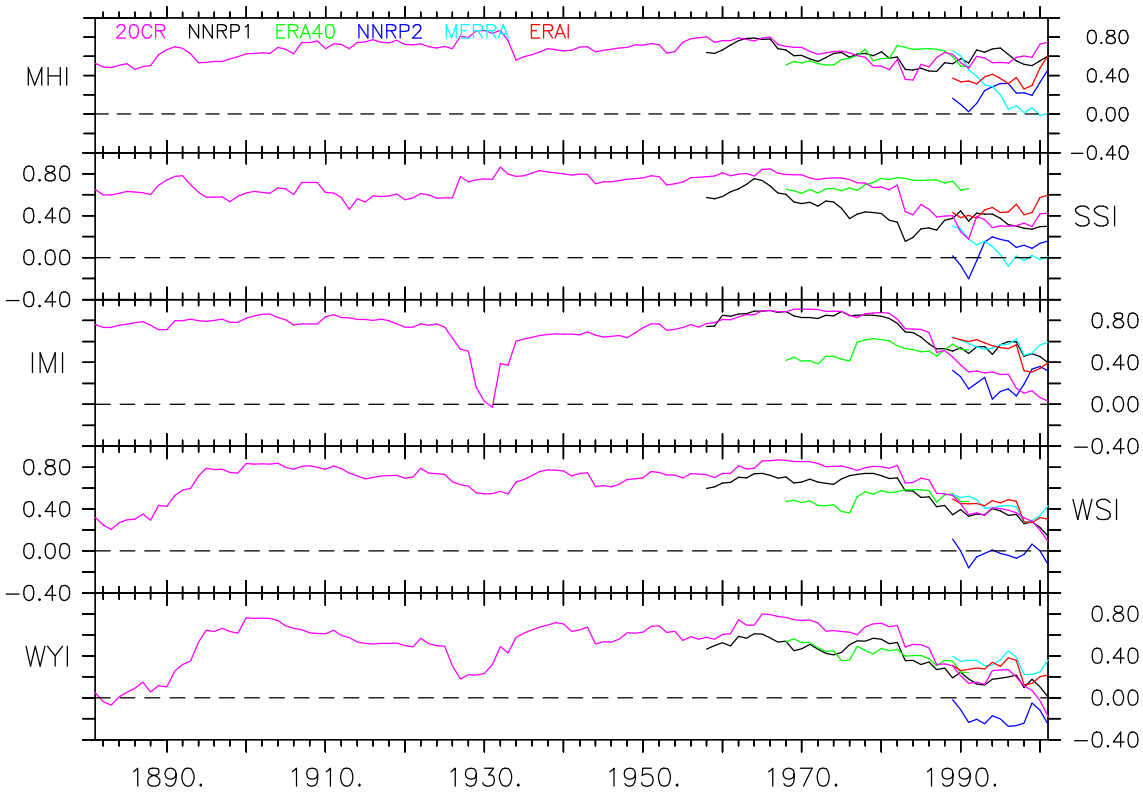

Fig. 3.S4 Sliding correlation (21 year window) between reanalysis MCIs and reanalysis ISMR.

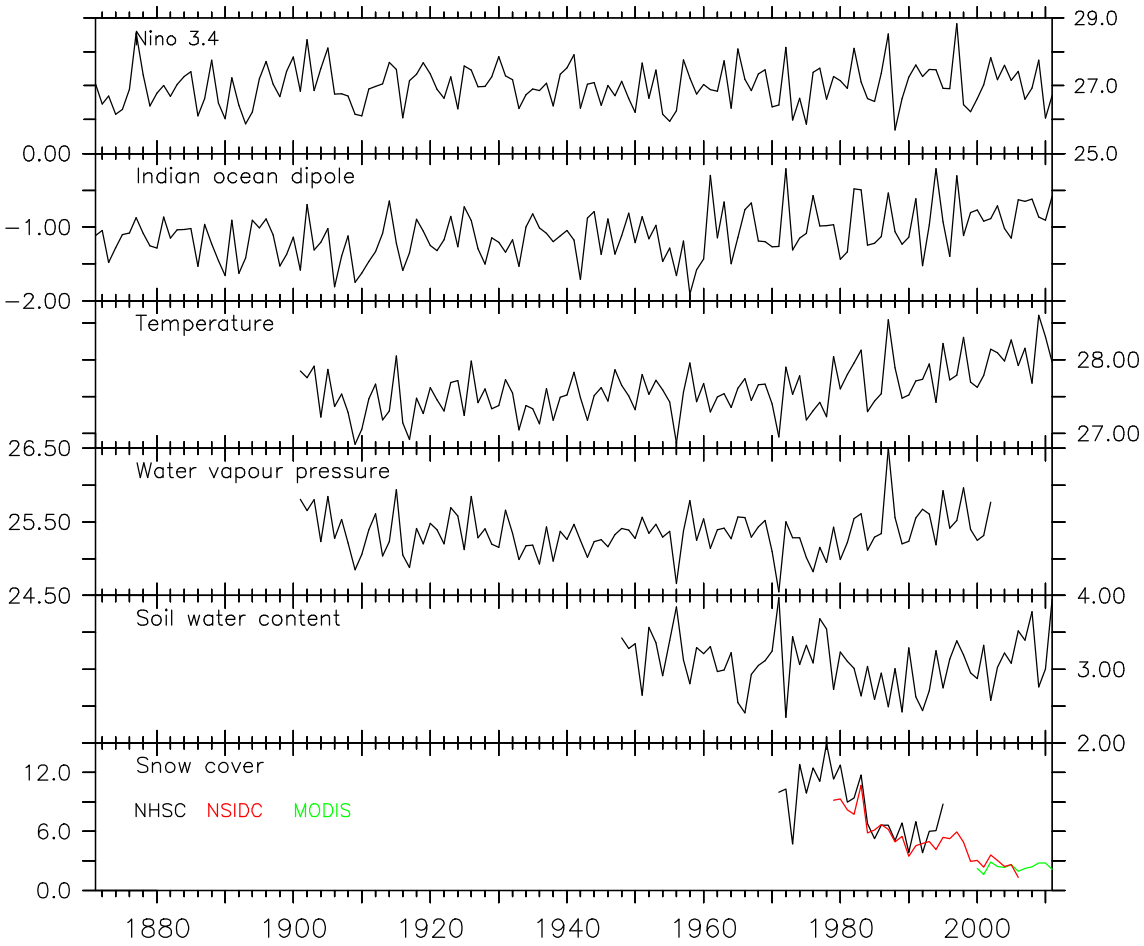

Fig. 3.S5 Monsoon mean time series for Nino 3.4 (unit: °C), Indian Ocean Dipole (unit: °C), Surface temperature (unit: °C), Water vapour pressure (unit: hpa), Soil water content (unit: m) and Snow cover (unit: %) series[1].

[1] See Table 3.S6 for further details.

4 Sensitivity of systematic biases in South Asian summer monsoon simulations to regional climate model domain size and implications for downscaled regional process studies

Synopsis

In the previous chapter, it is found that monsoon rainfall indices – monsoon circulation indices relationships exhibit considerable low frequency variability though the extent of variability differs for zonal and meridional wind based indices. In light of those findings, the paper suggested caution in interpreting such relationships in model simulations and recommended further research to establish the cause of contrasting variability. Based on those findings, monsoon circulation indices were considered to provide limited utility in assessment of model simulation in this chapter. In addition, they were not used in the subsequent chapters partly because the domain of RCM integration is smaller than the areal extent of the averaging region of any of the monsoon circulation indices.

This chapter seeks to address the research question no. 2 identified in chapter 2, which is: To what extent the choice of domain size and location affect the "added value" that an RCM can offer? To achieve this, simulations from the Hadley Centre global model – HadGEM3 and its regional version, run over a number of targeted domains, were assessed in order to investigate the nature of the inherent systematic errors in simulating SASM. As shown later, results suggest that RCM simulations are sensitive to the choice of domain size and its location. Further investigation reveals that systematic errors in the Hadley Centre model system are mainly produced by local processes in the simulation of the SASM and their key source regions lies at the periphery of the main area of interest (i.e. South Asian land mass). This enables setting up of a moderately sized domain that includes the main area of interest (South Asia) and also minimizes the systematic errors inherent in the model. This moderately sized domain is also used in subsequent chapters.

Authorship Declaration

I carried out all the analysis and writing of the paper. R. Jones and R. C. Levine contributed to the planning the paper through the discussion on the methodology and structure of the paper. They also helped select RCM simulations. R. C. Levine also gave useful advice on computation of the thermodynamic vertical profile. R. C. Levine and W. Moufouma-Okia carried out the model simulations and provided the data for analysis undertaken in this chapter. M. New helped plan the analysis and gave advice on the methodology. R. C. Levine and M. New edited text and all authors were involved in editing the drafts.

Sensitivity of systematic biases in South Asian summer monsoon simulations to regional climate model domain size and implications for downscaled regional process studies

J. Karmacharya[1,2], R.C. Levine[3], R. Jones[1,3], W. Moufouma-Okia[3] and M. New[1,4]

Affiliations:

[1] School of Geography and the Environment, University of Oxford, Oxford, United Kingdom

[2] Department of Hydrology and Meteorology, Kathmandu, Nepal

[3] Met Office Hadley Centre, Exeter, United Kingdom

[4] African Climate and Development Initiative, University of Cape Town, Cape Town, South Africa

Climate Dynamics, 45: 213-231. doi: 10.1007/s00382-015-2565-6

Received: 6 March 2014 / Accepted: 16 March 2015 / Published online: 31 March 2015

Abstract

Global climate models (GCMs) have good skill in simulating climate at the global scale yet they show significant systematic errors at regional scale. For example, many GCMs exhibit significant biases in South Asian summer monsoon (SASM) simulations. Those errors not only limit application of such GCM output in driving regional climate models (RCMs) over these regions but also raise questions on the usefulness of RCMs derived from those GCMs. We focus on process studies where the Hadley Centre RCM is driven by realistic lateral boundary conditions from atmospheric re-analysis which prevents remote systematic errors from influencing the regional simulation. In this context it is pertinent to investigate whether RCMs also suffer from similar errors when run over regions where their parent models show large systematic errors. Furthermore, the general sensitivity of the RCM simulation to domain size is informative in understanding remote drivers of systematic errors in the GCM and in choosing a suitable RCM domain that minimizes those errors. We investigate Met Office Unified Model systematic errors in SASM by comparing global and regional model simulations with targeted changes to the domain and forced with atmospheric re-analysis. We show that excluding remote drivers of systematic errors from the direct area of interest allows the application of RCMs for process studies of the SASM, despite the large errors in the parent global model. The findings in this study are also relevant to other models, many of which suffer from a similar pattern of systematic errors in global model simulations of the SASM.

Keywords:

South Asian summer monsoon, systematic bias, regional climate model, domain size

4.1 Introduction

Global climate models (GCMs) are the primary tool for global climate simulation (Nikulin 2012). They perform reasonably well at the global scale and are able to capture large scale climate features. However, due to their coarse resolution they lack fine scale details and climate extremes (e.g., Duffy et al. 2003). Moreover, they fail to resolve important local to regional scale processes which could lead to systematic regional biases. For example, many GCMs have difficultly simulating even the basics of South Asian summer monsoon (SASM) such as the distribution of seasonal mean precipitation. In particular, many GCMs have a systematic wet bias over the equatorial Indian Ocean (EIO) and dry bias over central India during the monsoon (Sperber et al. 2013). Historically GCMs (both atmosphere only and couple atmosphere-ocean) have difficulty simulating SASM (e.g., Annamalai et al. 2007a, Kripalani et al. 2007). Even though there has been overall progress in simulating SASM those systematic errors still persist. For example, Coupled Model Intercomparison Project-5 (CMIP5) models show improvement over Coupled Model Intercomparison Project-3 (CMIP3) models in simulating various aspects of the Asian summer monsoon, of which SASM is an integral part but significant biases still persist (Sperber et al. 2013).

Regional climate models (RCMs) are widely used for dynamical downscaling. This is applied both to the downscaling of relatively coarse resolution GCM output at high resolution over a limited area (Wilby and Fowler 2010) and to regional process studies where high-resolution simulations are forced at the boundaries by realistic fields from atmospheric re-analysis. RCMs currently operate at horizontal resolutions of the order of several tens of km or even less and provide physically consistent climatic information at fine spatial and temporal scale. Though RCMs were initially developed and tested for

the mid-latitudinal climate most of the RCMs have been used successfully across the globe including for tropical climate. In particular, a number of RCM have been successfully used in numerous studies on the SASM. Some of those studies focused on validation of RCMs under present climate (e.g., Dobler and Ahrens 2010, Philippe et al. 2011, Polanski et al. 2010, Saeed et al. 2012); while others tested the linkage of SASM with other climatic forcings such as Eurasian snow cover (e.g., Shekhar and Dash 2005). Yet others made future projection of SASM (Ashfaq et al. 2009, Kumar et al. 2011a, Kumar et al. 2011b, Kumar et al. 2006, Syed et al. 2014).

The standard approach used in dynamical downscaling using RCMs is to use the one way nesting technique in which the RCM receives the meteorological field from the coarse resolution (GCM or re-analysis) driving data at its lateral boundaries at regular intervals. Based on that information the RCM generates its own simulation within the domain while maintaining consistency with the driving field at the lateral boundary. In this regards size and location of the RCM domain plays an important role in its simulation. Given the sensitivity of the RCM simulation to its domain, it is advised that they should be large enough so that RCM can freely generate circulation within its domain but not so large that simulation deviates significantly from the large scale feature of the driving model (Jones et al. 1995). However, some recent studies recommended using very large domain with semi hemispheric extent. For example, Diaconescu and Laprise (2013) showed that RCMs run over a very large domain can reduce some of the large scale errors present in the driving field.

It is to be noted that above recommendations are based primarily on studies done over mid-latitude. In contrast, Bhaskaran et al. (1996) found that simulation of SASM large scale circulation in a RCM is relatively insensitive to the domain size, which they attributed to inherent differences between mid-latitude and tropical dynamics. On the

other hand, a recent study noted that SASM simulation of seasonal mean hydrological cycle and daily precipitation variability at a sub domain (that extends from 74°-90°E and 16°-28°N) is sensitive to the domain size (Bhaskaran et al. 2012). Nevertheless, the choice of the regional domain has generally been heuristic (Leduc et al. 2011). For example, very large domains are employed in COordinated Regional climate Downscaling EXperiment (CORDEX) framework so as to cover the continents with minimum sets of domains (Giorgi et al. 2009).

It is also worth noting the importance of using high quality large-scale data sets for dynamical downscaling. Irrespective of the quality of the RCM used for downscaling in the absence of a good quality driving field, good results cannot be expected (Giorgi and Mearns 1999). This leads to an interesting question: is it rational to run a RCM (derived from a GCM) forced by a realistic lateral boundary condition (LBC) over a region where the parent GCM simulation depicts significant systematic errors? This is a relevant question because RCM model physics are either the modified version of existing limited area model or the full physics of a GCM is implemented within a regional dynamical framework (Giorgi and Mearns 1999). In either case, all the physical components of RCMs are similar or more detailed than those in GCMs. It might be expected that RCMs would behave similar to its parent model. However, given the sensitivity of RCM simulations to its domain, can we select a suitable domain to overcome those systematic errors inherent in the parent model? It might be possible to exploit the sensitivity of a RCM towards its domain for identification of suitable domain provided parent model's inherent systematic errors over the region are largely forced by local processes and their key source regions lies at the periphery of the main area of interest.

This paper aims to address this question by focusing on the role of domain size in overcoming systematic errors inherent in parent (Global) model's simulation of SASM, when such model is used in regional mode, and with "unbiased" forcing/boundary conditions. In other words, we seek to demonstrate how a RCM with inherent SASM bias in parent model can be used for downscaled process studies with a careful selection of its domain. These results help understand how different elements of the systematic error interact within the monsoon region and inform the choice of domain size.

A brief survey of previous studies on SASM bias in global models is presented in section 4.2. The data and methods are described in section 4.3. The results are presented in section 4.4 followed by discussions and conclusion in section 4.5.

4.2 Previous studies on SASM bias in global models

Before presenting our results, we first briefly review some previous work on systematic errors in GCM SASM simulations, which help us understand interconnections among the different elements of systematic errors.

The systematic error in climate simulations of the SASM has been a long-term problem for the MetUM and other models, with the structure of the systematic error in MetUM simulations being robust since HadGEM1 and continuing through HadGEM2 and more recent climate configurations of the MetUM (Johnson et al. 2015, Levine and Turner 2012, Martin et al. 2010, Walters et al. 2013). Moreover, sensitivity tests have shown that changes in horizontal resolution (up to N512) have minimal impact on the systematic error in these configurations of the MetUM, though they have a somewhat larger impact in the most recent MetUM configurations (e.g. GA5 and GA6) (Johnson et al. 2015). The typical systematic error has persisted in both atmosphere only and

ocean-atmosphere coupled configurations of the MetUM since HadGEM1 (Levine and Turner 2012, Martin et al. 2006) and is composed broadly of three elements: a wet bias over the EIO, a wet bias over the Himalayas, and a dry bias over a zonal band covering central India, the Western Ghats and the western BoB (Fig. 4.S1) (Levine and Turner 2012, Martin et al. 2006). Most of the CMIP3 and CMIP5 models and their respective multi model ensemble means also have similar biases (e.g., Annamalai et al. 2007a, Bollasina and Nigam 2009, Bollasina and Ming 2013, Sperber et al. 2013).

Excessive precipitation over the EIO seems to be an inherent feature of the MetUM rooted in its convection scheme which develops preferential convection over areas of large heat and moisture availability such as the EIO (Levine and Turner 2012). Martin et al. (2010) noted that excess EIO precipitation also appears in MetUM's short time-scale (1 to 5 day) forecasts, and before the dry bias develops over India, suggesting a direct effect of convection parameterization on the equatorial bias. This also suggests excessive convection over EIO may play a role in driving the Indian dry bias by weakening the moisture transport towards India. Furthermore, sensitivity studies have shown that targeted weakening of the EIO bias such as–suppression of the EIO convection via introduction of a cold EIO SST anomaly in the MetUM results in enhanced moisture transport towards India and enhanced Indian precipitation (Levine and Turner 2012). In addition, a MetUM experiment performed by Bush et al. (2014) found that suppression of the EIO convection by enhancing convective entrainment shifts precipitation towards India. On the other hand Levine and Turner (2012) noted that excess precipitation over the Himalayas appears to be a MetUM inherent deficiency in resolving the interaction of low-level monsoon flow with the Himalayan orography. They also found enhanced orographically induced precipitation over the Himalayan foothills in scenarios which reduce precipitation over central India, suggesting a link

between these two biases. These results suggest that the dry bias over central India is coupled with the wet bias over the EIO and the Himalaya.

Many other models have comparable biases in simulation of the SASM and similar mechanisms have been proposed to explain them. For example, Rockel and Geyer (2008) noted that overestimation of precipitation over mountains and warm oceans seem to remove too much moisture from the atmosphere resulting in less water vapour transport towards other areas. Similarly Bollasina and Ming (2013) suggested that spring-time wet EIO biases, arising from excessive model response to the local meridional SST gradient through enhanced near-surface meridional wind convergence, are associated with a consistent anomalous precipitation and circulation pattern over the whole Indian region via establishment of an anomalous Hadley-type meridional circulation, whose northern branch subsides over northeastern India significantly affecting the monsoon evolution and supressing early monsoon rainfall.

4.3 Data and methods

4.3.1 Data

The European Centre for Medium-Range Weather Forecasts interim reanalysis (ERAI) (Dee et al. 2011) is used to drive a nudged global model and all RCMs as described below. It is also used to evaluate model simulated upper-level atmospheric circulations.

Precipitation observations came from the global precipitation climatology project (GPCP) version 2.2 (Huffman et al. 2009) at monthly resolution and GPCP One-Degree daily version 1.2 (Huffman et al. 2001). GPCP monthly dataset is derived by combining the multi-satellite estimate with a precipitation gauge analysis and its One-Degree daily

precipitation dataset is based on a merged Infrared radiometers over the 40°N-40°S latitude band and a rescaled Television and Infrared Observation Satellite Operational Vertical Sounder at higher lititudes. To ensure temporal homogeneity of these produces GPCP reprocessed the entire record with the new gause analysis.

Daily precipitation is also taken from the station based product of APHRODITE's APHRO_MA_V1003R1 (Yatagai et al. 2009). The monsoon Asia sector (60°-155° E, 0°-55°N) of this daset is based on around 3000 to 8500 stations (vary from year to year), which were selected after extensive quality control procedure at each station Indian meteorological department (IMD) gridded daily precipitation data (Rajeevan and Bhate 2009) is also used. This dataset is based on 3500 stations on the average but the station density varies from year to year. So there is a possibility of temporal inhomogeneities in the above datasets. APHRODITE is chosen as the reference dataset because of its high temporal and spatial coverage and station density especially over the Himalayas. Finally, an independent observational dataset is also considered: the tropical rainfall measuring mission (TRMM) 3B42V6 at daily resolution (Huffman et al. 2007). The daily accumulated precipitation product is derived from a 3-hourly product (3B42), which is estimated from the combination of microwave and infrared observations. In common with other short interval precipitation estimates these estimates show considerably more uncertainity. Different precipitation datasets provide an estimate of observational uncertainty.

4.3.2 Models

A recent configuration of the UK Met Office Unified Model (MetUM) is used in this study. The MetUM is a highly flexible model that is designed to use in both climate research and numerical weather prediction (NWP) activities at global as well as regional

configurations (Cullen 1993). The dynamical core of the atmospheric component of the MetUM uses a semi-implicit, semi-Langrangian formulation to solve the non-hydrostatic, fully-compressible deep atmosphere equations of motion (Davies et al. 2005) and includes a comprehensive set of parameterizations describing the land surface (Best et al. 2011, Clark et al. 2011), boundary layer (Lock et al. 2000), convection (Gregory and Rowntree 1990) and cloud microphysics (Wilson and Ballard 1999).

In this study, climate configurations of the MetUM in atmosphere-only mode (HadGEM) are applied; specifically the Global Atmosphere versions 2 and 3 (GA2 and GA3) (Walters et al. 2011). The model systematic errors in climate simulations of the SASM are robust across these model versions and earlier climate configurations of the MetUM (Johnson et al. 2015, Levine and Turner 2012, Martin et al. 2010, Walters et al. 2013). The two model versions are similar but there are a few notable differences in their formulation, such as treatment of ozone absorption in the ultra-violet, microphysics scheme, shallow convection diagnosis, land surface scheme etc. Walters (2011) provides detail description of the model physics and the differences in two model versions and their impacts.

4.3.3 Experimental framework

Three types of experiments are carried out to understand influence of domain size and shape on the inherent model biases.

a) A GCM simulation – to identify the inherent SASM systematic biases in the model

b) A nudged GCM simulation - to separate out circulation related biases in SASM simulation from moisture and convection related biases

c) RCM simulations over four different domains – to understand interaction of different elements of the systematic error within the South Asia region and identify appropriate domain.

A brief summary of these simulations and the underlying reason behind running them are discussed below and recapped in Table 4.1.

Table 4.1 List of model simulations.

Sr. no.	Run ID	Model version and resolution	Spatial coverage, (area in million square km)	Initialization	Analysis period
a)	GA	GA3 (N216, ~0.83°)	Global	Jan 1979	Dec 1989-Nov 2008
b)	GAN	GA2 (N96, ~1.88°)	Global with nudging over CORDEX South Asia domain (CSAD)	Jan 1989	“
c)	R3	GA3-RA, 0.44°	CSAD, (69.1)	Jan 1989	“
d)	R3B	“	Small reference domain, (24.6)	“	“
e)	R2N	GA2-RA, 0.44°	CSAD, but exclude equatorial Indian Ocean, (42)	“	Dec 1989-Nov 1998
f)	R2S	“	CSAD, but exclude northern part, (49)	“	Dec 1989-Nov 1999

4.3.3.1 Global Atmosphere climate model simulations

a) GA – GA3 (i.e. HadGEM3) simulation at high resolution (N216, approximately 0.83°) forced only by daily observed SSTs and sea ice, so atmospheric simulation is unconstrained. The simulation depicts the systematic errors inherent in the model. As shown later, basic structure of this bias has persisted across different versions and horizontal resolution of GA.

b) GAN – GA2 (i.e. HadGEM2) simulation at coarse resolution (N96, approximately 1.88°) with large-scale dynamical fields nudged towards driving reanalysis over the CORDEX South Asia domain (CSAD) (Giorgi et al. 2009). Grid-point nudging is done for zonal and meridional wind and potential temperature fields at upper and mid atmospheric levels. The simulation has the freedom of unconstrained simulation over the globe outside the CSAD. As the integration is nudged towards the driving data within the CSAD this simulation serves to indicate the performance of the modelling system over this region in the absence of large-scale mid to upper- level atmospheric biases.

As shown later, the resolution difference in GA and GAN has minimal impact compared to the impact of the nudging. This is because the Global Atmosphere physical formulation is designed to be independent of horizontal resolution and thus to perform consistently across a wide range of applications. Model evaluation across a range of horizontal resolutions shows that there are generally no large changes in the basic atmospheric state (Walters et al. 2011); however, the simulation at increasing resolution does enable the model to represent the details of both regional and local climate better. A more in depth analysis of sensitivity of MetUM simulations to horizontal resolution is discussed in Johnson et al. (2015).

4.3.3.2 Regional climate model simulations

As mentioned above, regional configuration of HadGEM (i.e. HadGEM-RA) is employed in this study, which is described below:

a) R3 – GA3-RA (regional configuration of the GA3) simulation over CSAD. See Fig. 4.1 for boundaries of all RCM domains. CSAD is the largest RCM domain used in this study. This simulation covers almost all local systems/regions relevant to SASM. Also the large size of the domain allows it to simulate its internal circulation more independently from the near-perfect LBC. Hence, systematic errors seen in this experiment can be attributed to regional forcing.

b) R3B – GA3-RA simulation using a smaller sub-domain, which is the same as the smallest domain in Bhaskaran et al. (1996). This domain includes the major topographical feature of the Himalayas and is presented as an example of an appropriate domain in which the effects of inherent systematic errors on our region of interest (South Asia) are minimised.

c) R2N – GA2-RA (regional configuration of the GA2) simulation over a truncated CSAD that excludes roughly the southern one-third (including EIO) from the CSAD. As shown later, the EIO is a region of large wet bias, so this simulation serves to quantify impacts of exclusion of a key bias prone region from CSAD in simulation of SASM over rest of the region.

d) R2S – Same as R2N but excludes the northern one-third (including the Himalayas) from the CSAD. As shown later, the Himalayas is a region of large wet bias, so this simulation serves to quantify impacts of excluding another bias prone region from CSAD. Note that, for consistency, R2N and R2S are compared against R2 (regional configuration of GA2), which is same as R3 except for the model version. As shown

later, SASM precipitation climatology difference in R2 and R3 is rather small compared to their biases.

Note that the final two experiments are performed to get an estimate of sensitivity of the model simulation to extreme domain set ups which entirely exclude a key bias prone region, and are by no means considered viable domains for SASM simulations.

All RCM simulations are performed on a rotated coordinate system, at 0.44° horizontal resolution and with a buffer zone of eight grid-points at the lateral boundary. They are driven by ERAI initial and lateral boundary condition, and the latter is updated every six hours. Eight grid-points along the rim of RCM outputs in the native grid are discarded and the remaining grid-points are transferred onto a standard lat-long grid of 0.5° resolution using bilinear interpolation whereas the global model simulation are on a standard lat-long grid. All the analysis are confined within South Asia represented by a region that extends from 40° - 110° E and 10° S - 40° N.

In all the simulations SST and sea-ice fraction are prescribed at lower boundary from a high resolution (0.25°) dataset (Reynolds et al. 2007) at daily interval. Simulations are initialized from January 1989 except for GA which is initialized from January 1979. A minimum of 11 months at the beginning is left as spin up, so data is available for analysis from December 1989 to November 2008 except for the R2N and R2S which is available for a shorter period (about 9-10 years) but that should not be problematic as the sole purpose of those simulations is to test sensitivity of the RCM to an extreme domain configuration.

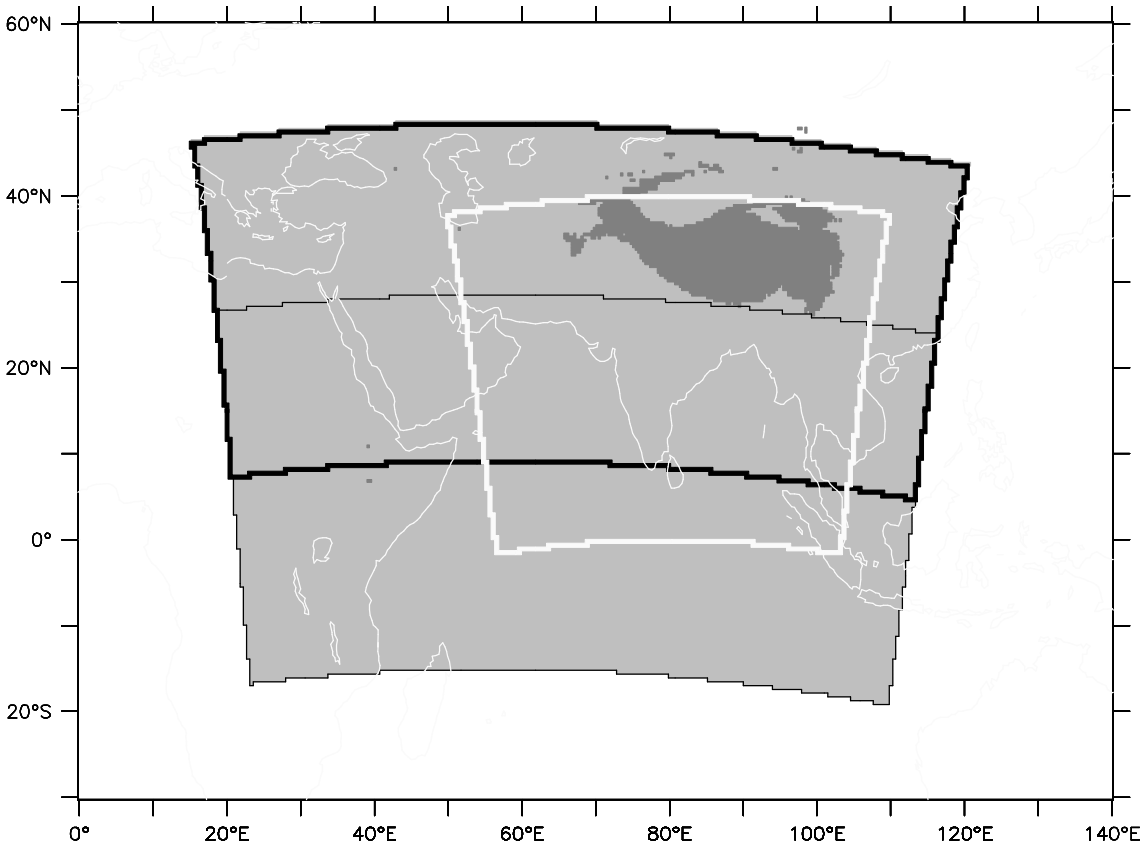

Fig. 4.1 RCM domains. The CSAD is shaded in light grey. R2N domain excludes area south of thick black line and R2S domain excludes area north of thin black line. R3B domain is enclosed by white line. Elevation above 3000 m is shaded grey.

4.3.4 Analysis methods

We focus our analysis on monsoon precipitation variability at climatological, interannual and intraseasonal timescales using daily and monthly mean data extracted for the relevant variables from the models and the observations. We also investigate interannual variability of monsoon circulation indices (MCIs). A number of monsoon indices, based on seasonal mean precipitation and circulation are used to investigate interannual variability of the SASM (Table 4.2). It is noted that R3B domain covers only about 80% of the monsoon Hadley index (MHI) (Goswami et al. 1999) computation region and about 60% or less of other MCI computation regions. Hence,

only MHI is computed for R3B. Also, a sensitivity test showed that the slight difference in the regions used for the MCI computations has only a small impact on the result. Furthermore, a central Himalayas monsoon rainfall index (CHMRI) is defined as the seasonal (monsoon) mean precipitation averaged over 80°– 88° E, 26°–30° N.

Table 4.2 Monsoon indices.

Name	Definition	Reference
Indian Summer Monsoon Rainfall (ISMR)	JJAS seasonal mean precipitation averaged over 70°–90° E, 5°–25° N (land points only)	Parthasarathy et al. (1992)
Monsoon Hadley Circulation Index (MHI)	JJAS seasonal mean meridional wind shear at lower tropospheric level (LTL) and upper tropospheric level (UTL), averaged over 70° –110° E, 10°–30° N	Goswami et al. (1999)
Webster and Yang index (WYI)	JJAS seasonal mean zonal wind shear at LTL and UTL, averaged over 40°–110° E, 0°–20° N	Webster and Yang (1992)
Westerly Shear Index (WSI)	JJAS seasonal mean zonal wind shear at LTL and UTL averaged over 40°–80° E, 5°–20° N	Wang and Fan (1999)
Indian Monsoon Index (IMI)	Difference in JJAS seasonal mean LTL zonal wind averaged over 40°–80° E, 5°–15° N and 70°–90° E, 20°–30° N	Wang et al. (2001)

Taylor diagrams are used to evaluate spatial patterns of climatological monsoon precipitation and interannual variability of monsoon indices. These diagrams provide a concise statistical summary of how well patterns (not restricted to spatial dimensions) of a variable from different sources match with each other in terms of their correlation, root mean square difference (RMSD) after removing the means and ratio of their variances (Taylor 2001). It is also useful in comparing several diagnostics and models

in combinations. In (normalized) Taylor diagrams, the radial distance from the origin to a point is proportional to the (normalized) standard deviation (SD) of the fields and the azimuthal positions give the correlation coefficient between the test and reference fields. Similarly the distance between the test and the reference points give (normalized) RMSD after removing the means. Note that RMSD hereafter refers to the normalized RMSD after removing the mean. Also all normalization is done with respect to the SD of the reference field and the reference point is situated at abscissa equal to 1 in the normalized Taylor diagram.

Northward propagation of summer monsoon intraseasonal oscillation is analysed as a measure of model skill in simulating intraseasonal aspect of SASM precipitation. It is isolated as follows: i) All observed and simulated daily precipitation data is interpolated to a common 1° resolution grid using linear interpolation and filtered using 30-50 day lanczos bandpass filter, ii) Data for the monsoon period are extracted for each year and iii) the lag correlation is computed between resulting 30-50 day filtered monsoon precipitation, zonally averaged between 70-100° E, with respect to itself at 85° E, 12° N (Lin et al. 2008). Note that the reference point is shifted by 2° N in case of R2N as its inner domain only reaches to 13° N at its southern end.

4.4 Results

4.4.1 Mean state

4.4.1.1 Basic systematic errors in the global models

Fig. 4.2a shows spatial distribution of SASM mean precipitation in observations (APHRODITE over land and GPCP over ocean). Precipitation maxima are located over the windward side of the mountains (e.g. the Western Ghats, the Arkan mountains,

northeast India and the central Himalayas), northeast Bay of Bengal (BoB) and east-central India, and the minima over the leeward side of the Western Ghats, the Arkan mountains (i.e. interior of Myanmar), the Himalayas (i.e. Tibetan Plateau) and western part of South Asia. The GA, similar to its predecessors, simulates excess precipitation over EIO and the Himalaya, and deficient over India (Fig. 4.2b). As discussed earlier, the excess precipitation over EIO and the Himalayas is directly linked with the precipitation deficit over central India.

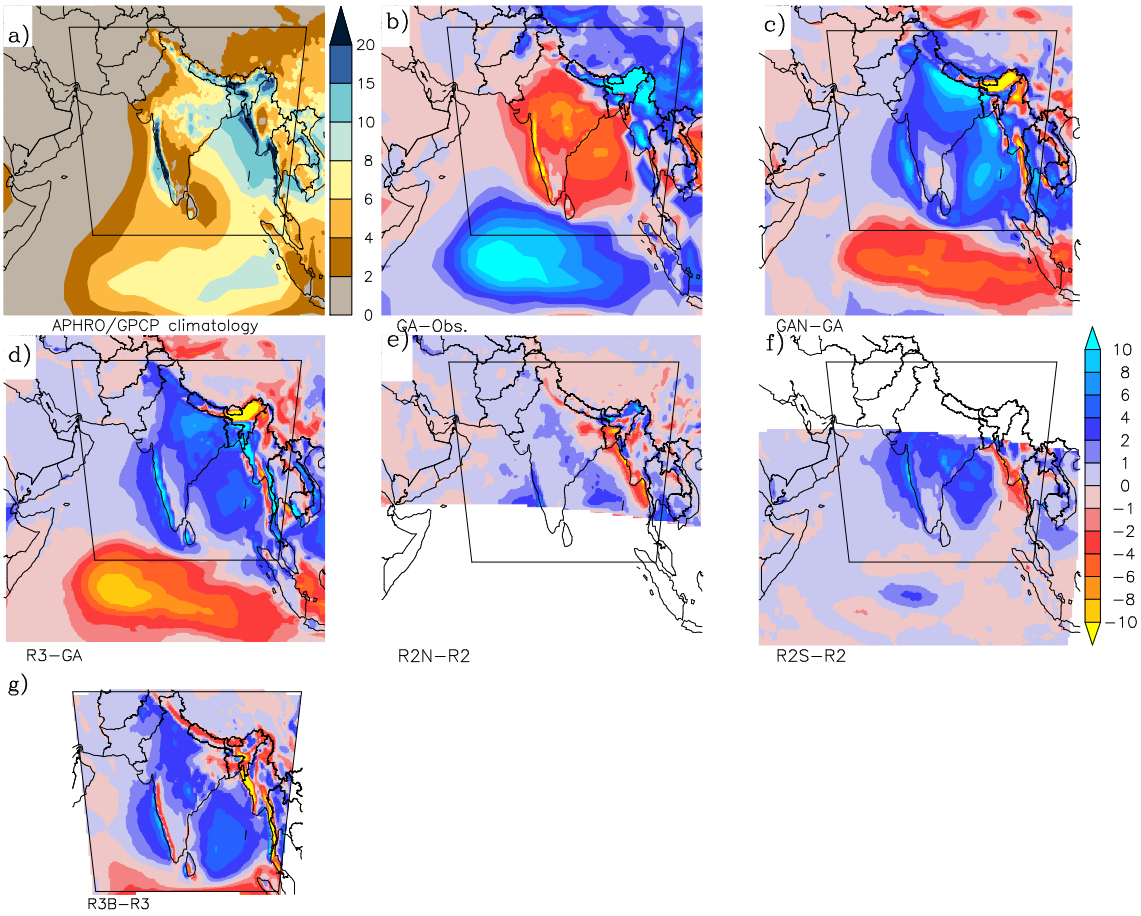

Fig. 4.2 Climatological monsoon mean precipitation for a) APHRODITE (1990-2007) over land and east of 60° E longitude and GPCP (1990-2008) over the rest, and the differences in b) GA from the observed climatology in a), (c-d) GAN and R3 from GA, (e-f) R2N and R2S from R2 and g) R3B from R3. Difference is calculated for 1990-2008 in (c-g) except for e) 1990-1998 and f) 1990-1999. R3B inner domain is also drawn in all plots. Unit: mm/day.

It is well known that the monsoon is associated with seasonal reversal of winds and that monsoon precipitation is largely controlled by the strength of the monsoon circulation. Fig. 4.3 and 4.4 shows the lower and upper level SASM mean circulation. The SASM circulation is characterised by the Findlater jet - a core of strong southwesterly wind off the Somali coast - and the monsoon trough over north India at the lower tropospheric level (LTL: 850 hpa) (Fig. 4.3a) and Tibetan anticyclone over the Himalayas and easterly jet over peninsular India at the upper tropospheric level (UTL: 200 hpa) (Fig. 4.4a). At the LTL, GA has a weaker Findlater jet than observations. The jet tends to diverge at landfall over India, resulting in an anomalously strong branch of westerly flow over north India. Overall there is anomalous anticyclonic circulation over central India and much weaker moisture flux towards the peninsular and north India (Fig. 4.S2b). Seasonal mean thermodynamic diagram at a location over central India (80° E, 22° N) shows that GA simulation is several degree warmer in the lower level (up to 700 hpa) and dryer throughout the troposphere compared to ERAI (Fig. 4.S3). Though, the atmosphere is in conditionally unstable state, lifting condensation level is much higher (~700 hpa) due to lack of low level moisture. This is consistent with the GA dry bias over India. On the other hand, the convergence and anomalous strong low-level flow into the eastern Himalayas is consistent with the large wet bias over north-east India. Moreover, the GA simulation shows excessive low-level convergence over the EIO with anomalous drawing in of air from both sides of the equator (Fig. 4.3b) consistent with the wet bias. Similarly, the simulation shows excessive upper-level divergence with anomalous north- and southwards outflow from the excessive EIO convection (Fig. 4.4b).

In the nudged GAN simulation mean precipitation is reduced over the EIO, eastern Himalayas, and increased over most of India, BoB and the eastern Arabian Sea

(windward side of the Ghats) compared to GA. This results in a reduction of rainfall biases over most areas, though GAN has further excessive precipitation over the Himalayan foothills (Fig. 4.2c). Note that GA and GAN use different model versions, but as discussed in section 4.3 and shown in Fig. 4.S1 the model systematic biases are robust across model configurations, and GAN and the other GA2-RA simulations are used here for the purpose of general sensitivity experiments. We also note that the horizontal resolution differs between GA and GAN, but the impact of the resolution difference (N216 Vs N96) is minimal compared to that of nudging (Fig. 4.S4).

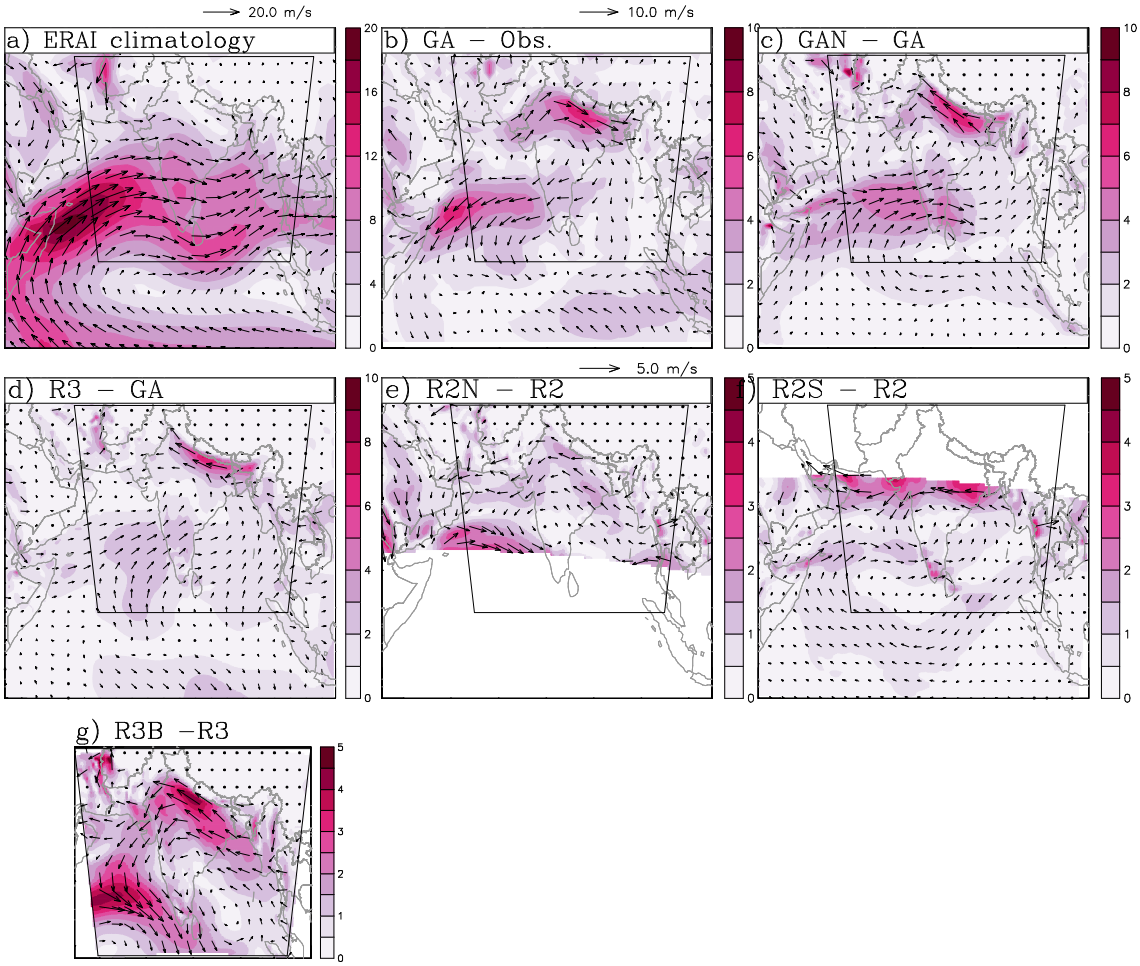

Fig. 4.3 As in Fig. 4.2 but for circulation at lower tropospheric level (850 hpa). ERAI circulation for 1990-2008 is shown in a). Arrows and shading show wind vectors and wind speed respectively. Unit: m/s.

GAN, being a nudged experiment, has minimal circulation biases, especially at mid to upper levels. Hence, most of the GA circulation biases are rectified in GAN. For example, removal of the upper level divergence (Fig. 4.4c) and also weakening of the lower level convergence over the EIO (Fig. 4.3c) coincides with suppression of the EIO wet bias. As mentioned earlier, this favours precipitation over India (e.g., Bush et al. 2014, Levine and Turner 2012). But despite near-perfect winds, a dry bias persists over central India owing to deficits in lower level moisture influx from the Arabian Sea (Fig.

4.S2c). Furthermore, precipitation is concentrated over the Himalayan foothill, highlighting the inherent MetUM orographic bias (Levine and Turner 2012).

Thermodynamic profiles over central India reveal the presence of a very dry stable layer in the lower atmosphere in the control simulation (GA), as evidenced by the close alignment of the temperature profile with the dry adiabat and lack of moisture at low-levels, which provides very unfavourable conditions for the development of convection. The vertical profiles are much improved in GAN compared to GA, and are in good agreement with ERAI, except for a slight dryness at lower levels. This can be anticipated because of the nudging at the upper levels and is consistent with enhanced inflow of moisture and precipitation over central India compared to GA (Fig. 4.S3).

Hence, GAN shows that a large portion of the systematic error in the GA climatology resides in its circulation related deficiencies which can be removed by nudging the GCM circulation towards the reanalysis. Clearly, GA circulation errors are forced both remotely as well as locally; though GAN rectifies almost all circulation biases, this experiment does not reveal their source. Next we isolate the local/regional circulation biases in the model over the South Asian region by forcing the regional version of the model with reanalysis which provide unbiased boundary forcing. RCM simulations over different domain allow us to examine the model sensitivity to size/location of the domain and isolate the key bias prone regions in South Asia.

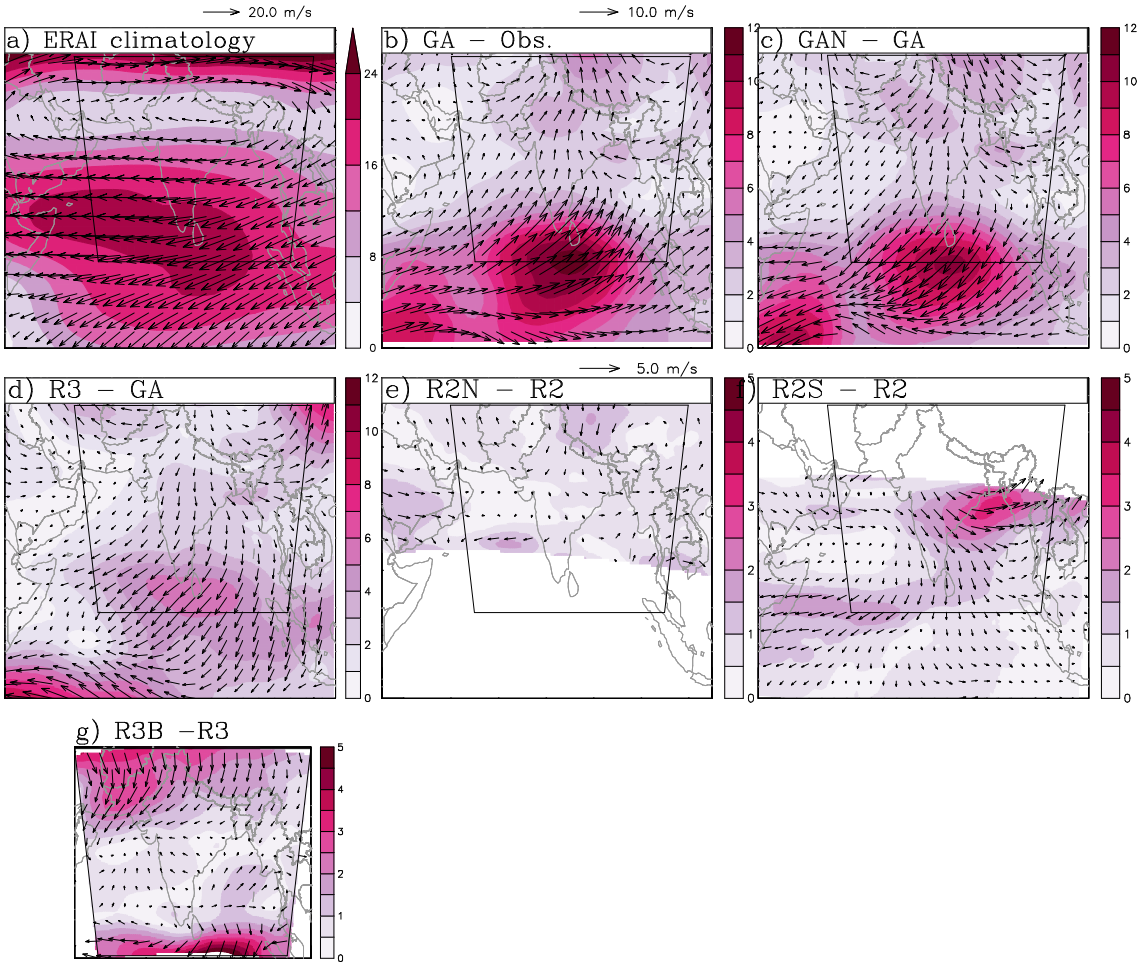

Fig. 4.4 Same as Fig. 4.3 but for upper tropospheric level (200 hpa).

4.4.1.2 Sensitivity of the systematic errors in RCM simulations

The R3 simulation of mean precipitation is broadly similar to GAN, with precipitation reduction over the EIO and eastern Himalayas and enhancement over central India, BoB and the Western Ghats (Fig. 4.2d). This shows that even though the high resolution global model has large systematic biases in simulating the SASM, there is scope for using its regional configuration for realistic simulation of SASM precipitation by imposing circulation constraints at its lateral boundaries. Yet it can be inferred from Fig. 4.2b and 4.2d that biases still persist in R3. The direct effect of the boundary conditions can be seen as substantial changes in the wind fields near the southern boundary of the

RCM domain. Similar to GAN simulation, the location of the southern boundary directly prevents anomalous exchange of air with the southern hemisphere at both lower and upper levels which weakens the lower level convergence (Fig. 4.3d) and the upper level divergence (Fig. 4.4d). This will act to modulate the magnitude of the model preferred convection and rainfall over the EIO. The increase in rainfall over India and the BoB is likely a response to the suppressed EIO convection (e.g., Bush et al. 2014, Levine and Turner 2012)

We next present some examples of the impact of size and location of the RCM domain on the simulation of mean precipitation. But first we note that similar to GCM simulations, difference in RCM configurations (GA2-RA Vs GA3-RA) has minimal impact on SASM simulation, which can be inferred by comparing seasonal mean precipitation difference in the two versions against their biases (Fig. 4.S5).

Comparing R2N to R2, there are only small changes, with a slight increase in mean precipitation mainly over the eastern Himalayas and the Western Ghats, and a small decrease over the north-eastern BoB (Fig. 4.2e). Hence, in this case the exclusion of the bias prone EIO region from the RCM simulation domain does not lead to significant improvement in the simulation of mean precipitation. This result is a bit surprising as several studies have indicated the EIO precipitation bias is linked to other deficiencies in SASM precipitation. Also, GCM sensitivity experiments that reduce EIO diabatic heating or relax the EIO meridional SST gradient indicate that improvement in EIO precipitation biases would significantly improve biases over India as well (Bollasina and Ming 2013). However, our result may relate to the EIO convection already being strongly supressed in the standard RCM domains used in R2 and R3 (Fig. 4.2d). This could also partly be due to intrinsic deficiencies of the model to produce diurnal convection over land (Turner et al. 2015), and subsequent changes in the larger-scale

circulation due to a lack of latent heating over India. Circulation changes in R2N compared to R2 are relatively small, with somewhat stronger westerly flow over the Arabian Sea and easterly flow over north India at lower level leading to anomalous cyclonic circulation over central India (Fig. 4.3e). At upper level, a weak anomalous cyclonic circulation is noted over Tibet in R2N compared to R2 (Fig. 4.4e).

We would like to reemphasize that despite R2N-R2 showing little change, we know that EIO bias plays a huge role. Apparent lack of improvement on exclusion of a key bias prone region (EIO) could relate to the fact that even in the standard domain modulation of EIO convection is already quite strong, via boundary constraints on the low level convergence and upper level, and subsequent effects on the thermodynamical vertical profile and triggering of convection over the EIO. What the limited change in R2N-R2 does highlight is that, beside remote effects of the EIO bias, there are also local contributions to the MetUM dry bias over India such as lack of convection over land (Turner et al. 2015).

In contrast, the R2S simulation shows larger increases in mean precipitation over central India and neighbouring oceans compared to R2 (Fig. 4.2f). Furthermore, removing the Himalayas from the domain weakens the anomalous strong branch of the westerly over northern India found in the control (Fig. 4.3f). This highlights the model problems in simulating realistic interaction between the strong moisture-laden monsoon flow and steep orography (Levine and Turner 2012). The R2S simulation suggests that, in other global and regional configurations, the Himalayan wet bias is directly related to the Indian dry bias by creating an area of excessive convergence along the steep southern slopes of the Himalayas and diverting moisture from central India. This may be a two-way process, as divergence of the low-level monsoon flow at landfall (as typically found in the MetUM, Fig. 4.3b) in response to difficulty to convect over the Indian

peninsula will enhance the flow into the Himalayas. Enhancement of lower level cyclonic flow over peninsular India (Fig. 4.3f) and anomalous upper level divergence over the head BoB (Fig. 4.4f) in R2S compare to R2 is consistent with the enhanced precipitation over central India and nearby oceans.

While the R2S experiment is useful to understand model behaviour, clearly it is undesirable to exclude the Himalayas from the RCM domain for realistic studies of the SASM. Hence, in the selection of the optimal domain for SASM simulation the focus should not only be on the exclusion of the entire bias prone regions such as the Himalayas but on selection of a domain that minimizes the overall bias while still including the entire area of interest. We argue that R3B is one such domain which performs well in the simulation of SASM precipitation when forced by reanalysis LBCs. Compared to R3, mean precipitation is increased over northwest and central India, the BoB and parts of the Arabian Sea and decreased over most of the mountains (the Western Ghats, the Himalayas and the Arkan mountains) and the northern EIO (Fig. 4.2g). The further improvements in R3B compared to the R3 simulation are likely related to the direct effects of the eastward shift of the western boundary. Both GA and R3 simulations show a weak westerly inflow through the latitudinal section corresponding to the R3B western boundary, which corresponds to the approximate location of the core of the Findlater jet (Fig. 4.3b,d), while the westerly inflow is substantially enhanced at the western boundary in R3B. The R2N experiment suggests that the northward shift of the southern boundary in R3B has only a secondary effect.

Thermodynamic profiles show that R3 and R3B have very similar vertical structures over central India, except for a slightly warmer lower atmosphere and drier low- mid-levels in R3 (Fig. 4.S3). Compared to GA, these vertical profiles are in good agreement with ERAI and comparable to that of GAN, although they are slightly drier and warmer

at the lower levels, with the larger bias found in R3, which is also slightly drier at mid-levels (~400 hpa). This is consistent with circulation and precipitation related improvements seen in R3B compared to R3 and in both RCMs relative to GA.

Table 4.3 show the area average seasonal mean precipitation bias in the models over three regions. GA has the largest ISMR dry bias (-66%) and wet bias over the west equatorial Indian Ocean (WEIO) (192%) though CHMRI bias in lowest (18%) which is likely due to cancelation of errors over the Himalayas and its southern plains. Both ISMR and WEIO biases are reduced in GAN though it has the highest CHMRI bias cause by reinforcement of the orographic bias as described earlier. Compared to both GCMs, biases are smaller in R3 over all region except of CHMRI bias with is larger than GA. These biases are further reduced in R3B compared to R3 over ISMR and CHMRI.

Table 4.3 Climatological monsoon mean bias (%) compare to APHRODITE for ISMR and CHMRI, and to GPCP over west equatorial Indian Ocean (WEIO) [1]

Model	ISMR	CHMRI	WEIO
GA	-66	18	192
GAN	-18	101	127
R3	-16	49	60
R3B	-2	46	X

[1] WEIO bias not computed for R3B as it only covers a fraction of the averaging area

Fig. 4.5 shows the normalized Taylor diagram for the spatial pattern of observed and simulated monsoon mean precipitation over land regions of ISMR (in grey) and over a common validation area (CVA: 60°-100° E, 5°-35° N, land only, in black) against APHRODITE located at abscissa 1. As expected, the three observational datasets (GPCP, TRMM and IMD) mostly have lower RMSDs indicating good inter-observational agreement. In contrast, GA RMSDs are either highest or second highest over the two regions arising from low correlation and large differences in variance compared to the reference. GAN RMSDs for those regions are also highest or second highest because of relatively poor correlation though its variances are comparable to the reference. The poor spatial correlation, despite improved areal average, is likely due to its coarser resolution. Both R3 and R3B have comparable RMSDs over the two regions which are smaller than those of GCMs but the latter has the lowest RMSDs amongst the four models. This again shows the good skill of R3B in simulating the spatial distribution of the SASM mean precipitation.

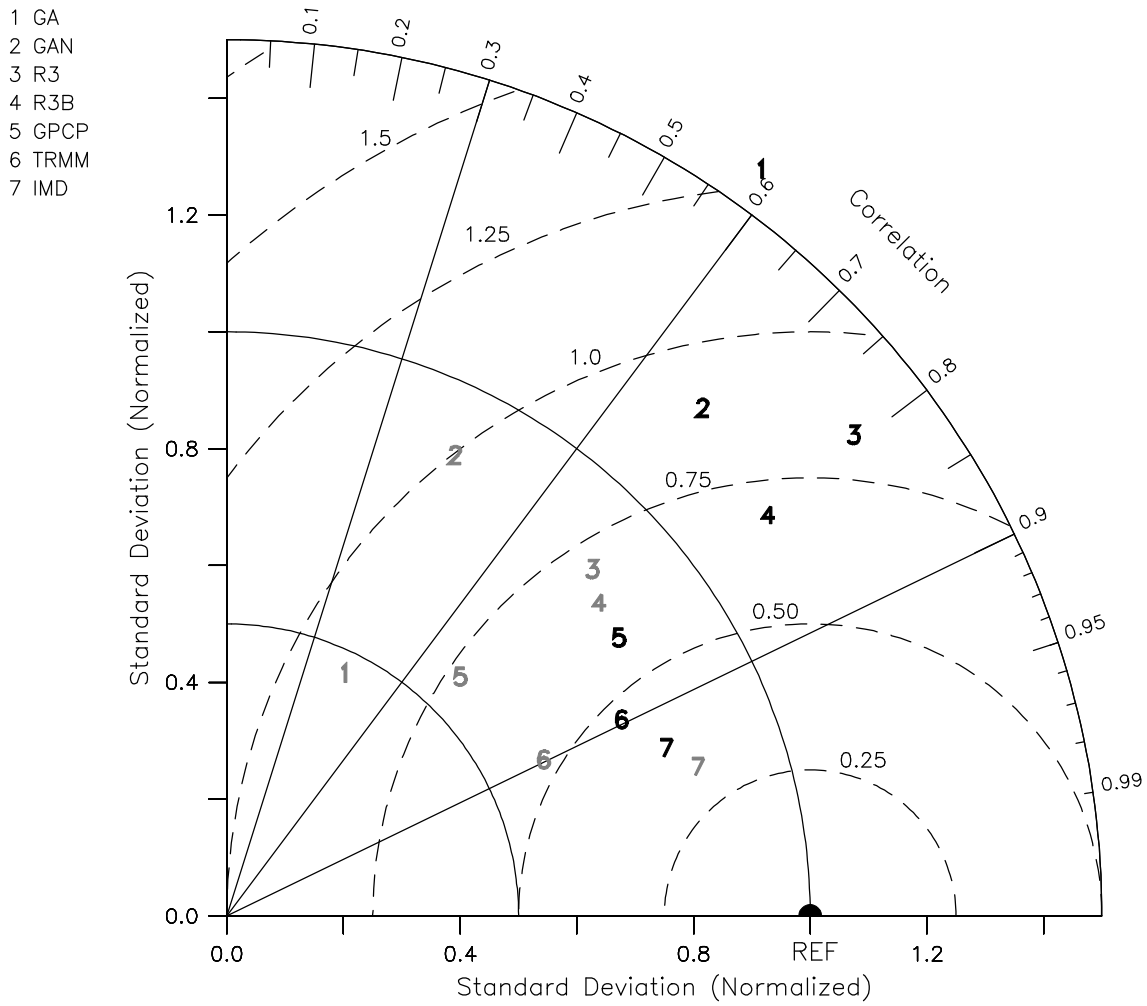

Fig. 4.5 Normalized Taylor diagram for the observed and simulated spatial patterns of climatological monsoon mean precipitation over ISMR region (70°-90° E, 5°-25° N) (numbers in grey) and a common validation area (60°-100° E, 5°-35° N) (numbers in black) compared to APHRODITE. Land points only. Note that R2N and R2S are not included because of their limited coverage.

4.4.2 Seasonal cycle

A primary manifestation of the SASM is the distinct seasonal variation of precipitation over the South Asia (Gadgil and Sajani 1998). Moreover simulation of the seasonal cycle poses a stringent test of model performance. Fig. 4.6 shows mean seasonal cycle of precipitation averaged over the three main regions of precipitation bias. The observed

seasonal cycle (grey envelop) shows strong dominance of summer monsoonal precipitation over the central India (Fig. 4.6a) and the Himalayas (Fig. 4.6b); in contrast there is only minor observed seasonal variation over the WEIO (Fig. 4.6c). As noted earlier, GA fails to capture the enhanced summer monsoon precipitation over central India which is partly due to excess WEIO precipitation during summer. Relatively good agreement between observations and GA in the seasonal cycle averaged over the central Himalayas is due to error cancellation of excessive precipitation over the mountains and the deficits over the foothills, which is an extension of the dry bias over central India (Fig. 4.2b). GAN fairly well simulate seasonal cycle over central India but overestimate monsoon precipitation over the central Himalaya due to reinforcement of the orographic bias as described earlier. Over the WEIO, GAN relatively better simulates both the magnitude and seasonality of the seasonal cycle compared to GA. However, RCMs simulated seasonal cycles are better or at least similar to those simulated by the GCMs over the three regions. We note that though seasonal cycles are well represented in some simulations, there are still spatial biases within the averaging area that compensate.

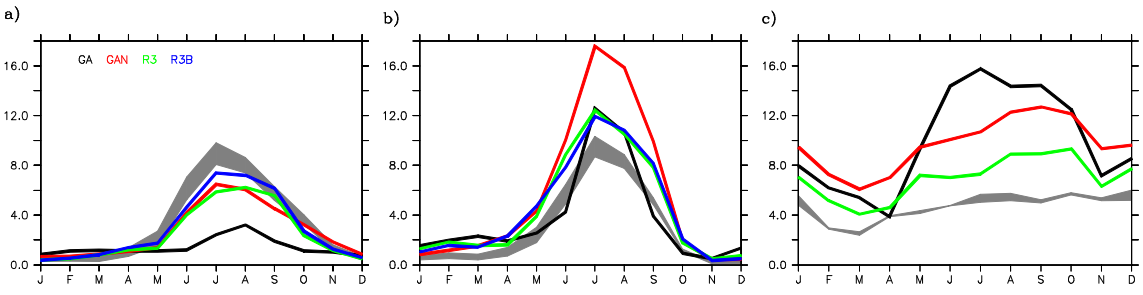

Fig. 4.6 Climatological mean seasonal cycle of precipitation (mm/day) averaged over a) ISMR region (land points only), b) CHMRI region (80°-88° E, 26°-30° N) and c) west equatorial Indian Ocean (60°-75° E, 5° S-5° N). Observational spread of APHRODITE, GPCP, TRMM and IMD (Only the former three in b) and only GPCP and TRMM in c)) is shown in grey envelop and simulations are shown in solid lines. The averaging period

is 1990-2008 except for APHRODITE (1990-2007), TRMM (1998-2008) and IMD (1990-2005)[1].

[1] Note that R2N and R2S are not included as they do not cover one or more averaging region. Same for R3B in c).

The onset of monsoon is heralded by the northward propagation of the Intertropical convergence zone (ITCZ) from the ocean (about 10° S) towards the Indian subcontinent (Pokhrel et al. 2013). Its manifestation can be seen in the rapid movement of observed precipitation maxima from about 10° N to 28° N during the monsoon onset period (Fig. 4.7). A large systematic error is seen in GA, with a stagnant band of intense precipitation over the EIO during summer and little sign of northward propagation of the ITCZ, resulting in dry conditions over central India. In comparison GAN relatively better capture the northward movement of the ITCZ but strong precipitation belt persists over EIO. Among the RCMs, northward propagation is weak in R3 with a stagnant EIO precipitation band in summer but the EIO bias is much reduced in R2S suggesting the previously described coupling between EIO and Indian convection can also work in the opposite direction, with an enhancement of Indian convection, due to exclusion of the Himalayas in R2S, and subsequent enhanced convergence of air from the EIO into the Indian subcontinent weakening EIO convection. The EIO is largely (entirely) absent in R3B (R2N) but among the models the northward propagation is most realistic in R3B.

However, models fail to closely replicate the observed movement of the maximum precipitation band (> 8.5 mm/day) from about 10° N to 28° N during the onset. The pattern correlations between GPCP hovmoller diagram and that of TRMM and other models for the monsoon season show their relative skill in capturing the observed pattern. The high correlation in TRMM (0.98) indicates the observational agreement,

whereas the negative correlation in GA (-0.03) reflects its poor skill (Table 4.4). This is improved in GAN but still the correlation is low; R3 correlation is comparable to GAN but R3B has relatively higher correlation (0.64) indicating its improved performance. These results again suggest a linkage (coupling) between wet EIO bias and dry central India bias. Similar linkage has also been suggested by many others (e.g., Rockel and Geyer 2008) in addition to those discussed above.

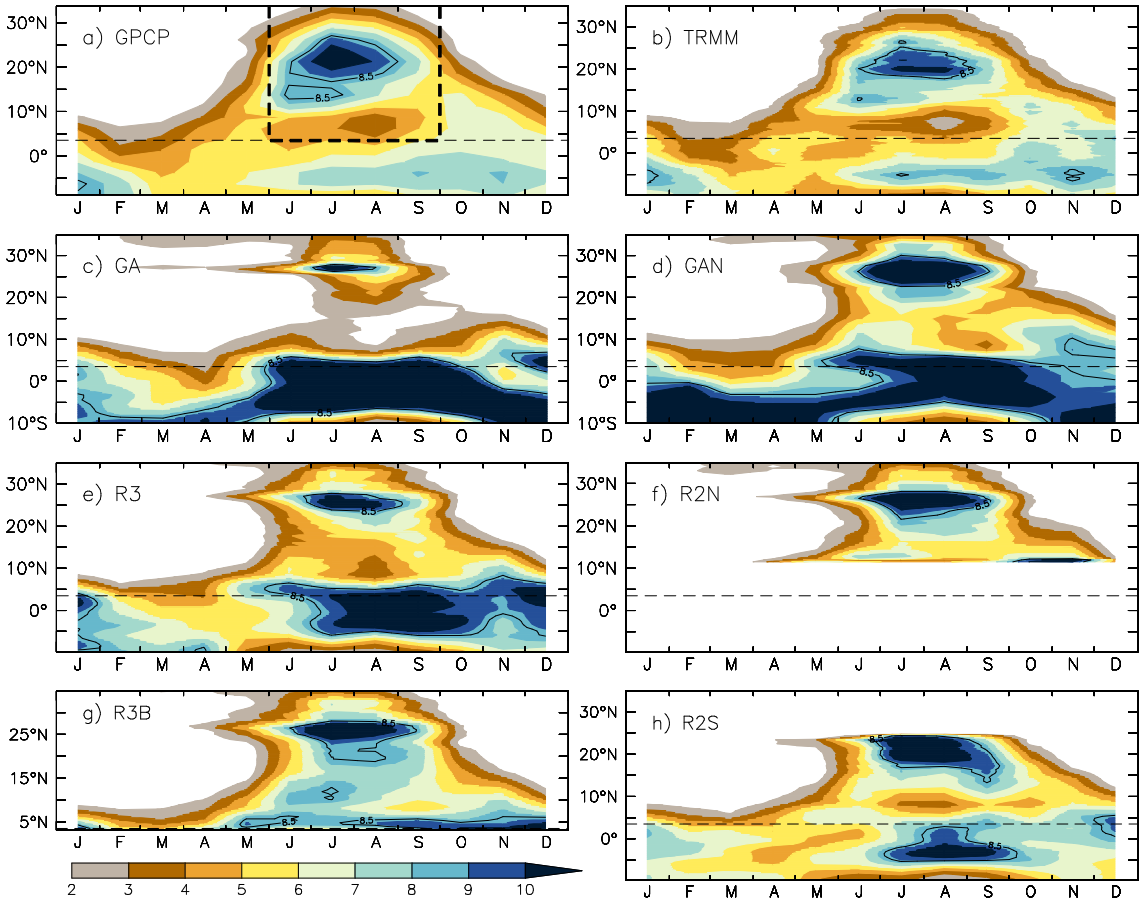

Fig. 4.7 Hovmoller diagram of climatological mean monthly precipitation evolution (mm/day) averaged over the longitudinal belt of 70°–90° E. Dash line at 3.5° N is drawn to highlight that R3B is absent south of that latitude. Box in thick dash line in top left plot represents the region over which pattern correlation is computed.

Table 4.4 Pattern correlations between GPCP and the other observation and models for the box enclosing 3.5° - 35° N and June- September in Hovmoller diagram (thick dashed box in Fig. 4.7a)

TRMM	GA	GAN	R3	R3B
0.98	-0.03	0.36	0.32	0.64

4.4.3 Inter-annual variability

Another important metric in model evaluation is its ability to replicate the observed variability. Hindcast simulation of the models provides an opportunity to directly compare observed and simulated interannual variability of the SASM. A number of monsoon indices based on precipitation and circulation have been defined for this purpose (e.g., Parthasarathy et al. 1992, Wang et al. 2001, Webster and Song Yang 1992) . A subset of those indices is considered in this study (Table 4.2).

Fig. 4.8 shows a normalized Taylor diagram for interannual variability of seasonal mean precipitation averaged over the central India land region (ISMR) (in grey) and the central Himalayas (in black). APHRODITE is the reference data at abscissa 1 against which other observations and model precipitations are normalized. GPCP shows good agreement for correlation and variance for both regions resulting in small RMSDs. Surprisingly, agreement is relatively poor for other two observational datasets (TRMM and IMD) leading to larger RMSDs (see also Collins et al. 2013). Note that IMD data is available only for India. GA RMSDs for both regions are amongst the highest mainly due to its low correlations. In contrast GAN RMSDs are amongst the lowest having slightly larger variances than the reference and relatively better correlations. R3 has low correlations for both regions leading to moderate to high RMSDs. Among the four

simulations R3B has the lowest (second lowest) RMSD over the central Himalaya (central India). Relatively small RMSDs in GAN and R3B are likely due to the stronger influence of boundary forcing in these models owing to nudging and a relatively small domain respectively. Hence, a reasonably sized small domain has added benefit in simulating interannual variability in addition to improved simulation of the mean state.

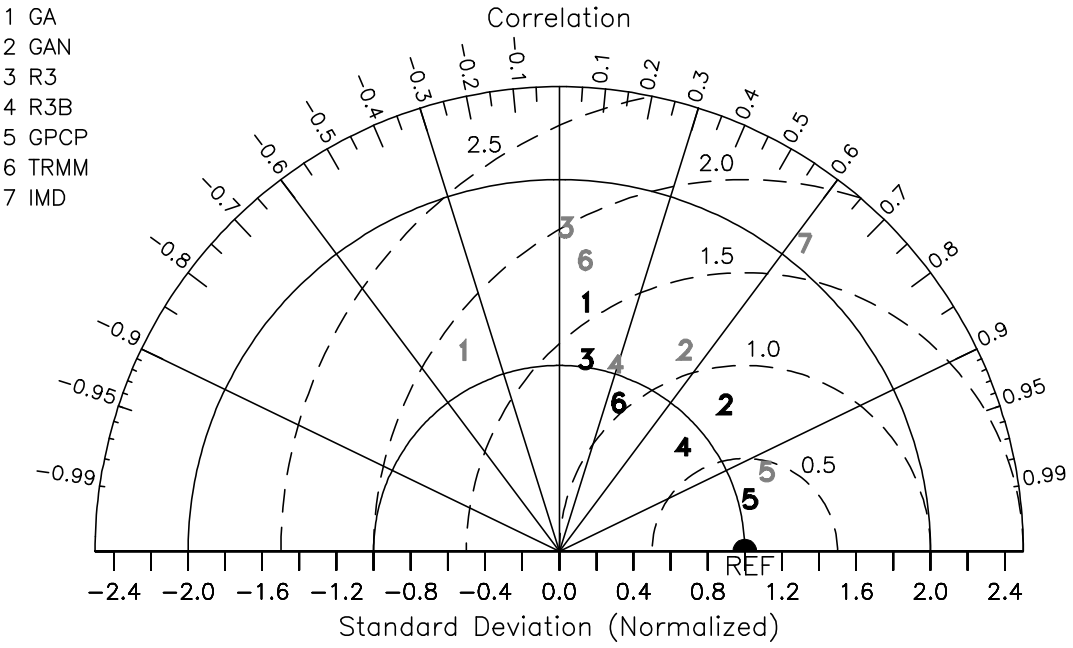

Fig. 4.8 Normalized Taylor diagram for ISMR (numbers in grey) and CHMRI (numbers in black) interannual time series for 1990-2007 except for TRMM (1998-2007) and IMD (1990-2005). APHRODITE is the reference data located at abscissa equal to 1[1].

[1] Note that IMD data is not available for CHMRI. Also note that R2N and R2S are not included as they do not cover one or more averaging region(s).

Next, model simulated interannual variability of two MCIs (MHI and Webster and Yang index - WYI) are compared against ERAI in a normalized Taylor diagram (Fig. 4.9). GA has highest RMSDs for both MCIs, owing to poor correlations and variances.

But note that unlike other simulations, it is not forced by ERAI. On the other hand, GAN has lowest RMSDs for both MCIs, resulting from good correlations and variances. This is likely due to strong control of boundary forcing via nudging. Both R3 and R3B have variances close to that of ERAI, but their RMSDs, particularly that of R3 for MHI, are relatively higher than that of GAN due to inferior correlations. Still R3B MHI RMSD is only slightly higher than that of GAN which is also likely due to the stronger influence of driving force owing to the smaller domain. We again note that only about 80% of MHI computation region is available in R3B due to its small domain with the eastern part missing. But, this should have little impact in our main results since values are only slightly altered when we recomputed MHI for ERAI and other models using the same MHI computation region as in R3B. Similar results are found for Westerly shear index (WSI) (Wang and Fan 1999) and Indian monsoon index (IMI) (Wang et al. 2001) statistics (not shown).

In conclusion, R3B is also able to reduce the GA systematic errors in simulating inter-annual variability of both precipitation and circulation. However, note that only MHI is computed for R3B due to limited coverage of other MCI computation areas.

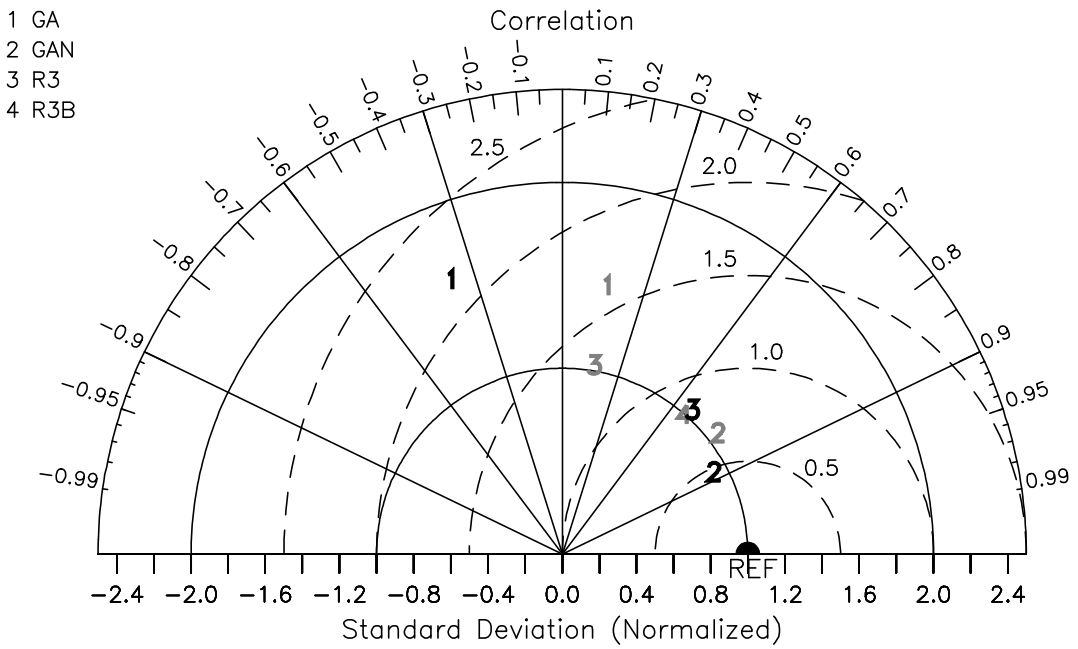

Fig. 4.9 Normalized Taylor diagram for MHI (numbers in grey) and WYI (numbers in black) interannual time series for 1990-2007. ERAI is the reference data located at abscissa equal to 1[1].

[1] Note that WYI is not computed for R3B due to its small domain. Also note that R2N and R2S are not included as they do not cover one or more averaging region(s).

4.4.4 Intra-seasonal variability

The SASM, along with other components of the Asian summer monsoon, has strong sub-seasonal variability with two dominant modes: an eastward- and northward-propagating intra-seasonal oscillation (Lin et al. 2008). These sub-seasonal modes have large impacts on the monsoon onset and breaks, as well as the formation, intensification and tracks of the tropical cyclones (Liebmann et al. 1994). It has been noted that models that simulate seasonal mean features well are those that are able to simulate intraseasonal features well (Sperber et al. 2000). Fig. 4.10 depicts the northward propagation of the summer monsoon intraseasonal oscillation. GPCP shows prominent northward propagating signals with phase speed of about 1.3 m/s. All models are able to

correctly simulate the phase speed of northward propagation but there are other deficiencies. In GA the lag correlation is rather weak and initiates only from around 5° N unlike GPCP in which it originates just south of the equator. The pattern and strength of positive correlation is slightly improved in GAN. RCMs show diverse skill in capturing the observed pattern and R3B arguably best capture the observed pattern and magnitude (confined to north of 3.5° N due to its small domain).

This suggests that R3B simulation improves the MetUM systematic errors on all time-scales from intra-seasonal to climatological means.

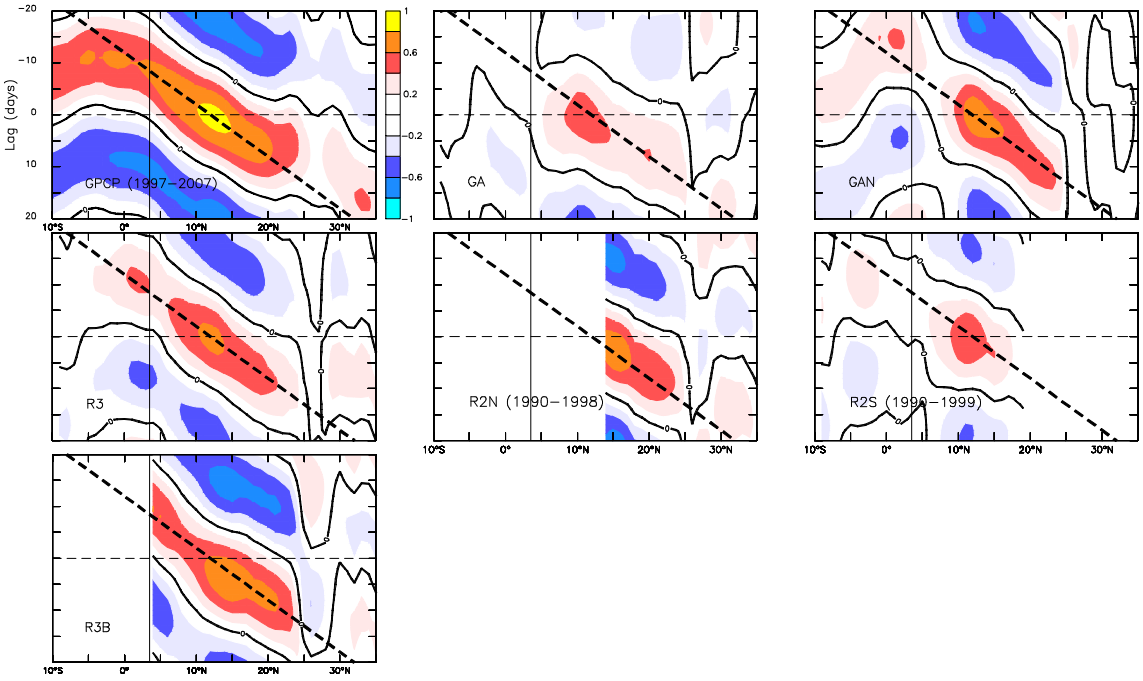

Fig. 4.10 Lag correlation of 30-50 day filtered daily monsoon precipitation, averaged between 70°-100° E, with respect to itself at 85° E, 12° N, except for R2N for which it is 85° E, 14° N. Data is analysed for 1990-2007 except for GPCP, R2N and R2S. Contour of zero correlation is overlaid and thick dash lines correspond to phase speeds of 1.3 m/s. Vertical line at 3.5° N is drawn to highlight that R3B is absent south of that latitude.

4.5 Conclusions and discussion

GCMs are the most scientifically sound tool for global climate simulation but they generally suffer from significant systematic errors at regional scale such as the simulation of the SASM. RCMs are used to downscale GCM or reanalysis global outputs to a higher resolution regional domain. However, irrespective of the quality of the RCM a prerequisite for realistic dynamical downscaling is the availability of a good quality driving field. The majority of present generation GCMs has large systematic errors in simulating the SASM (Sperber et al. 2013). Hence, application of GCM data as LBCs for RCMs over those regions where the global model has large systematic errors may limit the reliability of the resulting simulations. Moreover, since RCMs are developed from GCMs or have many commonalities in their physics/ dynamics, it would be interesting to see if they also suffer from similar errors when run over regions where their parent models show large systematic errors, even if they are driven by near-perfect LBCs from re-analysis. In particular, we investigate the role of the RCM domain size in minimizing systematic errors in the SASM simulation inherent in the parent model using MetUM global and regional model configurations. As well as informing the choice of regional model domain this approach provides information on the nature of the parent model systematic errors.

We found that the global model simulation (GA) has large systematic errors in simulation of various features of the SASM. The main features are the weak seasonal cycle of precipitation over the Indian subcontinent, excessive precipitation over the EIO and Himalayas and a dry bias over central India. The corresponding circulation features include excessive low-level (upper-level) convergence (divergence) over the EIO, a weak monsoon jet core and excessively strong low-level flow into the Himalayas.

Another notable error is the weak intraseasonal northward propagation, while there are also errors in the interannual variability of precipitation and circulation. All such errors are also common amongst many current GCMs (Sperber et al. 2013). Previous MetUM studies suggest that the bias over the EIO spins up rapidly within a few days and is very likely a direct effect of convection parameterization problem (Martin et al. 2010). Furthermore, sensitivity studies have shown that targeted weakening of the EIO bias results in enhanced moisture transport towards India and enhanced Indian precipitation (e.g., Bush et al. 2014, Levine and Turner 2012). This suggests that any RCM domain that excludes (part of) the EIO may show an improved SASM simulation.

A further global simulation with nudging of winds to re-analysis data (GAN) shows that enforcing near-perfect winds substantially reduces the magnitude of the model systematic errors in precipitation. However, the systematic error pattern remains, albeit with a smaller magnitude, highlighting the persistence of the inherent model biases and again indicating problems with model physics parameterizations. Furthermore, the excessive rainfall over the Himalayas is further enhanced in the nudged experiment reflecting the model's problems with convection when strong moist flow is incident upon steep orography. The strong coupling, as described in this paper, between different areas of the SASM may exacerbate the biases near the Himalayas.

The large domain RCM simulation (R3) replicates most of the GA biases, albeit with smaller magnitude, which is likely due to the constraints imposed by the lateral boundaries. In particular, the weakening of excessive low-level convergence over the EIO through excessive inflow of air from either side of the equator is likely a direct consequence of the prescribed LBCs through the southern R3 boundary, while there is a similar weakening of upper-level divergence. Both of these changes will act to suppress EIO convection, which in turn will promote moisture transport within the monsoon jet

towards India. However, the remaining biases, which are similar to the GA, indicate that the MetUM systematic errors in the simulation of the SASM are largely forced by local processes. However there are other source regions of the Indian dry bias in addition to the EIO convection. This is evident in the persistence of the central Indian dry bias in a regional simulation that excludes the EIO region (R2N). This may be the result of intrinsic difficulty of the model to produce diurnal convection over land, indeed the Indian precipitation is found to be sensitive to land distribution and its surface type (Turner et al. 2015) as well as vegetation distribution (McCarthy et al. 2012).

The model's ability to represent flow over steep orography may also play a role in the Indian dry bias. A regional simulation that excludes the northern parts of the CSAD (R2S) substantially enhances rainfall over central India. This suggests that the Himalayan wet bias diverts moisture from central India and contributes to the dry bias. This idea is consistent with additional simulations (not shown) that weaken the convergence over the Himalayas by reducing the steep orographic gradients of the southern slopes of the Himalayas and shift rainfall towards central India. R2S simulation also shows a slight weakening of the EIO bias, suggesting that in the model the Indian bias also feeds back onto the EIO bias.

Clearly in a study of the SASM it is not realistic to exclude the Himalayas from the RCM domain and the emphasis should be on selecting a domain that effectively minimizes the systematic error while including the area of interest and allowing a large enough area for the model to produce its own internal circulation. Our results shows that R3B, that is of reasonable size and partly excludes EIO, is one such domain that has a relatively small dry bias over central India. This is achieved by partly excluding the EIO from the domain and also narrowing the lateral extent of the domain, which limits errors in the location and strength of the Findlater jet. Moreover, we have shown that

the R3B simulation substantially reduces the GA systematic errors at all time-scales from intra-seasonal upwards.

In conclusion, unless a RCM is able to simulate all aspect of SASM well, the systematic error in one area will have detrimental impacts in other areas if the domain is too large. Here, we have shown this can be minimized by selecting an appropriately small domain. Finally, the MetUM systematic errors are common amongst current GCMs and they also have similar mechanisms of early onset of bias over EIO region which then adversely affect circulation and moisture flow over rest of the South Asia (e.g., Bollasina and Ming 2013). Hence, it can be expected that other RCMs, derived from such GCMs, would likely have larger bias in SASM simulation when run over large domains such as CWAD compared to simulations carried over smaller domain such as that of R3B. However, the exact boundaries of an appropriate domain for other RCMs are likely to be sensitive to model configuration, such as the choice of convection scheme and other parameterizations. Nevertheless our results should be relevant for other RCMs in selection of an appropriate domain.

Acknowledgements

First author thanks the Felix Scholarships for funding his DPhil. The model simulations were carried out at Met Office. Richard Levine and Richard Jones were supported by the Joint DECC/Defra Met Office Hadley Centre Climate Programme (GA01101). The authors would like to thank Gill Martin for comments on earlier drafts of the manuscripts, and two anonymous reviewers for comments which helped to significantly improve the manuscript.

Supplementary Information: Chapter 4

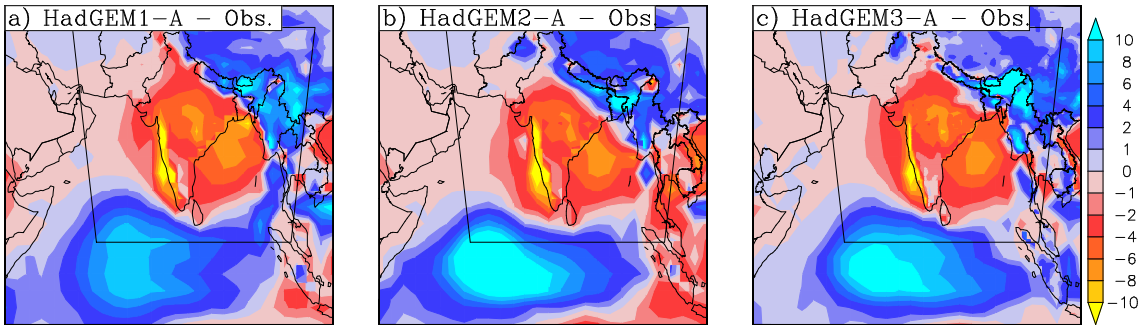

Fig. 4.S1 Climatological monsoon mean precipitation bias (mm/day) in a) HadGAM1-A (1982-2000), b) HadGEM2-A (1990-2008) and c) HadGEM3-A (i.e. GA3, same as Fig. 4.2b) (1990-2008) compared to observed in Fig. 4.2a. Averaging period is constricted by the data availability.

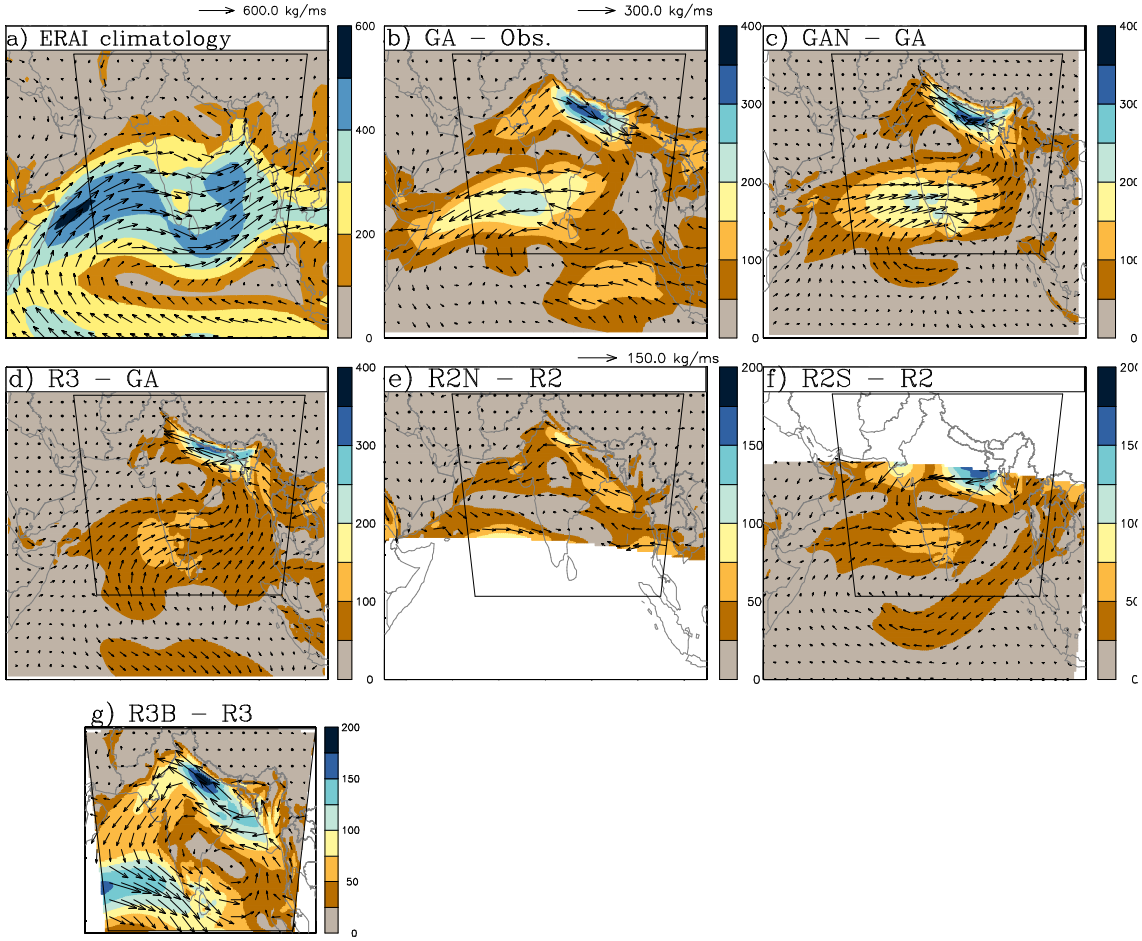

Fig. 4.S2 Climatological monsoon mean vertically integrated moisture flux for a) ERAI, and the differences in b) GA from ERAI, (c-d) GAN and R3 from GA, (e-f) R2N and R2S from R2 and g) R3B from R3, averaged for 1990-2008 except for e) 1990-1998 and f) 1990-1999. Arrows and shading show moisture flux vectors and its magnitude respectively. Unit: kg/ms.

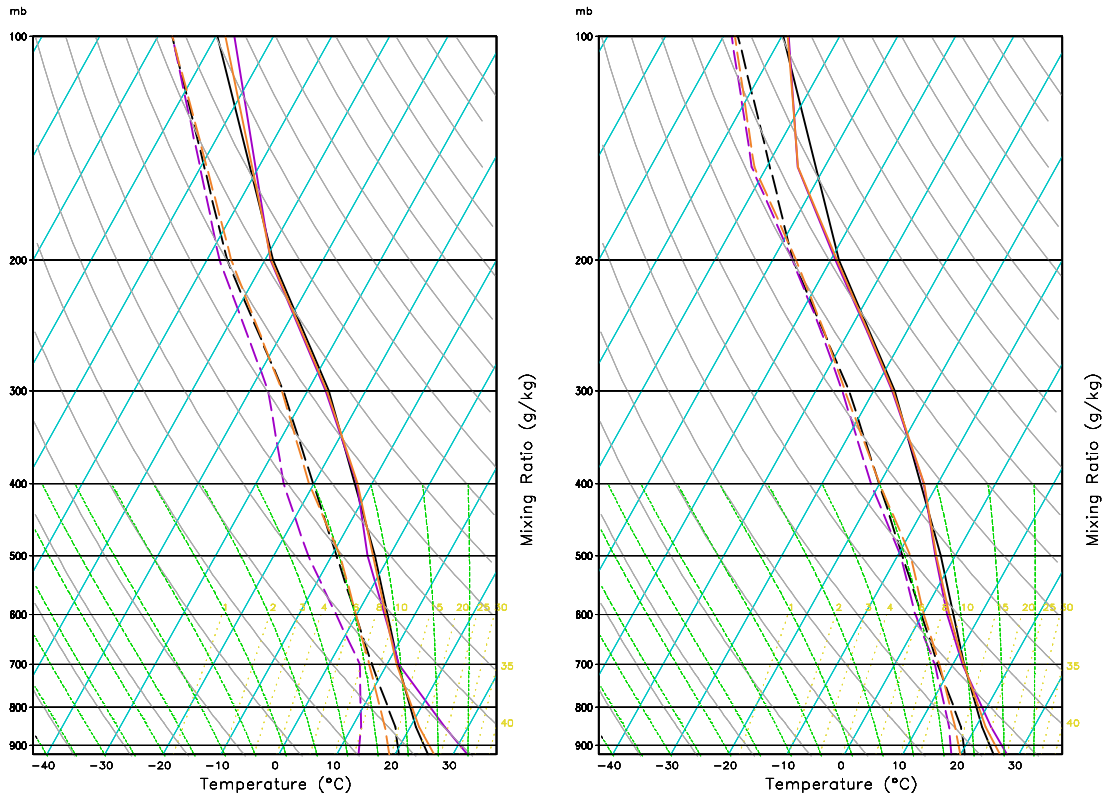

Fig. 4.S3 Climatological monsoon mean SkewT-logP diagram over central India (80° E, 22° N) for ERAI (black), GA (purple) and GAN (orange) in the left panel, and ERAI (black), R3 (purple) and R3B (orange) in the right panel.

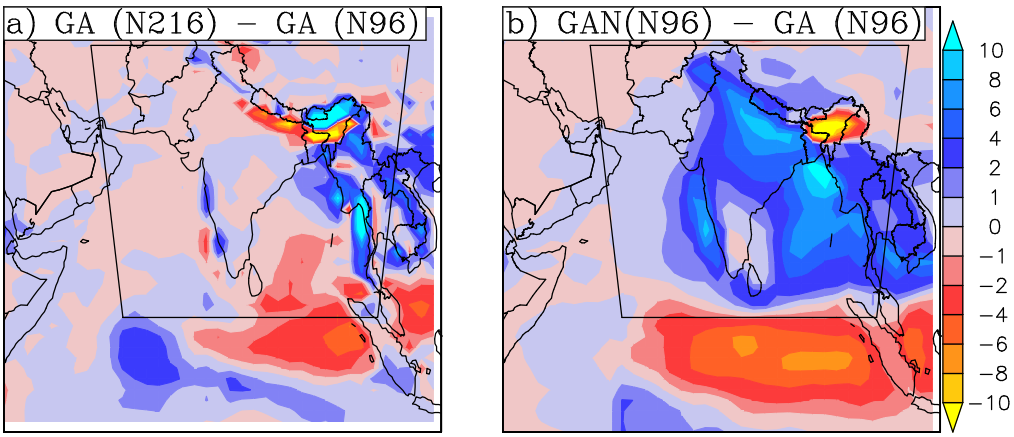

Fig. 4.S4 Same as Fig. 4.S1but for difference between coarse resolution GA (N96) simulation and a) GA and b) GAN.

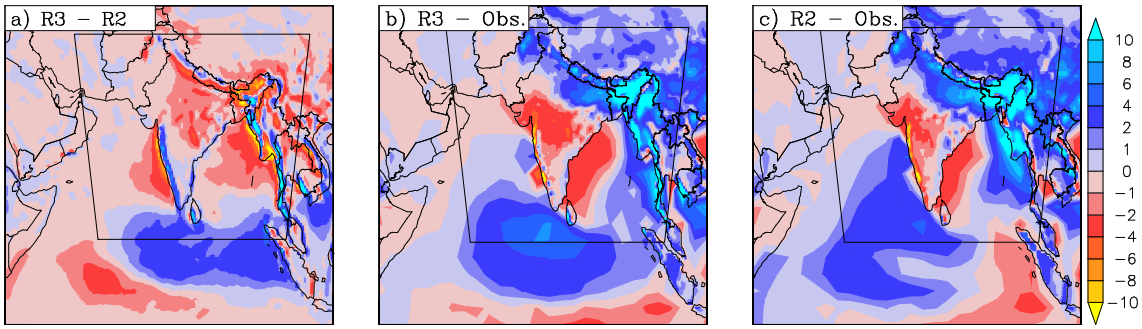

Fig. 4.S5 Same as Fig. 4.S1 but for a) R3-R2, b) R3-Obs and c) R2-Obs.

5 Evaluation of the added value of a high-resolution regional climate model simulation of the South Asian summer monsoon climatology

Synopsis

In the previous chapter, it is found that both global and regional versions of Hadley Centre climate model have similar patterns of the systematic errors in simulation of the SASM provided the domain of integration of the regional climate model is large. This suggests that systematic errors in simulation of the SASM in the Hadley Centre model system are mainly produced by local processes. Further experiments with domains of different size shows that key source regions of the systematic errors lies on the periphery of the Indian landmass which allows setting up of a moderately size domain that include the main area of interest (South Asia) and also minimize the systematic errors inherent in the model.

Using the same optimal domain identified in the previous chapter the added value of high resolution RCM simulation of SASM is assessed in this chapter. For this, RCM simulations were performed over an identical domain at high (0.11°) and low (0.44°) resolutions. Through the assessment of those simulations, this chapter seek to partially address the research question no. 3 identified in chapter 2 which is: for the Hadley Centre regional climate model what is the extent of added value in going from 50 km to 12 km resolution, and if so, where does the added value lie? This is achieved through the assessment of the model simulated SASM climatologies against the observed with focus mainly on precipitation.

As shown later, the high resolution RCM simulation adds value compared to the coarse resolution simulation, in terms of reduction of bias, in many aspects of the SASM, mainly those associated with precipitation. However, in contrast to many other studies, improvement in the high resolution simulation of the mean precipitation mainly occurs over the homogeneous Indo-Gangetic plain and is achieved through reduction of the wet

bias in the coarser simulation. Other noticeable improvements in the high resolution simulation are seen in the intensity distribution of daily precipitation, spatial distribution of precipitation extremes, wet day frequencies, seasonal mean low level circulation and moisture flux etc. These results clearly demonstrate the added value of the Hadley Centre RCM at high resolution regarding simulation of the South Asian monsoon climatology, mainly the precipitation.

Authorship Declaration

I did the analysis for this paper and wrote the text. R. Jones helped design the model simulation. W. Moufouma-Okia carried out the RCM simulation. M. New helped plan the analysis, and gave advice on the methodology for investigations. Both R. Jones and M. New gave comments on the findings. All co-authors commented on a draft of the paper.

Evaluation of the added value of a high-resolution regional climate model simulation of the South Asian summer monsoon climatology

J. Karmacharya[1,2] R. Jones[1,3] W. Moufouma-Okia[3] and M. New[1,4]

Affiliations:

1 School of Geography and the Environment, University of Oxford, Oxford, United Kingdom

2 Department of Hydrology and Meteorology, Kathmandu, Nepal

3 Met Office Hadley Centre, Exeter, United Kingdom

4 African Climate and Development Initiative, University of Cape Town, Cape Town, South Africa

Submitted to: *International Journal of Climatology*

Abstract

The South Asian summer monsoon (SASM) is a continental scale weather system, which fluctuates at a range of temporal and spatial scales. The majority of current generation global climate models are broadly able to simulate the large scale characteristics of the SASM, but they suffer from major deficiencies such as large errors in the spatial distribution of SASM mean precipitation. Higher resolution regional climate models (RCMs) have been proposed as options to better simulate fine temporal and spatial scale features and variability, which should lead to an improved mean state. Here, we analyse SASM simulations using a contemporary Hadley Centre RCM, forced by ERA-Interim reanalysis and observed sea surface temperature, at medium (0.44°) and high (0.11°) horizontal resolutions. Evaluation of the results show that the high resolution RCM is able to better resolve the interaction of the low level monsoon flow with the Himalayan orography leading to added value in simulating many aspects of SASM precipitation such as the seasonal mean, relative frequency distribution of daily precipitation, and various metrics of precipitation extremes. Though errors still persist, and so further improvements in the RCM are required, the results suggest that the use of a higher resolution RCM has the potential to add value when downscaling global climate model climate change projections.

5.1 Introduction

Regional climate models (RCMs) have made substantial progress from the first application of “nested” regional modelling techniques for climate applications in the late 1980s by Dickinson et al. (1989) and they have been widely used for dynamical downscaling over different parts of the globe. In the past, RCM simulations were generally performed at a resolution of ~50 km. However, they have been run at higher and higher resolution in recent years (e.g., Cardoso et al. 2013, Mukhopadhyay 2010, Soares et al. 2012). Various factors have contributed to increase in RCM resolution such as demand for detailed climatic information at regional to local levels, the potential to improve the representation of physical processes, accessibility and transferability of the models, access to higher computational capacity at affordable price.

Climate information at fine scales is generally required in the planning of climate change adaptation and some mitigation measures. For example, detailed climate information is needed to run impact assessment models such as hydrological river catchment models, especially for modelling of smaller regions (Berg et al. 2013). Moreover, Alpine glacier models require information at spatial resolutions as fine as 10s of metres (Jarosch et al. 2012). In this connection, Im et al. (2010) noted that RCMs might have to be run at resolution higher than 10 km to provide useful information for input into basin hydrology studies over complex areas such as the Alps. However, statistical bias correction techniques might still need to be applied on such RCM outputs before using those in hydrological models as systematic biases often prevail in those outputs (Dobler et al. 2012).

High resolution RCMs have better representation of coastlines and topography (Chan et al. 2012) and generally have improved representation of the physical processes and

interactions (e.g., the dynamical structure of weather systems or cloud complexes; the location of major circulation features) (Rauscher et al. 2010). Moreover, the large-scale dynamics of the climate systems are partially determined by nonlinear processes, whose characteristic scales might be unresolved at coarse resolutions (Marvel et al. 2013) but might have explicitly resolved at higher resolution as more and more processes could be resolved at high resolution. With these improvements, they are expected to simulate local and regional weather phenomena more accurately (Marvel et al. 2013) leading to improved simulation of the distribution of events at finer temporal scales e.g. daily and in particular extreme events (Frei et al. 2003, Kendon et al. 2012). Hence, model fidelity could also improve by explicitly resolving, rather than parameterizing, those processes (Hack et al. 2006) as has been demonstrated in convection-permitting RCMs (Kendon et al. 2012).

However, achieving added value from high resolution RCM simulation is not a trivial issue as simply increasing model resolution does not automatically results in improved model performance (e.g. Jacob et al. 2007, Rauscher et al. 2010). High resolution simulations may lack any added value or even show degradation owing to problems in the lateral forcing of the RCMs (Warner et al. 1997), domain size (Leduc and Laprise 2009, Vannitsem and Chomé 2005), parameterization inadequacies (Jiao and Caya 2006), or a combination of several of those factors (e.g. Castro et al. 2005). For example, in a study using HadAM3, Pope and Stratton (2002) reported overall degradation in precipitation climatology at higher resolution. Lack of improvement with higher resolution is also reported by several other authors in various recent studies (e.g. Dobler and Ahrens 2010, Haslinger et al. 2013) and these provide enough motives to investigate model performance in simulating the South Asian summer monsoon (SASM) at high and low resolutions.

Additionally, model performance at the higher resolution could be sensitive to seasonality and geography as they dictate the climate regime and hence the precipitation type (Chan et al. 2012, Iorio et al. 2004, Rauscher et al. 2010). There are also few reports of diminishing returns with increasing resolutions (Mass et al. 2002). In a study over Southeast England using a Met Office limited area model, Chan et al. (2012) concluded that generally there was no evidence of 1.5 km simulation being superior to 12 km or vice versa in climate simulations of precipitation at daily timescales. In particular, they found no benefit of increasing model resolution beyond 12 km for winter season. They attributed this to scale of dynamical process that drive winter precipitation events in Europe, caused by fronts and depressions of scale of the order of 100-1000 km, which is 2-3 order of magnitude larger than highest model resolution (1.5 km) in their study. Interestingly, from the analysis of same set of simulations, Kendon et al. (2012) found clear improvements at the sub-daily time scale for metrics such as variability, duration and spatial extent of precipitation. So, the issue of added value appears to depend also on temporal scale and statistics considered for evaluation. Further, using another recent Met Office RCM (same as the one used in this study) at a range of resolution from 150 to 12 km over the CORDEX-Africa domain Moufouma-Okia and Jones (2014) found improvements in simulation of rainfall variability over Africa with increased horizontal resolution, though some errors persist.

RCMs have been used in the study of the SASM since mid-1990s (e.g. Bhaskaran et al. 1996, Chen and Yen 1994) and most of them have horizontal resolution of about 50 km (e.g. Dobler and Ahrens 2010, Kumar et al. 2011a, Philippe et al. 2011, Polanski et al. 2010). However, higher resolution models, not limited to RCMs, are increasingly being used for SASM simulations. For example, Rajendran et al. (2012) assessed the performance of a very high resolution (20 km) atmospheric global climate model

(AGCM) to simulate SASM and illustrated that SASM rainfall is strongly controlled by processes and parameterised physics, which need to be resolved with adequately high resolution for accurate assessment of local- and regional- scale climate and its changes. Using a variable resolution global climate model (with resolution < 35 km over South Asia), Sabin et al. (2013) found large improvements in simulating various aspects of SASM such as more realistic precipitation distribution and circulation features (e.g. monsoon trough and synoptic disturbances). However, many centres, that have the ability to run RCMs, lack the infrastructure and/or technical capacity to carry out GCM simulations; therefore, understanding the potential for higher resolution RCM simulations over the region remains an important question.

Higher resolution RCMs have also been used in a few studies on SASM in recent years. For example, Akhtar et al. (2008) ran a RCM (PRECIS) at 25 km forced by a GCM (HadAM3P) and used the outputs to drive hydrological models in order to estimate impact of climate change in three small river basins in the western Himalaya. They found rather uniform warming throughout the year and across the basin in future (i.e. in late 21st century compared to base line). Similarly, in all three basins precipitation was projected to increase in all seasons but with larger increase in winter than summer. They also noted that projected changes were comparable to those made for neighbouring regions using coarser RCM and statistical methods. Ashfaq et al. (2009) found that a RCM (RegCM3) simulation at high (25 km) and medium (50 km) resolution depict very similar spatial pattern of changes in mean convective precipitation. They further noted that despite higher resolution of the RCM, its convective parameterization was inadequate to resolve interaction among convective organization, orography and the diurnal cycle, which influence the life cycle and spatial coherence of large scale circulation. Mukhopadhyay (2010) assessed the sensitivity of high resolution (15 km)

WRF RCM simulations of the Indian summer monsoon to three cumulus parameterization schemes and found that Betts–Miller–Janjic´ (BJF) scheme was able to produce a reasonable mean precipitation pattern compared to other two schemes (i.e. Grell–Devenyi, Kain–Fritsch) owing to its reasonable heating profile, along with the realistic moist instability and seasonal cycle of evaporation and condensation. Srinivas et al. (2013) also obtained similar result in comparison of moderate resolution (30 km) WRF simulation with the same three convection schemes. They further argued that 30 km resolution is adequate to produce regional climate features such as off-shore trough, heat low and spatial variations of rainfall.

Similarly, Bhaskaran et al. (2012) ran a Met Office RCM (HadRM3P) at 50 and 25 km to study sensitivity of the hydrological cycle to domain size and showed that seasonal mean hydrological cycle and the day-to-day precipitation variations of a sub-region within the model domain were sensitive to the domain size though largely insensitive to resolution. Ménégoz et al. (2013) ran RCM at 20 km to simulate precipitation and snow cover over the Himalaya for few years and noted that although the RCM was able to capture the spatial variability of precipitation and snow cover over the Himalaya, it underestimated precipitation and snowfall. Moreover, a season-long very high resolution (1.5 km) integration of the SASM has been performed recently in Met Office (Webster S, personal communication), but it will take more time to extend this work to climate time scale given the tremendous computational cost involved. However, none of those studies directly compared the performance of RCMs at higher and coarser resolutions.

However, Sinha et al. (2013) employed double nesting technique to run RegCM3 at 90 km and 30 km, forced by a GCM at outer domain, to simulate SASM for three seasons (dry, wet and normal) and three different convection schemes. They found that rainfall

intensity and distribution was best captured by different convection schemes at different resolutions. Nevertheless, the high resolution model captures those aspects better compared to the coarser simulation, as well as generates more rainfall over most parts of India. Further, based on the findings they argued that it is adequate to run the model at 30 km resolution so as to evaluate the results against the observation at 1° resolution (the highest they were able to find). Clearly, daily precipitation data over South Asia is available at much higher resolution, so they might have concluded differently about adequacy of the model resolution had they compared their result with such dataset. In addition, even the horizontal resolution of 25 km seems to be generally inadequate for realistic representation of spatiotemporal variability of SASM such as precipitation, particularly over complex regions such as the Himalaya. In any case, there have been only a few RCM based studies on SASM that employ high resolution compared to plethora of such studies over other regions, in particular over mid-latitudes, in recent years (e.g., Barrera-Escoda et al. 2013, Gorter et al. 2014, Li et al. 2012).

The previous Hadley Centre regional model, PRECIS, is widely used but applies the hydrostatic approximation in its representation of atmospheric dynamics. This limits the horizontal resolution it can use (it is formulated to run at resolutions of 50 and 25 km) and its usefulness in studying benefits of higher resolution. However, the recent version of the Hadley Centre RCM is relevant in this context as it uses a non-hydrostatic formulation and thus can run at (much) higher resolutions.

The main aim of this paper is then to compare performance of a recently developed Hadley Centre RCM (HadGEM3-RA) in simulating various aspect of SASM at medium (0.44°) and high (0.11°) horizontal resolutions with particular focus on precipitation. We wish to answer the question of whether running the Hadley Centre RCM at high resolution adds sufficient value (compared to added computational costs) to be of use in

climate change impact work, such as catchment scale hydrological impacts modelling (Berg et al. 2013).

The rest of the paper is arranged as follows. In section 5.2, the model formulation, experimental design and observational data are discussed. In section 5.3, we evaluate the high and low resolution model performances focusing on various aspects of precipitation using a comprehensive analysis of various statistics associated with daily and monthly precipitation such as seasonal mean distribution, relative frequency distribution and extremes. Conclusions are drawn in section 5.4.

5.2 Methods

5.2.1 Model and experimental design

HadGEM3-RA is the limited area component of the third Global Atmosphere (GA3) modelling system; where the GA3 configuration of the Met Office Unified Model (MetUM) itself is derived from the HadGEM3 global model. It is a merged weather and climate prediction system formulated in a way that allows atmospheric processes to be modelled and parameterized seamlessly across time scales and spatial resolutions. For a more detailed description of the model formulation readers are referred to Walters et al. (2011).

HadGEM3-RA has a fully elastic and non-hydrostatic dynamical core, employing a semi-implicit and semi-Lagrangian scheme (Davies et al. 2005). Prognostic fields are discretized horizontally with the Arakawa staggering C-grid (Arakawa and Lamb 1977) and the vertical decomposition is done through Charney-Philips terrain following and hybrid-height levels (Charney and Phillips 1953). The HadGEM3-RA physical

formulation includes the following parameterizations: deep convection—based on the mass flux scheme CMODS4A (Gregory and Rowntree 1990) with convective available potential energy closure, which originates from Frisch and Chappell (1980), and various extensions to include down-draughts (Gregory and Allen 1991) and convective momentum transport; large scale precipitation—based on the updated cloud microphysics scheme of Wilson and Ballard (1999) and uses the fall velocities of Abel and Shipway (2007) for a better representation of the drizzle drop spectrum; turbulent motions and boundary layer mixing processes are calculated using the scheme of Brown et al. (2008). Large scale clouds are dealt with using the prognostic cloud fraction and condensate scheme PC2 (Wilson et al. 2008), and soil–vegetation–atmosphere interactions are calculated using the Joint UK Land Environment Simulator (JULES, Best et al. 2011).

The model employs 63 vertical levels and can be run, in theory, at any desired horizontal resolution. The latitude–longitude grid is rotated so that the equator lies always inside the region of interest, in order to obtain a quasi-uniform grid box area throughout the region of interest. The model has been used over different regions of the globe and it is one of the models participating in the Coordinated Regional Climate Downscaling Experiment (CORDEX, Giorgi et al. 2009, wcrp-cordex.ipsl.jussieu.fr).

HadGEM3-RA is run at 0.44° and 0.11° horizontal resolution (i.e. approximately 50 and 12 km resolution respectively; henceforth RCM50 and RCM12) over an identical South Asian domain (Fig. 5.1), which is same as the smallest domain in Bhaskaran et al. (1996). A previous study on sensitivity of the model simulation to the domain size found that the model, run at 0.44°, has better skill in simulating the SASM over this domain compared to several larger domains (Karmacharya et al. 2015, Chapter 4 - this

thesis). Both simulations are run on a rotated latitude-longitude grid with the rotated grid equator in the middle of the domain to ensure quasi-uniform grid-boxes across the domain and the outputs are interpolated to 50- and 12- km latitude-longitude grid, using bilinear interpolation after discarding the outer 8 and 28 grid points from the coarser and finer simulations respectively. Except where otherwise stated, to facilitate inter-comparison, interpolated RCM12 outputs are aggregated to the 50 km latitude-longitude grid, which is consistent with treatment of model output as areal average verses a set of point estimates (Chen and Knutson 2008).

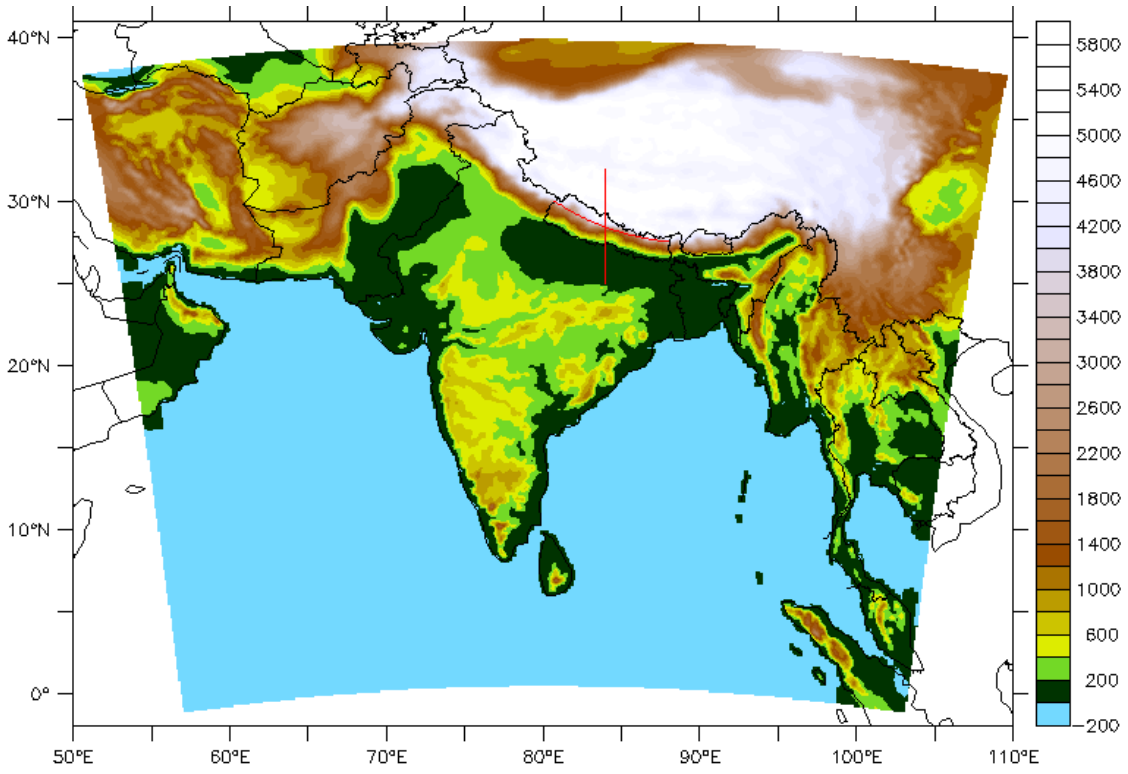

Fig. 5.1 RCM domain common to both RCM simulations. Orography of RCM12 is also shown. Red lines represent the line along which transects of orography is drawn in Fig. 5.S1.

Both simulations are forced by ERA-Interim (ERAI) reanalysis (Dee et al. 2011) at the lateral boundaries. ERAI has a T255 spatial resolution (~0.75° or ~80 km) and 60 hybrid vertical levels. Temporally, the reanalysis is prescribed at the lateral boundaries every 6 hours. ERAI also provides initial condition for the RCM50, which was initialized on 1 January 1989 and ran continuously till the end of 2008. In contrast, output of RCM50 is used to initialize RCM12 which start on the 1st April and ran till the end of September for each year from 1990 to 2008. This is done so RCM12 is run only over the season of interest but also to ensure that it has the same initial condition at the start of premonsoon season as in the RCM50. In both simulations, sea surface temperature (SST) is prescribed from observed high-resolution (0.25°) SST (Reynolds et al. 2007) at daily interval. The first year of the coarser simulation is discarded as spin up so summers of 1990 to 2008 is the common data available period in both the simulations, out of which monsoon seasons (June-September) of 1990 to 2007 are analysed.

Although each simulation uses identical physics, a few changes were made in RCM12 to maintain the model stability, such as shorter time step and diffusion settings. The RCM12 orography was also slightly smoothed to overcome a valley cooling problem found with the default orography. This smoothing was confined to the high mountainous regions and resulting differences in elevation for any grid point is less than 200 m. For numerical stability, RCM topography is often smoothed to filter out the smallest topographical wave corresponding to a wavelength of twice the grid interval (Dimri 2009, Im et al. 2006). In addition, topographical smoothing has also been employed to improve RCM performance, for example, to reduce precipitation overestimation in the steepest topographical slopes (Pal et al. 2007). Despite the slight smoothing the 12 km model orography is more realistic than that used in the 50 km

model as can be seen clearly from a comparison of transects along and across the central Himalaya at high and low resolutions in both the models and an observation (Fig. 5.S1).

5.2.2 Observational datasets

The following datasets are used for model evaluation.

i) Daily precipitation is taken from the station based gridded product of APHRODITE available at 0.25° resolution (APHRO_MA_V1003R1) (Yatagai et al. 2009). This dataset is chosen because of its high temporal and spatial coverage and station density, especially over the central Himalayas.

Even though TRMM (Huffman et al. 2007) is a relatively high resolution dataset based on remote sensing (e.g. TRMM-3B42 available at resolution of 25 km at 3 hourly intervals), it is not employed here for model evaluation for two reasons. Firstly, it is available only from 1998. Secondly similar to other remote sensing data, it does not capture the precipitation distribution at elevation higher than 1 km well and also underestimates precipitation in mountainous regions (Andermann et al. 2011).

ii) Global precipitation climatology project (GPCP) version 2.2 (Huffman et al. 2009) at monthly resolution – a satellite and gauge measurement based product available at 2.5° resolution. The dataset is used for model evaluation over the ocean, where APHRODITE data is not available.

iii) ERAI is also used to evaluate model performance in simulating circulation and other atmospheric features associated with the SASM.

5.3 Results and discussions

5.3.1 Monsoon climatology

The observed (APHRODITE over land and east of 60° E, and GPCP over the rest) summer monsoon seasonal mean precipitation for 1990-2007 is shown in Fig. 5.2a. The Observed mean precipitation maxima are located over the Western Ghats, east central and north east India, foothills of the central Himalaya, the Arkan hills, Bangladesh and north Bay of Bengal. In contrast, observed precipitation minima lie on the leeward sides of the mountains such as the Western Ghats, the Arkan hills and the Himalaya. Also, a west-northwest to east-southeast gradient of precipitation is found over the Indo Gangetic plain (IGP) arising from diminishing moisture content in the monsoonal flow further inland (Fig. 5.S2).

The coarser model simulated mean precipitation exhibits a wet bias over the IGP, northeast and east peninsular India, east Bay of Bengal and east Arabian sea (Fig. 5.2b). A dry bias is seen over the west central and west peninsular India and west Bay of Bengal. Wet bias over the warm ocean and dry bias Indian land areas are common and long standing problems in climate model simulations (e.g. Annamalai et al. 2007a, Sperber et al. 2013). In particular wet biases over the warm ocean found in atmosphere only models have been partly attributed to the use of prescribed SSTs, which, by design, lack the negative correlation between SST and rainfall over warm oceans with weak SST gradients (Krishna Kumar et al. 2005), and it has been shown to reduce with coupling an ocean component to an atmosphere only RCM (Ratnam et al. 2009). This wet bias, caused by lack of atmosphere-ocean coupling, could in turn affect intraseasonal oscillation and seasonal variations of monsoon (Krishnan et al. 2006).

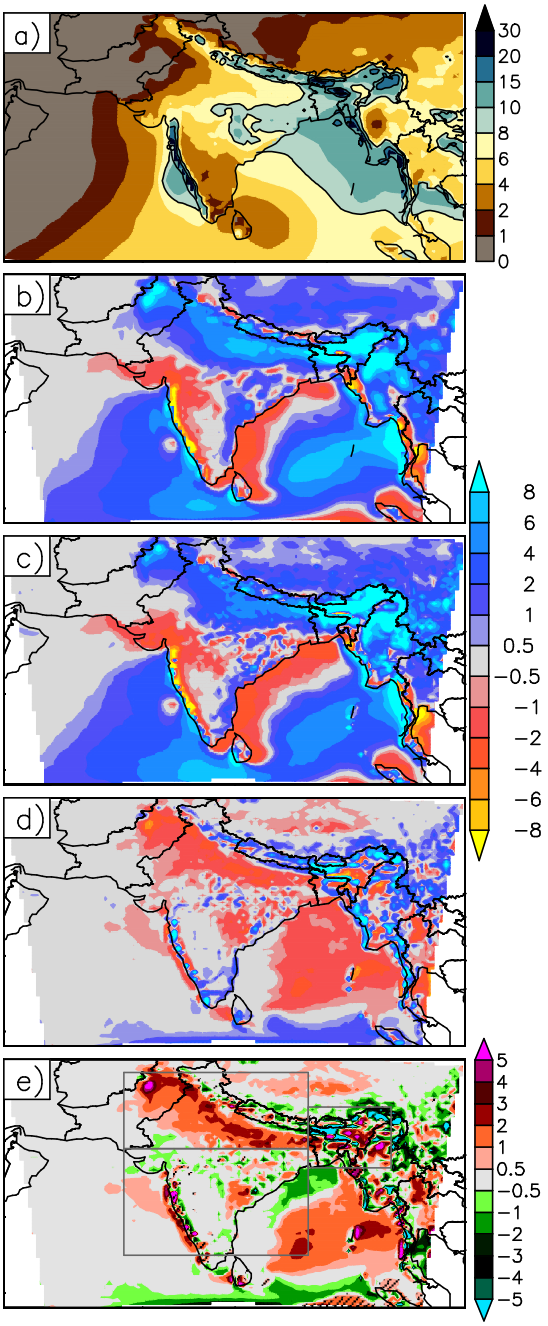

Fig. 5.2 a) Observed monsoon mean precipitation for 1990-2007 (APHRODITE over land and east of 60° E, and GPCP over the rest), (b-c) bias in RCM50 and RCM12 relative to a), d) RCM12 difference from RCM50, e) added value of RCM12. Areas having dry bias in RCM50 and added value more than 0.5 are

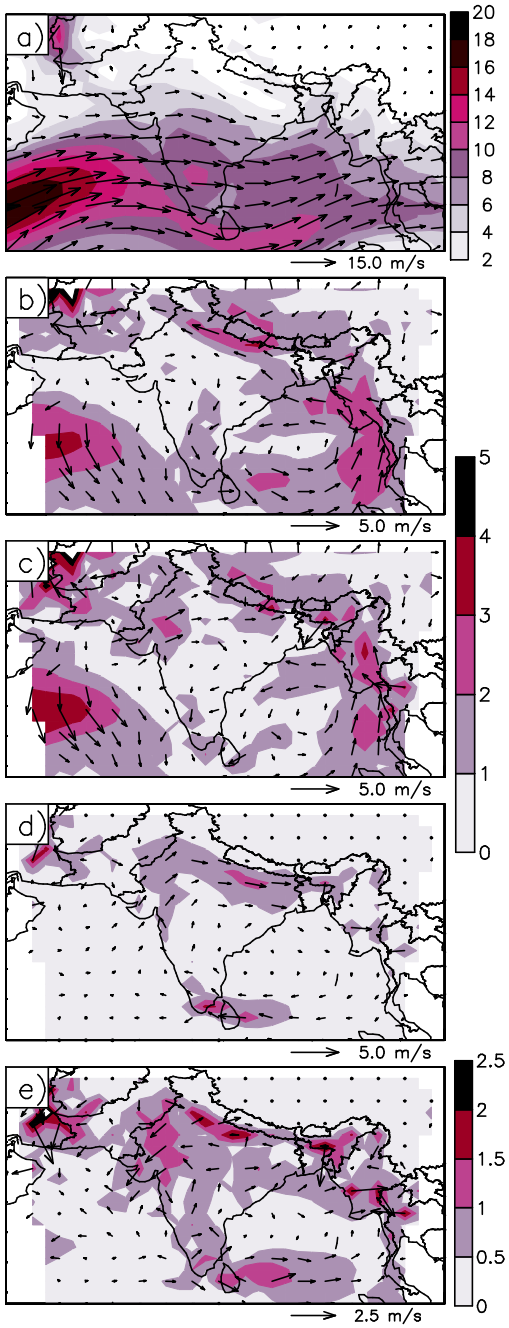

Fig. 5.3 a) Observed (ERAI) monsoon mean circulation at lower tropospheric level for 1990-2007, (b-c) bias in RCM50 and RCM12, d) RCM12 difference from RCM50. e) added value of RCM12[1].

[1] wind vectors with southerly or westerly components represent added values for meridional and zonal components of wind

hashed. Unit: mm/day[1].

[1] Here, added value = | (RCM50 - Obs.) | - | (RCM12 - Obs.)

respectively whereas those with northerly and easterly components represent negative added value for the respective wind components. Arrows and shading show the wind vectors and speed respectively. Unit: m/s.

The RCM50 was also analysed in Karmacharya et al. (2015, Chapter 4 - this thesis) where the effect of domain size on regional monsoon climate was evaluated. They found that RCM50 was able to partially overcome the common MetUM problem of dry bias over the Indian landmass, but at the same time it introduces a large wet bias over north India reflecting the model's problems with convection when strong moisture-laden flow is incident upon steep orography – another MetUM inherent deficiency in resolving the interaction of low-level monsoon flow with the Himalayan orography (Levine and Turner 2012). Sensitivity tests show that the north Indian wet bias is directly related to central Indian dry bias by creating an area of excessive convergence along the steep southern slopes of the Himalayas and diverting moisture from central India. In the RCM50, there is anomalously strong southeasterly flow over the IGP at the lower atmospheric levels (Fig. 5.3b) resulting in anomalous vertical integrated moisture flux (VIMF) over the region from the Bay of Bengal (Fig. 5.S2b). On the other hand, divergence of the low-level monsoon flow at landfall (as typically found in the MetUM, Fig. 5.3 b-c) in response to difficulty to convect over the Indian peninsula (leading to dry bias over the west coast) enhances the flow into the Himalaya. Hence, the systematics errors within the domain are closely interlinked.

The RCM12's mean precipitation bias pattern resembles that of the coarser simulation (Fig. 5.2c). However, compared to RCM50 the wet bias over the IGP, Bay of Bengal

and parts of east central and northeast India is reduced (Fig. 5.2d). This demonstrates a clear benefit (or added value in the sense of smaller absolute biases) from the use of higher resolution, though the added value will be sensitive to the observational estimate used as reference and thus cannot be accurately quantified. Almost all the improvement seen at 12 km (Fig. 5.2e) is achieved by reduction of the wet bias in the RCM50 (compare Fig. 5.2d and 5.2e). It is noteworthy that previous studies generally reported increased precipitation with higher resolution simulations (e.g. Bhaskaran et al. 2012, Giorgi and Marinucci 1996, Leung and Qian 2003, Stephenson et al. 1999). For example, Sinha et al. (2013) reported increased precipitation in high resolution simulations over most part of India compared to its coarse resolution counter in RegCM3 simulations of SASM. However, here not only precipitation is reduced over the IGP in the higher resolution simulation, but it results in reduced wet bias in almost all those areas.

Consistent with its large wet bias over IGP and east-central Bay of Bengal (Fig. 5.2b), RCM50's low level flow has anomalously strong southeasterly flow over the IGP and cyclonic circulation over the Bay of Bengal (Fig. 5.3b). Again, RCM12 has anomalous westerly flow over the IGP and anticyclonic circulation over the Bay of Bengal at the low level relative to RCM50 (Fig. 5.3d), which is consistent with its reduced precipitation over those regions compared RCM50. These differences in circulation lead to reduction of moisture in flux over the IGP from the Bay of Bengal and over south Bay of Bengal from the Arabian sea in RCM12 (Fig. 5.S2d). Hence, there is a clear connection between the precipitation and circulation improvements in RCM12 relative to RCM50. Further, low level circulation differences in the two simulations over land is mainly confined along the Himalayan foothills, which is likely due to the model's ability to better resolve the interaction between the orography and the low level flow at

the higher resolution. This shows that one of the MetUM's inherent deficiencies can be partly overcome by employing simulations at higher resolution. However, compared to ERAI, RCM12 has anomalous low level westerly flow over large parts of north India (Fig. 5.3c) and the added value in both components of the wind is confined to east-central coast of India and small parts of northwest and peninsular Indiabut there is deterioration in both components of the wind over west-central India (Fig. 5.3e). Nevertheless, these results are consistent with other previous studies that relate model ability to realistically simulate the spatial distribution of precipitation as well as its frequency and intensity at higher horizontal resolution with its improved simulation of certain circulation features (Rauscher et al. 2010). Such features include ITCZ position and migration (Rauscher et al. 2006), the genesis and evolution of tropical storms (Oouchi et al. 2006), monsoon circulations (Gao et al. 2006), orographic precipitation, and topographic effects (Duffy et al. 2003, Iorio et al. 2004, Leung and Qian 2003).

For further insight into the source of precipitation reduction in the high resolution simulation, we compared the terms of water balance equation described in Bhaskaran et al. (2012) in the two simulations averaged over a rectangular region that encompasses the landmass of north and central parts of India (74-83° E, 18-27° N). In the high resolution simulation, area average precipitation and evapotranspiration rate, and convergence of VIMF into the region are reduced by 0.73, 0.46 and 0.25 mm/day respectively compared to the coarser resolution (Table 5.1). Hence, roughly two thirds of the reduction in precipitation is accounted for by reduced local moisture recycling and one third by reduced moisture convergence. These inter-links between rate of precipitation and evapotranspiration, and convergence changes are consistent with those reported by Bhaskaran et al. (2012).

Table 5.1 Terms of water balance equation (in mm/day) [1].

Model	S	P	E	D	P - E
RCM50	0.16	7.55	3.10	-4.6	4.45
RCM12	0.18	6.82	2.65	-4.35	4.17
RCM12 - RCM50		-0.73	-0.46	0.25	-0.28

[1] S, P, E and D represent local change in the atmospheric water vapour storage, precipitation rate, evapotranspiration rate, divergence of vertically integrated moisture flux respectively.

5.3.2 Distribution of daily precipitation

Next, we analyse various aspects of the daily precipitation data to gain further insight into factors contributing to the mean precipitation bias.

5.3.2.1 Frequency of wet day

In the APHRODITE observed gridded rainfall, the pattern of mean wet day frequency (days with precipitation exceeding 1 mm/day) is broadly similar to mean precipitation (Fig. 5.4a). In comparison, the frequency of wet days is too high in RCM50 over most parts of South Asia with the highest overestimation over central Pakistan (up to 80 days; Fig. 5.4b). It seems that the anomalous low level southeasterly flow over the IGP in RCM50 aids moisture advection all the way to central Pakistan resulting in excessive wet days over the region. Reduction of the anomalous low level flow in RCM12 leads to substantial reduction in the number of wet days, especially over the IGP with the largest reduction over central Pakistan (up to 50 days), though large bias still persists (Fig. 5.4c). On the other hand, frequencies of wet days in both models are similar to the observed over the west Indian coast, where models have similar dry biases. A plot of

simple daily intensity index[5] (wet day precipitation rate) shows that both models have similar distribution of the biases (both magnitude and pattern) over South Asia including IGP (not shown), so the differences in low level flow over the IGP in the two models mainly modulates the number of wet days without altering the precipitation intensity. Hence, the improvements in mean precipitation over land in the high resolution simulation mainly arise from a reduced number of wet days.

Moreover, RCM12's improved simulation of the frequency of wet days implies that it has better skill in simulating other metrics commonly used in model evaluation, which are associated with wet day frequency, such as mean consecutive wet days, mean dry spell etc. For example, mean consecutive wet days are relatively better simulated in RCM12 compared to RCM50 over large parts of South Asia (Fig. 5.S3).

5.3.2.2 Relative frequency distribution

While the wet day frequency provides some insight into causes of wet bias over the IGP, it does not explain the differences across the range of observed and modelled precipitation intensities - this information can be gained from the frequency distribution of the daily precipitation. Hence, we compare relative frequency distribution of monsoon daily precipitation for both simulations and observation over three land regions outlined in Fig. 5.2e. For each dataset and region, the relative frequency distribution is computed as follows: daily precipitation from each of the common 50 km grids within a region is binned in 0.5 mm wide bins for the entire period (monsoons season, 1990-2007) and the resulting histogram is expressed relative to the total sample size, which is the product of total duration (days) of monsoon and number of common 50 km grids in the region. Each region is selected based on its distinct seasonal mean

[5] Simple daily intensity index is defined as the ratio of wet day cumulative precipitation to number of wet days where days with more than 1 mm precipitation are considered wet days

precipitation pattern or specific features of its representation in the two simulations warranting further investigation: a) north India and neighbourhood – a wet bias region but showing large improvement in the RCM12, b) central and south India – a dry bias region with overall slight deterioration in the RCM12 and c) northeast India and surrounds – the region of highest observed precipitation in South Asia, where RCM12 shows improvement in some areas but deterioration in some other areas.

Across all three regions, the RCM12 simulated relative frequency distribution is closer to observation for light and moderate precipitation (up to 20-40 mm/day) (Fig. 5.5). The 50 km (12 km) simulated extreme tail is in good agreement with the observed for north (central and south) India however it is overestimated by both models for northeast India. Hence, the wet bias in RCM50 over north India comes from the overestimation of the light to moderate precipitation (2.5-40 mm/day). Overall, there are improvements in the 12 km simulated relative frequency distribution over all three regions including those regions where there is no added value in mean precipitation.

The role of model horizontal resolution in simulating precipitation extremes has been well recognized (Kopparla et al. 2013, Pope and Stratton 2002). At higher resolution models are better able to resolve atmospheric motions and orographic forcing. Moreover, smoothing resulting from a coarse model grid box representing a large area acts disproportionately in reducing extreme precipitation (Iorio et al. 2004). Hence, although RCM12 overestimated extreme tails in two regions, this might partly be due to sparser observational network. For example, from an experiment over grid boxes that have a sufficiently dense local station network, Hofstra et al. (2010) showed that gridded daily precipitation is over-smoothed when fewer than all the available stations (within the interpolation search radii) are used to calculate grid-box average. Moreover,

the smoothing is greater for higher percentile, and hence it has disproportionate effect on extremes.

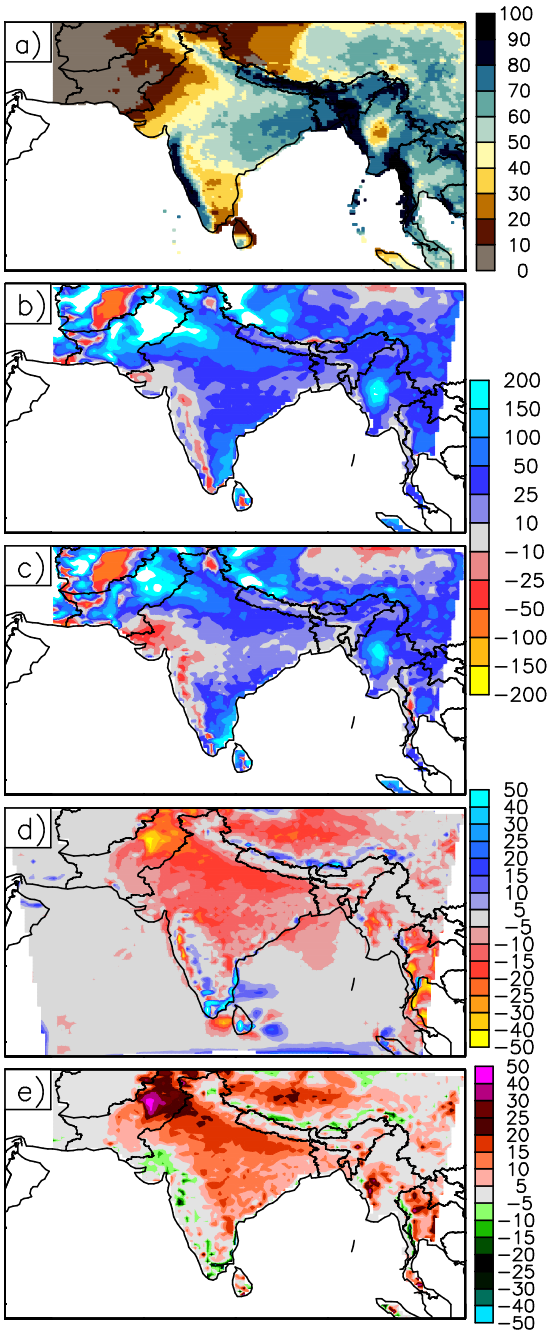

Fig. 5.4 a) Observed (APHRODITE) monsoon wet day climatological for 1990-2007 expressed as % of total days in monsoon, (b-c) bias in RCM50 and RCM12 (in %), d) RCM12 difference from RCM50 (days) e) added value of RCM12 (days).

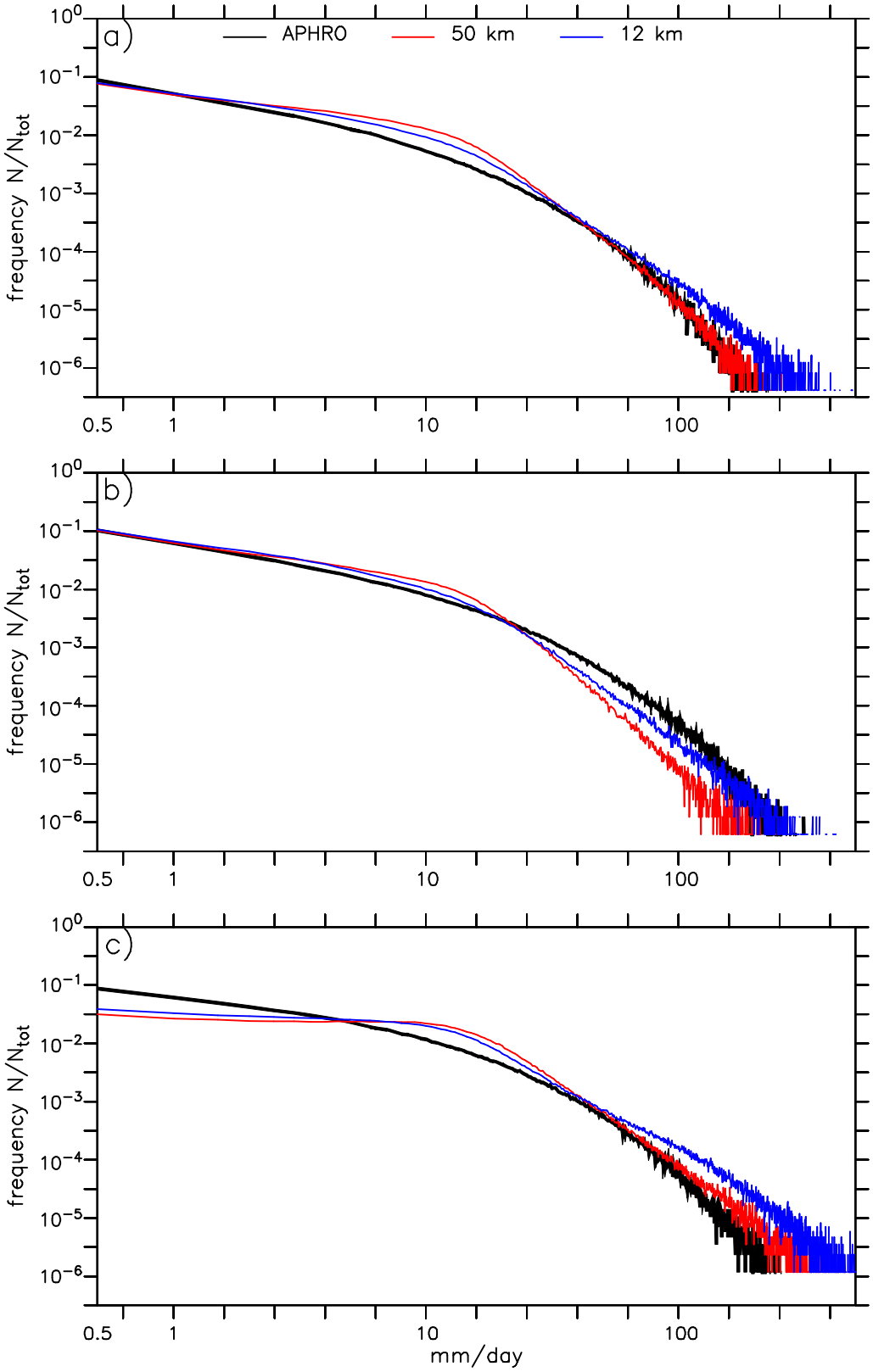

Fig. 5.5 Relative frequency distribution of daily precipitation in APHRODITE, RCM50 and RCM12 over a) north India and neighbourhood, b) central and south India and c) north east India and neighbourhood (land only). See Fig. 5.2e for outline of the regions.

5.3.2.3 Extremes

Manifestation of the improved distribution of daily precipitation can also be seen in the precipitation extremes, which is computed by considering precipitation during wet days only. The observed 95th percentile of the daily precipitation (95PDR) shows maxima along the Western Ghats, the Arkan hill and northeast India (Fig. 5.6a). The RCM50 95PDR shows a dry bias over much of the South Asia except parts of the IGP and northeast India (Fig. 5.6b), which is consistent with the large dip at the extreme tail of relative frequency distribution over South India in the RCM50 compared to the observation. The dry bias over central Indian is reduced in RCM12, while wet bias over IGP and northeast India is enhanced (Fig. 5.6c-d). Overall, there are improvements over central India and a few parts of the mountainous regions in the RCM12, but differences are minimal over other regions in the two simulations. In addition, RCM50 has an excess number of very wet days (i.e. days with precipitation amounts larger than 95PDR) compared to observed over much of South Asia with maximum overestimation in the western IGP region (Fig. 5.S4b). The excess number of very wet days in the RCM50 is actually an artefact of excess wet days in the simulation as, by definition, there will always be 5 percentile of days above the 95th percentiles. Hence, this bias is also reduced in the RCM12 over most of the South Asia with largest improvements over central Pakistan (Fig. 5.S4c-e).

In the observation, the contribution of very wet days cumulative precipitation (R95pTOT) to the seasonal total is at a maxima over the central India, which is possibly associated with the normal cyclone track – south of the monsoon trough over the IGP bringing exceptionally heavy precipitation (compared to the mean) along the route (Fig. 5.S5a). Compared to the observations, the contribution of R95pTOT to the seasonal total is underestimated over much of the South Asia in RCM50 (Fig. 5.S5b), while it is

overestimated over the IGP and parts of the central India in RCM12 (Fig. 5.S5c). However, this translates into increased absolute bias over the central Himalayan foothills and parts of northwest and west central India in RCM12, whereas improvements are noted over peninsular India, east coast of India etc. (Fig. 5.S5e). Excessive contribution of R95pTOT to the seasonal total in RCM12 is likely to arise from the occasional occurrence of grid point storms in high resolution simulation (Giorgi et al. 2014), which appears despite aggregation of both 12 km and APHRODITE data to the 50 km grid. The coarser resolution of observation may also play a role.

Similar results are obtained for the extreme wet day (99^{th} percentile) metric (not shown). Overall, these results indicate general improvements in simulation of precipitation extremes in the high resolution simulation.

5.3.3 Seasonal evolution of climatological daily precipitation

In this section, we investigate the evolution of climatological daily precipitation through the monsoon season in the observations and model simulations. This analysis reveals model performance at sub-seasonal scale i.e. early, mature and late phases of monsoon. Fig. 5.7 shows the daily climatology of the fraction of total precipitation due to light (<5 mm), moderate (5-30 mm) and heavy (>30 mm) precipitation respectively averaged over the same three regions outlined in Fig. 5.2e.

Both models have very similar seasonal evolution for the fraction of total precipitation due to light precipitation over all three regions. This shows that process of generation of the light precipitation is likely to be similar in both the models and differences in precipitation distributions in the two models come mainly from the differences in the

higher intensities. The seasonal evolution of the contribution of light precipitation is similar to observed over north India, but the ratio remains below observed over northeast India throughout the season. However, over central and south India it is much higher than observed during initial phase of monsoon (i.e. up to mid-July) but it approaches the observed ratio as monsoon progresses.

In general, fractions of total precipitation due to moderate and heavy precipitation respectively are closer to observed in RCM12 compared to RCM50 for all three regions. In fact, the evolution of those fractions are closer to observed in RCM12 throughout the season over north and, central and south (northeast) India regions except for first half of June (initial phase of monsoon).

Hence, RCM12 exhibits improved skill not only for relative frequency distribution of daily precipitation aggregated for the whole period, but it also performed better throughout the season. In other words, improvements in RCM12 compared to RCM50 is not due to the better performance during a particular phase of monsoon (e.g. early, peak, late), rather it performs persistently better throughout the season, at least in the climatological sense. Moreover, these results are not sensitive to slight alteration of the thresholds used to define different precipitation categories, which indicates the robustness of the result.

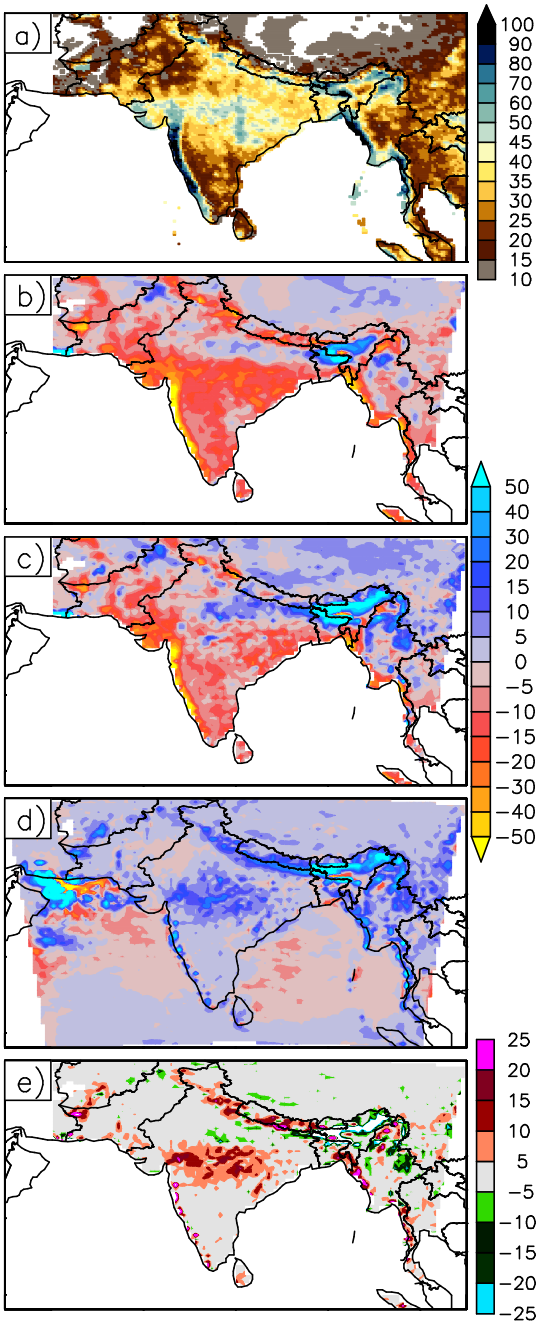

Fig. 5.6 Observed (APHRODITE) 95th percentile of the daily precipitation (95PDR), (b-c) bias in RCM50 and RCM12, d) RCM12 difference from RCM50 e) added value of RCM12. Unit: mm/day.

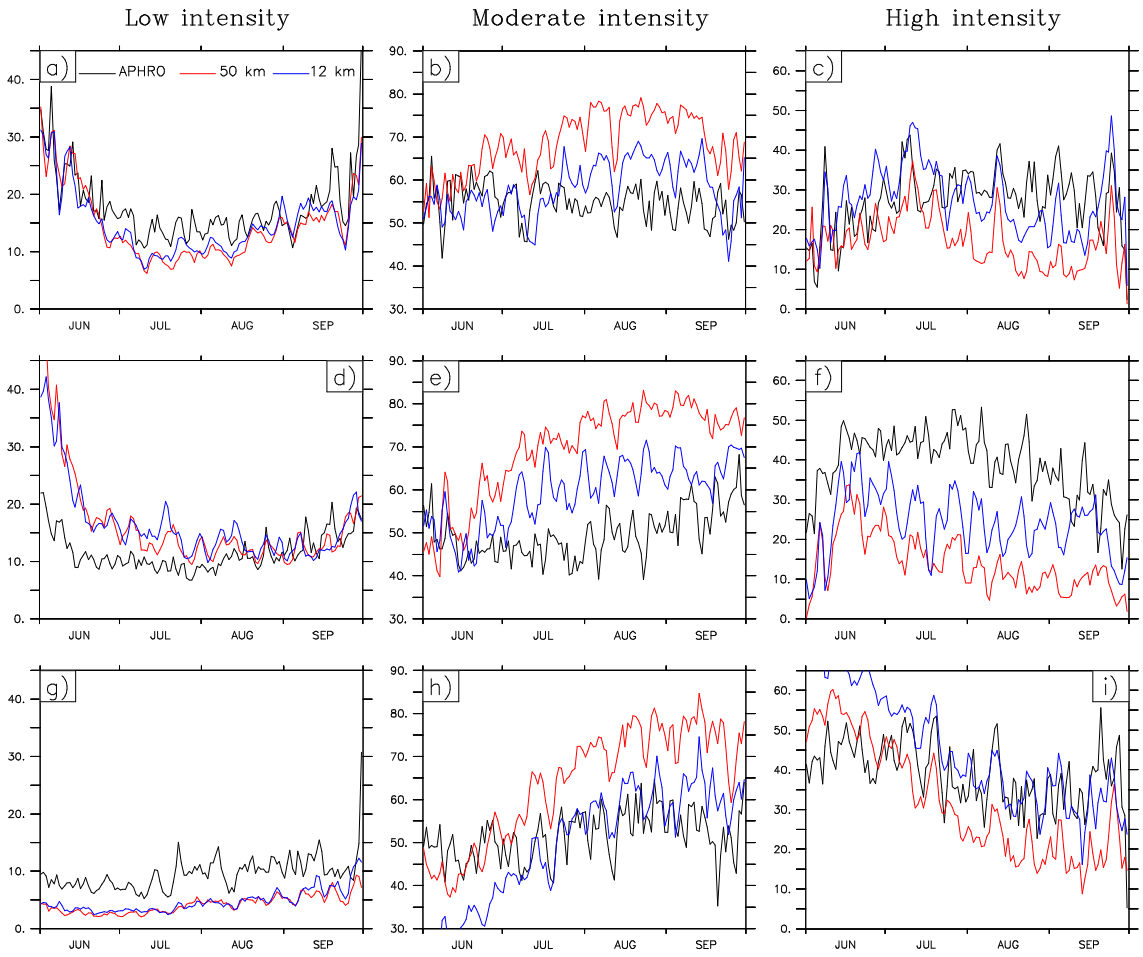

Fig. 5.7 Observed and simulated daily climatology for contribution of light (<5 mm), moderate (5-30 mm) and heavy (>30 mm) precipitation to total precipitation (%) over north India and neighbourhood (a-c), central and south India (d-f) and northeast India and neighbourhood (g-i) (land only).

5.4 Conclusions

Regional climate models (RCMs) that have conventionally been run at a resolution of 25-50 km are now being run at resolutions of 10 km or less. The use of higher resolutions is motivated by an expected added value from improved representation of land surface heterogeneity, improved physics and dynamics, and capacity to simulate small scale processes. Importantly, it is also motived by the demand from the user

community for higher resolution climate projections. This raises the question whether the higher resolution brings additional useful information or simply the same information as coarser resolution simulations at apparently finer scales. The added value of high resolution simulations are often investigated in precipitation – a variable with high fine scale heterogeneity and of high socio-environmental significance. Many studies have reported improvements in higher resolution simulation of precipitation, but others reported lack of improvement or even deterioration. So, higher resolution does not necessarily lead to improved simulation; for example, a strengthening or weakening of the hydrological cycle could either reduce or enhance an underlying bias seen at coarser resolution.

We investigated the added value of high resolution regional climate modelling in simulating various characteristics of the South Asian summer monsoon precipitation using the HadGEM3-RA model at 50- and 12- km resolutions. The large scale circulation simulated by both the models at low level are generally similar except for the flow over i) the Indo-Gangetic plains, which arguably comes from the enhanced model skill at the high resolution to resolve the interaction of the moisture laden low level flow with the Himalayan steep orography, and ii) over the Bay of Bengal. This partial improvement in simulation of low level circulation in the high resolution simulation leads to improved simulation of the South Asian Summer monsoon (SASM) mean precipitation specially over the Indo-Gangetic plain (IGP) and the Bay of Bengal, and it better simulates many other aspects of SASM precipitation such as frequency of wet days, relative frequency distribution of the daily precipitation, and precipitation extremes.

We found that improvements in higher resolution simulation of mean precipitation is achieved mostly through the reduced wet bias (arising from reduced wet days at least

over the IGP) and the largest added value over land is seen over the IGP rather than regions of complex terrain such as mountains or coasts. Both these results are significant given many previous studies reported increased mean precipitation and complex, rather than homogeneous, regions being the likely area of improvements at higher resolution. It is noteworthy that increasing resolution without tuning model physics could potentially increase the model bias (Rauscher et al. 2010). Met Office models are designed to run at a range of resolution keeping the model physics the same (Walters et al. 2011). So these results, in agreement with Pope and Stratton (2002) and Duffy et al. (2003), indicate the need for improved model parameterizations and model tuning at higher resolution in order to further improve model performance.

While some studies reported improvements with high resolution modelling for the season in which precipitation is mainly produced by the resolved scheme, rather than the convective parameterization, with fewer improvements for the season when convective scheme dominates (Chan et al. 2012, Iorio et al. 2004). Others reported improvements even for summer convective precipitation (Prein et al. 2013). Among other factors, presence or lack of added value in high resolution simulation also depends on the metrics used for the evaluation (Chan et al. 2012). In any case, convective precipitation contributes about half of total SASM precipitation in the observation, but its contribution is even higher in the model simulations. Hence, improvement of convection scheme might be a key component for further improvements in high resolution model simulation of the SASM. Model simulations at convection permitting scale (1-4 km) would also provide further insight.

However, our results are encouraging enough to extend this work to test the sensitivity of the RCM SASM simulation to horizontal resolution when forced by imperfect boundary forcings from GCMs.

Acknowledgements

First author thanks the Felix Scholarships for funding his DPhil and the Christ Church for partially funding final year of study. The model simulations were carried out at Met Office. Richard Jones was supported by Joint DECC/Defra Met Office Hadley Centre Climate Programme (GA01101). We acknowledge use of the MONSooN system, a collaborative facility supplied under the Joint Weather and Climate Research Programme, which is a strategic partnership between the Met Office and the Natural Environment Research Council. We thank two anonymous reviewers for comments which helped to significantly improve the manuscript. We also acknowledge use of the Ferret program, product of NOAA's Pacific Marine Environmental Laboratory, for analysis and graphics in this paper.

Supplementary Information: Chapter 5

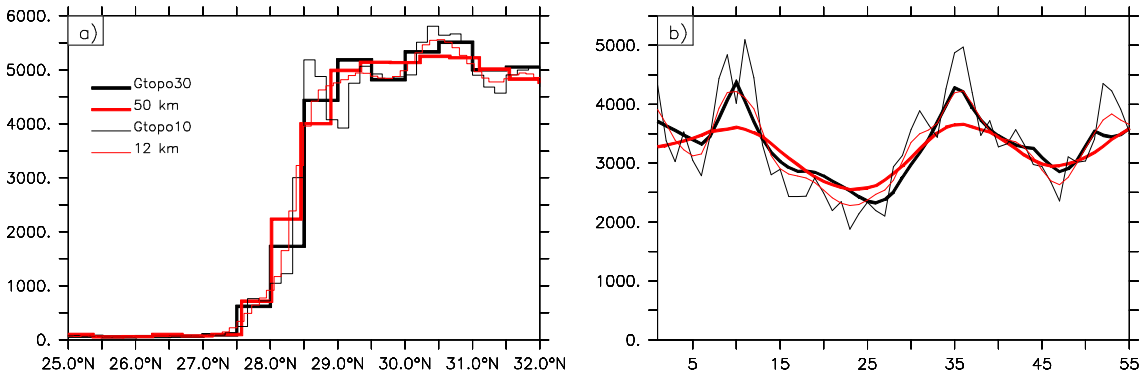

Fig. 5.S1 a) North-south transect of topography over the central Himalaya for GTOPO-30 min, GTOPO-10, RCM50 and RCM12, b) same as a) but for elevation sampled along the arc approximately parallel to the central Himalaya. See Fig. 5.1 for the location of the line/arc.

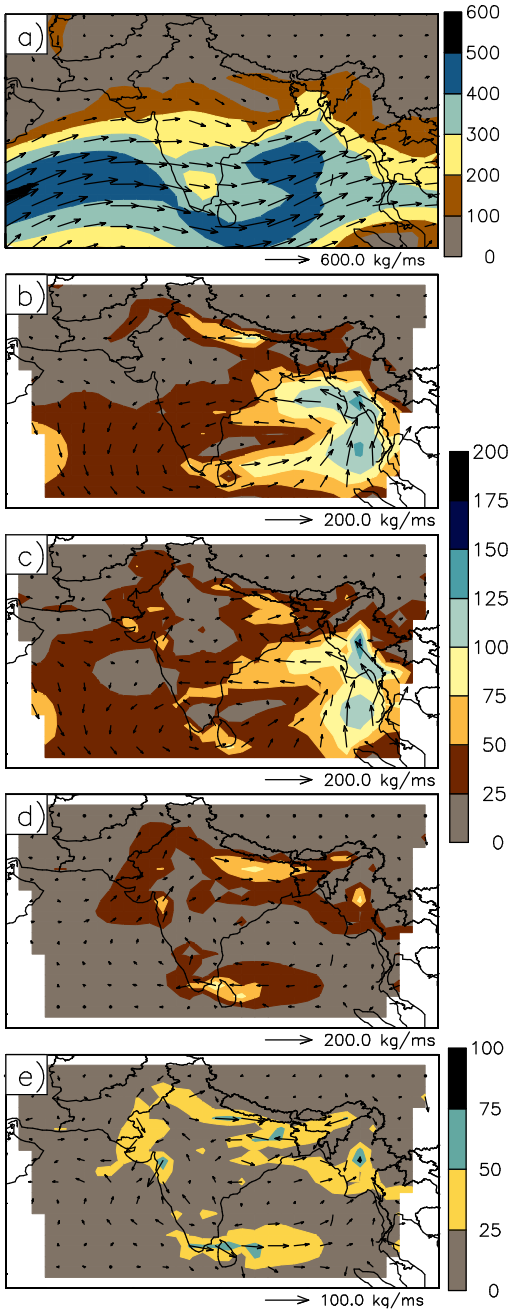

Fig. 5.S2 a) Observed (ERAI) monsoon mean vertical integrated moisture flux, (b-c) bias in RCM50 and RCM12, d) RCM12 difference from RCM50, e) added value of RCM12. See Fig. 5.3 for interpretation of the added value. Arrows and shading show moisture flux vectors and its magnitude respectively. Unit: kg/ms.

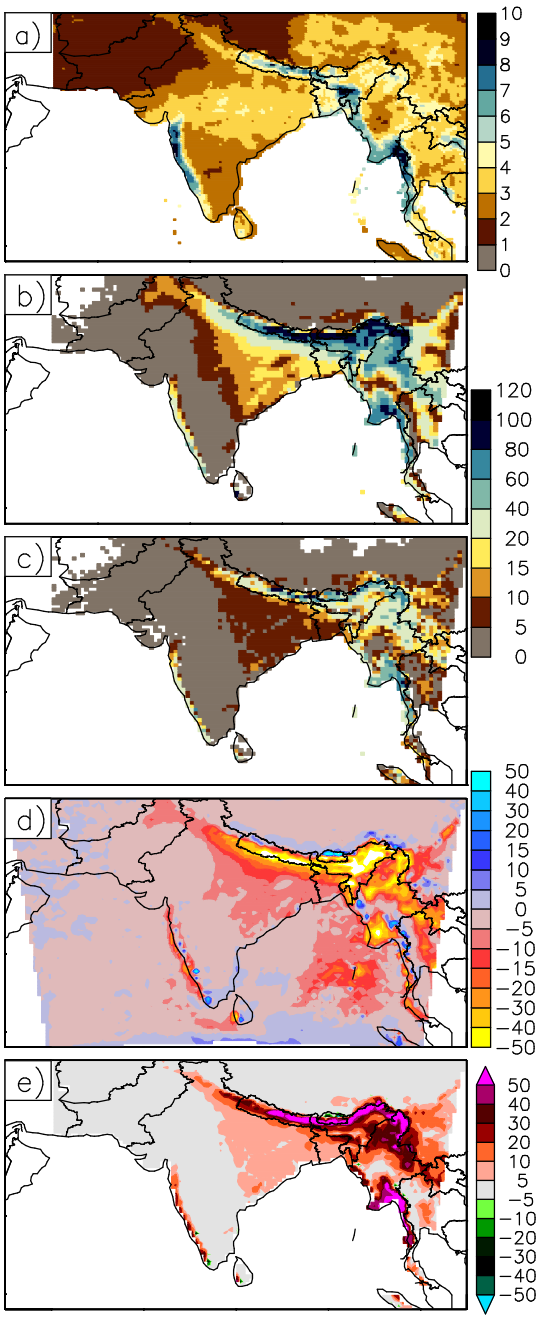

Fig. 5.S3 a) Observed (APHRODITE) monsoon mean consecutive wet days, (b-c) bias in RCM50 and RCM12, d) RCM12 difference from RCM50, e) added value of RCM12. Unit: days.

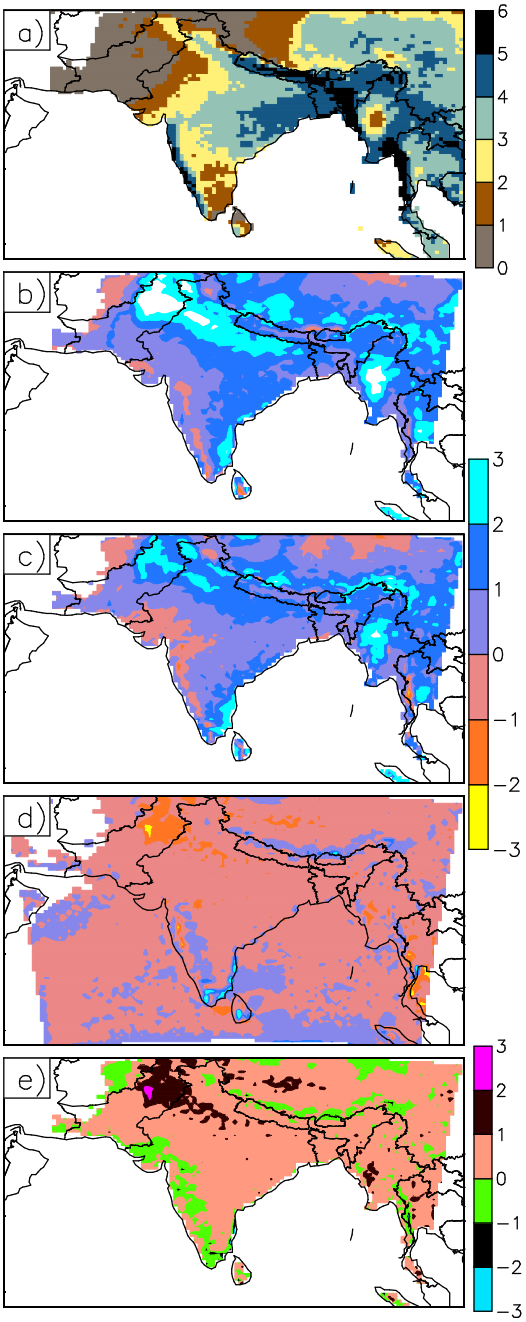

Fig. 5.S4 a) Observed (APHRODITE) monsoon mean frequency of very wet days, (b-c) bias in RCM50 and RCM12, d) RCM12 difference from RCM50, e) added value in RCM12. Unit: days.

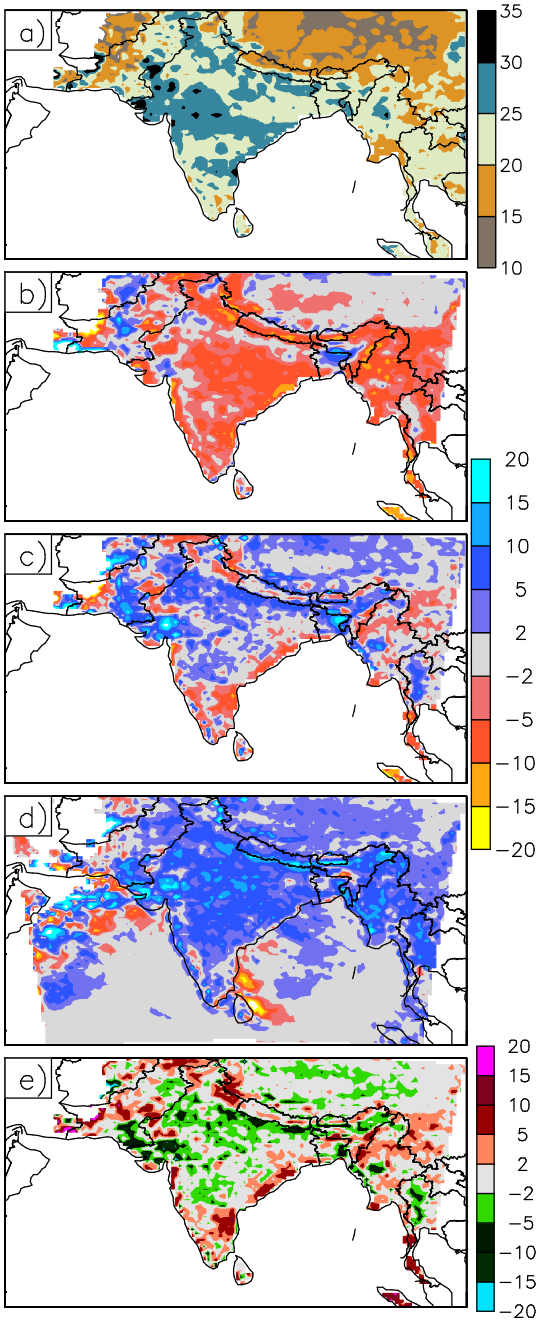

Fig. 5.S5 a) Observed (APHRODITE) monsoon climatology of the contribution of very wet day precipitation (R95pTOT) to seasonal total (%), (b-c) bias in RCM50 and RCM12, d) RCM12 difference from RCM50, e) added value in RCM12.

6 Added value of a high resolution regional climate model in simulation of intraseasonal variability of the South Asian summer monsoon

Synopsis

The previous chapter demonstrated the added value of the high resolution Hadley Centre RCM in simulating SASM climatology, mainly its precipitation. The largest improvement in high resolution model's simulation of mean precipitation is seen over the Indo-Gangetic plain, and is achieved through the reduction of excess wet bias and wet days in the coarser model. In addition added value was seen in many other aspects such as intensity distribution of daily precipitation, spatial distribution of precipitation extremes, wet day frequencies, seasonal mean low level circulation and moisture flux etc.

In continuation of the previous chapter, this chapter also assesses the added value of high resolution RCM simulation of SASM but here the focus of the assessment is: intraseasonal aspects of the SASM, mainly the precipitation. The assessment utilizes the same two RCM simulations described in the previous chapter and again attempts to address the same research question, which is: for the Hadley Centre regional climate model what is the extent of added value in going from 50 km to 12 km resolution, and if so, where does the added value lie? So, this chapter complements the previous chapter in quest for addressing the research questions.

As for the monsoon climatology, the high resolution RCM exhibits added value in simulating various intraseasonal characteristics of the SASM. For example, the high resolution RCM has improved simulation of active and break composite precipitation rates with large added value over the Indo-Gangetic plain. However, the high resolution model does not show consistently improved results for temporal statistics associated with active and break events. Nevertheless, the high resolution model better simulates precipitation extremes over the central Himalaya (Nepal) in terms of timing of their

occurrence relative to peak monsoon months and the break spell, and contribution of the extreme cumulative precipitation to the seasonal total. These results clearly demonstrated added value of high resolution Hadley centre RCM simulation of monsoon intraseasonal characteristics.

Authorship Declaration

I carried out all the analysis and wrote the paper. R. Jones and M. New contributed to narrow the area of investigations. M. New helped plan the analysis, and gave advice on the methodology for investigations particularly concerning large scale features associated with intraseasonal aspects. Both R. Jones and M. New contributed to interpretation of the findings and their comments were helpful in rewriting the manuscript. They both commented on a draft of the paper.

Added value of a high resolution regional climate model in simulation of intraseasonal variability of the South Asian summer monsoon

J. Karmacharya[1,2], M. New[1,3] and R. Jones[1,4]

Affiliations:

[1] School of Geography and the Environment, University of Oxford, Oxford, United Kingdom

[2] Department of Hydrology and Meteorology, Kathmandu, Nepal

[3] African Climate and Development Initiative, University of Cape Town, Cape Town, South Africa

[4] Met Office Hadley Centre, Exeter, United Kingdom

Submitted to: *International Journal of Climatology*

Abstract

The South Asian summer monsoon (SASM) exhibits large variability in the intraseasonal scale with dominant modes of variability at 10-20 days and 30-60 days. Phases of these modes manifest as the active and break cycles of monsoon, which have been subject of many model based studies, as improved simulation of intraseasonal features also leads to better representation of the seasonal mean characteristics. We evaluate a recent Hadley centre regional climate model's performance, at low and high resolutions and forced by a reanalysis, in simulating various characteristics associated with intraseasonal variability of SASM. In particular, we compare the spatial patterns of precipitation and upper level circulation composites for active and break spells and, timing, frequency and duration of those spells. We found improvements in simulation of active and break composite precipitation rate in the high resolution simulation. These improvements likely come from i) improved position of the monsoon trough particularly over west India for active composite, ii) improved low level flow particularly south of the Himalaya for break composite. Moreover, enhanced capacity of the model at high resolution to resolve convection and interaction of moisture laden low level flow with the steep Himalayan orography is likely to contribute in reduction of excess precipitation over Indo-Gangetic plain and, improvements over east Nepal for break spells are likely to come from model's ability to effectively capture precipitation enhancements that arise from orographic-forced and mid-tropospheric ascending motions. However, mixed results are obtained for temporal statistics associated with occurrence of active and break events.

We also compare the model performance in simulating precipitation extremes over Nepal. The timing of extreme precipitation occurrence in relation to peak monsoon

months and break spells, and contribution of the extreme cumulative precipitation to the seasonal total are improved in the high resolution simulation.

6.1 Introduction

While the South Asian summer monsoon (SASM) is one of the most stable components of the global climate system on interannual time scales, it exhibits large variability in shorter time scales. A substantial component of the variability arises from the fluctuations in the intraseasonal scale (Rajeevan et al. 2010). The dominant time scales of intraseasonal variation are 10-20 days (Goswami et al. 2006b, Krishnamurti and Bhalme 1976) and 30-60 days (Krishnamurthy and Shukla 2000, Murakami and Nakazawa 1985). While the 30–60 day mode of variability has a prominent poleward propagation over South Asia, the 10–20 day mode is characterized by a westward phase propagation (Goswami et al. 2006b) associated with monsoon depression (Bhaskaran et al. 1996, Krishnamurti and Bhalme 1976) and has the spatial structure of convection more regional to the monsoon domain with a prominent east-west orientation (Annamalai and Slingo 2001, Goswami et al. 2006b). In contrast, 30-60 day variability has large spatial structure with a quadrupole pattern that consists of enhanced convection over the Indian subcontinent, extending over the Bay of Bengal, Maritime Continent and equatorial west Pacific, but reduced convection over the equatorial Indian Ocean and northwest tropical Pacific (Annamalai and Slingo 2001, Turner and Slingo 2009). Phases of these modes manifest as the active and break cycles of monsoon (Kulkarni et al. 2011).

Though the mechanisms responsible for the intraseasonal variations are not fully understood (Klingaman et al. 2008, Krishnamurthy and Shukla 2000), broadly speaking, monsoon Intra-seasonal oscillations (MISOs) are fluctuations of the intratropical convergence zone (ITCZ) between its two favoured locations, one over central India and the other over the equatorial Indian Ocean, and repeated propagation from its

oceanic to continental regimes with characteristic time scales of 10-20 days and 30-60 days (Goswami and Xavier 2003, Sikka and Gadgil 1980). Its basic genesis and temporal and spatial scale selection seemingly arise from atmospheric internal dynamics involving convective feedbacks (Goswami et al. 2006b, Jiang et al. 2004), but they are modified by air–sea interactions (Fu et al. 2003, Waliser et al. 2004).

During the active phase, precipitation is enhanced over central India and the Western Ghats, and suppressed over the Himalayan foothills and south eastern peninsular India and the opposite happens in the break phase (Krishnamurthy and Shukla 2000, Turner and Slingo 2009). Waliser et al. (1999) demonstrated that these recurring active and break spells give SASM an intra-seasonal variability (ISV) greater than its interannual variability. Also, frequency and duration of active and break spells within a season could potentially influence the seasonal mean precipitation. Hence, the timing and duration of active and break events potentially has huge socioeconomic impacts. It is particularly important in agriculture and water resources management. For example, a long break in critical growth periods of crops can lead to a substantial reduction in agricultural yield (Gadgil and Rao 2000, Lal et al. 1999).

Models that simulate intraseasonal features well also have better representation of the seasonal mean features (Sperber et al. 2000). Hence, aside from numerous theoretical and observational studies, there have been many modelling studies of MISO. Several authors have noted that coupled global climate models (GCMs) have better skill in simulating MISO compare to atmosphere only models (e.g., Fu et al. 2002, Fu et al. 2007, Sharmila et al. 2013). However, Klingaman et al. (2008) showed that MISO is well simulated even in atmosphere only GCMs, when forced by realistic SST at high temporal resolution. Goswami et al. (2010) suggested that given the huge spatial scale of the MISO, GCMs might be required for its realistic simulation, but at very high

resolution. However, if a regional climate model (RCM) is to be employed in such studies, they recommend using boundary forcing with correct MISO signals.

RCMs have also been used in study of MISOs. Bhaskaran et al. (1996) argued that since MISOs arise from interaction between convections in the ITCZ and the large scale dynamics, RCMs, by virtue of its higher resolution, have potential to better simulate MISO related regional dynamics compared to GCMs as the regional ITCZ are generated internally within the RCM. By using a Hadley Centre model, they demonstrated that a moderate resolution RCM (0.44°) can produce a realistic representation of the SASM ISV, responding to both the global forcing via the lateral boundary conditions and independent internal dynamics. Moreover, Bhaskaran et al. (1998) showed that the RCM captured fine scale spatial details of precipitation associated with active and break monsoon which are not present in the driving model, particularly those over the Himalayan foothills. They attributed this to interaction of the MISO signal with the enhanced orography in the RCM. Other studies have also shown that RCMs (e.g. RegCM3) are able to satisfactorily simulate ISV of SASM (e.g., Dash et al. 2006, Dash et al. 2013). Using an RCM coupled with an ocean model Ratnam et al. (2009) showed that a coupled RCM has better skill in simulating the mean state as well as MISO, which they attributed to improved ocean atmosphere interaction in the coupled model. However, RCM simulations are still predominantly done in atmosphere only mode though they are increasingly run at higher horizontal resolutions (e.g. 10 km or less).

As mentioned above heavy precipitation occurs over the central and eastern Himalayan (CEH) foothills and north east India during break spells (Dhar et al. 1984, Dhar and Nandargi 2000, Vellore et al. 2014), among which the south-eastern plain of Nepal receives the highest fraction of seasonal total precipitation (above 16%, not shown). Hence, break spells have special significance over those regions. The aim of this paper

is to evaluate performance of a recent Hadley Centre RCM, run at low (50 km) and high (12 km) resolutions, in simulating characteristics associated with both break monsoon and extreme precipitation over the central Himalaya (Nepal). However, the paper first looks at active and break characteristics across the wider South Asian domain to see if there is an overall improvement at high resolution before focusing on the central Himalaya. In a companion paper, we evaluated performance of the low and high resolution simulations and found improvements in the latter for several aspects of SASM precipitation such as seasonal mean distribution, relative frequency distribution and various metrics of extremes (Karmacharya et al., submitted, Chapter 5). Here, we focus our analysis on intraseasonal aspects of monsoon.

The remainder of the paper is arranged as follows. Section 6.2 describes the model and methodology. The spatial patterns of precipitation and circulation during different phases of monsoon are compared in section 6.3. Temporal agreement in occurrence of active and break spells, and precipitation extremes over Nepal are also analysed. A summary and conclusions are drawn in section 6.4.

6.2 Data and Methods

6.2.1 Model and experimental design

The regional configuration of the Hadley Centre Global Environmental Model version 3 (HadGEM3-RA, Walters et al. 2011) is used in this study. HadGEM3-RA has 63 vertical levels and shares common atmospheric and land surface model components with HadGEM3, but it is applied over a limited area. The readers are referred to Walters et al. (2011) and Moufouma-Okia and Jones (2014) for detailed descriptions of the model formulations.

In this study, HadGEM3-RA is run at 0.44° and 0.11° horizontal resolution (i.e. approximately 50 and 12 km resolution respectively; hereafter RCM50 and RCM12) over an identical South Asian domain on the rotated grid coordinate system. Bhaskaran et al. (1996, 1998) showed that an earlier Hadley Centre RCM was able to simulate MISO features well when run over the same domain. Both simulations are forced by the European Centre for Medium range Weather Forecasting (ECMWF) reanalysis dataset ERA-Interim (ERAI) (Dee et al. 2011) at the lateral boundaries. ERAI has a T255 (~0.75° or ~80 km) spatial resolution, 60 hybrid vertical levels and temporal resolution of 6 hours. ERAI also provides initial condition for 50 km simulation, which is initialized on 1 January 1989 and ran continuously till the end of 2008. In contrast, output of RCM50 is used to initialize RCM12 each season on the 1st April and ran till the end of September for each year from 1990 to 2008. This is done to have same initial condition at the start of premonsoon season in both simulations. Sea surface temperature (SST) is prescribed from observed high-resolution (0.25°) daily SST (Reynolds et al. 2007). The first year of the coarser simulation is discarded as spin up, so summers of 1990 to 2008 are the common data available period in both the simulations, out of which monsoon seasons (June-September) of 1990 to 2007 are analysed, limited by the observational data constraints. These runs are same as those employed in Karmacharya et al. (submitted; chapter 5), which has additional details on experimental design and data processing. But unlike in that paper, here all analysis is done in standard latitude-longitude grids at resolutions comparable to model grid resolutions. Only when algebraic operation is to be performed between the variables on different grids, data at fine resolution are linearly interpolated to 50 km model grid.

6.2.2 Observational data

The following data are used for model evaluation.

i) APHRODITE (APHRO_MA_V1003R1) daily precipitation - gridded dataset at 0.25° resolution generated from station observations (Yatagai et al. 2009). This dataset is used as the main observational reference as it is available for entire South Asia. Moreover, it is a high resolution dataset and has relatively high station density over Nepal. However, it is available only up to 2007.

ii) Indian Meteorological Department (IMD) daily precipitation - gridded dataset at 0.5° resolution generated from station observations in India (Rajeevan and Bhate 2009). These data are used to estimate observational uncertainty in occurrence of active and break spells. It is available only up to 2005.

iii) ERAI upper level wind – ERAI dataset is described above. Its upper level wind and geopotential data are used to evaluate model fidelity in simulating circulation characteristics associated with different phase of monsoon.

6.2.3 Active and break monsoon index

A number of break monsoon criteria have been proposed in the past. For example, Ramamurthy (1969) used synoptic criteria to define break spells. Others defined active and break spells based on different variables such as outgoing long-wave radiation (OLR), zonal wind etc. (e.g., Krishnamurthy and Shukla 2000, Manoj 2011, Webster et al. 1998, Xavier et al. 2010). In several studies active and break spells are defined from precipitation over India (e.g., Annamalai and Slingo 2001, Gadgil and Joseph 2003, Krishnamurthy and Shukla 2000).

Here, following Rajeevan et al. (2010), daily precipitation over central India is used to identify active and break monsoon spells. According to this definition, a spell is defined as active (break) monsoon if standardized daily precipitation averaged over central India (so called monsoon core zone that extends roughly from 18.0°N to 28.0°N, and 65.0°E to 88.0°E but excludes Himalaya region) is above 1 (below -1) for at least three consecutive days during the peak monsoon months of July and August. Nevertheless, Rajeevan et al. (2010) found that break spells they identified were comparable with those defined by Ramamurthy (1969) and De et al. (1998) and there is a very large overlap with those identified by Gadgil and Joseph (2003). However, they found their criterion to be slightly more stringent than the ones they compared against. They argued that some break spells identified in previous studies rather corresponds to weak monsoon spells as the precipitation composites for those period lack the distinct positive (negative) anomaly over the foothills of Himalaya and peninsular India (central India). Rajeevan et al. (2010) criterion has also been used in several recent studies (e.g., Dash et al. 2013).

6.3 Results

6.3.1 Characteristics of active and break periods

Characteristics of the SASM during the active and break spells are investigated by computing the composites for the respective spells. As explained above Rajeevan et al. (2010)'s criteria has been used to identify those spells in each dataset using the daily precipitation data of the respective dataset averaged over the core monsoon zone. So the total duration of an active (break) spell and its date of occurrence differ among the observations as well as model simulations. Temporal distribution and statistics of active

and break spells are discussed in section 6.3.2. This section presents analysis of active and break composites for precipitation, low level circulation and zonally averaged upper air pressure anomaly.

6.3.1.1 Precipitation distribution

Precipitation shows distinct characteristics during the active and break phases of the monsoon. As pointed out in previous studies, such as Krishnamurthy and Shukla (2000), during the active phase, in the observations above normal precipitation occurs over central India (with a daily precipitation rate more than 5 times the seasonal average rate over drier west central India), whereas below normal precipitation occurs over the Himalayan foothills and the east peninsular India (Fig. 6.1a). On the other hand, during break phases little precipitation occurs over central India, but above normal precipitation occurs over the Himalayan foothills and the peninsular India with daily precipitation rate higher than 3 times the seasonal average rate over foothills of the eastern Nepal Himalaya (Fig. 6.1b). Similar to previous studies (e.g., Rajeevan et al. 2010), observed active and break monsoon composite precipitation distributions are nearly a mirror image of each other. The out of phase relationship between active and break phases is highlighted by the difference in active and break composite precipitation which shows large excess over the central Himalayan foothills and large deficit over the core monsoon zone (Fig. 6.1c). Both the higher and lower resolution simulations are able to broadly capture the observed precipitation distribution during the active and the break phases (Fig. 6.1 d-e, g-h) and their differences in the two phases (Fig. 6.1 f, i). However, the magnitude of the maxima appears to be better captured in RCM12 in both phases. This will be investigated further in the section 6.3.3.

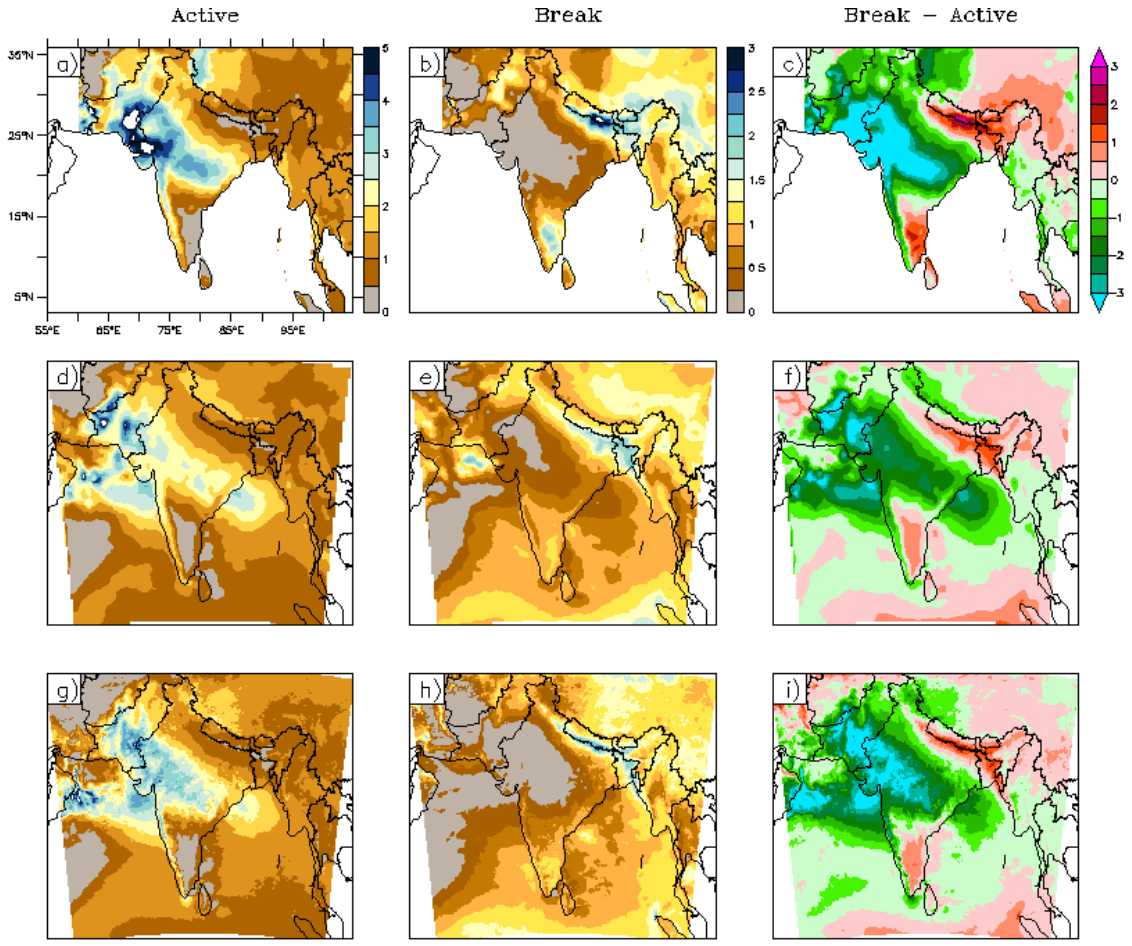

Fig. 6.1 Active and break monsoon composite precipitation rate and difference of the two expressed as ratio of the seasonal mean rate for (a-c) APHRODITE, (d-f) RCM50 and (g-i) RCM12. Unit less.

6.3.1.2 Lower and upper level circulation

As with precipitation, circulation also shows distinct characteristics during the active and break phases of monsoon. During the active phase, observed low level flow (in reanalysis) is stronger than normal resulting in enhanced cyclonic vorticity over central India; also a stronger low level jet (LLJ) impinges upon peninsular India nearly head-on (Fig. 6.2a). These results are in agreement with earlier studies (e.g., Muraleedharan et al. 2013). Likewise, the upper level easterly jet is stronger than usual with the core located southeast of peninsular India, which has north-easterly flow (Fig. 6.S1). The

centre of the subtropical high is also shifted west of its mean position. During the break spell, low level flow is comparable to the seasonal mean south of about 22° N latitude with the LLJ bypassing peninsular India, which is in line with earlier studies (e.g., Gadgil and Joseph 2003, Ramamurthy 1969, Vellore et al. 2014). But unlike the seasonal mean, a westerly flow anomaly prevails over all of India up to the Himalayan foothills with the development of anticyclonic vorticity, especially in the latitude belts between 15° to 25° N (Fig. 6.3a, see also Muraleedharan et al. 2013, Rajeevan et al. 2010, Ramamurthy 1969). At the upper level the easterly jet is slightly stronger and broader than usual and is elongated from peninsular India westwards with zonal wind flow (Fig. 6.S2a, see also Sathiyamoorthy et al. 2007, Vellore et al. 2014). The centre of the subtropical high is located over the central Himalayan foothills which enhances the uplift of the low level convergence over the region that aids heavy precipitation. According to Rajeevan et al. (2010), during the break phase the atmosphere over central India achieves a stable state which persists until it is disturbed by a synoptic scale system or a northward propagating ITCZ; for this reason, as seen later, break spells generally last longer than active spells.

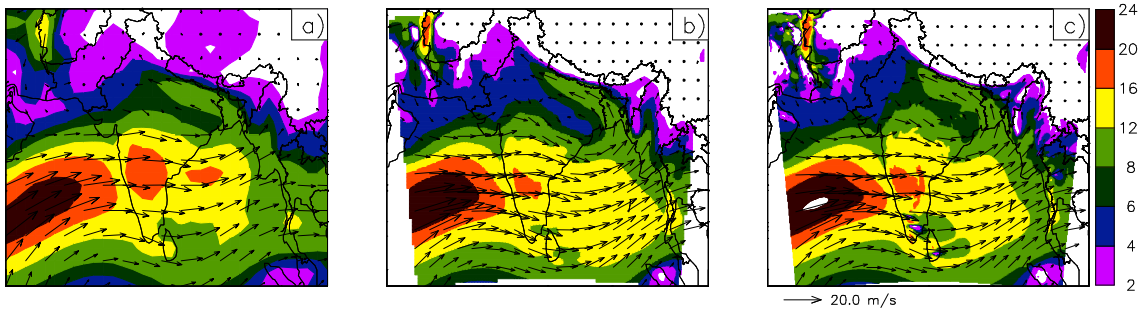

Fig. 6.2 850 hpa active monsoon composite circulation for a) ERAI, b) RCM50 and c) RCM12. Arrows show wind vectors and shading show wind speed. Unit: m/s.

Both RCM simulations are able to broadly capture the observed circulation features at the lower and upper levels during active and break spells (Fig. 6.2, 6.3, 6.S1, 6.S2). However, there are some differences, the most prominent of which is the break composite low level circulation south of the central Himalaya. Similar to observations, the low level flow remains westerly to north-westerly south of the central Himalaya in RCM12, but it is easterly over the Himalayan foothills in the RCM50.

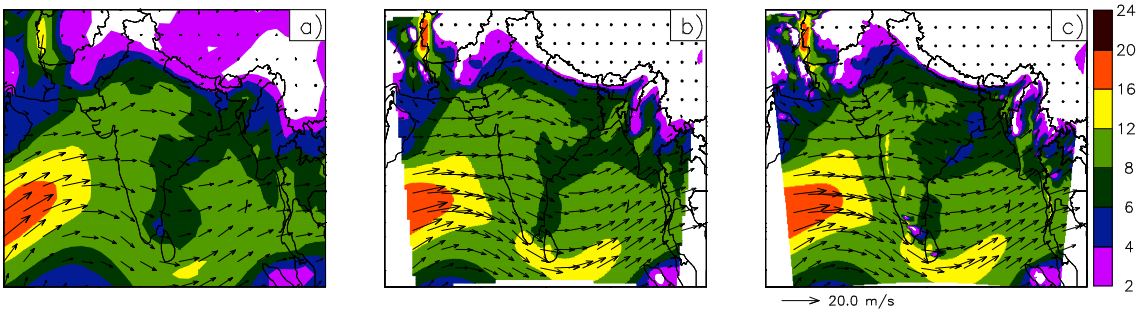

Fig. 6.3 Same as Fig. 6.2 but for break monsoon.

6.3.1.3 Zonal average pressure anomaly

A north-south transect of zonal average (75-85° E) pressure anomaly shows that during the active spell there is strong low pressure anomaly over central India up to mid tropospheric levels with a southward shift of the anomaly with height (Fig. 6.4). During the break spell, there is a weak high pressure anomaly over central India (e.g., Choudhury and Krishnan 2011, Ramamurthy 1969, Vellore et al. 2014) and low pressure anomaly over the Himalayan foothills at the lower level, extending only weakly up to the mid tropospheric levels. Both the RCM simulations replicate the observed variation of the pressure anomaly along the north-south transect during both active and break phases, though there are slight differences in the amplitude.

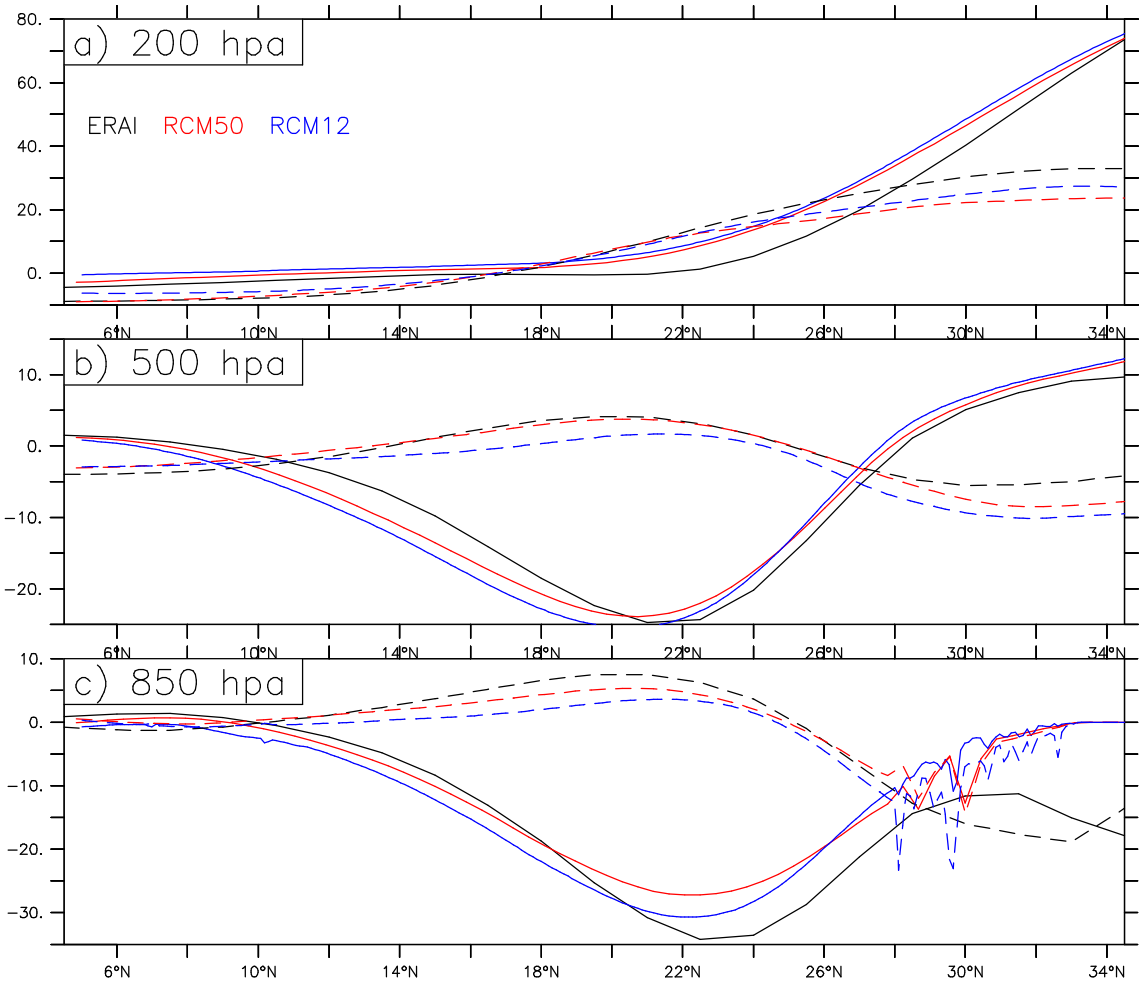

Fig. 6.4 North-South transects of active (solid line) and break (dash line) composite GPH anomaly zonally averaged over 75-85° E at a) 200 hpa, b) 500 hpa and c) 850 hpa for ERAI, RCM50 and RCM12. Unit: m.

6.3.2 Occurrence of active and break spells

Next we compare the occurrence of active and break spells in the RCM simulations and two observed data sets, IMD and APHRODITE, noting that IMD data are available only up to 2005. Overall there is a good agreement in broad occurrence of the active and break spells in the two observations for 1990-2005 (Fig. 6.5), but the dates of those spells do not always match exactly. Inter-observational agreement is relatively better for break spells than active spells as shown by the persistent higher Peirce skill score (PSS)

between the two observations for the break spells compared to the active spells (Table 6.1). The table also shows that even though (magnitude of) the PSS is sensitive to the dataset used as reference, the rank of higher and lower PCCs is maintained irrespective of the dataset used as reference. Also, there are some difference in numbers of active and break spells and the total duration of those spells in the two observations, in particular total duration is shorter in APHRODITE for both phases despite its longer data availability (Table 6.2). Similarly, it has fewer active events despite coverage of two additional seasons. These differences could be due to several factors such as difference in stations sampled, resolution, length of data availability etc. However, this does bring out the high sensitivity of the definition of the spells to the criteria used.

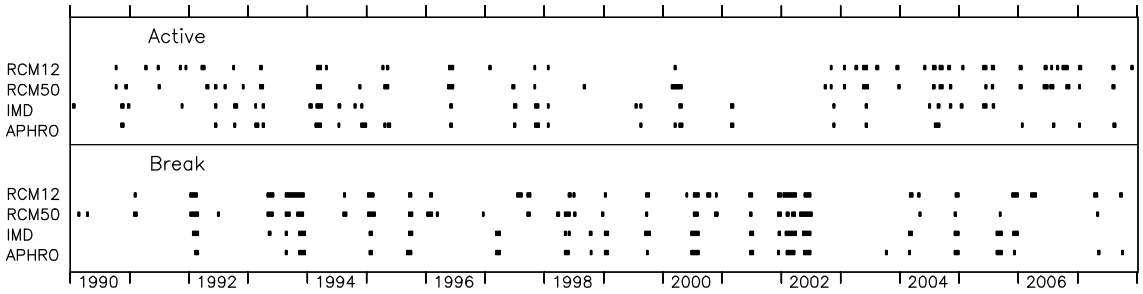

Fig. 6.5 Active and break monsoon spells in observations and RCM simulations. Note that IMD data is available only up to 2005.

Table 6.1 Peirce skill score for active and break spells with respect to APHRODITE and IMD for common period (1990-2005).

	WRT APHRODITE			**WRT IMD**	
Dataset	**Active**	**Break**	**Dataset**	**Active**	**Break**
IMD	0.70	0.91	APHRODITE	0.58	0.80
RCM50	0.37	0.50	RCM50	0.27	0.51
RCM12	0.28	0.57	RCM12	0.25	0.64

The RCM simulations are broadly able to capture observed occurrence and length of the active and break spells (Fig. 6.5). Agreement is particularly good in a few years (e.g. break spells in 1999, 2001-2002 and low numbers of active spells in 1998-1999, 2001-2002), but it is poor in some other years (e.g. too many active spells in 2003, 2006-2007). As for the observations, in both simulations PSS is higher for break spells than the active with respect to both the observations (Table 6.1). PSS is higher in the RCM50 for the active spell but higher in the RCM12 for the break spell. So, neither of the simulation performs consistently better. Also, both frequency and the total duration of active and break spells are higher in both simulations compared to APHRODITE with RCM12 mostly depicting a larger bias, though APHRODITE itself is likely to underestimates them. But the simulated mean and median durations of active and break spells are close to those observed in both models. For example, in agreement with Rajeevan et al. (2010), mean and median duration of active spells are shorter than break spells in the observations and model simulations. Hence, the overestimation of total duration of the simulated active and break spells mainly arise from higher frequency of those events in model simulations.

Table 6.2 Statistics of observed and simulated active and break monsoon spells[1].

Dataset	No. of spell	Spell duration (days)				SD of annual cumulative spell duration
		Total	mean	median	Maximum	
Active						
APHRODITE	25	100	4.0	3	8	3.6
IMD	29	108	3.7	3	8	5.0
RCM50	32	136	4.3	3.5	12	4.3
RCM12	38	145	3.8	3	7	6.0
Break						
APHRODITE	22	114	5.2	5	10	3.7
IMD	21	125	6.0	5	13	4.5
RCM50	31	155	5.0	4	14	6.3
RCM12	29	175	6.0	5	21	6.9

[1] IMD data spans for 1990-2005 only, others cover 1990-2007

To summarize, RCM12 performs better on some active/break associated temporal statistics, but it is worse on some others. Thus it is not clearly superior to the RCM50 for these statistics. In addition, observational spread also means that clear conclusions could not be drawn on the models' skill in simulating these statistics.

6.3.3 Improvements in composite precipitation in the high resolution simulation

Next we compare the simulated active and break composite precipitation rates against the observed and identify any regions of added values in RCM12. We define added value as difference of absolute bias (from observation) in RCM50 from that in RCM12 (i.e. added value = | (RCM50 - Obs.) | - | (RCM12 - Obs.) | (Karmacharya et al., submitted, Chapter 5). Hence, there is added value over the regions where the absolute bias in RCM12 is less than that in RCM50.

The observed active composite precipitation rate is the highest over central India and the Western Ghats (above 30 mm/day), but there is little precipitation over north India and east peninsular India (Fig. 6.6a). Compared to APHRODITE, precipitation rate is subdued over central India and the Western Ghats in RCM50 but enhanced over the Indo-Gangetic plain (IGP), the CEH and northeast India (Fig. 6.6b) resulting in large biases over those regions. Compared to RCM50, precipitation rate in RCM12 is reduced over the IGP, parts of the CEH foothills but enhanced over west central India and parts of the Western Ghats (Fig. 6.6c) resulting in reduced absolute bias, and hence added value, over those regions (Fig. 6.6d).

The observed break composite precipitation rate is the highest over the central Himalayan foothills, but there is little precipitation over the rest of India, except northeast India and the Western Ghats (Fig. 6.7a). RCM50 overestimates the precipitation rate over most of India, except the southern tip and east Nepal with the largest overestimation over the IGP and northeast India (Fig. 6.7b). Both the magnitude and spread of the wet bias are larger than in the case of its bias for the seasonal mean precipitation (see Karmacharya et al., submitted, Chapter 5). RCM12 is drier compared to RCM50 over most of India, but it is wetter over most of the CEH (Fig. 6.7c). This results in reduced absolute bias in RCM12 over the IGP, east Nepal and parts of central India, with maximum added value over the IGP (> 5mm/day). Vellore et al. (2014) also noted enhanced intensity and added mesoscale details on the organization of precipitation over the southern slopes of CEH in the finer WRF model simulation (10 km and less) which was absent in the coarser simulation. They attributed this to the higher resolution RCM's ability to more effectively capture precipitation enhancements that arise from orographic forcing and mid-tropospheric ascending motion.

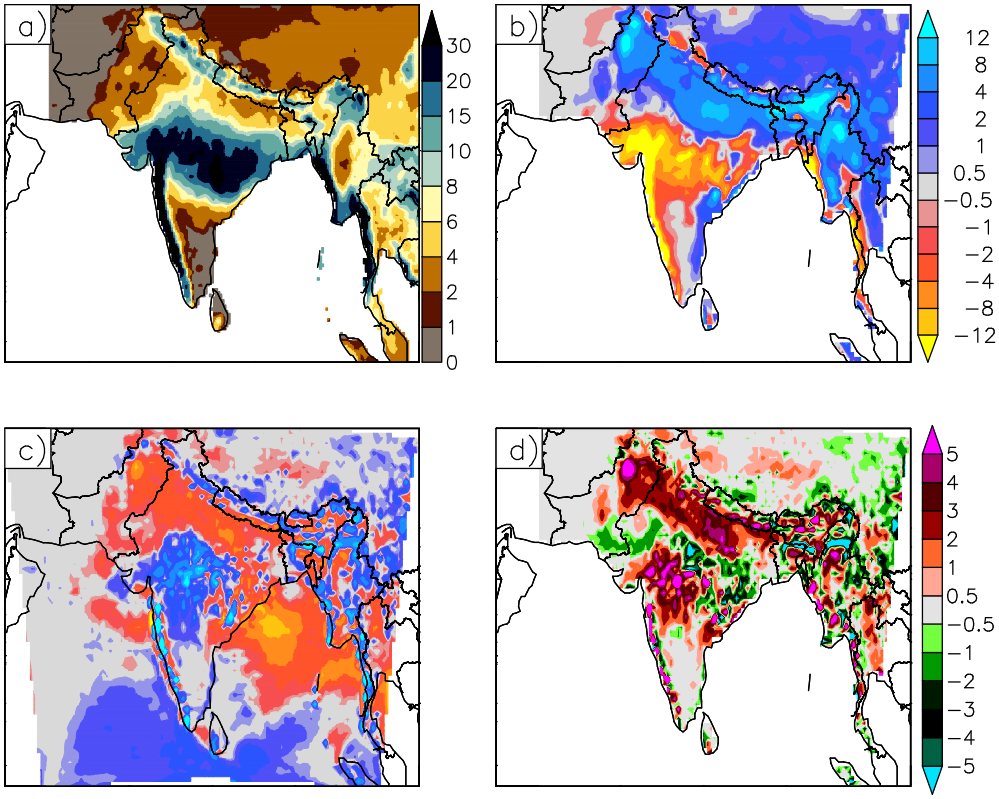

Fig. 6.6 Active monsoon composite precipitation rate a) in APHRODITE, b) bias in RCM50, c) RCM12 minus RCM50, d) added value of RCM12 compared to the RCM50. Unit: mm/day.

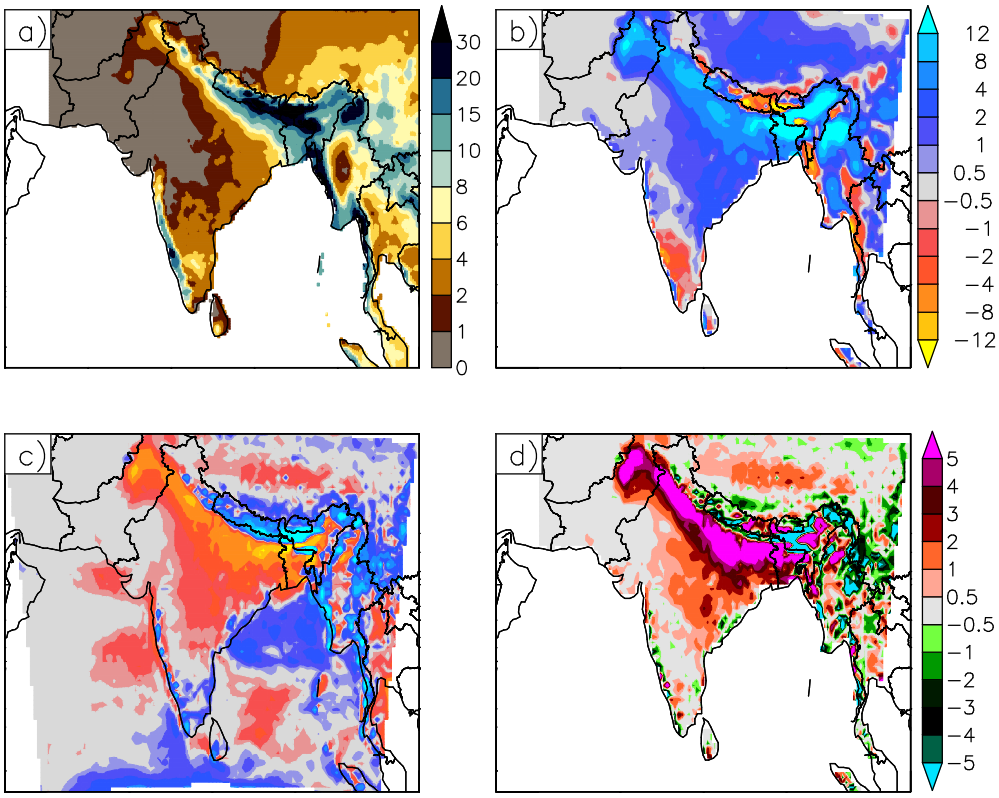

Fig. 6.7 Same as Fig. 6.6 but for break composite.

For both active and break composites, added value in RCM12 is spread over a larger region than where there is no added value; further, the added value in these periods is greater than if only the seasonal mean precipitation added value is considered (Karmacharya et al., submitted, Chapter 5).

6.3.4 Possible sources of improvement in composite precipitation in the high resolution simulation

As noted above, there is little difference in active and break composite circulation at upper level, so the improvement in simulation of composite precipitation rate in the high resolution model is likely to arise from other sources. Some of the possible sources of improvements are explored below, but firstly we note that excessive active composite precipitation intensity in RCM50 over the IGP is likely a consequence of a long

standing Met Office Unified model (MetUM) problem of simulating excess precipitation over the Himalayan foothills arising from poor representation of the interaction of the moisture laden flow with the steep Himalayan orography (Levine and Turner 2012). As for the seasonal mean, this is much reduced in RCM12 owing to improved model ability to handle convection and interaction of moist flow with Himalayan orography at high resolution.

6.3.4.1 Progression of the composite monsoon trough

As the frequency and duration of the active and break spells are dictated by the propagation of the MISOs, we compared the progression of the monsoon trough during active and break spells in the reanalysis and the RCM simulations by considering the composite position of the trough on the days before and after the active and break spells. For this purpose, the position of the monsoon trough is determined from the meridional minima of the 850 hpa geopotential height with the search band confined to 10 to 33° N. A five point binomial smoothing is also applied to smooth the trough. In addition, in case of the RCMs, data is first linearly interpolated to the ERAI grid and Tibet is also masked (i.e. GPH < 1300 m).

In the observations, the position of the active composite monsoon trough is distinct from its composite positions on the lag and lead days especially over west India and the entire length of the trough is located over central India, south of its normal position (Muraleedharan et al. 2013), with east-west orientation (Fig. 6.8a, also see Choudhury and Krishnan 2011), which is conducive to enhanced of precipitation over the core monsoon zone and suppression in other regions. Also, lows and depressions frequently form over Bay of Bengal and move across the core monsoon zone in this phase (Rajeevan et al. 2010).

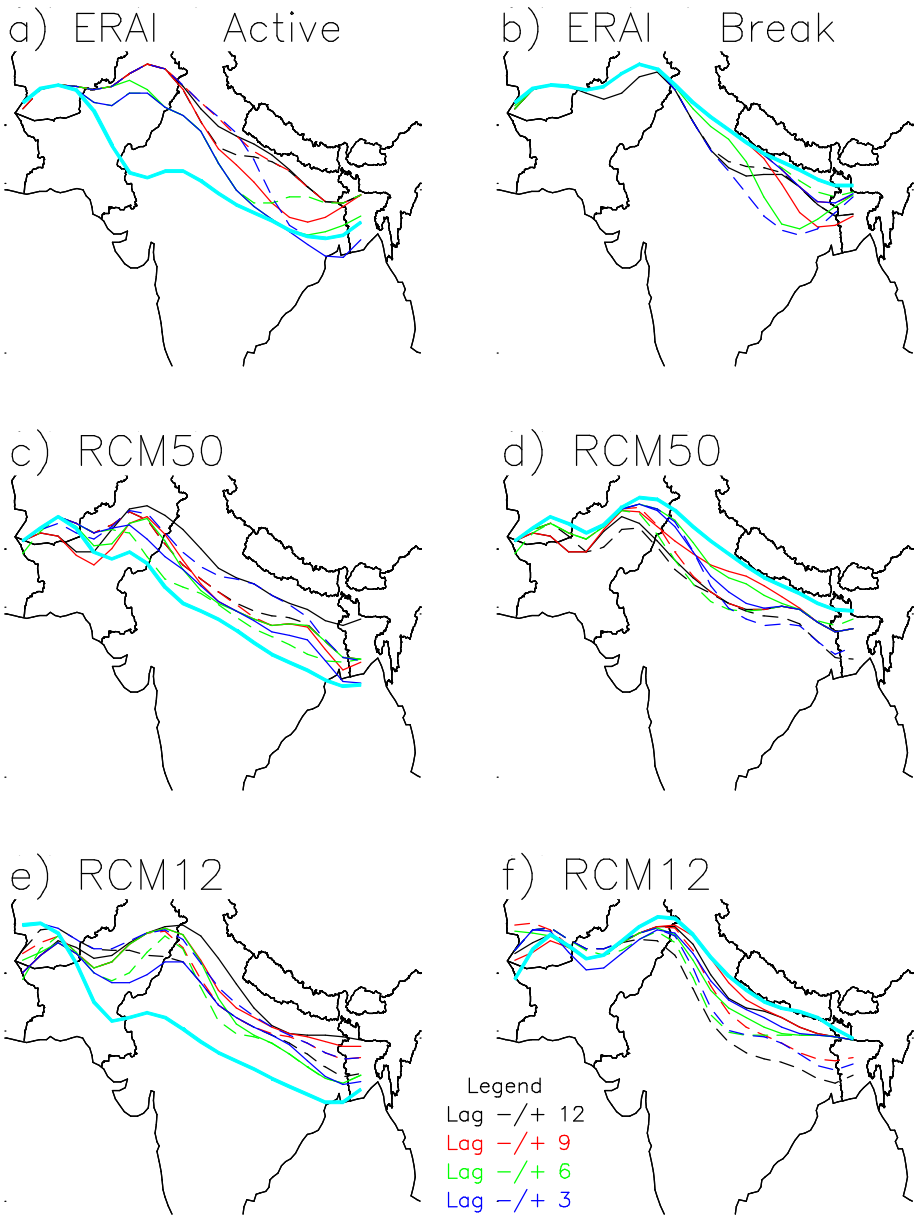

Fig. 6.8 Lagged monsoon trough at 850 hpa for active (left panel) and break (right panel) composites. Solid, dash and thick blue lines correspond to lag, lead and active (break) composite monsoon trough respectively.

Next, the observed and simulated composite positions of the monsoon trough on the lead/lag days are investigated to explore if this provides some insight on difference in the active (break) composite precipitation distribution in the RCM simulations. Here, the start and end of the active (break) spell is taken as day zero, so, for example, lag -3

corresponds to 3 days before the start of active (break) spell and lag +3 corresponds to 3 days after the end of the active (break) spell. In RCM50 the position of the active composite monsoon trough on the lead/lag days are generally south of the observed position over west India on those days, while it is several degrees north of that observed over west India for the active composite (Fig. 6.8c). On the other hand, the position of the active composite monsoon trough is similar to observation in the RCM12 (Fig. 6.8e) which is likely to contribute to improved distribution of active composite precipitation rate. Moreover, a realistic monsoon trough position also sets the stage for better trajectories for lows and depressions. In fact, low and depression trajectories in RCM12 are closer to those observed, whereas they are displaced northwards in RCM50 especially over west India (R. Levine, personal communication). In RCM12, the composite position of troughs on the lead/lag days are confined over the IGP and close to each other though their positions are not necessarily better than in the RCM50.

The observed break composite monsoon trough lies close to the Himalayan foothills and is in the northern most position compared to its lag and lead composite positions (Fig. 6.8b, see also Choudhury and Krishnan 2011, Ramamurthy 1969, Vellore et al. 2014). This is conducive for precipitation enhancement over the CEH foothills and reduction over rest of India. The composite position of the trough on the lag and lead days is rather scattered over the IGP and does not depict orderly north-south propagations (also for active lag/lead composites). Both RCMs capture the position of the trough for break composite well, but though their composite position on the lag/ lead days are generally similar to those observed there is no one to one correspondence and neither of the models performs persistently better (Fig. 6.8 d, f).

6.3.4.2 Wet days and precipitation distribution

Excess precipitation over the Himalayan foothills is a common problem in MetUM, and it has been attributed to poor representation of the interaction of the moisture laden flow with the steep Himalayan orography (Levine and Turner 2012). A previous study, using the same RCM simulations, as this paper found that excess seasonal mean precipitation over the IGP in RCM50 is mainly due to this model simulating too many wet days, and that a reduction in the seasonal wet bias in RCM12 is similarly associated with a reduction in the wet-day bias (Karmacharya et al., submitted, Chapter 5). This is supported by the fact that both simulations have comparable simple daily intensity index values, indicating they have comparable precipitation on wet days. Here we build on this previous work to compare the observed and simulated wet days during active and break spells.

In the observations, wet days during active spells exceed 90% of the total number of active spells (days) over the core monsoon zone, the Western Ghats and the central Himalaya but remain below 60% over the IGP (Fig. 6.9a). On the other hand, for break spells it exceeds 90% of the total number of break days over the CEH, but it is reduced to 10-40% over large parts of India including the core monsoon zone (Fig. 6.9d). RCM50 shows considerable bias in wet days: during active spells wet days exceed 95% over entire north and central India (Fig. 6.9b); during break spells they exceed 95% over the entire Himalayan range and its foothills (Fig. 6.9e). Though active spell wet days exceeds 85% over almost entire north and central India in RCM12, it exceeds 95% only over central India and the Himalayan range (Fig 6.9c). Likewise, break spell wet days exceeds 95% only over Nepal and northeast India (Fig. 6.9f). Hence, a reduced wet bias over IGP in RCM12 compared to RCM50 for both active and break composites is associated with more realistic simulation of the dry and wet days in RCM12.

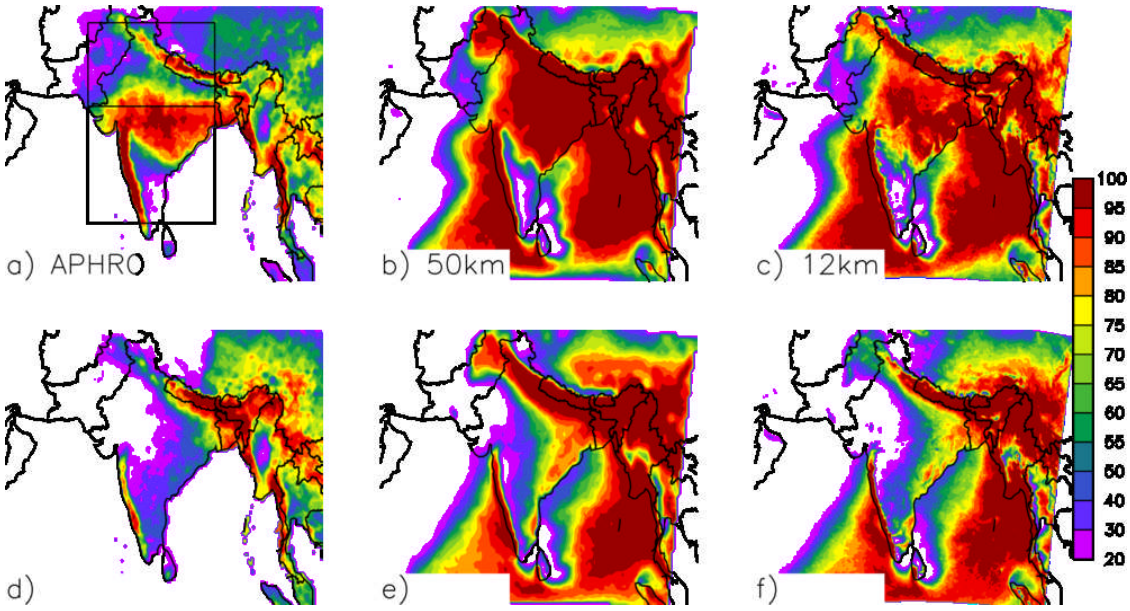

Fig. 6.9 Active (upper panel) and break (lower panel) composite wet days (standardized as the % of total active and break days).

6.3.4.3 Relative frequency distribution of daily precipitation

For further insight into the distribution of daily precipitation during the active and break spells, we compared also the relative frequency distribution of the daily precipitation during those spells over north and south India.

In all cases, RCM50 overestimates moderate precipitation, even when there is overall dry bias as in the case of active composite precipitation over south India (Fig. 6.10c). Also the tails of distribution are underestimated in RCM50 for active spell over both north and south India with larger underestimation in the latter (Fig. 6.10 a, c). Active spell relative frequency distribution is relatively better simulated in the RCM12. Though, the tails of the break spell relative frequency distribution simulated by both

RCMs are comparable to that observed over both regions, as stated earlier RCM50 overestimate moderate precipitation, but those biases are reduced in the RCM12.

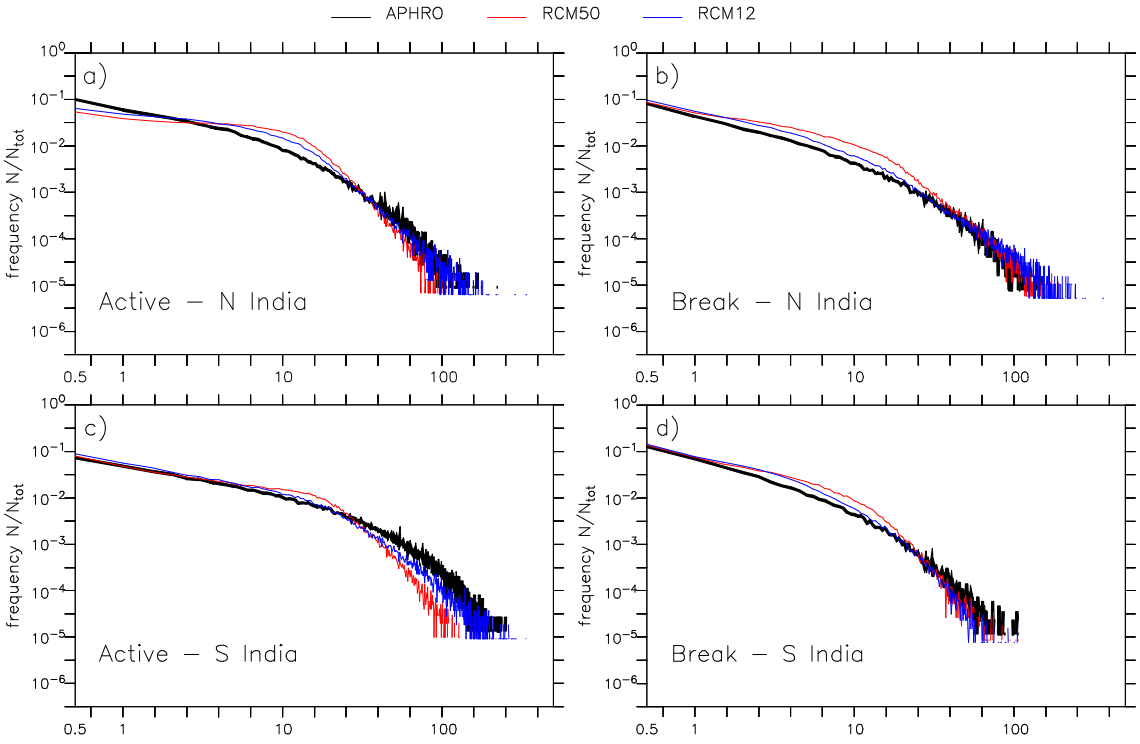

Fig. 6.10 Relative frequency distribution of daily precipitation for active and break spells.

6.3.5 Extreme precipitation over Nepal

Though break spells are associated with heavy precipitation over the CEH foothills, it is of highest significance over south eastern Nepal, where break monsoon cumulative precipitation makes maximum contribution to the seasonal total (above 16% of the seasonal total, not shown). Hence, we next compare the Nepal average precipitation during break spells vis-à-vis extremes. For this purpose, we define events (days) that exceed 95th percentile of Nepal average daily precipitation for the monsoon seasons of 1990-2007 as extremes. Daily monsoonal precipitation over Nepal can be considered

fairly homogeneous and Nepal averaged precipitation as representative of precipitation across Nepal as correlations between observed Nepal averaged daily precipitation time series and daily precipitation time series at individual grids within Nepal are 0.6-0.8 except for a few grids for which it is 0.4-0.5 (not shown).

Almost 90% of the observed extreme rainfall days (hereafter very wet days) over Nepal falls in the peak monsoon months of July-August, with about 21% of those days occurring in the break spells (Table 6.3). The relatively low overlap between very wet days and break spells is a little surprising given how break spell creates a conducive environment for precipitation enhancement over the CEH foothills. However, it is worth noting that irrespective of the length of break spell (having mean of 5-6 days) intense precipitation over the CEH typically occurs only on first 1-2 days of the break spell (Vellore et al. 2014).

Table 6.3 Occurrence of days exceeding 95th percentile of Nepal average daily precipitation (very wet days) (%).

Very wet days falling in …	APHRODITE	RCM50	RCM12
the month of Jul-Aug	87.2	50.5	66.4
break monsoon	21.1	17.4	30.0
break monsoon (per hundred break days)	18.5	11.2	17.1
active monsoon	0.0	0.0	0.0

In RCM50, 50% of very wet days fall in July-August and 17% during the break spells. In RCM12, 66% of very wet days fall in July-August and 30% in the break spell. Even though ratio of occurrence of very wet days in July-August is relatively better captured in RCM12, it has higher co-occurrence of very wet days and break spells. But this is likely a consequence of excessive number of break days in the model simulation. So, an

alternative comparison would be to consider the fraction of occurrence of very wet days in break spell scaled by the total number of break spell in each case. With this scaling, the fraction of occurrence of the very wet days in break spell are about 19, 11 and 17 per hundred break days in the observation, RCM50 and RCM12 respectively. In this regard, RCM12 better captures the observed distribution of very wet days both in July-August and break spells. But, both models correctly capture lack of occurrence of very wet days in the active spell in a similar manner to the observations.

On the average, observed very wet days cumulative precipitation contributes above 15% of the seasonal total precipitation along the southern side of Nepal, which rises up to 25% over the south central parts (Fig. 6.11a). In contrast, the contribution of very wet day cumulative precipitation to the seasonal total is less than 5% over central India, which shows the out of phase relationship of occurrence of extreme precipitation over Nepal and central India. Though RCM50 correctly simulates the pattern of contribution of very wet day cumulative precipitation to the seasonal total and the position of the maxima, the maximum contribution remains below 15% (Fig. 6.11b). In contrast, in RCM12 the contribution is above 15% along the southern side of Nepal, which reaches 20-25% over its south-eastern plains (Fig. 6.11c). Hence, the high resolution simulation also improves simulation of this metric of extreme rainfall. This improvement is likely to come from the model's ability to effectively capture precipitation enhancements that arise from orography-forced as well as mid-tropospheric ascending motions at the higher resolution (Vellore et al. 2014).

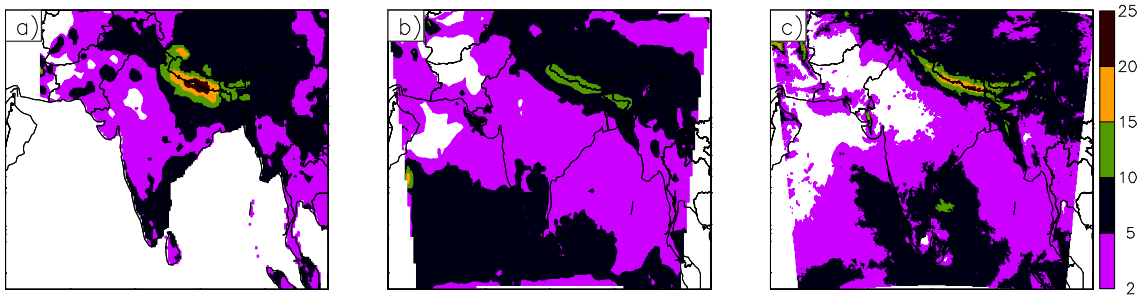

Fig. 6.11 Contribution of precipitation on days exceeding 95th percentile of Nepal average daily precipitation to the seasonal total for a) APHRODITE, b) RCM50 and c) RCM12. Unit: %.

Finally, wet day composite low level circulation is similar to the corresponding break composite circulation in the observation as well as model simulations (Fig. 6.S3), which suggests close correspondence between those events.

6.4 Summary and conclusion

The South Asian summer monsoon is a stable component of the regional climate system on interannual time scales, but it exhibits large variability in shorter time scales. A substantial component of the variability arises from fluctuations at intra-seasonal time-scales, most prominent of which is variability in 10-20 day and 30-60 day modes. Both these modes manifest as active and break cycles of the monsoon with potential for large socioeconomic impacts in the region through the spatiotemporal modulation of precipitation.

Coupled models are generally found to better simulate monsoon intra-seasonal variability. However, this variability has also been successfully simulated using regional climate models, provided they are forced by a realistic monsoon intra-seasonal

oscillation (MISO) signal at their lateral boundary. Here, we evaluated fidelity of an RCM at low and high resolutions in simulating various characteristics associated with monsoon intraseasonal variability such as active and break monsoon and precipitation extremes over the central Himalaya.

Clear improvements are seen in the active and break composite precipitation intensity at the higher RCM resolution, with the largest improvements over Indo-Gangetic plain. Improvements are also seen over the west central India in active composite and eastern Nepal in break composite. These improvements likely come from i) improved position of the monsoon trough particularly over west India for active monsoon periods, ii) improved low level flow particularly south of the Himalaya for break periods. With regard to seasonal mean precipitation, enhanced capacity of the model at high resolution to resolve convection and interaction of moisture laden low level flow with the steep Himalayan orography is likely to contribute in reducing excess precipitation over Indo-Gangetic plain in both phases. Similarly improvements over east Nepal for break spells is likely to arise from model ability to effectively capture precipitation enhancements that arise from orography-forced and mid-tropospheric ascending motions (Vellore et al. 2014) .

Apart from the differences in circulation and the position of the monsoon trough mentioned above there are no other significant differences in the position of the monsoon trough and the upper level circulation for active and break composites between the different resolution simulations. Also, little difference is noted in propagation of the monsoon intraseasonal oscillation, as depicted by the migration of the monsoon trough associated with two phases. These minimal differences could either be due to stronger control of the driving field, owing to smaller domain, that prevents

internal generation of circulation or that even the coarser model has adequate resolution to resolve those systems.

There is little improvement in the temporal statistics associated with active and break spells such as their timing, frequency and duration. However, clear conclusions could not be drawn on the models' relative skill in simulating these statistics due to observational spread.

In the observations, cumulative Nepal extreme precipitation (i.e. upper 5 percentile) contributes up to about 25% of the seasonal total over southern plains of central Nepal and is associated with composite low level circulation similar to that in monsoon break spells. The high resolution model is able to relatively better capture these features; it is also better able to capture the timing of occurrence of extreme precipitation over Nepal in relation to peak monsoon and break spells.

These results are in line with other recent studies which show improved performance of higher resolution model in simulating various features of the SASM. For example, Rajendran et al. (2013) found marked improvements in capturing spatial pattern of seasonal mean precipitation and its frequency distribution at higher resolution. Likewise, Sabin et al. (2013) found large improvements in higher resolution such as ability to capture the heavy precipitation along the mountainous regions and simulation of realistic monsoon trough together with marked improvements in associated precipitation and circulation features. However, those studies employed GCMs but similar studies using RCMs are lacking. This study (and the companion paper, Chapter 5) shows that similar improvement can be achieved in high resolution RCM simulation of SASM, but the study needs to be repeated with multiple realizations and different RCMs before arriving at a robust conclusion.

Acknowledgements

First author thanks the Felix Scholarships for funding his DPhil and the Christ Church for partially funding final year of study. The model simulations were carried out at Met Office. Richard Jones was supported by Joint DECC/Defra Met Office Hadley Centre Climate Programme (GA01101). We acknowledge use of the MONSooN system, a collaborative facility supplied under the Joint Weather and Climate Research Programme, which is a strategic partnership between the Met Office and the Natural Environment Research Council. We thank two anonymous reviewers for comments which helped to significantly improve the manuscript. We also acknowledge use of the Ferret program, product of NOAA's Pacific Marine Environmental Laboratory, for analysis and graphics in this paper.

Supplementary Information: Chapter 6

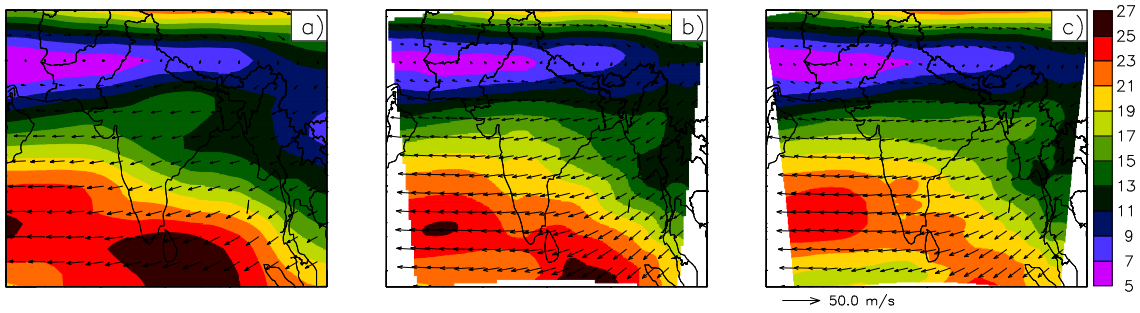

Fig. 6.S1 200hpa active monsoon composite circulation for a) ERAI, b) RCM50 and c) RCM12. Unit: m/s.

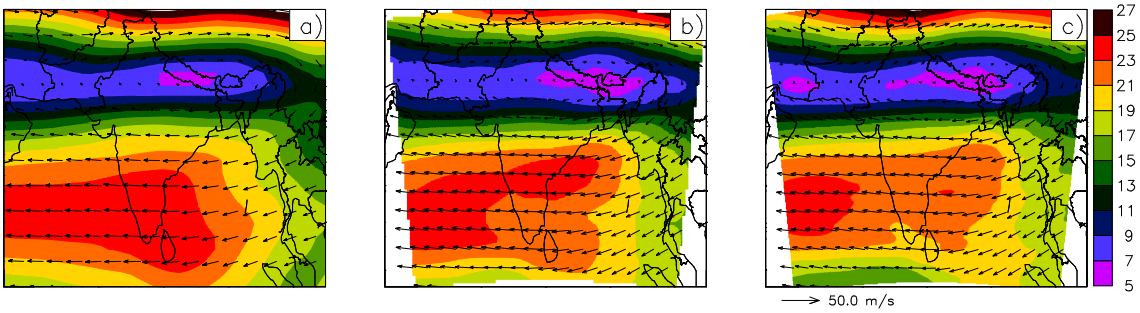

Fig. 6.S2 200hpa break monsoon composite circulation for a) ERAI, b) RCM50 and c) RCM12. Unit m/s.

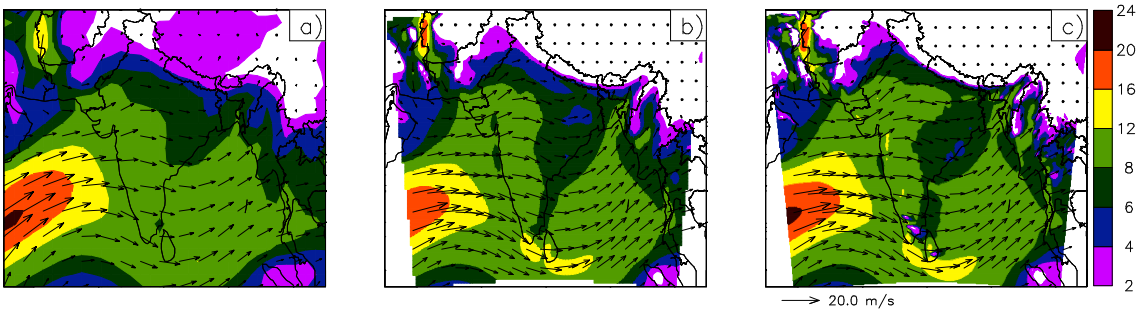

Fig. 6.S3 850 hpa composite circulation for days exceeding 95th percentile of Nepal average daily precipitation for a) ERAI, b) RCM50 and c) RCM12. Unit: m/s.

7 Conclusion

7.1 Summary and conclusion

The aim of the thesis is to evaluate sensitivity of a regional climate model simulation of the South Asian summer monsoon to its domain size and spatial resolution, and then to identify optimal domain as well as added value of high resolution modelling. In addition, suitability of monsoon circulation indices as a benchmark metric for evaluating model performance in simulating SASM is also evaluated. To meet the objective, following three prong approach is employed: i) Assessment of monsoon indices for their potential application as metric for rapid model evaluation: ii) Evaluation of sensitivity of a RCM simulation of SASM climatology to domain size and identification of optimal domain: iii) Evaluation of role of RCM spatial resolution on realistic simulation of SASM. The approaches were selected following the identification of the research gaps in the literature review (chapter 2), which sets out following research objectives:

1) *Investigate the strength and stability of relationships between monsoon precipitation indices and a number of large scale monsoon circulation indices at interdecadal scale.*

2) *Evaluate sensitivity of RCM simulation of SASM climatology, mainly precipitation, to the size and location of the domain.*

3) *Evaluate added value of high resolution RCM simulation of SASM with focus on various characteristic of precipitation.*

Referring back to those objectives the main findings of the research are summarized below:

Findings related to research objective 1

The seasonal mean time series for each MCI and MRI are extracted from six reanalyses and three precipitation observations respectively. Bootstrapping of the sliding correlation is carried out on each MCI-MRI pair, provided those series are normal and independent, to identify whether a low frequency variability of the MCI-MRI relationship is significantly more or less variable than expected from sampling variability at specified confidence level.

Decadal and multi-decadal shifts are noted in the strength of the correlation between 20CR MCIs and AIMR (the longest series) with prominent shift occurring around 1890, 1930, 1955 and then a more gradual shift to lower correlations in the 1980s.

There is broad agreement in evolution of MCI-AIMR relationships among the MCIs which depict highest correlation for 1960-1980 followed by gradual decline in the recent decades. However, the decline appears to be faster for zonal wind-based MCIs than meridional wind-based MCIs.

Overall, the relationship between SASM rainfall indices and circulation indices show considerable low frequency variability. Nevertheless, interdecadal variability of the relationship between meridional wind based monsoon circulation indices and monsoon rainfall indices are within the limit of sampling variability for 1948-2011 but that between zonal wind based circulation indices and monsoon rainfall indices exceed the limit of sampling variability.

Local variability of the indices generally shows good correlation with the contemporary strength of MCI-MRI relationships. However, this study did not reveal any further insight in contrasting variability of zonal and meridional based MCIs with MRI.

Findings related to research objective 2

Met Office Unified Model's inherent SASM systematic errors and interaction of different elements of the systematic errors within the South Asia region is investigated by comparing a global, a nudged global, and a regional climate model simulation over four carefully selected domains. All simulations were forced by an observed SST at the surface and nudged global and RCM simulations were forced by an atmospheric reanalysis. The assessment focuses on monsoon precipitation variability at climatological, interannual and intraseasonal timescale.

RCM simulation of SASM with large domain (CORDEX South Asia domain) and forced by ERAI reanalysis has many of the systematic errors similar to that in its parent Hadley Centre GCM – HadGEM3, albeit of reduced magnitude, which indicates that systematic errors is largely produced by local processes in the Hadley model system. Further, many of the large systematic errors seen in HadGEM in simulation of SASM are common amongst many current GCMs.

In Hadley Centre models northern EIO is a region of large wet bias where systematic error spins up rapidly within a few days, probably due to the problem in convective parameterization, which then has direct detrimental impact on simulation of SASM through circulation and moisture flux anomalies (Martin et al. 2010). Likewise, the Himalayan wet bias, another common error in model simulations, causes dryness over central India through diversion of moisture flux. Hence, different elements of systematic errors interact among each other resulting in a composite anomaly field even when simulation is forced by near perfect forcings at the boundary. So, the challenge is to exploit the sensitivity of a RCM simulation towards its domain to identify a domain setup that minimizes the systematic errors inherent in the parent model.

It is seen that among the simulations investigated, RCM simulation with moderately sized domain (R3B), that partly exclude the EIO and has narrow lateral extension, has i) relatively better spatial distribution of seasonal mean precipitation, in particular reduced dry bias over central India, ii) stronger low level circulation closer to the observed, iii) most realistic northward progression of convection with the onset of monsoon, iv) arguably best intraseasonal variability of precipitation, v) improved interannual variability of seasonal mean precipitation and circulation. Hence, among the different RCM domain setups and GCM simulations, the RCM simulation with moderately sized domain performs best in almost all aspects of the SASM. This is achieved due to the fact that i) the parent model's inherent systematic SASM errors are largely forced by local process and their key source regions (e.g. EIO) lie at the periphery of the main area of interest (i.e. South Asian land mass), ii) The moderately sized domain is small enough to exclude the main bias prone region, but large enough to include other key regions and able to produce its own internal circulation.

Findings related to research objective 3

A recent Hadley Centre RCM (HadGEM3-RA), forced by reanalysis and observed SST, is run at a medium (0.44°) and a high (0.11)° resolution over an identical South Asian domain (same as the best performing moderately size domain identified above). While the low resolution simulation is a continuous integration, the high resolution simulation consists of a series of runs over the summer seasons, initialized on 1st of April each year from 1990 to 2008, using the low resolution output as the initial condition. The two model simulations are compared against the observations, and their absolute biases computed, from which added value (or lack of added value) of the high resolution simulation is derived (as described in section 2.5.3).

The model evaluation again mainly focuses on precipitation and consists of two parts (spread in two chapters): evaluation of i) climatological and ii) intraseasonal characteristics.

Findings related with climatological characteristics

The high resolution RCM simulation adds value (i.e. has reduced bias compared to the coarser resolution simulation) in many, but not all, aspects of the SASM, mainly those associated with precipitation. One interesting finding of the study is that improvements in the high resolution model simulation of seasonal mean precipitation are seen mainly over the homogeneous Indo-Gangetic plain and they are achieved through reduction of large wet bias in the coarser simulation. But other studies mostly indicated improvement in precipitation simulation over the complex/heterogeneous regions (e.g., Haensler 2011, Prein et al. 2013) and generally increased precipitation at higher resolution (e.g., Bhaskaran et al. 2012, Sinha et al. 2013).

Excessive precipitation over the IGP in the coarser model is likely a continuation of a long standing MetUM problem of poor representation of the interaction of the moisture laden flow with the steep Himalayan orography (Levine and Turner 2012). Improved simulation of precipitation over the IGP in the high resolution RCM indicates that MetUM is able to overcome this inherent deficiency, simply by increasing its horizontal resolution.

Other main improvements in the high resolution RCM simulation of the SASM climatology are summarized in Table 7.1. The table also identifies regions where there is deterioration in the high resolution RCM simulation compared to the coarser simulation.

Findings related with intraseasonal characteristics

The high resolution RCM exhibits added value in simulation of various intraseasonal characteristic of the SASM and in some cases the added value achieved is larger than that obtained for comparable statistics for the seasonal mean. However, the added value is not distributed uniformly across all the variables or metrics.

The high resolution model improves simulation of active and break composite precipitation rate with large added value over the IGP in both phases and over west central India in active phase and east Nepal in the break phase. These improvements are achieved by reduction of the coarser model's wet bias over the IGP and, dry bias over west central India and east Nepal. More realistic simulation of active and break composite precipitation rate in the high resolution simulation is likely to arise from improved simulation of monsoon trough during active spells and improved low level flow, particularly south of the Himalaya during break spells. In addition, enhanced model ability at high resolution to better resolve convection and interaction of moisture laden low level flow with the steep Himalayan orography is likely to contribute to the reduction of excess precipitation over the IGP. Similarly, improvements over east Nepal is likely to come from model's ability to effectively capture precipitation enhancements that arise from orography-forced and mid-tropospheric ascending motions.

The high resolution simulation also better simulates precipitation extremes over Nepal regarding timing of their occurrence in relation to peak monsoon months and break spells, and also to the contribution of the extreme cumulative precipitation to the seasonal total.

Some temporal statistics associated with timing, duration and frequency of active and break events are closer to observed in the high resolution simulation, but the coarse

resolution model performs better for some other statistic. So, the high resolution model does not show persistently better results for temporal statistics associated with active and break events.

Table 7.2 provides a summary of the performance of the high resolution model in simulating intraseasonal characteristics of SASM relative to its coarse resolution counterpart for different evaluation criteria/metrics

Table 7.1 Added value (or loss of value) of high resolution RCM relative to its coarser counterpart in simulating various features associated with SASM climatology.

Variable/ metric	Statistic/measure	Main area of improvement	Main area of deterioration	Related figure
precipitation	Spatial distribution of seasonal mean	Indo Gangetic Plain (IGP)	N. BoB, parts of the east and central Himalaya	Fig. 5.2
"	Relative frequency distribution of daily precipitation	Entire land region	Tail of distribution over north and northeast India[1]	Fig. 5.5
Extreme precipitation (95^{th} percentile)	Spatial distribution	Central India, parts of the central Himalaya	The eastern Himalayan foothills[2]	Fig. 5.6
Wet day frequency	"	IGP	Almost none	Fig. 5.4
Very wet day frequency	"	Western IGP	Almost none	Fig. 5.S4
Contribution of very wet day precip. to seasonal total	"	East Indian coastal, South Pakistan, Uttaranchal etc.	Central India, the central Himalayan foothills	Fig. 5.S5
Mean consecutive wet days	"	The east and central Himalaya	None	Fig. 5.S3
Low level circulation	"	West Gangetic plain	West central India	Fig. 5.3
Moisture flux	"	West Gangetic plain	East Gangetic plain, northern part of the Western Ghat	Fig. 5.S2

[1] But this could well be manifestation of coarser resolution of the observation and/or insufficient station samples (see section 5.3.2.3).

2 Again lack of sufficient station network might have partly contributed to excessive bias.

Table 7.2 Performance of high resolution RCM relative to its coarse resolution counterpart in simulating various intraseasonal characteristics of SASM.

Metric/measure	Main area of improvement	Main area of deterioration	Related figure/table
Active composite precipitation rate	IGP, west central India	Along the mean position of the monsoon trough	Fig. 6.6
Break composite precip. rate	IGP, East Nepal, parts of northeast India	Parts of northeast India and the central Himalayan foothills	Fig. 6.7
A/B[1] composite circulation	Break composite low level flow over the central Himalayan foothills	Weaker than observed Easterly Jet at 200 hpa for both active and break composites	Fig 6.3, 6.S1, 6.S2
A/B composite zonal average pressure anomaly	Both models are in good agreement with the observation.	-	Fig. 6.4
Occurrence of A/B spells and associated statistics	Mixed result	-	Table 6.1, 6.2
Position of the A/B composite monsoon trough	Active composite trough over west central India	None	Fig. 6.8
Lagged monsoon trough position for A/B composites	None (difficult to quantify from present analysis)	-	Fig. 6.8
A/B composite wet days	IGP and central India for the active and the Himalayan foothills for the break	None	Fig. 6.9
Relative frequency distribution of daily precip. for A/B spells	Overall Improved distribution of moderate and extremes precip. over both region and spells	Slight over (under) estimation of the tail of distribution over north (south) India for beak spells	Fig. 6.10

Occurrence of “Nepal very wet days”	In better agreement with the observation for very wet days falling in Jul-Aug, & co-occurrence of those days and break spells scaled by the total duration of the break spells	Co-occurrence of very wet days and break spells too high compared to the observed.	Table 6.3
Contribution of cumulative precipitation during “Nepal very wet days” to the seasonal total	The contribution over the core region (the central Himalayan foothills) closer to the observed.	None	Fig. 6.11

[1] A/B refer to Active/Break

7.2 Implications of the research

The research findings mentioned above could have following implications in the field of climate modelling, in particular modelling of the SASM.

- As monsoon rainfall indices are considered the best indicator of the strength and variability of the SASM, the variability of the SASM might not be best represented by the monsoon circulation indices. This is because the relationship between monsoon rainfall indices and monsoon circulation indices depict considerable low frequency variability. This implies that monsoon circulation indices might not be an appropriate metric for rapid appraisal of model skill in simulating SASM. Moreover, low frequency variability of correlation between the circulation based and rainfall based indices implies the correlation is not an appropriate metric for model evaluation unless the comparison is done between simulated and observed correlation for the same period. In particular, higher than observed correlation in the model simulation does not necessarily indicate higher model skill as postulated in some studies (e.g., Dobler and Ahrens 2010, Saeed et al. 2012), rather they might indicate model deficiencies.

- The sensitivity of RCM simulation to domain size indicates the importance of choosing appropriately sized domain through sensitivity studies so as to minimise the systematic errors, and maximise the potential for added value. This remains a necessity unless a RCM is able to simulate all aspect of SASM well; otherwise systematic error in one area will have detrimental impact on rest of the domain, especially if the domain is too large. As many of the current GCMs suffer from common systematic errors and they also have similar mechanisms of

early onset of bias over the EIO which then adversely affect circulation and moisture flow over rest of the South Asia (e.g., Bollasina and Ming 2013), conclusion drawn here should be largely valid for other RCMs derived from those GCMs. However, exact boundaries of an appropriate domain for other RCMs are likely to be sensitive to model configuration, such as the choice of convection scheme and other parameterizations.

- Also, CORDEX South Asia domain may or may NOT be a good domain as it includes the bias prone EIO region. However, there is still some scope of realistic simulation of SASM with the CORDEX South Asia domain if the given RCM does not have similar bias as running the RCM over the domain may remove the bias in the driving GCM. But if a given RCM also suffers from similar bias, then one might need to run the RCM over a smaller domain (such as the moderate domain used in this study) as well as force it with GCMs that does not have this bias.

- Nevertheless, intercomparison of the various model simulations over CORDEX South Asia domain would provide interesting insight regarding sensitivity of SASM simulation to model physics and parameterization independent of the sensitivity to the domain size.

- The enhanced performance of the high resolution model in simulation of many aspects of SASM, in particular those associated with precipitation, promotes application of high resolution RCMs in simulation of SASM. This result is consistent with the previous studies that show much improved performance of high resolution model in simulating various aspects of SASM (e.g., Rajendran et

al. 2013, Sabin et al. 2013). Those studies employed GCMs, but similar studies using high resolution RCMs are lacking so far.

7.3 Evaluation of the research

7.3.1 Contribution of the thesis

This thesis brings out the unstable relationship between the precipitation based and circulation based rainfall indices, which need to be taken into account while evaluating models in simulating those aspects.

It brings back the debate on sensitivity of the RCM SASM simulation to domain size, which has not received much attention heretofore. The study also shows that despite the large errors in the parent GCM, its regional version can still be used in processes studies when run over an appropriately size domain that excludes remote drivers of systematic errors from the direct area of interest.

A simple approach is used in the thesis to find the added value, which involve comparison of absolute bias in the model simulations i.e. added value = | (Model-A - Obs.) | - | (Model-B - Obs.) |. This approach might be suitable for other similar studies that evaluate the added value of high resolution model simulation for the present climate.

This thesis shows that reanalysis forced RCM run at high resolution but moderately sized domain (~25,000,000 sq. km) simulates SASM more realistically compared to that at coarser resolution and larger domain.

7.3.2 Limitations of the thesis

- The conclusion drawn in the study of monsoon rainfall and circulation based indices are based on the limited data (two reanalysis dataset for 64 years), which is not sufficient for a study on interdecadal variability. Also, the correlation between AIMR and 20th century reanalysis MCIs drop sharply around 1950; however, the thesis did not investigate its likely causes. This might reveal further insight on the fluctuation of the relationship between the two indices.

- The main limitation of the modelling studies is that only one RCM is employed and only a single integration is carried out for each experiment, which makes it difficult to generalize the results and conclusions drawn here without reasserting those findings using multiple RCMs and multiple realizations. This is because there is always a danger that the results obtained from a single RCM/realization are due to some unknown limitations in the model physics or parameterization and the results are not driven by plausible physical processes. Further, even when the given model is free from such errors, internal variability of the model could have relatively large influence on the model outputs, especially those with fine scale features such as precipitation. But it is not possible to have an estimate of internal variability with a single simulation, unless such experiments are repeated several times with slight perturbations, such as using slightly different initial conditions.

- Furthermore, the Hadley Centre model used in this work is not among the best contemporary models for simulation of SASM. Particularly, its deficiency in simulating SASM precipitation climatology with large wet EIO bias and dry

central India bias is well known. It is possible that RCMs, which simulate SASM much better, through model tuning, or otherwise, show entirely different sensitivity to the domain size. In particular, if such RCMs are able to better handle the convection, it is likely that inclusion of EIO region in the domain will not generate the big erroneous response seen in this study. In such an event, the difference between large and small domain simulation might be small, which in turn imply that RCM simulation of SASM is relatively insensitive to domain size and thus invalidate one major finding of the thesis.

- The Met Office Unified models are designed to run across a range of resolution and configurations (such as NWP, climate model - both global and regional) employing an unique model physics and parameterization, so the model configuration is relaxed to allow maximum flexibility. However, this generalization is likely to hamper the model performance particularly at the high resolution. This is because models are generally tested and optimized for simulations at most commonly used resolutions, but high resolution simulations require that the model parameterizations are adjusted to or fit for the scales of the high resolution simulation being sought (Jacob and Brasseur 2013[6]). However, the Met Office philosophy discourages such endeavours and no such attempts have been made in this study as well.

- Contrary to common practise, the high resolution RCM simulation analysed in this study consists of a series of discrete season long runs initialized each year using the moderate resolution RCM output (this is done to have same initial

[6] Oral presentation at International Conference on Regional Climate – CORDEX 2013, Brussels, Belgium, available at: http://cordex2013.wcrp-climate.org/plenary_A6/Pl_A6_01_jacob.pdf

condition in the two runs). So, the set up prevents the high resolution simulation from having continuity and freedom to generate its own circulation internally at longer than a seasonal time scale. So, it is plausible that the high resolution simulation considered here differs from the one that would have been obtained from a continuous integration. Compared to the latter, the present setup might have prevented both the emergence of additional added value and also the emergence of additional deteriorations compared to the coarser simulation.

- There is a mismatch between the horizontal resolution of the RCM simulations and the observations used for comparison. While the RCMs have resolution of 50- and 12- km approximately their outputs are compared against ERAI for upper level fields and against APHRODITE at 25 km resolution for precipitation. While the resolution difference of the simulated and observed large scale atmospheric fields might have limited impact in model evaluation, the coarser resolution of the precipitation dataset might have detrimental impact on evaluation of high resolution simulation such as the extremes.

7.4 Suggestions for future work

The research undertaken brings out a number of topics on which further research would be beneficial.

The conclusion of the thesis is drawn from comparison of unique RCM simulation for each experimental setup. However, model simulations, in particular precipitation, are sensitive to both external forcings as well as internal RCM physics. Hence, a logical extension of present work is to repeat the experiments on sensitivity of RCM simulation to domain size and added value of high resolution modelling, using multiple realisations

and then to evaluate the outputs from individual members as well as ensemble mean. Such study would provide an estimate of the internal model physics related uncertainty associated with the conclusions drawn here.

The present study evaluates the performance RCM simulation up to a horizontal resolution of 0.11° and finds a number of improvements compared to the coarser simulation. However, RCM simulations at convection resolving horizontal resolution of 1-4 km have recently been carried out for various regions. Though computationally astonishingly expensive, such runs are now feasible with rapidly growing computation capacity. The main attraction of convection permitting climate simulations is that error-prone deep convection parameterization schemes, which is the source of spatial and case dependent sensitivity and high systematic errors in model simulations (Warrach-Sagi et al. 2013), can be omitted as deep convection can be (at least partly) resolved explicitly (Weisman et al. 1997). Hence, simulation at convective resolving horizontal resolution of 1-4 km would also provide interesting insight into the debate of added value of high resolution simulation of SASM, which might provide further insight into apparent lack of added value over complex and heterogeneous regions, such as the Himalaya in the present study.

However, evaluation of higher resolution simulation needs to be carried out with comparable high resolution observations. Use of coarser observation in evaluation of high resolution simulation might mask the improvement in the high resolution simulation and in some cases even indicate deterioration erroneously. Hence, another relevant research task is the development of sufficiently high resolution gridded dataset over the regions where dense network of station observation exist. This would assist evaluation of very high resolution models, at least over those regions. Even though relatively high resolution datasets based on remote sensing exist, (e.g., TRMM available

at resolution of 25 km at 3 hourly intervals) they have a number of limitations especially over the elevated regions such as the Himalaya (where precipitation often comes as snow, as light drizzle and during short intense storms), as remote sensors generally have difficulty detecting short-lasting and light precipitation as well as frozen precipitation. For example, TRMM-3B42 does not capture well the precipitation distribution at elevation higher than 1 km and underestimates precipitation in mountainous regions (Andermann et al. 2011). This limits their application in evaluation of high resolution models.

The thesis shows that with careful selection of domain, RCM forced by realistic boundary condition is able to simulate SASM well in spite of large systematic errors in its parent GCM simulation. However, the sensitivity of the RCM to domain size and resolution when forced by imperfect boundary forcings remains unanswered. So, the present work can be further extended by forcing the RCM with imperfect boundary conditions from different GCMs. This could provide an estimate of the sensitivity of the RCM simulation to domain size and horizontal resolution when forced by imperfect forcings.

The Hadley Centre model used in this study is not among the best contemporary models for realistic simulation of SASM, particularly precipitation, owing to its inherent deficiency in convection scheme and orographic bias (Levine and Turner 2012). Hence, repeating the research in this thesis with 2-3 different RCMs would provide further insight to the sensitivity of SASM simulation to domain size and horizontal resolution. In particular, such a study would reveal whether the findings of the thesis are valid universally or limited to the model considered in this study. Then after, those RCMs could be run with different GCMs creating a grand ensemble, something akin to

ongoing CORDEX initiative on RCM intercomparison, which would allow a host of assessments, including a more systematic assessment of parent-daughter issue.

7.5 Concluding remarks

Finally, I would like to conclude this thesis with few final thoughts that has not been dwelled upon in proceeding sections.

The first relates to the sensitivity of RCM simulation to its domain.

Though extent of sensitivity may vary from region to region or season to season, it is clear that RCM simulations are sensitive to the domain size and its location. So the importance of choosing an appropriate domain has been well documented. In this connection, a number of recommendations can be found in literature regarding judicious selection of domain. For example, few common recommendations are: domain should be large enough to allow full development of internal model mesoscale circulations and include relevant regional forcing but they should not be so big that its large scale circulation significantly deviates from that of the driving LBC. But, it is difficult to set out a general criterion for the choice of a RCM domain as the choice depends on the region and experiment design.

For example, if the aim is to interrogate RCM outputs to further the scientific understanding on the physical controls of regional biases then heuristic choice of domains would be useful as analysis of those outputs would provide insight into different elements of systematic errors and their interactions. However, if the aim is to reliably downscale global projections at sub regional level RCM integration might have to be carried out on several carefully selected domains as recent studies (e.g., Bhaskaran et al. 2012) suggest that there exist no single optimum domain which is suitable for

RCM applications in climate change assessments on all sub regions within the model domain.

Ideally, there is a need to develop a methodology for dynamical downscaling which renders the sensitivity of RCM simulations to domain size while ensuring the physical consistency between the RCM and large scale forcings. Promising results have been obtained through the application of large scale or spectral nudging which constrains the synoptic scales to follow the driving data while allowing the RCM to develop the small scale dynamics responsible for precipitation. Recent studies (e.g., Miguez-Macho et al. 2004)show that nudging large scales greatly eliminates the dependency of simulation fields such as precipitation on domain size and locations. Further research is need in this direction to promote application of these techniques in dynamical downscaling.

And the final issue relates with the association between a RCM's skill to simulate historic mean climate to its skill to simulate the climate change projections.

Unlike weather forecasts which can be verified in few days to weeks (i.e. after the forecast validity period), a major difficulty in evaluating model simulated future climate projections is that associated observation to validate those projections against does not exist at present. So, it is not possible to assess the model's future climate projections in "traditional manner". To circumvent the problem, it is customary to evaluate model skill in simulating present or past climate against the observations of the corresponding periods. Here, the past climate refers to climate from recent past up to paleoclimate time scale. Compared to models that show poor skill in simulating past or current climate, models that well simulate those periods are considered better and their future projects are considered more trustworthy. This is based on the hypothesis that given the dynamical downscaling is physically based, if a model performs well under one climatic

condition it should also perform well in other climatic conditions as governing equations remain invariant under diverse climatic conditions.

However, correlating model skill to simulate historic climate with its skill to project future climate may be problematic because the approximations and parametrizations in the model that gives good results in present climate might not perform equally well in future climatic condition as climate system operates in nonlinear manner. In addition, sudden breakdown in some components of climate regime in future cannot be ruled out. It is unlikely that present climatic pattern would prevail in such scenario which would limit the applicability of climate change scenario developed based on current climatic conditions.

Furthermore, Racherla et al. (2012) found that RCM's skill in reproducing historic climatological mean conditions is not closely associated with its skill in capturing climate change in the recent decades. Rather RCM skill is strongly limited by the skill of the driving GCM itself. Under that scenario, attempts to link model skill to simulate present climate with its future climate projections could be futile. However, additional research is needed on this matter before drawing firm conclusions.

References

Abel SJ, Shipway BJ (2007) A comparison of cloud-resolving model simulations of trade wind cumulus with aircraft observations taken during RICO. Q J R Meteorol Soc 133:781-794. doi: 10.1002/qj.55

Adler RF, Huffman GJ, Chang A, Ferraro R, Xie P-, Janowiak J, Rudolf B, Schneider U, Curtis S, Bolvin D, Gruber A, Susskind J, Arkin P, Nelkin E (2003) The version-2 global precipitation climatology project (GPCP) monthly precipitation analysis (1979-present). J Hydrometeorol 4:1147-1167. doi: 10.1175/1525-7541(2003)004<1147:TVGPCP>2.0.CO;2

Akhtar M, Ahmad N, Booij MJ (2008) The impact of climate change on the water resources of Hindukush-Karakorum-Himalaya region under different glacier coverage scenarios. Journal of Hydrology 355:148-163. doi: 10.1016/j.jhydrol.2008.03.015

Andermann C, Bonnet S, Gloaguen R (2011) Evaluation of precipitation data sets along the Himalayan front. Geochem Geophys Geosyst 12:Q07023. doi: 10.1029/2011GC003513

Anders AM, Roe GH, Hallet B, Montgomery DR, Finnegan NJ, Putkonen J (2006) Spatial patterns of precipitation and topography in the Himalaya. Special Paper of the Geological Society of America:39-53

Annamalai H, Hamilton K, Sperber KR (2007a) The South Asian summer monsoon and its relationship with ENSO in the IPCC AR4 simulations. J Clim 20:1071-1092. doi: 10.1175/JCLI4035.1

Annamalai H, Okajima H, Watanabe M (2007b) Possible impact of the Indian Ocean SST on the northern hemisphere circulation during El Nino. J Clim 20:3164-3189. doi: 10.1175/JCLI4156.1

Annamalai H, Slingo JM (2001) Active/break cycles: diagnosis of the intraseasonal variability of the Asian Summer Monsoon. Clim Dyn 18:85-102

Arakawa A, Lamb C (1977) Computational design of the basic dynamic processes of the UCLA general circulation model. Methods Comput Phys 17:173-265

Armstrong RL, Brodzik MJ, Knowles K, Savoie M (2005) Global Monthly EASE-Grid Snow Water Equivalent Climatology. Boulder, CO: National Snow and Ice Data Center. Digital media.

Ashfaq M, Shi Y, Tung W-, Trapp RJ, Gao X, Pal JS, Diffenbaugh NS (2009) Suppression of south Asian summer monsoon precipitation in the 21st century. Geophys Res Lett 36. doi: 10.1029/2008GL036500

Ashok K, Guan Z, Yamagata T (2001) Impact of the Indian Ocean dipole on the relationship between the Indian monsoon rainfall and ENSO. Geophys Res Lett 28:4499-4502. doi: 10.1029/2001GL013294

Bansod SD, Singh HN, Patil SD, Singh N (2012) Recent changes in the circulation parameters and their association with Indian summer monsoon rainfall . J Atmos Solar Terr Phys 77:248 <last_page> 253. doi: 10.1016/j.jastp.2012.01.015

Barnett TP, Adam JC, Lettenmaier DP (2005) Potential impacts of a warming climate on water availability in snow-dominated regions. Nature 438:303-309

Barrera-Escoda A, Gonçalves M, Guerreiro D, Cunillera J, Baldasano JM (2013) Projections of temperature and precipitation extremes in the North Western Mediterranean Basin by dynamical downscaling of climate scenarios at high resolution (1971-2050). Clim Change:1-16. doi: 10.1007/s10584-013-1027-6

Barros AP, Kim G, Williams E, Nesbitt SW (2004) Probing orographic controls in the Himalayas during the monsoon using satellite imagery. Natural Hazards and Earth System Science 4:29-51

Bawiskar SM (2009) Weakening of lower tropospheric temperature gradient between Indian landmass and neighbouring oceans and its impact on Indian monsoon. J Earth Syst Sci 118:273-280. doi: 10.1007/s12040-009-0029-2

Berg P, Wagner S, Kunstmann H, Schädler G (2013) High resolution regional climate model simulations for Germany: Part I-validation. Clim Dyn 40:401-414. doi: 10.1007/s00382-012-1508-8

Best MJ, Pryor M, Clark DB, Rooney GG, Essery RLH, Menard CB, Edwards JM, Hendry MA, Porson A, Gedney N, Mercado LM, Sitch S, Blyth E, Boucher O, Cox PM, Grimmond CSB, Harding RJ (2011) The Joint UK Land Environment Simulator (JULES), model description - Part 1: Energy and water fluxes. Geoscientific Model Development 4:677-699. doi: 10.5194/gmd-4-677-2011

Bhaskaran B, Ramachandran A, Jones R, Moufouma-Okia W (2012) Regional climate model applications on sub-regional scales over the Indian monsoon region: The role of domain size on downscaling uncertainty. J Geophys Res 117:D10113. doi: 10.1029/2012JD017956

Bhaskaran B, Murphy JM, Jones RG (1998) Intraseasonal oscillation in the Indian summer monsoon simulated by global and nested regional climate models. Mon Weather Rev 126:3124-3134

Bhaskaran B, Jones RG, Murphy JM, Noguer M (1996) Simulations of the Indian summer monsoon using a nested regional climate model: Domain size experiments. Clim Dyn 12:573-587

Bolch T, Kulkarni A, Kääb A, Huggel C, Paul F, Cogley JG, Frey H, Kargel JS, Fujita K, Scheel M, Bajracharya S, Stoffel M (2012) The State and Fate of Himalayan Glaciers. Science 336:310-314. doi: 10.1126/science.1215828

Bollasina M, Nigam S (2009) Indian Ocean SST, evaporation, and precipitation during the South Asian summer monsoon in IPCC-AR4 coupled simulations. Clim Dyn 33:1017-1032. doi: 10.1007/s00382-008-0477-4

Bollasina MA, Ming Y (2013) The general circulation model precipitation bias over the southwestern equatorial Indian Ocean and its implications for simulating the South Asian monsoon. Clim Dyn 40:823-838. doi: 10.1007/s00382-012-1347-7

Bollasina MA, Ming Y, Ramaswamy V (2011) Anthropogenic aerosols and the weakening of the south asian summer monsoon. Science 334:502-505. doi: 10.1126/science.1204994

Boville BA (1991) Sensitivity of Simulated Climate to Model Resolution. J Climate 4:469-485. doi: 10.1175/1520-0442(1991)004<0469:SOSCTM>2.0.CO;2

Brown AR, Beare RJ, Edwards JM, Lock AP, Keogh SJ, Milton SF, Walters DN (2008) Upgrades to the Boundary-Layer Scheme in the Met Office Numerical Weather Prediction Model. Bound -Layer Meteorol 128:117-132. doi: 10.1007/s10546-008-9275-0

Browne NAK, Sylla MB (2012) Regional climate model sensitivity to domain size for the simulation of the West African summer monsoon rainfall. Int J Geophys 2012. doi: 10.1155/2012/625831

Bush SJ, Turner AG, Woolnough SJ, Martin GM, Klingaman NP (2014) The effect of increased convective entrainment on Asian monsoon biases in the MetUM general circulation model. Q J R Meteorol Soc. doi: 10.1002/qj.2371

Caldwell P (2010) California wintertime precipitation bias in regional and global climate models. J Appl Meteorol Climatol 49:2147-2158. doi: 10.1175/2010JAMC2388.1

Cardoso RM, Soares PMM, Miranda PMA, Belo-Pereira M (2013) WRF high resolution simulation of Iberian mean and extreme precipitation climate. Int J Climatol 33:2591-2608. doi: 10.1002/joc.3616

Castro CL, Pielke Sr. RA, Leoncini G (2005) Dynamical downscaling: Assessment of value retained and added using the Regional Atmopsheric Modeling System (RAMS). J Geophys Res D Atmos 110:1-21. doi: 10.1029/2004JD004721

Chan SC, Kendon EJ, Fowler HJ, Blenkinsop S, Ferro CAT, Stephenson DB (2012) Does increasing the spatial resolution of a regional climate model improve the simulated daily precipitation?. Clim Dyn:1-21

Charney JG, Phillips NA (1953) Numerical integration of the quasi-geostrophic equations for barotropic and simple baroclinic flows. J Meteor 10:71-99. doi: 10.1175/1520-0469(1953)010<0071:NIOTQG>2.0.CO;2

Chen C-, Knutson T (2008) On the verification and comparison of extreme rainfall indices from climate models. J Clim 21:1605-1621. doi: 10.1175/2007JCLI1494.1

Chen H, Ding Y, He J (2007) Reappraisal of Asian summer monsoon indices and the long-term variation of monsoon. Acta Meteorologica Sinica 21:168-178

Chen T-, Yen M- (1994) Interannual variation of the Indian monsoon simulated by the NCAR community climate model: Effect of the tropical Pacific SST. J Clim 7:1403-1415

Choudhury AD, Krishnan R (2011) Dynamical response of the South Asian monsoon trough to latent heating from stratiform and convective precipitation. J Atmos Sci 68:1347-1363. doi: 10.1175/2011JAS3705.1

Christensen JH, Carter TR, Rummukainen M, Amanatidis G (2007) Evaluating the performance and utility of regional climate models: The PRUDENCE project. Clim Change 81:1-6

Clark DB, Mercado LM, Sitch S, Jones CD, Gedney N, Best MJ, Pryor M, Rooney GG, Essery RLH, Blyth E, Boucher O, Harding RJ, Huntingford C, Cox PM (2011) The Joint UK Land Environment Simulator (JULES), model description - Part 2: Carbon fluxes and vegetation dynamics. Geoscientific Model Development 4:701-722. doi: 10.5194/gmd-4-701-2011

Colin J, DéQué M, Radu R, Somot S (2010) Sensitivity study of heavy precipitation in Limited Area Model climate simulations: Influence of the size of the domain and the use of the spectral nudging technique. Tellus Ser A Dyn Meteorol Oceanogr 62:591-604. doi: 10.1111/j.1600-0870.2010.00467.x

Collins M, Achutarao K, Ashok K, Bhandari S, Mitra AK, Prakash S, Srivastava R, Turner A (2013) Observational challenges in evaluating climate models. Nat Clim Change 3:940-941. doi: 10.1038/nclimate2012

Compo GP, Whitaker JS, Sardeshmukh PD, Matsui N, Allan RJ, Yin X, Gleason BE, Vose RS, Rutledge G, Bessemoulin P, BroNnimann S, Brunet M, Crouthamel RI, Grant AN, Groisman PY, Jones PD, Kruk MC, Kruger AC, Marshall GJ, Maugeri M, Mok HY, Nordli O, Ross TF, Trigo RM, Wang XL, Woodruff SD, Worley SJ (2011) The Twentieth Century Reanalysis Project. Q J R Meteorol Soc 137:1-28. doi: 10.1002/qj.776

Cook KH, Vizy EK, Launer ZS, Patricola CM (2008) Springtime intensification of the great plains low-level jet and midwest precipitation in GCM Simulations of the twenty-first century. J Clim 21:6321-6340. doi: 10.1175/2008JCLI2355.1

Cook KH, Vizy EK (2006) Coupled model simulations of the West African monsoon system: Twentieth- and twenty-first-century simulations. J Clim 19:3681-3703. doi: 10.1175/JCLI3814.1

Coppola E, Giorgi F, Raffaele F, Fuentes-Franco R, Giuliani G, LLopart-Pereira M, Mamgain A, Mariotti L, Diro GT, Torma C (2014) Present and future climatologies in the phase I CREMA experiment. Clim Change. doi: 10.1007/s10584-014-1137-9

Cullen MJP (1993) The Unified Forecast Climate Model. Meteorol Mag 122:81-94

Dai A (2006) Precipitation characteristics in eighteen coupled climate models. J Clim 19:4605-4630. doi: 10.1175/JCLI3884.1

Daly C (2006) Guidelines for assessing the suitability of spatial climate data sets. Int J Climatol 26:707-721. doi: 10.1002/joc.1322

Dash SK, Mamgain A, Pattnayak KC, Giorgi F (2013) Spatial and Temporal Variations in Indian Summer Monsoon Rainfall and Temperature: An Analysis Based on RegCM3 Simulations. Pure Appl Geophys 170:655-674

Dash SK, Shekhar MS, Singh GP (2006) Simulation of Indian summer monsoon circulation and rainfall using RegCM3. Theoretical and Applied Climatology 86:161-172

Davies T, Cullen MJP, Malcolm AJ, Mawson MH, Staniforth A, White AA, Wood N (2005) A new dynamical core for the Met Office's global and regional modelling of the atmosphere. Q J R Meteorol Soc 131:1759-1782. doi: 10.1256/qj.04.101

De Sales F, Xue Y (2011) Assessing the dynamic-downscaling ability over South America using the intensity-scale verification technique. Int J Climatol 31:1205-1221. doi: 10.1002/joc.2139

De US, Lele RR, Natu JC (1998) Breaks in southwest monsoon. Indian Meteorological Department, Report No. 1998/3

Dee DP, Uppala SM, Simmons AJ, Berrisford P, Poli P, Kobayashi S, Andrae U, Balmaseda MA, Balsamo G, Bauer P, Bechtold P, Beljaars ACM, van de Berg L, Bidlot J, Bormann N, Delsol C, Dragani R, Fuentes M, Geer AJ, Haimberger L, Healy SB, Hersbach H, Hólm EV, Isaksen L, Kållberg P, Köhler M, Matricardi M, Mcnally AP, Monge-Sanz BM, Morcrette J-, Park B-, Peubey C, de Rosnay P, Tavolato C, Thépaut J-, Vitart F (2011) The ERA-Interim reanalysis: Configuration and performance of the data assimilation system. Q J R Meteorol Soc 137:553-597. doi: 10.1002/qj.828

Delsole T, Shukla J (2012) Climate models produce skillful predictions of Indian summer monsoon rainfall. Geophys Res Lett 39. doi: 10.1029/2012GL051279

DelSole T, Shukla J (2009) Artificial skill due to predictor screening. J Clim 22:331-345. doi: 10.1175/2008JCLI2414.1

Denis B, Laprise R, Caya D, Côté J (2002) Downscaling ability of one-way nested regional climate models: The Big-Brother Experiment. Clim Dyn 18:627-646

Dhar ON, Nandargi S (2000) A study of floods in the Brahmaputra basin in India. Int J Climatol 20:771-781. doi: 10.1002/1097-0088(20000615)20:7<771::AID-JOC518>3.0.CO;2-Z

Dhar ON, Soman MK, Mulye SS (1984) Rainfall over the southern slopes of the Himalayas and the adjoining plains during ' breaks' in the monsoon. Journal of Climatology 4:671-676

Di Luca A, de Elía R, Laprise R (2012) Potential for added value in precipitation simulated by high-resolution nested Regional Climate Models and observations. Clim Dyn 38:1229-1247. doi: 10.1007/s00382-011-1068-3

Diaconescu EP, Laprise R (2013) Can added value be expected in RCM-simulated large scales?. Clim Dyn 41:1769-1800. doi: 10.1007/s00382-012-1649-9

Dickinson RE, Errico RM, Giorgi F, Bates GT (1989) A regional climate model for the western United States. Clim Change 15:383-422. doi: 10.1007/BF00240465

Dimri AP (2013) Interannual variability of Indian winter monsoon over the Western Himalayas. Global Planet Change 106:39-50. doi: 10.1016/j.gloplacha.2013.03.002

Dimri AP (2009) Impact of subgrid scale scheme on topography and landuse for better regional scale simulation of meteorological variables over the western Himalayas. Clim Dyn 32:565-574

Dimri AP, Mohanty UC (2009) Simulation of mesoscale features associated with intense western disturbances over western Himalayas. Meteorol Appl 16:289-308

Dimri AP (2004) Impact of horizontal model resolution and orography on the simulation of a western disturbance and its associated precipitation. Meteorol Appl 11:115-127

Dobler A, Ahrens B (2011) Four climate change scenarios for the Indian summer monsoon by the regional climate model COSMO-CLM. J Geophys Res D Atmos 116. doi: 10.1029/2011JD016329

Dobler A, Ahrens B (2010) Analysis of the Indian summer monsoon system in the regional climate model COSMO-CLM. J Geophys Res D Atmos 115. doi: 10.1029/2009JD013497

Dobler C, Hagemann S, Wilby RL, StÃtter J (2012) Quantifying different sources of uncertainty in hydrological projections in an Alpine watershed. Hydrol Earth Syst Sci 16:4343-4360. doi: 10.5194/hess-16-4343-2012

Duffy PB, Govindasamy B, Lorio JP, Milovich J, Sperber KR, Taylor KE, Wehner MF, Thompson SL (2003) High-resolution simulations of global climate, part 1: Present climate. Clim Dyn 21:371-390

Elguindi N, Giorgi F, Turuncoglu U (2014) Assessment of CMIP5 global model simulations over the subset of CORDEX domains used in the Phase I CREMA. Clim Change 125:7-21. doi: 10.1007/s10584-013-0935-9

Fan F, Mann ME, Lee S, Evans JL (2012) Future changes in the South Asian summer monsoon: An analysis of the CMIP3 multimodel projections. J Clim 25:3909-3928. doi: 10.1175/JCLI-D-11-00133.1

Fan F, Mann ME, Lee S, Evans JL (2010) Observed and modeled changes in the South Asian summer monsoon over the historical period. J Clim 23:5193-5205. doi: 10.1175/2010JCLI3374.1

Fan F, Mann ME, Ammann CM (2009) Understanding changes in the Asian summer monsoon over the past millennium: Insights from a long-term coupled model simulation. J Clim 22:1736-1748. doi: 10.1175/2008JCLI2336.1

Feser F, Rrockel B, Storch H, Winterfeldt J, Zahn M (2011) Regional climate models add value to global model data a review and selected examples. Bull Am Meteorol Soc 92:1181-1192. doi: 10.1175/2011BAMS3061.1

Feser F (2006) Enhanced detectability of added value in limited-area model results separated into different spatial scales. Mon Weather Rev 134:2180-2190. doi: 10.1175/MWR3183.1

Feser F, von Storch H (2005) A spatial two-dimensional discrete filter for limited-area-model evaluation purposes. Mon Weather Rev 133:1774-1786. doi: 10.1175/MWR2939.1

Frei C, Christensen JH, Déqué M, Jacob D, Jones RG, Vidale PL (2003) Daily precipitation statistics in regional climate models: Evaluation and intercomparison for the European Alps. J Geophys Res D Atmos 108:ACL 9-1 - ACL 9-19

Fritsch JM, Chappell CF (1980) Numerical Prediction of Convectively Driven Mesoscale Pressure Systems. Part I: Convective Parameterization. J Atmos Sci 37:1722-1733. doi: 10.1175/1520-0469(1980)037<1722:NPOCDM>2.0.CO;2

Fu X, Wang B, Waliser DE, Tao L (2007) Impact of atmosphere-ocean coupling on the predictability of monsoon intraseasonal oscillations. J Atmos Sci 64:157-174. doi: 10.1175/JAS3830.1

Fu X, Wang B, Li T, McCreary JP (2003) Coupling between Northward-propagating, intraseasonal oscillations and sea surface temperature in the Indian Ocean. J Atmos Sci 60:1733-1753. doi: 10.1175/1520-0469(2003)060<1733:CBNIOA>2.0.CO;2

Fu X, Wang B, Li T (2002) Impacts of air-sea coupling on the simulation of mean Asian summer monsoon in the ECHAM4 model. Mon Weather Rev 130:2889-2904

Gadgil S, Joseph PV (2003) On breaks of the Indian monsoon. Proceedings of the Indian Academy of Sciences, Earth and Planetary Sciences 112:529-558

Gadgil S, Rao PRS (2000) Farming strategies for a variable climate - A challenge. Curr Sci 78:1203-1215

Gadgil S, Sajani S (1998) Monsoon precipitation in the AMIP runs. Clim Dyn 14:659-689

Gao X, Xu Y, Zhao Z, Pal JS, Giorgi F (2006) On the role of resolution and topography in the simulation of East Asia precipitation. Theor Appl Climatol 86:173-185. doi: 10.1007/s00704-005-0214-4

Gershunov A, Schneider N, Barnett T (2001) Low-frequency modulation of the ENSO - Indian monsoon rainfall relationship: Signal or noise?. J Clim 14:2486-2492

Giorgi F (2014) Introduction to the special issue: the phase I CORDEX RegCM4 hyper-matrix (CREMA) experiment. Clim Change. doi: 10.1007/s10584-014-1166-4

Giorgi F, Coppola E, Raffaele F, Diro GT, Fuentes-Franco R, Giuliani G, Mamgain A, Llopart MP, Mariotti L, Torma C (2014) Changes in extremes and hydroclimatic regimes in the CREMA ensemble projections. Clim Change. doi: 10.1007/s10584-014-1117-0

Giorgi F, Jones C, Asrar GR (2009) Addressing climate information needs at the regional level: The CORDEX framework. WMO Bull 58:175-183

Giorgi F, Mearns LO (1999) Introduction to special section: Regional climate modeling revisited. J.Geophys.Res. 104:6335-6352

Giorgi F, Marinucci MR (1996) An investigation of the sensitivity of simulated precipitation to model resolution and its implications for climate studies. Mon Weather Rev 124:148-166

Giorgi F, Mearns L, Shields C, McDaniel L (1998) Regional Nested Model Simulations of Present Day and 2 Ã— CO2 Climate over the Central Plains of the U.S. Clim Change 40:457-493. doi: 10.1023/A:1005384803949

Gorter W, van Angelen JH, Lenaerts JTM, van den Broeke MR (2014) Present and future near-surface wind climate of Greenland from high resolution regional climate modelling. Clim Dyn 42:1595-1611. doi: 10.1007/s00382-013-1861-2

Goswami BB, Mukhopadhyay P, Mahanta R, Goswami BN (2010) Multiscale interaction with topography and extreme rainfall events in the northeast Indian region. Journal of Geophysical Research D: Atmospheres 115

Goswami BN, Venugopal V, Sangupta D, Madhusoodanan MS, Xavier PK (2006a) Increasing trend of extreme rain events over India in a warming environment. Science 314:1442-1445. doi: 10.1126/science.1132027

Goswami BN, Wu G, Yasunari T (2006b) The annual cycle, intraseasonal oscillations, and roadblock to seasonal predictability of the Asian summer monsoon. J Clim 19:5078-5099

Goswami BN, Xavier PK (2003) Potential predictability and extended range prediction of Indian summer monsoon breaks. Geophys Res Lett 30:ASC 9-1 - 9-4

Goswami BN, Krishnamurthy V, Annamalai H (1999) A broad-scale circulation index for the interannual variability of the Indian summer monsoon. Q J R Meteorol Soc 125:611-633

Gregory D, Allen S (1991) The effect of convective downdraughts upon NWP and climate simulations. In: Nineth conference on numerical weather prediction:122-123

Gregory D, Rowntree PR (1990) A Mass Flux Convection Scheme with Representation of Cloud Ensemble Characteristics and Stability-Dependent Closure. Mon Weather Rev 118:1483-1506. doi: 10.1175/1520-0493(1990)118<1483:AMFCSW>2.0.CO;2

Grotch SL, MacCracken MC (1991) The Use of General Circulation Models to Predict Regional Climatic Change. J Climate 4:286-303. doi: 10.1175/1520-0442(1991)004<0286:TUOGCM>2.0.CO;2

Hack JJ, Caron JM, Danabasoglu G, Oleson KW, Bitz C, Truesdale JE (2006) CCSM-CAM3 climate simulation sensitivity to changes in horizontal resolution. J Clim 19:2267-2289. doi: 10.1175/JCLI3764.1

Haensler A (2011) Dynamical downscaling of ERA40 reanalysis data over southern Africa : added value in the simulation of the seasonal rainfall characteristics. Int J Climatol 31:2338-2349

Hall DK, Riggs GA, Salomonson VV (2006) MODIS snow and sea ice products. Earth Sci Satell Rem Sens : Sci Instruments 1:154-181

Harris I, Jones PD, Osborn TJ, Lister DH (2014) Updated high-resolution grids of monthly climatic observations - the CRU TS3.10 Dataset. Int J Climatol 34:623-642. doi: 10.1002/joc.3711

Haslinger K, Anders I, Hofstätter M (2013) Regional climate modelling over complex terrain: An evaluation study of COSMO-CLM hindcast model runs for the Greater Alpine Region. Clim Dyn 40:511-529. doi: 10.1007/s00382-012-1452-7

Held IM, Soden BJ (2006) Robust responses of the hydrological cycle to global warming. J Clim 19:5686-5699. doi: 10.1175/JCLI3990.1

Hofstra N, New M, McSweeney C (2010) The influence of interpolation and station network density on the distributions and trends of climate variables in gridded daily data. Clim Dyn 35:841-858. doi: 10.1007/s00382-009-0698-1

Hofstra N, Haylock M, New M, Jones PD (2009) Testing E-OBS European high-resolution gridded data set of daily precipitation and surface temperature. J Geophys Res D Atmos 114. doi: 10.1029/2009JD011799

Hofstra N, Haylock M, New M, Jones P, Frei C (2008) Comparison of six methods for the interpolation of daily, European climate data. J Geophys Res D Atmos 113. doi: 10.1029/2008JD010100

Huffman GJ, Adler RF, Bolvin DT, Gu G (2009) Improving the global precipitation record: GPCP Version 2.1. Geophys Res Lett 36. doi: 10.1029/2009GL040000

Huffman GJ, Adler RF, Bolvin DT, Gu G, Nelkin EJ, Bowman KP, Hong Y, Stocker EF, Wolff DB (2007) The TRMM Multisatellite Precipitation Analysis (TMPA): Quasi-global, multiyear, combined-sensor precipitation estimates at fine scales. J Hydrometeorol 8:38-55. doi: 10.1175/JHM560.1

Huffman GJ, Adler RF, Morrissey MM, Bolvin DT, Curtis S, Joyce R, McGavock B, Susskind J (2001) Global precipitation at one-degree daily resolution from multisatellite observations. J Hydrometeorol 2:36-50. doi: 10.1175/1525-7541(2001)002<0036:GPAODD>2.0.CO;2

Hurrell JW, Trenberth KE (1998) Difficulties in obtaining reliable temperature trends: reconciling the surface and satellite microwave sounding unit records. J Clim 11:945-967

Im E-, Coppola E, Giorgi F, Bi X (2010) Validation of a high-resolution regional climate model for the alpine region and effects of a subgrid-scale topography and land use representation. J Clim 23:1854-1873

Im E-, Park E-, Kwon W-, Giorgi F (2006) Present climate simulation over Korea with a regional climate model using a one-way double-nested system. Theor Appl Climatol 86:187-200. doi: 10.1007/s00704-005-0215-3

Immerzeel WW, Van Beek LPH, Bierkens MFP (2010) Climate change will affect the asian water towers. Science 328:1382-1385

Iorio JP, Duffy PB, Govindasamy B, Thompson SL, Khairoutdinov M, Randall D (2004) Effects of model resolution and subgrid-scale physics on the simulation of precipitation in the continental United States. Clim Dyn 23:243-258. doi: 10.1007/s00382-004-0440-y

Jacob D, Bärring L, Christensen OB, Christensen JH, De Castro M, Déqué M, Giorgi F, Hagemann S, Hirschi M, Jones R, Kjellström E, Lenderink G, Rockel B, Sánchez E, Schär C, Seneviratne SI, Somot S, Van Ulden A, Van Den Hurk B (2007) An inter-comparison of regional climate models for Europe: Model performance in present-day climate. Clim Change 81:31-52. doi: 10.1007/s10584-006-9213-4

Jarosch AH, Anslow FS, Clarke GKC (2012) High-resolution precipitation and temperature downscaling for glacier models. Clim Dyn 38:391-409. doi: 10.1007/s00382-010-0949-1

Ji Z, Kang S (2013) Double-Nested Dynamical Downscaling Experiments over the Tibetan Plateau and Their Projection of Climate Change under Two RCP Scenarios . J Atmos Sci 70:1278 <last_page> 1290. doi: 10.1175/JAS-D-12-0155.1

Jiang X, Li T, Wang B (2004) Structures and mechanisms of the northward propagating boreal summer intraseasonal oscillation. J Clim 17:1022-1039

Jianhua Ju, Slingo J (1995) The Asian summer monsoon and ENSO. Quarterly Journal - Royal Meteorological Society 121:1133-1168

Jiao Y, Caya D (2006) An investigation of summer precipitation simulated by the Canadian Regional Climate Model. Mon Weather Rev 134:919-932. doi: 10.1175/MWR3103.1

Johnson SJ, Levine RC, Turner AG, Martin GM, Woolnough SJ, Schiemann R, Mizielinski MS, Roberts MJ, Vidale PL, Demory M-, Strachan J (2015) The resolution sensitivity of the South Asian monsoon and Indo-Pacific in a global 0.35° AGCM. Clim Dyn. doi: 10.1007/s00382-015-2614-1

Jones RG, Noguer M, Hassell DC, Hudson D, Wilson SS, Jenkins GJ, Mitchell JFB (2004) Generating high resolution climate change scenarios using PRECIS. Met Office Hadley Centre, Exeter, UK

Jones RG, Murphy JM, Noguer M (1995) Simulation of climate change over Europe using a nested regional-climate model. I: Assessment of control climate, including sensitivity to location of lateral boundaries. Q J R Meteorol Soc 121:1413-1449

Joseph PV, Simon A (2005) Weakening trend of the southwest monsoon current through peninsular India from 1950 to the present. Curr Sci 89:687-694

Kalnay E, Kanamitsu M, Kistler R, Collins W, Deaven D, Gandin L, Iredell M, Saha S, White G, Woollen J, Zhu Y, Chelliah M, Ebisuzaki W, Higgins W, Janowiak J, Mo KC, Ropelewski C, Wang J, Leetmaa A, Reynolds R, Jenne R, Joseph D (1996) The NCEP/NCAR 40-year reanalysis project. Bull Am Meteorol Soc 77:437-471

Kamal-Heikman S, Derry LA, Stedinger JR, Duncan CC (2007) A Simple Predictive Tool for Lower Brahmaputra River Basin Monsoon Flooding. Earth Interact 11:1-11. doi: 10.1175/EI226.1

Kanamitsu M, Dehaan L (2011) The Added Value Index: A new metric to quantify the added value of regional models. J Geophys Res D Atmos 116. doi: 10.1029/2011JD015597

Kanamitsu M, Ebisuzaki W, Woollen J, Yang S-, Hnilo JJ, Fiorino M, Potter GL (2002) NCEP-DOE AMIP-II reanalysis (R-2). Bull Am Meteorol Soc 83:1631-1643+1559

Kang S, Xu Y, You Q, Flügel W-, Pepin N, Yao T (2010) Review of climate and cryospheric change in the Tibetan Plateau. Environmental Research Letters 5

Karmacharya J, Levine RC, Jones R, Moufouma-Okia W, New M (2015) Sensitivity of systematic biases in South Asian summer monsoon simulations to regional climate model domain size and implications for downscaled regional process studies. Clim Dyn 45:213-231. doi: 10.1007/s00382-015-2565-6

Kehrwald NM, Thompson LG, Yao Tandong, Mosley-Thompson E, Schotterer U, Alfimov V, Beer J, Eikenberg J, Davis ME (2008) Mass loss on Himalayan glacier endangers water resources. Geophys Res Lett 35:L22503. doi: 10.1029/2008GL035556

Kendon EJ, Roberts NM, Fowler HJ, Roberts MJ, Chan SC, Senior CA (2014) Heavier summer downpours with climate change revealed by weather forecast resolution model. Nat Clim Change 4:570-576. doi: 10.1038/nclimate2258

Kendon EJ, Roberts NM, Senior CA, Roberts MJ (2012) Realism of rainfall in a very high-resolution regional climate model. J Clim 25:5791-5806. doi: 10.1175/JCLI-D-11-00562.1

Kharin VV, Zwiers FW (2005) Estimating extremes in transient climate change simulations. J Clim 18:1156-1173. doi: 10.1175/JCLI3320.1

Kim O-, Wang B, Shin S- (2013) How do weather characteristics change in a warming climate?. Clim Dyn 41:3261-3281. doi: 10.1007/s00382-013-1795-8

Klingaman NP, Inness PM, Weller H, Slingo JM (2008) The Importance of High-Frequency Sea Surface Temperature Variability to the Intraseasonal Oscillation of Indian Monsoon Rainfall. J Climate 21:6119-6140. doi: 10.1175/2008JCLI2329.1

Konwar M, Parekh A, Goswami BN (2012) Dynamics of east-west asymmetry of Indian summer monsoon rainfall trends in recent decades. Geophys Res Lett 39. doi: 10.1029/2012GL052018

Kopparla P, Fischer EM, Hannay C, Knutti R (2013) Improved simulation of extreme precipitation in a high-resolution atmosphere model. Geophys Res Lett 40:5803-5808. doi: 10.1002/2013GL057866

Kripalani RH, Oh JH, Kulkarni A, Sabade SS, Chaudhari HS (2007) South Asian summer monsoon precipitation variability: Coupled climate model simulations and projections under IPCC AR4. Theoretical and Applied Climatology 90:133-159. doi: 10.1007/s00704-006-0282-0

Krishna Kumar K, Hoerling M, Rajagopalan B (2005) Advancing dynamical prediction of Indian monsoon rainfall. Geophys Res Lett 32:1-4. doi: 10.1029/2004GL021979

Krishnamurthy V, Shukla J (2000) Intraseasonal and interannual variability of rainfall over India. J Clim 13:4366-4377

Krishnamurti TN, Bhalme HN (1976) OSCILLATIONS OF A MONSOON SYSTEM - 1. OBSERVATIONAL ASPECTS. J Atmos Sci 33:1937-1954

Krishnan R, Sabin TP, Ayantika DC, Kitoh A, Sugi M, Murakami H, Turner AG, Slingo JM, Rajendran K (2013) Will the South Asian monsoon overturning circulation stabilize any further?. Clim Dyn 40:187-211. doi: 10.1007/s00382-012-1317-0

Krishnan R, Ramesh KV, Samala BK, Meyers G, Slingo JM, Fennessy MJ (2006) Indian Ocean-monsoon coupled interactions and impending monsoon droughts. Geophys Res Lett 33. doi: 10.1029/2006GL025811

Krueger O, Schenk F, Feser F, Weisse R (2013) Inconsistencies between long-term trends in storminess derived from the 20CR reanalysis and observations. J Clim 26:868-874. doi: 10.1175/JCLI-D-12-00309.1

Kulkarni A (2012) Weakening of Indian summer monsoon rainfall in warming environment. Theor Appl Climatol 109:447-459. doi: 10.1007/s00704-012-0591-4

Kulkarni A, Kripalani R, Sabade S, Rajeevan M (2011) Role of intra-seasonal oscillations in modulating Indian summer monsoon rainfall. Clim Dyn 36:1005-1021; 1021. doi: 10.1007/s00382-010-0973-1

Kumar KK, Kamala K, Rajagopalan B, Hoerling M, Eischeid J, Patwardhan S, Srinivasan G, Goswami B, Nemani R (2011a) The once and future pulse of Indian monsoonal climate. Clim Dyn 36:2159-2170; 2170. doi: 10.1007/s00382-010-0974-0

Kumar KK, Patwardhan SK, Kulkarni A, Kamala K, Rao KK, Jones R (2011b) Simulated projections for summer monsoon climate over India by a high-resolution regional climate model (PRECIS). Curr Sci 101:312-326

Kumar KK, Rajagopalan B, Hoerling M, Bates G, Cane M (2006) Unraveling the mystery of Indian monsoon failure during El Niño. Science 314:115-119

Kumar KK, Rajagopalan B, Cane MA (1999) On the weakening relationship between the indian monsoon and ENSO. Science 284:2156-2159. doi: 10.1126/science.284.5423.2156

Kumar RK, Sahai AK, Krishna Kumar K, Patwardhan SK, Mishra PK, Revadekar JV, Kamala K, Pant GB (2006) High-resolution climate change scenarios for India for the 21st century. Curr Sci 90:334-345

Kusunoki S, Mizuta R, Matsueda M (2011) Future changes in the East Asian rain band projected by global atmospheric models with 20-km and 60-km grid size. Clim Dyn 37:2481-2493. doi: 10.1007/s00382-011-1000-x

Lal M, Singh KK, Srinivasan G, Rathore LS, Naidu D, Tripathi CN (1999) Growth and yield responses of soybean in Madhya Pradesh, India to climate variability and change. Agric For Meterol 93:53-70. doi: 10.1016/S0168-1923(98)00105-1

Laprise R (2003) Resolved scales and nonlinear interactions in limited-area models. J Atmos Sci 60:768-779

Lau K-, Kim K-, Yang S (2000) Dynamical and boundary forcing characteristics of regional components of the Asian summer monsoon. J Clim 13:2461-2482

Leduc M, Laprise R (2009) Regional climate model sensitivity to domain size. Clim Dyn 32:833-854. doi: 10.1007/s00382-008-0400-z

Leduc M, Laprise R, Moretti-Poisson M, Morin J (2011) Sensitivity to domain size of mid-latitude summer simulations with a regional climate model. Clim Dyn 37:343-356; 356. doi: 10.1007/s00382-011-1008-2

Lee J-, Hong S- (2014) Potential for added value to downscaled climate extremes over Korea by increased resolution of a regional climate model. Theor Appl Climatol 117:667-677. doi: 10.1007/s00704-013-1034-6

Leung LR, Qian Y (2003) The sensitivity of precipitation and snowpack simulations to model resolution via nesting in regions of complex terrain. J Hydrometeorol 4:1025-1043. doi: 10.1175/1525-7541(2003)004<1025:TSOPAS>2.0.CO;2

Levine RC, Turner AG (2012) Dependence of Indian monsoon rainfall on moisture fluxes across the Arabian Sea and the impact of coupled model sea surface temperature biases. Clim Dyn 38:2167-2190. doi: 10.1007/s00382-011-1096-z

Li H, Kanamitsu M, Hong S- (2012) California reanalysis downscaling at 10 km using an ocean-atmosphere coupled regional model system. J Geophys Res D Atmos 117. doi: 10.1029/2011JD017372

Li L, Li W, Jin J (2014) Improvements in WRF simulation skills of southeastern United States summer rainfall: physical parameterization and horizontal resolution. Clim Dyn:1-15. doi: 10.1007/s00382-013-2031-2

Liebmann B, Hendon HH, Glick JD (1994) The relationship between tropical cyclones of the western Pacific and Indian Oceans and the Madden-Julian oscillation. J.Meteor.Soc.Japan 72:401-412

Lin J-, Weickman KM, Kiladis GN, Mapes BE, Schubert SD, Suarez MJ, Bacmeister JT, Lee M- (2008) Subseasonal variability associated with Asian summer monsoon simulated by 14 IPCC AR4 coupled GCMs. J Clim 21:4541-4567

Lo JC-, Yang Z-, Pielke Sr. RA (2008) Assessment of three dynamical climate downscaling methods using the Weather Research and Forecasting (WRF) model. J Geophys Res D Atmos 113. doi: 10.1029/2007JDO09216

Lock AP, Brown AR, Bush MR, Martin GM, Smith RNB (2000) A new boundary layer mixing scheme. Part I: Scheme description and single-column model tests. Mon Weather Rev 128:3187-3199. doi: 10.1175/1520-0493(2000)128<3187:ANBLMS>2.0.CO;2

Manoj MG (2011) Absorbing aerosols facilitate transition of Indian monsoon breaks to active spells. Clim Dyn 37:2181-2198

Martin GM, Milton SF, Senior CA, Brooks ME, Ineson S, Reichler T, Kim J (2010) Analysis and reduction of systematic errors through a seamless approach to modeling weather and climate. J Clim 23:5933-5957. doi: 10.1175/2010JCLI3541.1

Martin GM, Ringer MA, Pope VD, Jones A, Dearden C, Hinton TJ (2006) The physical properties of the atmosphere in the new Hadley Centre Global Environmental Model (HadGEM1). Part 1: Model description and global climatology. J Clim 19:1274-1301. doi: 10.1175/JCLI3636.1

Martin GM, Arpe K, Chauvin F, Ferranti L, Maynard K, Polcher J, Stephenson DB, Tschuck P (2000) Simulation of the Asian Summer Monsoon in Five European General Circulation Models. Atmospheric Science Letters 1:X-XXVIII

Marvel K, Ivanova D, Taylor KE (2013) Scale space methods for climate model analysis. Journal of Geophysical Research: Atmospheres 118:5082-5097

Mass CF, Ovens D, Westrick K, Colle BA (2002) Does increasing horizontal resolution produce more skillful forecasts? The results of two years of real-time numerical weather prediction over the Pacific Northwest. Bull Am Meteorol Soc 83:407-430+341

Masson D, Knutti R (2011) Spatial-scale dependence of climate model performance in the CMIP3 ensemble. J Clim 24:2680-2692. doi: 10.1175/2011JCLI3513.1

McCarthy MP, Sanjay J, Booth BBB, Kumar KK, Betts RA (2012) The influence of vegetation on the ITCZ and South Asian monsoon in HadCM3. Earth Syst Dyn 3:87-96. doi: 10.5194/esd-3-87-2012

McSweeney CF (2007) Daily rainfall variability at point and areal Scales: evaluating simulations of present and future climate. PhD Thesis. University of East Anglia, Norwich

McSweeney CF, Jones RG, Booth BBB (2012) Selecting ensemble members to provide regional climate change information. J Clim 25:7100-7121. doi: 10.1175/JCLI-D-11-00526.1

Ménégoz M, Gallée H, Jacobi HW (2013) Precipitation and snow cover in the Himalaya: From reanalysis to regional climate simulations. Hydrol Earth Syst Sci 17:3921-3936. doi: 10.5194/hess-17-3921-2013

Miguez-Macho G, Stenchikov GL, Robock A (2004) Spectral nudging to eliminate the effects of domain position and geometry in regional climate model simulations. J Geophys Res D Atmos 109:D13104 1-14. doi: 10.1029/2003JD004495

Mizuta R, Oouchi K, Yoshimura H, Noda A, Katayama K, Yukimoto S, Hosaka M, Kusunoki S, Kawai H, Nakagawa M (2006) 20-km-mesh global climate simulations using JMA-GSM model - Mean climate states. J Meteorol Soc Jpn 84:165-185. doi: 10.2151/jmsj.84.165

Molinari J, Dudek M (1992) Parameterization of convective precipitation in mesoscale numerical models: a critical review. Mon Weather Rev 120:326-344

Moufouma-Okia W, Jones R (2014) Resolution dependence in simulating the African hydroclimate with the HadGEM3-RA regional climate model. Clim Dyn 44:609-632. doi: 10.1007/s00382-014-2322-2

Mukhopadhyay P (2010) Indian summer monsoon precipitation climatology in a high-regional climate model: impacts of convective parameterization on systematic biases. Weather and forecasting 25:369-387

Murakami T, Nakazawa T (1985) Tropical 45 day oscillations during the 1979 Northern Hemisphere summer. J Atmos Sci 42:1107-1122

Muraleedharan PM, Mohankumar K, Sivakumar KU (2013) A study on the characteristics of temperature inversions in active and break phases of Indian summer monsoon. J Atmos Sol -Terr Phys 93:11-20. doi: 10.1016/j.jastp.2012.11.006

Murugavel P, Pawar SD, Gopalakrishnan V (2012) Trends of Convective Available Potential Energy over the Indian region and its effect on rainfall. Int J Climatol 32:1362-1372. doi: 10.1002/joc.2359

Nikulin G (2012) Precipitation Climatology in an Ensemble of CORDEX-Africa Regional Climate Simulations. J Clim 25:6057-6078

Oouchi K, Noda AT, Satoh M, Wang B, Xie S-, Takahashi HG, Yasunari T (2009) Asian summer monsoon simulated by a global cloud-system-resolving model: Diurnal to intra-seasonal variability. Geophys Res Lett 36. doi: 10.1029/2009GL038271

Oouchi K, Yoshimura J, Yoshimura H, Mizuta R, Kusunoki S, Noda A (2006) Tropical cyclone climatology in a global-warming climate as simulated in a 20 km-mesh global atmospheric model: Frequency and wind intensity analyses. J Meteorol Soc Jpn 84:259-276. doi: 10.2151/jmsj.84.259

Paeth H, Mannig B (2012) On the added value of regional climate modeling in climate change assessment. Clim Dyn:1-10. doi: 10.1007/s00382-012-1517-7

Pal JS, Giorgi F, Bi X, Elguindi N, Solmon F, Gao X, Rauscher SA, Francisco R, Zakey A, Winter J, Ashfaq M, Syed FS, Bell JL, Differbaugh NS, Karmacharya J, Konari A, Martinez D, Da Rocha RP, Sloan LC, Steiner AL (2007) Regional climate modeling for the developing world: The ICTP RegCM3 and RegCNET. Bull Am Meteorol Soc 88:1395-1409

Panitz H-, Dosio A, Büchner M, Lüthi D, Keuler K (2014) COSMO-CLM (CCLM) climate simulations over CORDEX-Africa domain: Analysis of the ERA-Interim driven simulations at 0.44° and 0.22° resolution. Clim Dyn 42:3015-3038. doi: 10.1007/s00382-013-1834-5

Pant GB, Kumar KR (1997) Climates of South Asia. Wiley; Belhaven Studies in Climatology

Parthasarathy B, Munot AA, Kothawale DR (1994) All-India monthly and seasonal rainfall series: 1871-1993. Theoretical and Applied Climatology 49:217-224

Parthasarathy B, Kumar KR, Kothawale DR (1992) Indian summer monsoon rainfall indices: 1871-1990. Meteorol Mag 121:174-186

Philippe PL, Christensen JH, Saeed F, Kumar P, Asharaf S, Ahrens B, Wiltshire AJ, Jacob D, Hagemann S (2011) Can Regional Climate Models Represent the Indian Monsoon? RID A-7439-2008. J Hydrometeorol 12:849-868. doi: 10.1175/2011JHM1327.1

Pielke RA, Sr. (2002) Mesoscale Meteorological Modeling. 2nd ed. Academic Press

Pokhrel S, Dhakate A, Chaudhari HS, Saha SK (2013) Status of NCEP CFS vis-a-vis IPCC AR4 models for the simulation of Indian summer monsoon. Theoretical and Applied Climatology 111:65-78

Polanski S, Rinke A, Dethloff K (2010) Validation of the HIRHAM-Simulated Indian Summer Monsoon Circulation. Advances in Meteoroloy 2010. doi: 10.1155/2010/415632

Pope VD, Stratton RA (2002) The processes governing horizontal resolution sensitivity in a climate model. Clim Dyn 19:211-236. doi: 10.1007/s00382-001-0222-8

Prein AF (2013) Importance of Regional Climate Model Grid Spacing for the Simulation of Heavy Precipitation in the Colorado Headwaters. J Clim 26:4848-4857

Prein AF, Gobiet A, Suklitsch M, Truhetz H, Awan NK, Keuler K, Georgievski G (2013) Added value of convection permitting seasonal simulations. Clim Dyn 41:2655-2677. doi: 10.1007/s00382-013-1744-6

Racherla PN, Shindell DT, Faluvegi GS (2012) The added value to global model projections of climate change by dynamical downscaling: A case study over the continental U.S. using the GISS-ModelE2 and WRF models. J Geophys Res D Atmos 117. doi: 10.1029/2012JD018091

Rajeevan M, Gadgil S, Bhate J (2010) Active and break spells of the indian summer monsoon. Journal of Earth System Science 119:229-247

Rajeevan M, Bhate J (2009) A high resolution daily gridded rainfall dataset (1971-2005) for mesoscale meteorological studies. Curr Sci 96:558-562

Rajendran K, Sajani S, Jayasankar CB, Kitoh A (2013) How dependent is climate change projection of Indian summer monsoon rainfall and extreme events on model resolution?. Curr Sci 104:1409-1418

Rajendran K, Kitoh A, Srinivasan J, Mizuta R, Krishnan R (2012) Monsoon circulation interaction with Western Ghats orography under changing climate: Projection by a 20-km mesh AGCM. Theoretical and Applied Climatology 110:555-571

Rajendran K, Kitoh A (2008) Indian summer monsoon in future climate projection by a super high-resolution global model. Curr Sci 95:1560-1569

Ramamurthy K (1969) Monsoon of India: Some aspects of the 'break' in the Indian southwest monsoon during July and August. Forecasting Manual

Ratnam JV, Giorgi F, Kaginalkar A, Cozzini S (2009) Simulation of the Indian monsoon using the RegCM3-ROMS regional coupled model. Clim Dyn 33:119-139

Ratnam MV, Krishna Murthy BV, Jayaraman A (2013) Is the trend in TEJ reversing over the Indian subcontinent?. Geophys Res Lett:n/a-n/a. doi: 10.1002/grl.50519

Rauscher SA, Coppola E, Piani C, Giorgi F (2010) Resolution effects on regional climate model simulations of seasonal precipitation over Europe. Clim Dyn 35:685-711. doi: 10.1007/s00382-009-0607-7

Rauscher SA, Seth A, Qian J-, Camargo SJ (2006) Domain choice in an experimental nested modeling prediction system for South America. Theor Appl Climatol 86:229-246. doi: 10.1007/s00704-006-0206-z

Rayner NA, Parker DE, Horton EB, Folland CK, Alexander LV, Rowell DP, Kent EC, Kaplan A (2003) Global analyses of sea surface temperature, sea ice, and night marine air temperature since the late nineteenth century. J Geophys Res D Atmos 108:ACL 2-1 - ACL 2-29

Reynolds RW, Smith TM, Liu C, Chelton DB, Casey KS, Schlax MG (2007) Daily high-resolution-blended analyses for sea surface temperature. J Clim 20:5473-5496. doi: 10.1175/2007JCLI1824.1

Rienecker MM, Suarez MJ, Gelaro R, Todling R, Bacmeister J, Liu E, Bosilovich MG, Schubert SD, Takacs L, Kim G-, Bloom S, Chen J, Collins D, Conaty A, Da Silva A, Gu W, Joiner J, Koster RD, Lucchesi R, Molod A, Owens T, Pawson S, Pegion P, Redder CR, Reichle R, Robertson FR, Ruddick AG, Sienkiewicz M, Woollen J (2011) MERRA: NASA's modern-era retrospective analysis for research and applications. J Clim 24:3624-3648. doi: 10.1175/JCLI-D-11-00015.1

Roberts NM, Lean HW (2008) Scale-selective verification of rainfall accumulations from high-resolution forecasts of convective events. Mon Weather Rev 136:78-97. doi: 10.1175/2007MWR2123.1

Robinson DA, Dewey KF, Heim Jr RR (1993) Global snow cover monitoring: an update. Bulletin - American Meteorological Society 74:1689-1696

Rockel B, Geyer B (2008) The performance of the regional climate model CLM in different climate regions, based on the example of precipitation. Meteorologische Zeitschrift 17:487-498. doi: 10.1127/0941-2948/2008/0297

Rojas M (2006) Multiply nested regional climate simulation for southern South America: Sensitivity to model resolution. Mon Weather Rev 134:2208-2223. doi: 10.1175/MWR3167.1

Rummukainen M (2010) State-of-the-art with regional climate models. Wiley Interdiscip Rev Clim Change 1:82-96. doi: 10.1002/wcc.8

Sabin TP, Krishnan R, Ghattas J, Denvil S, Dufresne J-, Hourdin F, Pascal T (2013) High resolution simulation of the South Asian monsoon using a variable resolution global climate model. Clim Dyn 41:173-194. doi: 10.1007/s00382-012-1658-8

Saeed F, Hagemann S, Jacob D (2012) A framework for the evaluation of the South Asian summer monsoon in a regional climate model applied to REMO. Int J Climatol 32:430-440. doi: 10.1002/joc.2285

Saeed S, Liu Y, Rasul G (2011) Multiyear hindcast simulations of summer monsoon over South Asia using a nested regional climate model-BCC_RegCM1.0. Theor Appl Climatol 103:249-264. doi: 10.1007/s00704-010-0297-4

Saji NH, Goswami BN, Vinayachandran PN, Yamagata T (1999) A dipole mode in the tropical Indian ocean. Nature 401:360-363

Sanchez-Gomez E, Somot S, Déqué M (2009) Ability of an ensemble of regional climate models to reproduce weather regimes over Europe-Atlantic during the period 1961-2000. Clim Dyn 33:723-736. doi: 10.1007/s00382-008-0502-7

Sathiyamoorthy V, Pal PK, Joshi PC (2007) Intraseasonal variability of the Tropical Easterly Jet. Meteorology and Atmospheric Physics 96:305-316. doi: 10.1007/s00703-006-0214-7

Scinocca JF, McFarlane NA (2004) The variability of modeled tropical precipitation. J Atmos Sci 61:1993-2015. doi: 10.1175/1520-0469(2004)061<1993:TVOMTP>2.0.CO;2

Seth A, Rauscher SA, Camargo SJ, Qian J-, Pal JS (2007) RegCM3 regional climatologies for South America using reanalysis and ECHAM global model driving fields. Clim Dyn 28:461-480

Sharmila S, Pillai PA, Joseph S, Roxy M, Krishna RPM, Chattopadhyay R, Abhilash S, Sahai AK, Goswami BN (2013) Role of ocean-atmosphere interaction on northward propagation of Indian summer monsoon intra-seasonal oscillations (MISO). Clim Dyn 41:1651-1669. doi: 10.1007/s00382-013-1854-1

Shekhar MS, Dash SK (2005) Effect of Tibetan spring snow on the Indian summer monsoon circulation and associated rainfall. Curr Sci 88:1840-1844

Shrestha AB, Wake CP, Dibb JE, Mayewski PA (2000) Precipitation fluctuations in the Nepal Himalaya and its vicinity and relationship with some large scale climatological parameters. Int J Climatol 20:317-327

Shrestha AB, Wake CP, Mayewski PA, Dibb JE (1999) Maximum Temperature Trends in the Himalaya and Its Vicinity: An Analysis Based on Temperature Records from Nepal for the Period 1971–94. J Climate 12:2775-2786. doi: 10.1175/1520-0442(1999)012<2775:MTTITH>2.0.CO;2

Sikka DR, Gadgil S (1980) On the maximum cloud zone and the ITCZ over Indian longitudes during the southwest monsoon. Mon Weather Rev 108:1840-1853

Sinha P, Mohanty UC, Kar SC, Dash SK, Kumari S (2013) Sensitivity of the GCM driven summer monsoon simulations to cumulus parameterization schemes in nested RegCM3. Theoretical and Applied Climatology 112:285-306

Soares P, Cardoso R, Miranda P, de Medeiros J, Belo-Pereira M, Espirito-Santo F (2012) WRF high resolution dynamical downscaling of ERA-Interim for Portugal. Clim Dyn:1-26. doi: 10.1007/s00382-012-1315-2

Sperber KR, Annamalai H, Kang I-, Kitoh A, Moise A, Turner A, Wang B, Zhou T (2013) The Asian summer monsoon: An intercomparison of CMIP5 vs. CMIP3 simulations of the late 20th century. Clim Dyn 41:2711-2744. doi: 10.1007/s00382-012-1607-6

Sperber KR, Slingo JM, Annamalai H (2000) Predictability and the relationship between subseasonal and interannual variability during the Asian summer monsoon. Q J R Meteorol Soc 126:2545-2574

Srinivas CV, Hariprasad D, Bhaskar Rao DV, Anjaneyulu Y, Baskaran R, Venkatraman B (2013) Simulation of the Indian summer monsoon regional climate using advanced research WRF model. Int J Climatol 33:1195-1210. doi: 10.1002/joc.3505

Stephenson DB, Rupa Kumar K, Doblas-Reyes FJ, Royer J-, Chauvin F, Pezzulli S (1999) Extreme daily rainfall events and their impact on ensemble forecasts of the Indian monsoon. Mon Weather Rev 127:1954-1966

Stowasser M, Annamalai H, Hafner J (2009) Response of the South Asian Summer Monsoon to Global Warming: Mean and Synoptic Systems. J Clim 22:1014-1036. doi: 10.1175/2008JCLI2218.1

Syed FS, Iqbal W, Syed A, Rasul G (2014) Uncertainties in the regional climate models simulations of South-Asian summer monsoon and climate change. Clim Dyn 42:2079-2097. doi: 10.1007/s00382-013-1963-x

Taylor KE (2001) Summarizing multiple aspects of model performance in a single diagram. Journal of Geophysical Research D: Atmospheres 106:7183-7192

Tokinaga H, Xie S-, Deser C, Kosaka Y, Okumura YM (2012) Slowdown of the Walker circulation driven by tropical Indo-Pacific warming. Nature 491:439-443. doi: 10.1038/nature11576

Tselioudis G (2012) Does dynamical downscaling introduce novel information in climate model simulations of precipitation change over a complex topography region?. Int J Climatol 32:1572-1578

Turner AG, Martin GM, Levine RC (2015) The role of peninsular India in the South Asian summer monsoon. Clim Dyn (submitted)

Turner AG, Annamalai H (2012) Climate change and the South Asian summer monsoon. Nature Climate Change 2:587-595

Turner AG, Slingo JM (2009) Subseasonal extremes of precipitation and active-break cycles of the Indian summer monsoon in a climate-change scenario. Q J R Meteorol Soc 135:549-567. doi: 10.1002/qj.401

Uppala SM, Kållberg PW, Simmons AJ, Andrae U, da Costa Bechtold V, Fiorino M, Gibson JK, Haseler J, Hernandez A, Kelly GA, Li X, Onogi K, Saarinen S, Sokka N, Allan RP, Andersson E, Arpe K, Balmaseda MA, Beljaars ACM, van de Berg L, Bidlot J, Bormann N, Caires S, Chevallier F, Dethof A, Dragosavac M, Fisher M, Fuentes M,

Hagemann S, Hólm E, Hoskins BJ, Isaksen L, Janssen PAEM, Jenne R, McNally AP, Mahfouf J-, Morcrette J-, Rayner NA, Saunders RW, Simon P, Sterl A, Trenberth KE, Untch A, Vasiljevic D, Viterbo P, Woollen J (2005) The ERA-40 re-analysis. Q J R Meteorol Soc 131:2961-3012. doi: 10.1256/qj.04.176

Van den Dool H, Huang J, Fan Y (2003) Performance and analysis of the constructed analogue method applied to US soil moisture over 1981-2001. J.Geophys.Res. 108:8617. doi: 10.1029/2002JD003114

Vannitsem S, Chomé F (2005) One-way nested regional climate simulations and domain size. J Clim 18:229-233. doi: 10.1175/JCLI3252.1

Vecchi GA, Soden BJ, Wittenberg AT, Held IM, Leetmaa A, Harrison MJ (2006) Weakening of tropical Pacific atmospheric circulation due to anthropogenic forcing. Nature 441:73-76. doi: 10.1038/nature04744

Vellore RK, Krishnan R, Pendharkar J, Choudhury AD, Sabin TP (2014) On the anomalous precipitation enhancement over the Himalayan foothills during monsoon breaks. Clim Dyn:1-23. doi: 10.1007/s00382-013-2024-1

Waliser DE, Murtugudde R, Lucas LE (2004) Indo-Pacific Ocean response to atmospheric intraseasonal variability: 2. Boreal summer and the Intraseasonal Oscillation. J Geophys Res C Oceans 109:C03030 1-26

Waliser DE, Jones C, Schemm J-E, Graham NE (1999) A statistical extended-range tropical forecast model based on the slow evolution of the Madden-Julian oscillation. J Clim 12:1918-1939

Walters DN, Williams KD, Boutle IA, Bushell AC, Edwards JM, Field PR, Lock AP, Morcrette CJ, Stratton RA, Wilkinson JM, Willett MR, Bellouin N, Bodas-Salcedo A, Brooks ME, Copsey D, Earnshaw PD, Hardiman SC, Harris CM, Levine RC, MacLachlan C, Manners JC, Martin GM, Milton SF, Palmer MD, Roberts MJ, Rodríguez JM, Tennant WJ, Vidale PL (2013) The Met Office Unified Model Global Atmosphere 4.0 and JULES Global Land 4.0 configurations. Geosci Model Dev Discuss 6:2813-2881. doi: 10.5194/gmdd-6-2813-2013

Walters DN, Best MJ, Bushell AC, Copsey D, Edwards JM, Falloon PD, Harris CM, Lock AP, Manners JC, Morcrette CJ, Roberts MJ, Stratton RA, Webster S, Wilkinson JM, Willett MR, Boutle IA, Earnshaw PD, Hill PG, MacLachlan C, Martin GM, Moufouma-Okia W, Palmer MD, Petch JC, Rooney GG, Scaife AA, Williams KD (2011) The Met Office Unified Model Global Atmosphere 3.0/3.1 and JULES Global Land 3.0/3.1 configurations. Geosci Model Dev 4:919-941. doi: 10.5194/gmd-4-919-2011

Wang B, Liu J, Kim H-, Webster PJ, Yim S-, Xiang B (2013) Intensified Northern Hemisphere summer monsoon [Earth, Atmospheric, and Planetary Sciences] . Proceedings of the National Academy of Sciences 110:5347-5352. doi: 10.1073/pnas.1219405110

Wang B, Wu R, Lau K- (2001) Interannual variability of the asian summer monsoon: Contrasts between the Indian and the Western North Pacific-East Asian monsoons. J Clim 14:4073-4090. doi: 10.1175/1520-0442(2001)014<4073:IVOTAS>2.0.CO;2

Wang B (2000) Reply. Bull Am Meteorol Soc 81:822-824. doi: 10.1175/1520-0477(2000)081<0822:REPLY>2.3.CO;2

Wang B, Fan Z (1999) Choice of South Asian Summer Monsoon Indices. Bull Am Meteorol Soc 80:629-638

Wang C, Jones R, Perry M, Johnson C, Clark P (2013) Using an ultrahigh-resolution regional climate model to predict local climatology. Q J R Meteorol Soc. doi: 10.1002/qj.2081

Warner TT, Peterson RA, Treadon RE (1997) A Tutorial on Lateral Boundary Conditions as a Basic and Potentially Serious Limitation to Regional Numerical Weather Prediction. Bull Am Meteorol Soc 78:2599-2617

Warrach-Sagi K, Schwitalla T, Wulfmeyer V, Bauer H- (2013) Evaluation of a climate simulation in Europe based on the WRF-NOAH model system: precipitation in Germany. Clim Dyn:1-20. doi: 10.1007/s00382-013-1727-7

Webster PJ, Magaña VO, Palmer TN, Shukla J, Tomas RA, Yanai M, Yasunari T (1998) Monsoons: processes, predictability, and the prospects for prediction. Journal of Geophysical Research C: Oceans 103:14451-14510

Webster PJ, Song Yang (1992) Monsoon and ENSO: selectively interactive systems. Q J R Meteorol Soc 118:877-926

Weisman ML, Skamarock WC, Klemp JB (1997) The resolution dependence of explicitly modeled convective systems. Mon Weather Rev 125:527-548

Wilby RL, Fowler HJ (2010) Regional climate downscaling. In: Fung CF, Lopez A, New M (eds) Modelling the Impact of Climate Change on Water Resources. Wiley-Blackwell, Chichester, U. K., pp 34-85

Wilson DR, Ballard SP (1999) A microphysically based precipitation scheme for the UK Meteorological Office Unified Model. Q J R Meteorol Soc 125:1607-1636. doi: 10.1256/smsqj.55706

Wilson DR, Bushell AC, Kerr-Munslow AM, Price JD, Morcrette CJ, Bodas-Salcedo A (2008) PC2: A prognostic cloud fraction and condensation scheme. II: Climate model simulations. Q J R Meteorol Soc 134:2109-2125. doi: 10.1002/qj.332

Winterfeldt J, Weisse R (2009) Assessment of value added for surface marine wind speed obtained from two regional climate models. Mon Weather Rev 137:2955-2965. doi: 10.1175/2009MWR2704.1

Xavier PK, John VO, Buehler SA, Ajayamohan RS, Sijikumar S (2010) Variability of Indian summer monsoon in a new upper tropospheric humidity data set. Geophys Res Lett 37. doi: 10.1029/2009GL041861

Xavier PK, Marzin C, Goswami BN (2007) An objective definition of the Indian summer monsoon season and a new perspective on the ENSO-monsoon relationship. Q J R Meteorol Soc 133:749-764

Yadav RK, Rupa Kumar K, Rajeevan M (2010) Climate change scenarios for Northwest India winter season. Quaternary International 213:12-19

Yatagai A, Kawamoto H (2008) Quantitative estimation of orographic precipitation over the Himalayas by using TRMM/PR and a dense network of rain gauges. Proceedings of SPIE - The International Society for Optical Engineering 7148

Yatagai A, Arakawa O, Kamiguchi K, Kawamoto H, Nodzu MI, Hamada A (2009) A 44-Year Daily Gridded Precipitation Dataset for Asia Based on a Dense Network of Rain Gauges. SOLA 5:137-140

Yim S, Wang B, Liu J, Wu Z (2013) A comparison of regional monsoon variability using monsoon indices. Clim Dyn:1-15. doi: 10.1007/s00382-013-1956-9

Zhang C, Zhang H (2010) Potential impacts of East Asian winter monsoon on climate variability and predictability in the Australian summer monsoon region. Theor Appl Climatol 101:161-177. doi: 10.1007/s00704-009-0246-2

Zhang M, Song H (2006) Evidence of deceleration of atmospheric vertical overturning circulation over the tropical Pacific. Geophys Res Lett 33. doi: 10.1029/2006GL025942

Zikova N, Holtanova E, Kalvova J (2013) Annual precipitation cycle in regional climate models: The influence of horizontal resolution. Theor Appl Climatol 112:521-533. doi: 10.1007/s00704-012-0749-0